2009-09-17

Neural Circuit Analyses of the Olfactory System in Drosophila: Input to Output: A Dissertation

Shamik DasGupta
University of Massachusetts Medical School

Neural Circuit Analyses of the Olfactory System in *Drosophila*: Input to Output

A Dissertation Presented

By

Shamik DasGupta

Submitted to the Faculty of the

University of Massachusetts Graduate School of Biomedical Sciences, Worcester

In partial fulfillment of the requirements for the degree of

Doctor of Philosophy

September 17, 2009

Neuroscience Program

Neural Circuit Analyses of the Olfactory System

in *Drosophila*: Input to Output

A Dissertation Presented By

Shamik DasGupta

The signatures of the Dissertation Defense Committee signify completion and approval as to style and content of the Dissertation

Scott Waddell, Ph.D., Thesis Advisor

Marc Freeman, Ph.D., Member of Committee

Paul Garrity, Ph.D., Member of Committee

Steven Reppert, M.D., Member of Committee

Neal Silverman, Ph.D., Member of Committee

The signature of the Chair of the Committee signifies that the written Dissertation meets the requirements of the Dissertation Committee

David Weaver, Ph.D., Chair of Committee

The signature of the Dean of the Graduate School of Biomedical Sciences signifies that the student has met all graduation requirements of the School

Anthony Carruthers, Ph.D.
Dean of the Graduate School of Biomedical Sciences

Neuroscience Program
September 17, 2009

To Shuvasree

Acknowledgements:

Joining Scott's lab was one of the best decisions I ever made. Scott offered everything I hoped to find in a PI. He is extremely intelligent, fun to work for and is very supportive to new, often wildly adventurous, ideas. For the first two years, I tried multiple projects that went nowhere and I suspected that I had the anti-Midas touch (a Chip Quinnism that Scott taught us: everything you touch turns to shit). Scott helped me survive this phase and constantly motivated me to work on projects of my interest. He spent hours with myself and Mike, teaching us how to make a presentation; how to write a paper, how to edit a thesis; how to give a talk; how to enjoy a single malt whisky (Mike never learned this part); you get the idea. I am grateful to Scott for everything he has done to support my career. And Scott, a special 'thank you' for all the slides I (we) stole from your presentations. All in all, I had a great time working for you and I will miss it a lot.

I appreciate the support I have received from my TRAC committee members: David Weaver, Marc Freeman, Mark Alkema, Tzumin Lee and Neal Silverman, throughout my graduate career. At times their shrewd questioning made me feel like a complete idiot and I used to curse myself for not having the insight to think about those things ahead of time. Their guidance helped me to become a better scientist. I am also grateful to Steven Reppert and Paul Garrity for agreeing to be on my defense committee.

I want to thank my wonderful labmates in the Waddell lab. Alex Keene guided me through my first few months in the lab and his success in grad school was a major motivating factor for me. Ben Leung is probably the most patient person I have ever seen in my life and was willing to spend hours with me discussing projects or editing my writing. He is smart, has a firm grasp of the scientific literature and his very fair and frank critique helped me to improve my scientific skills. I want to thank him for all the discussions we had, from science to science fiction and video games. Mike Krashes (aka Pinky) and I joined Scott's lab around the same time and immediately formed a close friendship because of our religious faiths. Mike is intelligent, extremely accommodating and hard working, and an avid environmentalist who was kind enough to recycle his meals in the form of odorous volatiles. My anosmia allowed us to function collaboratively in the lab and we were reasonably successful as a team (team Shamichael in Mikology). I firmly believe some day we will be able to take over the world (Pinky and the Brain anyone). Paola Perrat was my molecular biology guru and I want to thank her for the molecular biology (and cooking) tips. Jena Pitman is a recent addition to the Waddell clan and I really enjoyed our arguments over scientific literature and the uselessness of having a cat. Outside the lab, these people are very good friends and I wish them all the success in their careers. I also want to thank two former members of our lab, Ruth Brain and Richard Auclair. I enjoyed working with them and we miss them a lot. I want

to welcome two new members of our lab, Chris Burke and Wolf Hutteroth, and wish them good luck.

We have a wonderful department here at UMass and I enjoyed working with some very collaborative colleagues. I want to thank Rob Gegear for all the discussion on behavior and statistics. I am also thankful to Stanley Heinze, Christine Merlin, Raphaëlle Dubruille and Hung-Hsiang Yu (Sam) for their help.

I am very fortunate to have had some very gifted teachers throughout my schooling and I am indebted to them. I am especially thankful to Chandan Saha and Maitrayee Dasgupta for the time and effort they spent in tutoring me and convincing me to stay in academia.

On a more personal note, I am grateful to my wife and parents for their unwavering support. My mom was my first biology teacher and I aspire to become a compassionate teacher like her. I am thankful to my dad for his continuous support and calming influence. It is very comforting to know that I can always count on him if things go wrong. My wife Shuvasree is the nicest and most caring person I have ever met and I am really lucky to have her beside me. She always inspired me to follow my dreams and I cannot thank her enough for the sacrifices she made to support my career.

Last but not least, I want to thank all my friends here at UMass: Jassi, Shiven, Kamal, Rajarshi, Ramesh and Samriddha. We had some great times together and I hope we will stay in touch after finishing grad school.

Abstract

This thesis focuses on several aspects of olfactory processing in *Drosophila*. In chapter I and II, I will discuss how odorants are encoded in the brain. In both insects and mammals, olfactory receptor neurons (ORNs) expressing the same odorant receptor gene converge onto the same glomerulus. This topographical organization segregates incoming odor information into combinatorial maps. One prominent theory suggests that insects and mammals discriminate odors based on these distinct combinatorial spatial codes. I tested the combinatorial coding hypothesis by engineering flies that have only one class of functional ORNs and therefore cannot support combinatorial maps. These files can be taught to discriminate between two odorants that activate the single functional class of ORN and identify an odorant across a range of concentrations, demonstrating that a combinatorial code is not required to support learned odor discrimination. In addition, these data suggest that odorant identity can be encoded as temporal patterns of ORN activity.

Behaviors are influenced by motivational states of the animal. Chapter III of this thesis focuses on understanding how motivational states control behavior. Appetitive memory in *Drosophila* provides an excellent system for such studies because the motivational state of hunger promotes reliance on learned appetitive cues whereas satiety suppresses it. We found that activation of neuropeptide F

(dNPF) neurons in fed flies releases appetitive memory performance from satiety-mediated suppression. Through a GAL4 screen, we identified six dopaminergic neurons that are a substrate for dNPF regulation. In satiated flies, these neurons inhibit mushroom body output, thereby suppressing appetitive memory performance. Hunger promotes dNPF release, which blocks the inhibitory dopaminergic neurons. The motivational drive of hunger thus affects behavior through a hierarchical inhibitory control mechanism: satiety inhibits memory performance through a subset of dopaminergic neurons, and hunger promotes appetitive memory retrieval via dNPF-mediated disinhibition of these neurons.

The aforementioned studies utilize sophisticated genetic tools for *Drosophil*a. In chapter IV, I will talk about two new genetic tools. We developed a new technique to restrict gene expression to different subsets of mushroom body neurons with unprecedented precision. We also adapted the light-activated adenylyl cyclase (PAC) from *Euglena gracilis* as a light-inducable cAMP system for *Drosophila*. This system can be used to induce cAMP synthesis in targeted neurons in live, behaving preparations.

Table of Contents

List of Figures

Chapter I. Circuit dynamics of olfactory processing in *Drosophila*

Chapter II: Input to the system: Learned odor discrimination in *Drosophila* without combinatorial odor maps in the antennal lobe

Chapter III: Output from the system: A neural circuit mechanism integrating motivational state with memory expression in *Drosophila*

List of Tables

Chapter III: Output from the system: A neural circuit mechanism integrating motivational state with memory expression in *Drosophila*

Abbreviations

ACT	Antennocerebral tract
AL	Antennal lobe
cAMP	cyclic adenosine monophosphate
CC	Central complex
CS	Conditioned stimulus
CS+	Paired conditioned stimulus
CS-	Unpaired conditioned stimulus
DA	Dopamine
dNPF	*Drosophila* neuropeptide-F
DPM	Dorsal paired medial
FLP	Flippase recombination enzyme
FRT	Flippase recognition target
GABA	Gamma-aminobutyric acid
GFP	Green fluorescent protein
KC	Kenyon cell
LFP	Local field potential
LH	Lateral horn
MB	Mushroom body
MB-MP	Mushroom body-medial lobe and pedunculus
dNPFR	*Drosophila* neuropeptide-F receptor
OR	Olfactory receptor
ORN	Olfactory receptor neuron
PI	Performance Index
PN	Projection neuron
shi^{ts1}	temperature-sensitive *shibire*
SOG	Subesophageal ganglion
TH	Tyrosine hydroxylase

TRP	Transient receptor potential
TQ	Tully-Quinn apparatus
US	Unconditioned stimulus
VUMmx1	Ventral unpaired median

Copyright Page

The chapters of this dissertation have appeared in separate publications or as part of publications:

Rickmyre, J. L., **DasGupta, S**., Ooi, D. L., Keel, J., Lee, E., Kirschner, M. W., Waddell, S., and Lee, L. A. (2007). The Drosophila homolog of MCPH1, a human microcephaly gene, is required for genomic stability in the early embryo. J. Cell. Sci 120, 3565-3577.

DasGupta, S. & Waddell, S. (2008). Learned odor discrimination in Drosophila without combinatorial odor maps in the antennal lobe. Current Biology 18, 1668-74.

Pitman, J.L., **DasGupta, S**, Krashes, M.J., Leung, B., Perrat, P.N., and Waddell, S. (2009). There are many ways to train a fly. Fly 3, 3-9.

Krashes, M.J.*, **DasGupta, S**.*, Vreede, A., White, B., Armstrong, J.D., Waddell, S. (2009). A neural circuit mechanism integrating motivational state with memory expression in Drosophila. Cell, in press. * equal contribution

Chapter I: Circuit dynamics of olfactory processing in *Drosophila*

I.A. Introduction

Where does behavior come from?

For centuries, ethologists, psychologists and biologists have debated the origin of behavior. Early models proposed that behavior emerges from summation of reflexes. The term 'reflex' often means a linear relationship between a stimulus and behavior and has an element of predictability in it. However psychologists soon realized that the linear stimulus-response relationship, like that observed in the knee-jerk response, is an exception in complex neural systems. Most behaviors are highly unpredictable and more often than not, a stimulus fails to elicit a predictable behavioral response. To incorporate this non-linearity in the response, later models for behavior incorporated a greater appreciation for a motivational component in behavior. These models postulated that behaviors happen to neutralize different internal drives and generate a consummatory phase; hunger generates behaviors that lead to consumption of food, thirst leads to drinking, lust leads to sex, (masochism leads to graduate school).

However drive alone cannot explain decisions often made during behavior. Memory plays an integral role in the decision-making process. For example, when hungry, animals are often guided to certain foods using memory

of prior experience. With this in mind, some motivational theorists incorporated memory and internal state into their models for motivated behavior. This is simply illustrated in a model from Frederick Toates (1986) where he postulated that motivated behavior emerges from the integration between sensory information from incentive objects (e.g. smell, taste and the sight of food), memory for these incentive objects (past experience with food) and the internal physiological state of the animal, whether the animal is hungry or satiated (Toates, 1986 and Figure I.1).

In my thesis I will describe olfactory memory performance of *Drosophila* in light of this model. In Chapter 1 and 2, I will discuss our current understanding of olfactory circuit function. Chapter 3 focuses on how motivated behavior emerges from the olfactory circuit. Chapter 4 summarizes previous chapters and discusses the development of new genetic tools that should aid neural circuit analysis in *Drosophila*. Consistent with the general theme of my graduate research, I particularly emphasize circuit dynamics in *Drosophila* olfactory behavior. The molecular aspect of olfaction and olfactory behavior has been covered in detail in some excellent recent reviews (Keene and Waddell, 2007, Hallem et al., 2006).

Understanding the neural basis of behavior

An important objective of modern neuroscience research is to understand how neural circuits control behavior. To address this problem an investigator needs to

select a behavior, identify individual neurons that are necessary for generating that behavior, assemble these neurons into a meaningful neural circuit and understand the ensemble properties of the circuit that generate the behavior. Such a study is daunting and seems most achievable for behaviors that require simple circuits. Alternatively, one might pick a model organism with a rich repertoire of behaviors but a relatively simple nervous system. The human brain contains ~ 10^{11} neurons and with our very rudimentary current understanding of the neural circuits, it will take a while before we can explain human behavior in terms of defined circuits. *Drosophila melanogaster* on the other hand has 10^5 neurons and we have a rapidly improving anatomical view of the neural circuit detail. Further, despite their relatively small brain fruit flies have a rich behavioral repertoire. The ability to combine those characteristics with electrophysiology and remarkably precise neural circuit intervention provided has led many investigators to fruit flies to investigate the neural basis of behavior. Given the conservation of genes, there is the hope that the underlying principles of neural circuit organization may also be sufficiently similar that this knowledge will be applicable to humans.

I.B. Choosing a behavior: Olfactory behaviors of *Drosophila*

Despite its small size compared to mammals, the *Drosophila* brain orchestrates a diverse array of sophisticated behaviors (Pitman et al., 2009). Olfactory behavior is among the most frequently studied and the relatively simple olfactory neural

circuit of the fly is extremely well characterized. The accessibility of the peripheral olfactory circuitry has allowed researchers to monitor neural activity via electrophysiology and functional imaging. The olfactory system of the fly directs robust odor driven behaviors including a naive attraction to some odors and repulsion to others. Moreover one can assign value to 'behaviorally meaningless' odorants with olfactory conditioning, which allows researchers to study memory related plasticity in the olfactory system. Certain odors might be more meaningful to a fly on different times e.g. hungry flies might be more attracted to food but until our recent work an appreciation for how physiological state affects olfactory-driven behavior was missing. In Chapter IV I will describe the identification of a neural circuit that mediates such state-dependence and allows us to add an element of motivational control to olfactory memory performance. I hope I will be able to convince you that *Drosophila* olfactory system allows one to study all major components of motivated behavior with very high resolution.

I.B. Olfactory conditioning assays: Several assays have been developed to study plasticity in the olfactory system. Most popular of them is classical olfactory conditioning. Two paradigms are commonly used in *Drosophila*.

Olfactory aversive conditioning: The *Drosophila* olfactory memory field took a significant step forward with the development of a classical conditioning assay that involves a binary T-maze choice—from here referred to as the TQ assay

(Tully and Quinn 1985, Figure I.2A) that is performed under dim-red light or darkness. In this paradigm 100 flies are trapped in the training tube that has an electrifiable grid and the experimenter therefore has complete control over shock presentation, intensity and duration. Odors (referred as Conditioned Stimulus or CS) on an air current are piped into the training chamber. Training consists of a 1 minute presentation of an odor (CS+) with twelve one second electric shocks (referred as Unconditioned Stimuli or US) (at 5 second intervals), followed by 30 seconds of fresh air and another 1 minute presentation of a different odor without electric shock (CS-). Odor memory is tested at given times thereafter by transporting flies in the elevator to the T-maze where they are allowed 2 minutes to choose between tubes containing either of the two odorants they experienced during conditioning. A performance index (PI) is then calculated by subtracting the number of flies in the CS- from the number of flies in the CS+ and dividing the result by the total number of flies. A different population of the same genotype of flies is trained with the CS+ and CS- odors reversed and a final performance index is the average of the two reciprocal half experiments (Figure I.3). PI scores using the TQ paradigm can be higher than 0.9 (with a score of 1 representing learning in every fly) but generally range from 0.6–0.9. Memory can either be tested immediately after training (3 minute memory, referred to as ‘learning’ or short-term memory) or the flies can be transferred to food vials and housed until being tested at later time points to assess different memory phases (e.g., middle-term and long-term memory). A single training session does not form persistent memory in the TQ paradigm and performance is essentially absent 24 hr after

training. However, 6–10 training sessions with or without rest intervals forms memory that lasts for days.

Olfactory appetitive conditioning: Although training flies to avoid electric shock is effective, shock is not an ecologically relevant reinforcer. Tempel et al. (1983) described conditioning with odorants and sucrose reward using a variation of the Quinn-Harris-Benzer apparatus (Quinn et al. 1974). They used light (and negative geotaxis) to attract food-deprived flies into a training tube painted with a band of sucrose (US) and odor (CS+). Training consisted of two rounds of a 30 second exposure to odor A (CS-) with no reward, 30 seconds of rest, followed by odor B (CS+) with sucrose reward. Memory was assayed by allowing the flies 15 seconds to choose between the CS+ and CS- odor in a T-maze. Performance scores were calculated by subtracting the number of flies approaching the CS- from the number approaching the CS+, divided by the total number of flies tested. Once again, the final PI score is the average of two reciprocal experiments where the CS+ and CS- odorants are swapped.

Flies have to be hungry to learn and retrieve memory efficiently in the sugar-rewarded paradigm. Tempel et al. (1983) concluded that flies exhibit optimal learning after 19–20 hours of starvation, a treatment that did not affect their intrinsic odor preference or their learning performance in the TQ assay. They also found that sugar reinforced memory persists much longer than shock reinforced memory. Appetitive conditioning is becoming more popular and is now

routinely performed in a TQ-like manner (Keene et al. 2006 and Figure I.2B). The primary difference between shock and sucrose training in the TQ machine is that flies are trained in two separate tubes for appetitive conditioning; one lined with crystallized sucrose on filter paper and one lined with blank filter paper. Using this approach we have recently shown that a single 2-minute pairing of odorant and sucrose forms protein synthesis dependent long-term memory that lasts for days. Extended periods of starvation can confound the appetitive paradigm. However, it is possible to extend the use of the assay to two-three days following a single session of training by feeding the flies after training and re-starving them before testing memory (Krashes and Waddell, 2008).

IC. The circuit that drives the behavior: Anatomy of *Drosophila* olfactory system

Olfactory Receptor Neurons (ORNs): The anatomy of the *Drosophila* olfactory system has been studied in detail (Keller et al., 2003, Hallem et al. 2006 and Figure I.4). *Drosophila* olfactory receptor neurons (ORNs) (also known as olfactory sensory neurons) are housed in sensory hairs or sensilla on either of two sets of fly olfactory organs, the antennae and maxillary palps. Most ORNs co-express a single odor-responsive olfactory receptor (OR) gene with an obligate dimerization partner encoded by the OR83b gene (Larsson et al., 2004, Benton et al., 2006, Sato et al., 2008, Benton et al., 2009) (see chapter II for more detail on Or83b and Or83b-independent ORNs). OR83b is required for OR

dendritic targeting and stability (Larsson et al., 2004, Benton et al., 2006, Sato et al., 2008, Wicher et al., 2009) and together the different OR/OR83b dimers form odor-gated ion channels (Sato et al., 2008, Wicher et al., 2008). OR-containing ion channels reside in the dendritic membrane of the ORN. Each ORN extends a single axon that synapses with second-order neurons in the antennal lobe. The antennal lobes of *Drosophila* are divided into spatially distinct spherical substructures of neuropil called glomeruli and ORNs that express the same OR gene project their axons to the same glomerulus (Vosshall et al., 2000, de Bruyne et al., 2001, Dobritsa et al., 2003, Goldman et al., 2005, Hallem et al., 2006). Glomeruli contain at least four distinct classes of neurons; ORNs which carry odorant information into the antennal lobe, Projection Neuron (PNs) which carry odorant information from the antennal lobe to higher order brain centers (Figure I.4) and inhibitory and excitatory local interneurons, (Tanaka et al., 2009, Shang et. al., 2007, Wilson et al., 2005, Stopfer et al., 1997).

Local Interneurons (LNs): Both excitatory cholinergic local interneurons (Shang et al., 2007) and inhibitory GABAergic local neurons (Tanaka et al., 2009, Okada et al., 2009) project to multiple glomeruli and are believed to be involved in gain-control and oscillatory synchronization of the olfactory response. Recent studies reported morphological and functional subdivision among inhibitory local neurons (Tanaka et al., 2009) but such subdivision has yet to be reported excitatory local interneurons.

Projection neurons (PNs): Each glomerulus is innervated by multiple PNs but the dendrites from each PN exclusively synapse in only one glomerulus. There are about 150 PNs associated with about 50 glomeruli. PNs carry the odorant information to two distinct anatomical regions in the fly brain, the mushroom body and lateral horn. PNs project their axons to these regions through three axonal tracts (Tanaka et al., 2004, Jefferis et al. 2007, Lin et al. 2007 and Figure I.4B). Most of the PNs follow the inner antennocerebral tract (iACT) and project to the mushroom body calyx and the lateral horn. Few PNs send their axon along either the medial (mACT) or the outer (oACT) antennocerebral tracts and these bypasses the mushroom body and directly innervate the lateral horn. Detailed anatomical analysis has determined that most glomeruli are innervated by 3 PNs and these PNs are usually morphologically similar in their projection patterns. However, there are a few exceptions to this rule. For example, two separate PN types innervate the VA1lm glomerulus. One type follows the mACT tract, bypassing the mushroom body and projecting to the lateral horn, whereas the other type follows the iACT and arborizes in both MB and LH (Jefferis et al. 2007). However, the functional significance of this type of innervation is still unclear. A less understood PN class has multiglomerular dendrites and sends their axons along the mACT to the lateral horn (Lai et al., 2008).

Lateral horns (LH): Not much is known about the morphology of *Drosophila* LH neurons. In the locust, GABAergic projections from the LH provide inhibitory input to the MB (Jortner et al. 2007, Perez-Orive et al., 2002). In *Drosophila*

morphologically diverse groups of neurons innervate LH but feedback neurons from the LH to the MB, like the locust lateral horn inhibitory neurons, have not been reported.

Mushroom bodies (MB): The Mushroom bodies are amongst the most extensively studied structures in insect neurobiology. The general anatomy of the mushroom body can be subdivided into three parts, the calyx, peduncle, and lobes (Figure I.5). Mushroom body neurons, also known as Kenyon Cells (KCs), have their cell bodies localized in the dorsal-posterior part of the *Drosophila* brain. *Drosophila* has approximately 2,500 KCs in each mushroom body. Kenyon cells extend their dendrites in the calyx and their neurites then project down through the brain as a bundle called the peduncle. The peduncle projects to the anterior part of the brain where the individual KCs branch to form at least five anatomically distinct lobes; two vertical lobes known as α and α' lobes and three horizontal lobes, named β, β' and γ (Crittenden et al., 1998, Tanaka et al., 2008 and Figure I.5). The *Drosophila* KC population can be subdivided into at least three subtypes based on their morphology, developmental timing and gene expression patterns. The γ neurons only project to γ lobes of the mushroom body and are formed during the mid-larval stage. In larval stage, they are bifurcated and form two lobes. During metamorphosis they undergo significant pruning and transformation, which results in the formation of a single horizontal γ projection in adult flies. The $\alpha'\beta'$ neurons bifurcate at the anterior pedunculus and one branch projects vertically into the α' lobe and the other horizontally into the β' lobe.

Similarly, αβ neurons bifurcate and send one projection into the α lobe and the other into the β lobe (Lee et al., 1999; Zhu et al., 2003). It is unclear whether the different KCs are preferentially connected to particular PNs. The dendrites of the γ neurons preferentially occupy the center of the calyx whereas dendrites of the other types of KCs are more widespread across the calyx (Tanaka et al., 2004, Jefferis et al., 2007). However a recent report indicated more stereotyped projections of KC dendrites within the calyx (Lin et al., 2007).

Mushroom body extrinsic neurons: A large number of neurons project onto the MB (for a recent description, see Tanaka et al., 2008). However, only a few have been shown to be involved in olfactory processing, like the dorsal paired medial (DPM) neurons, the anterior paired lateral (APL) neurons, dopaminergic neurons and octopaminergic neurons. DPM neurons are a pair of neurons that arborize in all the MB lobes. They express the *amnesiac* gene, which encodes a putative neuropeptide (Waddell et al., 2000) and they may use acetylcholine (Keene et al., 2004) as a co-transmitter. APL neurons are a pair of GABAergic neurons with cell bodies localized in the anterior-lateral protocerebrum (Liu and Davis, 2009). Like DPM neurons, APL neurons project onto all MB lobes and in addition they innervate the entire peduncle and calyx. Dopaminergic neurons arborize extensively throughout the brain (Friggi-Grelin et al., 2003 and Figure I.10) and different subsets of dopaminergic neurons innervate discrete regions of the MB including the calyx, peduncle and different regions of the MB lobes. A detailed description of some of these dopaminergic neurons is provided in

chapter III. Like dopaminergic neurons, octopaminergic neurons form arborizations in the MB lobes and calyx (Sinakevitch et al., 2006 and Figure I.11). However the MB lobe innervation by these neurons is much sparser than that of dopaminergic neurons. Conversely, the antennal lobes are almost devoid of dopaminergic projections but are densely innervated by octopaminergic neurons (Sinakevitch et al., 2006 and Figure I.11).

PN-Third order neuron connectivity: The anatomical organization of PN synapses in the MB and LH has recently been investigated in great detail (Tanaka et al., 2004, Jefferis et al. 2007, Lin et al. 2007). PN projection data from 32 out of ~50 PN classes is now available. PN termini in the lateral horn are organized into distinct zones with the same classes of PNs projecting to the same region of the LH. PNs responding principally to fruit odors project to the posterior-dorsal part of the LH whereas PNs responding to pheromones project to the anterior-ventral region. Sexual dimorphism among the PN projection patterns in the LH has also been reported. The anatomy of LH output neurons has not been described in detail, although there are some indications that LH neurons may maintain the proposed segregation between fruit odor and pheromone information (Tanaka et al., 2004, Jefferis et al. 2007, Lin et al., 2007).

The organization of PN synapses in the mushroom body calyx is significantly different. PN synapses in the calyx can be sub-divided into 3 regions with PNs carrying pheromone information being separated from other PNs.

However, there is no obvious zonal segregation between the non-pheromone PN termini in the calyx (Tanaka et al., 2004, Jefferis et al., 2007, Lin et al., 2007).

Even with our current understanding of the anatomy, we only have a partial picture of the olfactory circuit. It is still unclear how motor centers are connected with the MB and LH. Moreover a synaptic connectivity map is still lacking. Development of trans-synaptic tracers and EM reconstruction of fly brain will provide a more detailed understanding of how neurons are connected in the olfactory circuit.

ID. Stimulus-response properties of the circuit: Dynamics of odor coding

Tremendous progress has been made in the last two decade towards understanding how neurons in the olfactory circuit respond to odors. There are two prevalent theories on how odor information is translated by the olfactory circuit; labeled-line theory and spatiotemporal coding theory. In next few paragraphs I will describe how different groups of neurons within the olfactory circuit responds to odors and point out the differences between the theories.

ORN responses: Olfactory receptors vary greatly in the number of odors they respond to. While some receptors respond to many odorants (receptors with wide tuning curves or odor generalists), others respond to one or very few odorants (receptors with narrow tuning curves or odor specialists) (Hallem et al.,

2006; Hallem et al., 2004). However, there is no clear dichotomy between specialist and generalist ORNs in terms of their tuning curves (Hallem et al., 2006). Rather a continuum of tuning breadths is observed among receptors. Specialist and generalist receptors occupy the ends of this spectrum. The temporal responses of ORNs to different odorants are highly diverse (Hallem et al., 2006). A given ORN can be activated or inactivated or not respond to different odorants and the same odorant evokes discrete patterns of responses in distinct classes of ORNs. The temporal patterns of odorant-evoked activities in ORNs are also highly varied and the information content of these temporal patterns is unclear (Hallem et al., 2006). While labeled-line theory postulates that odors are coded by simple activation/inactivation of ORNs (i.e., a binary code), spatiotemporal coding theory incorporates the coding capacity of odor-induced temporal dynamics of ORNs. Although there is obvious capacity of coding in this rich diversity of temporal responses, the information content remains unclear.

PN responses: How ORN responses are translated in the antennal lobe is a hotly debated issue. A receptor-glomerulus map is available for 44 ORs (Couto et al., 2005; Fishilevich et al., 2005) and a recent study has reported the responses of 24 ORs to a diverse collection of 110 odorants (Hallem et al., 2006). These studies indicate that each odorant has a unique pattern of ORN activation that will vary with concentration. Due to the ORN organization in the AL, these combinatorial activation patterns are represented in the antennal lobe glomeruli. The odortopy present in the AL suggests a mechanism of odor coding that

utilizes spatial patterns of glomerular activation to represent an odorant (Figure I.6). When an odorant binds to a specific subset of receptors, the binding in turn activates a specific subset of glomeruli and functional imaging data shows this pattern of glomerular activation is highly odor-specific and stereotyped in *Drosophila* (Ng et al., 2002; Wang et al., 2003). Moreover, functional imaging studies indicated that PN responses might arise from linear relay of ORN inputs supporting a labeled-line theory of odor coding in which odor quality is encoded by activation/inactivation of specific combinations of neurons though successive layers of the olfactory circuit (Ng et al., 2002; Wang et al., 2003) (Figure I.6).

An alternative model of odor coding has emerged from electrophysiological studies of odor-evoked responses in ORN and PN (Laurent et al., 1996, Wehr et al., 1996, Stopfer et al., 2003, Mazor et al., 2005, Tanaka et al., 2009, and Figure I.7). Electrophysiological recordings from PNs have indicated that a given odorant can produce excitatory responses in ~69% of PNs (Wilson et al., 2004). By directly comparing presynaptic and postsynaptic tuning curves corresponding to the DM2 glomerulus, Wilson et al. (2004) reported that PNs can be even more broadly tuned than their presynaptic ORN input. Lateral connectivity involving LNs within the antennal lobe facilitate PN populations to integrate information across different ORN information channels, despite their principally uniglomerular dendritic fields (Wilson et al., 2005, Shang et al., 2007, Tanaka et al., 2009). These data along with the studies on other insects support a model in which odor information is encoded by spatiotemporal activation

patterns in the PN ensemble (Laurent et al., 1996). Furthermore, odorants evoke a subthreshold oscillation in the local field potential of PNs and specific PNs fire axon potentials at different phases of this oscillatory cycle. These oscillatory-synchronized activities of PNs are believed to be a key component in encoding odor identity (Laurent et al., 1996 and Figure I.7).

Local neuron responses: Both theories of odor coding have started to recognize the role of local neurons in odor coding. The excitatory local interneurons are very broadly tuned to odors, innervate most, if not all glomeruli in the antennal lobe, and show little glomerular specificity in their synaptic output. It has been proposed that excitatory local interneurons add a diffuse excitatory offset to PN signals to amplify weak signals (Shang et al., 2007). A recent study has shown inhibitory local interneurons can be sub-divided into two classes. One class of inhibitory local interneurons (LN1) primarily arborize in the glomerular regions rich in ORN termini whereas the other class (LN2) of iLN synpses are presynaptic to PN dendrites (Tanaka et al., 2009). Several studies have shown inhibitory local interneurons prevent hyperactivation of PNs in the presence of strong ORN input (Root et al., 2008, Kazama et al., 2008). Tanaka et al. (2009) has recently demonstrated that in *Drosophila*, LN2 are responsible for the generation of odor-evoked oscillatory synchronization of PNs.

Third order neuron responses: How *Drosophila* LH neurons respond to odorants is still unknown. However studies from other insects, locusts in

particular, suggests LH output neurons shape MB responses to odors via inhibitory coupling (Perez-Orive et al., 2002, Jortner et al., 2007 and Figure I.7). KCs typically receive synaptic input from 10-50 % of all receptor channels (Jefferis et al. 2007), but their high firing thresholds ensure that each cell responds only to combinations of simultaneously active afferents (Perez-Orive et al., 2002, Jortner et al., 2007, Murthy et al., 2008, Turner et al., 2008). Patterns of receptor activation are thus compressed into synthetic, high-level features. This mechanism of feature extraction makes the system less prone to false-positive detection. It is unclear whether odorants are represented by combinatorial activation of KCs. Beautiful electrophysiological studies in the locust MB have shown that odorants are represented by evolving temporal patterns of KC activity (Figure I.7) and output from LH neurons and short-lived spike-time dependent plasticity in some mushroom body extrinsic neurons are required for establishing this response. Functional imaging studies using Ca^{2+} sensitive dyes or transgenic Ca^{2}+ indicators demonstrated sparse and distinct patterns of KCs are activated by specific odorants (Wang et al., 2003, Wang et al., 2004). However, the poor spatial and temporal resolution of these reporters prevented more detailed characterization of the responses (Jayaraman et al., 2007). A recent electrophysiological study has demonstrated that KC responses to odorants are not stereotyped at the level of individual KCs (Murthy et al., 2008), consistent with the conclusions drawn form studies in the locust (Mazor et al., 2005). Decorrelation of ORN inputs in the antennal lobe and subsequent

synthetic coding in MB population alleviates the requirement of having a stereotyped odor-code in the MB.

In spite of our detailed knowledge of the structural organization of the olfactory system, the mechanism of odor perception and discrimination has remained elusive. The spatiotemporal nature of olfactory responses is not unique to insects and is also observed in mammals (for review see Wilson and Mainen, 2006). It is still unclear how imaging and electrophysiological data can be correlated to behavior (In chapter II, I will demonstrate the importance of temporal dynamics in learned odor discrimination). Whereas anatomical and functional imaging data point towards a labeled-line like organization in the olfactory system, behavior and electrophysiological studies have demonstrated an important role of odor-evoked temporal dynamics in odor coding. It is possible the true scenario lies somewhere in-between where temporal dynamics within chemotopically/perceptually separated channels encode odorant identity. Notably studies in the honeybee olfactory system indicate disruption of oscillatory synchronization is detrimental towards discrimination of chemically similar odorants but does not affect discrimination between dissimilar odorants (Stopfer et al., 1997).

IE. Memory formation within the circuit: Olfactory memory of *Drosophila*

Behavioral versus cellular memory

Two distinct approaches are used to study memory; monitoring experience dependent changes in behaviors (behavioral plasticity) and monitoring changes in neural circuits based on stimulus exposure (cellular plasticity). Landmark studies on *Aplysia* defined changes in synaptic strength as the mechanism of storing associative memory (Castellucci and Kandel, 1976). Stability of the memory depends on the stability of the changes in synapses. Long-lived changes involve morphological remodeling of the synapses, require protein synthesis and the memory lasts for days; these referred to as long-term memories. A less stable form of memory is referred to as short-term memory that does not requires protein synthesis or morphological changes at synapses. All memories usually pass through a labile phase before being processed into more stable short/long term memories. Current models of *Drosophila* memory incorporate changes in synaptic strength as the mode for memory storage. Different models propose different anatomical regions and molecules involved in this process. In this section I will describe the proposed mechanisms and models of how memory related changes occur in the olfactory circuit. However it is important to note that the relationship between behavioral and cellular approaches is still unclear. Studies on *Aplysia* first demonstrated a direct correlation between cellular and behavioral plasticity, where quantifiable changes in synaptic strength lead to changes in behavioral response (Castellucci and Kandel, 1976). Numerous studies point toward necessity of synaptic changes for memory formation, establishing strong correlation between cellular and

behavioral plasticity. However until we can artificially create memory in specific synapses and demonstrate behavioral memory expression, the relationship between cellular and behavioral plasticity will remain, at best, correlative.

Memory genes and processes: The memory formed after single-trial aversive conditioning lasts for hours, does not require protein synthesis and can be divided into three phases- short-term memory, middle-term memory and anesthesia-resistant memory (ARM) (Quinn et al., 1979, Quinn and Dudai, 1976). Long-term olfactory memory (LTM) can be formed either by single trial appetitive conditioning (Krashes et al., 2008) or by multiple trial aversive conditioning (Folkers et al., 1993, Tully et al., 1994). LTM can last for days and requires protein synthesis (Tully et al., 1994). Mutant analysis studies have identified a large number of memory-associated genes, most notable of which are members of the cAMP signaling cascade like *rutabaga (rut)* (Livingstone et al., 1984, Levin et al., 1992). RUT is an adenylyl cyclase and it has a high level of expression in the mushroom body (Han et al., 1992). Memory defects of *rut* mutants can be rescued by expressing an UAS-*rut* transgene in the mushroom body of adult flies, demonstrating RUT function in MB is sufficient for memory and the *rut* phenotype does not result from developmental defects (Zars et al., 2000; McGuire et al., 2003; Mao et al., 2004 and Figure I.8). The current model of olfactory memory formation postulates that odor-evoked PN activity increases Ca^{2+} concentration in odor-specific KCs whereas shock/sugar stimuli activate G-protein coupled receptors (GPCRs) (Connolly et al. 1996) throughout MB. In KCs

where Ca^{2+} influx coincides with GPCR activation, RUT adenylyl cyclase is activated resulting in a synergistic increase in cellular cAMP concentration. Stability of memory depends on the duration of the cAMP surge. A prolonged increase in cAMP concentration results in formation of LTM via activation of cAMP-response-element-binding protein (CREB) (Yin et al., 1994, Yin et al., 1995, Perazzona et al., 2004). This model is supported by data from flies carrying mutations in genes associated with cAMP signaling like *dnc* (a cAMP phosphodiesterase) (Byers et al., 1981, Chen et al., 1986) and *DC0* (catalytic subunit of protein kinase A) (Skoulakis et al., 1993) which cause memory phenotypes indicating an important role of cAMP signaling in olfactory memory formation (reviewed in Keene and Waddell 2007, Figure I.8 and I.12).

Even after identification of more than 60 'memory genes' our understanding of the molecular pathways of olfactory memory formation remains rudimentary. It is unclear how these genes are related to neural circuit function. Some of these memory genes have already been implicated in other cognitive processes like attention (van Swinderen, 2007). It is also unclear whether expression of 'memory genes' in the MB is necessary for memory formation. Furthermore, it is unknown whether all memory genes function in the same cells the way depicted in most *Aplysia*-inspired models of *Drosophila* olfactory learning. I therefore believe that a circuit-oriented analysis of olfactory memory is essential to understand how olfactory memories are stored and retrieved in fly brain.

IF. How the circuit stores new information: Circuit dynamics of olfactory memory processing

To understand how memories are encoded in the brain, it is essential to understand how the neural circuit changes with memory formation. Several studies have investigated conditioning-induced plasticity in different parts of the olfactory circuit. An early functional imaging study identified short-lived plasticity in the antennal lobes (Yu et al., 2004) by imaging PN responses to odorants using synaptophluorin to monitor synaptic release (Miesenböck et al., 1998). The number of glomeruli responding to an odorant was seen to increase after presenting flies odorants in conjunction with electric shock. It was proposed that this plasticity contributes to memory formation immediately after training (Yu et al., 2004). Two behavior studies have also implicated the antennal lobe as a site for memory related plasticity. Thum et al. (2007) reported the PNs are a sufficient site for RUT-dependent plasticity for appetitive memory formation. Ashraf et al. (2006) demonstrated that aversive long-term memory formation is correlated with a change in level of Ca^{2+}/calmodulin-dependent kinase II (CaMKII) protein in the AL and postulated that synaptic protein synthesis in PNs is required for LTM formation.

All current models favor the MB as the site for CS-US association. Behavioral studies have demonstrated a requirement for the MB in olfactory learning. Mutant analysis and MB ablation studies have shown that the MB is required for olfactory learning whereas flies innate responses to odors appear to be MB-independent. This led to the hypothesis that the LH mediates innate olfactory behavior whereas MB is involved in mediating learned behavior (Heimbeck et al., 2001). However one study claimed MB output is required for innate odor attraction, but not for innate odor repulsion (Wang et al., 2003). More evidence supporting involvement of the MB in olfactory memory came from studies blocking MB output during different stages of memory processing. A temperature sensitive dominant mutant form of dynamin ,*Shi*^{ts1} (Kitamoto 2001), was used in these studies to block KC output. At high temperature (the restrictive temperature), this dominant mutant form of dynamin blocks neuronal output by inhibiting synaptic vesicle recycling. Using this approach several studies have implicated MB as the storage site for olfactory memory (Dubnau et al., 2001, McGuire et al., 2001, Schwaerzel et al., 2002 and Davis, 2005). Recently, using a similar approach, Krashes et al. (2007) demonstrated a differential requirement of the different MB neurons at different stages of aversive and appetitive olfactory memory processing. Output from the $\alpha'\beta'$ neurons is required for memory acquisition and consolidation whereas $\alpha\beta$ lobe output is exclusively required for memory retrieval. Since $\alpha\beta$ lobe output is required only during memory retrieval, current dogma implicates the α and β lobes as the storage site for appetitive and aversive olfactory memory (Yu et al., 2006, Krashes et al., 2007, Krashes and

Waddell, 2008 and Figure I.12). Mutant studies also implicated the mushroom body as the site for olfactory memory storage. Adult-restricted, MB-specific rescue of the putative coincidence detector encoded by *rutabaga* rescues the olfactory memory phenotype of *rut* mutant flies (McGuire et al., 2003; Mao et al., 2004) suggesting CS and US information is integrated in the MB. In support of behavioral studies, functional imaging studies observed increases in Ca^{2+} release in the α lobe tips following CS-US coupling that is sufficient for LTM formation (Yu et al., 2006). However it is still unclear how increased synaptic strength is correlated with increased Ca^{2+} release, as observed in functional imaging studies.

MB extrinsic neurons play a critical role in memory processes. Output from DPM neurons is required for memory consolidation. Blocking DPM neuron output using *shi*^{ts1} during consolidation abolishes both appetitive and aversive memory (Waddell et al., 2000, Keene et al., 2004, Keene et al., 2006; Krashes and Waddell, 2008). A functional imaging study found that DPM neurons respond to both shock and odorants stimuli used in conditioning. An odorant-specific enhancement of the odor-evoked response was detected in DPM neurons following the CS-US pairing and this conditioned response occurred during the same time period in which blocking DPM output impairs memory (Yu et al. 2005). Unlike DPM neurons, APL neurons are believed to be involved in suppressing olfactory learning; inhibiting GABA synthesis in APL neurons enhances olfactory learning. A functional imaging study found that like DPM neurons, APL neurons

are also activated by shock and odorants. However CS-US pairing reduces the APL neuron's response to conditioned odorants, implicating that olfactory learning involved suppressing output of these neurons in an odor specific manner (Liu and Davis, 2009).

Delivery of US information to the MB: Since the MB is regarded as the site for coincidence detection during classical olfactory conditioning, it is reasonable to assume CS and US circuits intersect at the MB. Dopamine and octopamine systems are believed to mediate reinforcement and play critical roles in delivering US information to the MB (Schwaerzel et al., 2003).

Electric-shock stimulus: It is still unclear whether a specific sensory mechanism is involved in electric-shock perception. Functional imaging studies with Ca^{2+} reporters have yielded conflicting results. Using the ratiometric Ca^{2+} sensor Chameleon, Riemensperger et al. (2005) reported that electric shock specifically depolarizes dopaminergic neurons (Riemensperger et al., 2005) whereas several other studies have observed widespread depolarization in response to electric shock (Yu et al., 2005, Yu et al., 2006, Liu and Davis 2009). Regardless of this inconsistency, both behavior and imaging studies have established the importance of the dopaminergic system in aversive memory formation. Tyrosine hydroxylase (TH) is a key enzyme for dopamine synthesis (Figure I.9) and a TH-GAL4 line has been generated fusing the TH promoter with GAL4 coding sequence. TH-GAL4 is specifically expressed in dopaminergic

neurons in *Drosophila*. Using TH-GAL4; uas-*Shi*^{ts1} combination to silence dopaminergic neurons, Schwaerzel et al. (2003) demonstrated that output from dopaminergic neurons is required for aversive memory formation but not for appetitive memory formation, indicating negative reinforcement requires dopaminergic neurons (Schwaerzel et al., 2003). In support of this hypothesis, a study of *Drosophila* larval olfactory learning has demonstrated that artificial activation of dopaminergic neurons during odor presentation is sufficient to form aversive olfactory memory (Schroll et al., 2006). Imaging studies noted that dopaminergic projections on the MB lobes are strongly activated by electric shock but weakly activated by odorants. Moreover the response to the conditioned odorant is significantly prolonged after CS-US coupling (Riemensperger et al., 2005). This last observation indicates that like mammals, *Drosophila* dopaminergic neurons are possibly providing predictive value to the conditioned stimulus. *Drosophila* have several subtypes of dopaminergic neurons and it is still unclear which are relevant for memory formation; MB projecting subtypes are the most likely candidates.

Sugar stimulus: Sugar is sensed by gustatory receptor neurons (GRNs) located on the tarsae, the proboscis and in internal mouthparts of *Drosophila* (Scott et al., 2001, Wang et al., 2004, Thorne et al., 2005, Marella et al., 2006, Dahanukar et al., 2007). These neurons project their axons to the subesophageal ganglion (SOG) of the brain where they are believed to interact with modulatory neurons. Octopaminergic neurons are believed to be the modulatory system that carries

the reinforcing effects of sugar to the MB in appetitive conditioning. Octopaminergic neurons (Sinakevitch et al., 2006) arborize in the SOG where they possibly receive direct input from GRNs. These neurons project extensively in the antennal lobe, MB and LH and therefore can potentially interact with the olfactory circuit. The role for such octopaminergic VUMmx1 neurons in appetitive conditioning was first demonstrated in honeybees where it was shown that electrical stimulation of VUMmx1 could replace the presentation of sucrose (Hammer et al., 1993). The TβH gene encodes an enzyme essential for octopamine synthesis (Figure I.9) and studies with TβH mutant flies revealed that TβH function is necessary for appetitive memory, but not for aversive memory formation (Schwaerzel et al., 2003). The memory defect of TβH mutant flies can be rescued either by feeding octopamine prior to training or by induction of a heat-shock promoter driven transgene; indicating octopamine acts acutely in appetitive conditioning (Schwaerzel et al., 2003). Consistent with this hypothesis, Schroll et al. (2006) demonstrated that artificial activation of tyraminergic and octopaminergic neurons during odor presentation can produce appetitive memory in larvae. Therefore it seems likely that octopaminergic neurons carry the US information to the MB.

How does MB output drive behavior? It is still unclear how MB output drives motor behavior. An anatomical structure called the central complex is believed to be the motor control center of *Drosophlila*. Mutants with developmental defects in CC are defective in locomotor behaviors (Strauss and Heisenberg 1993). Thus it

has been postulated that MB is directly or indirectly connected to the central complex. However no such connection has yet been reported in *Drosophila*.

Studies in locusts have indentified neurons postsynaptic to KCs but none of these project to the central complex. A recent study described a morphologically varied collection of MB extrinsic neurons in *Drosophila* (Tanaka et al., 2008). However the functional properties of these neurons remain to be tested.

IG. A circuit mechanism for memory storage

All *Drosophila* memory models, like the one described in Figure I.12 use coincidence detection at the mushroom body as the mechanism behind storing olfactory memory. A coincidence-based form of memory storage was first proposed by Donald Hebb (1949) who argued that learning involve coincident synaptic activation of neurons. These types of learning with 'Hebbian synapses', shown to exist in *Aplysia* (Antonov et al., 2003), have been proposed in many systems (Mayford et al., 1996, Tsien et al., 1996, Rogan et al., 1997, Oda et al., 1998, Tsvetkov et al., 2002) including insect olfactory system (for reviews see Keene and Waddell, 2007, Davis, 2005, Heisenberg, 2003). One such study examined transmission and plasticity between the synapse made by Kenyon cells onto one of the KC downstream target β-lobe neurons, using intracellular recordings. These synapses are strong and excitatory and display short-lived Hebbian spike-timing dependent plasticity (STDP) (Cassenaer and Laurent 2007). The authors postulated that this form of STDP enhances the

synchronization between the KCs and their targets and thereby helps to preserve the propagation of the odor-specific codes through the olfactory system. However a recent study on the moth *Manduca sexta* has found that odor-induced spiking in KCs cells can occur well before the US is delivered, indicating a non-Hebbian mechanism of memory formation (Ito et al., 2008). It is important to note that memory-associated changes in KCs (or in other parts of olfactory network) have not yet been demonstrated convincingly. It is unclear whether memory formation involves changes in specific synapses, like the one between KCs and yet to be identified fourth-order neuron, or a more global system-wide change is involved. If memory formation indeed involves a network-wide change, detecting such changes might prove extremely difficult because to our current inability to detect a population-wide neural communication with good spatiotemporal resolution. On the other hand, if olfactory memory is indeed stored form of changes in specific KC-output neuron synapse, identification of MB output neurons will allow direct testing of the hypothesis. To complicate matters further, in chapter III, I will add an additional element to the olfactory behavior; motivational control of olfactory memory performance. All these possibilities will keep *Drosophila* as an exciting model to study behavior systems for years to come.

Figure I.1

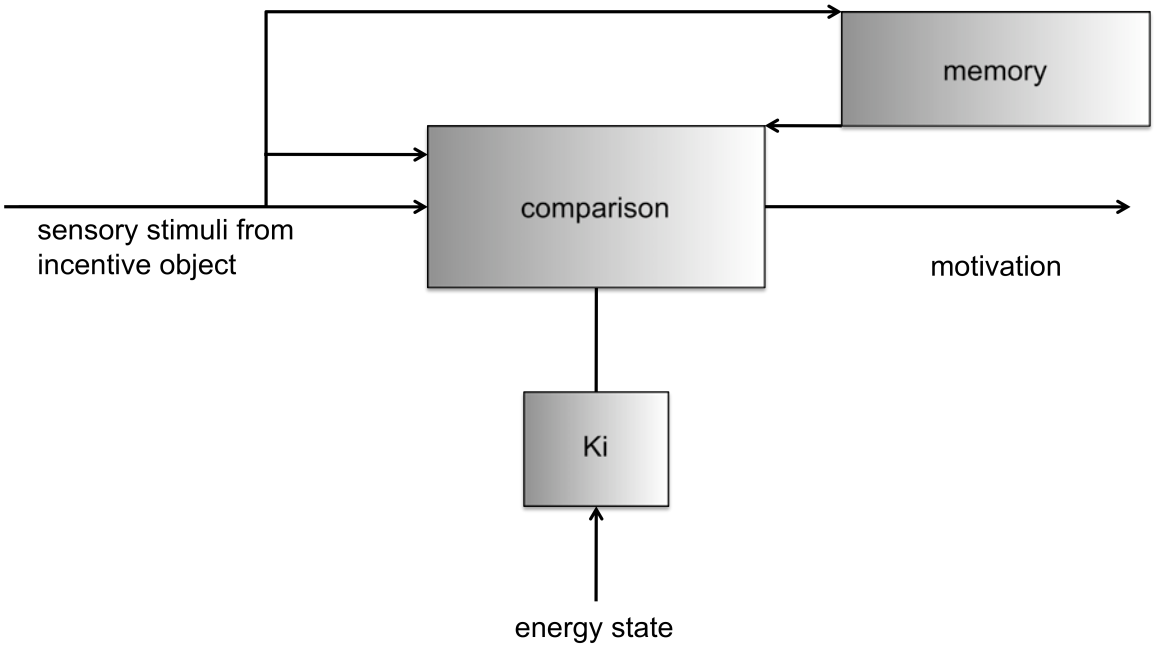

Figure I.1. A simple model for motivation. Motivated behavior was proposed to emerge from integration of sensory information, memories and internal states. Sensory information from incentive objects, like food impinge upon the nervous system. Internal states, such as nutritional state in the case of feeding, sensitizes the nervous system and makes it responsive to the sensory incentive. The term Ki, represents the 'gain' or 'sensitivity' of the system. Sensory stimuli revive a memory of past experience of the stimulus in question. If the integration is positive Ki will be relatively high and motivated behavior will be displayed. If the integration is negative, Ki will be low, and the system will either show no response or display active avoidance to the substance. (Adapted from Toates,1986).

Figure I.2

A.

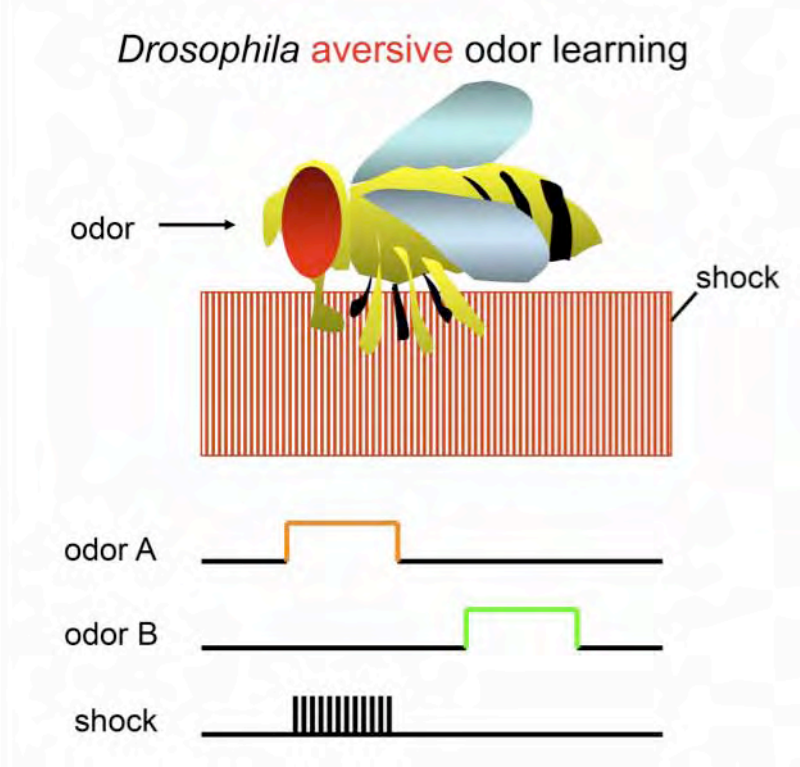
Drosophila aversive odor learning
odor
shock
odor A
odor B
shock

B.

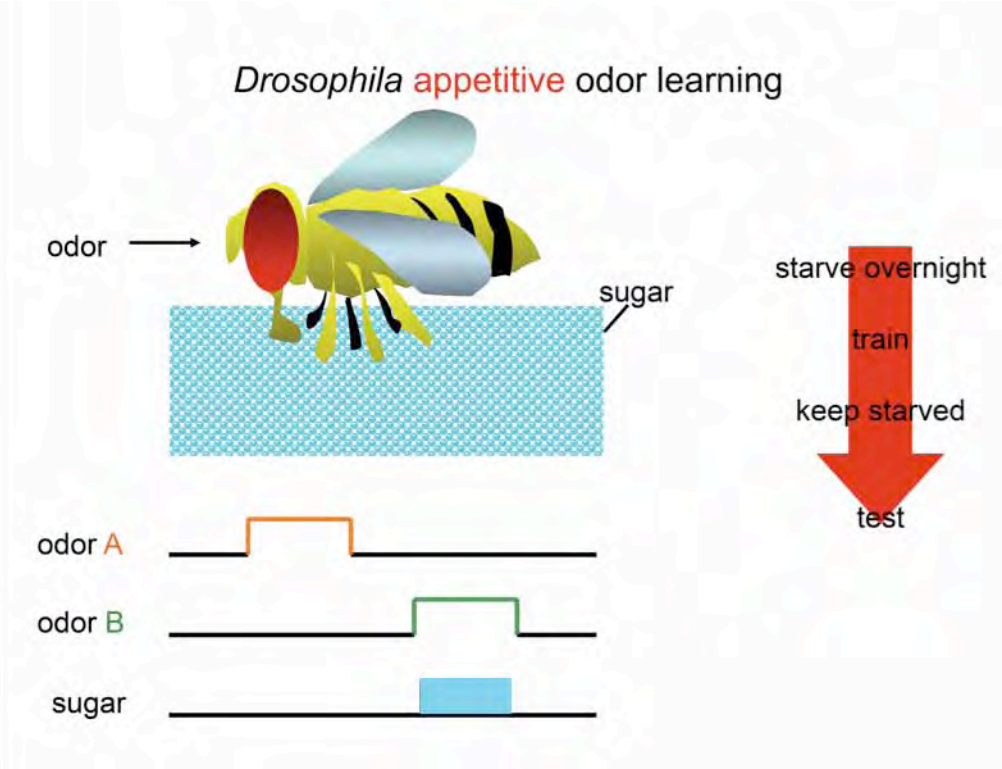
Drosophila appetitive odor learning
odor
sugar
starve overnight
train
keep starved
test
odor A
odor B
sugar

Figure I.2. Olfactory conditioning-Training. (A) Aversive conditioning paradigm. Flies are exposed to one odor for 1 minute coincident with 12 electric shock followed by 30 second of clean air. They then receive the second odor for 1 min without electric shock. **(B)** Appetitive conditioning paradigm. Starved flies are given one odor alone for 2min followed by a 30 second exposure to clean air. Then they receive the second odor with sugar to form an appetitive odor memory

Figure I.3

A.

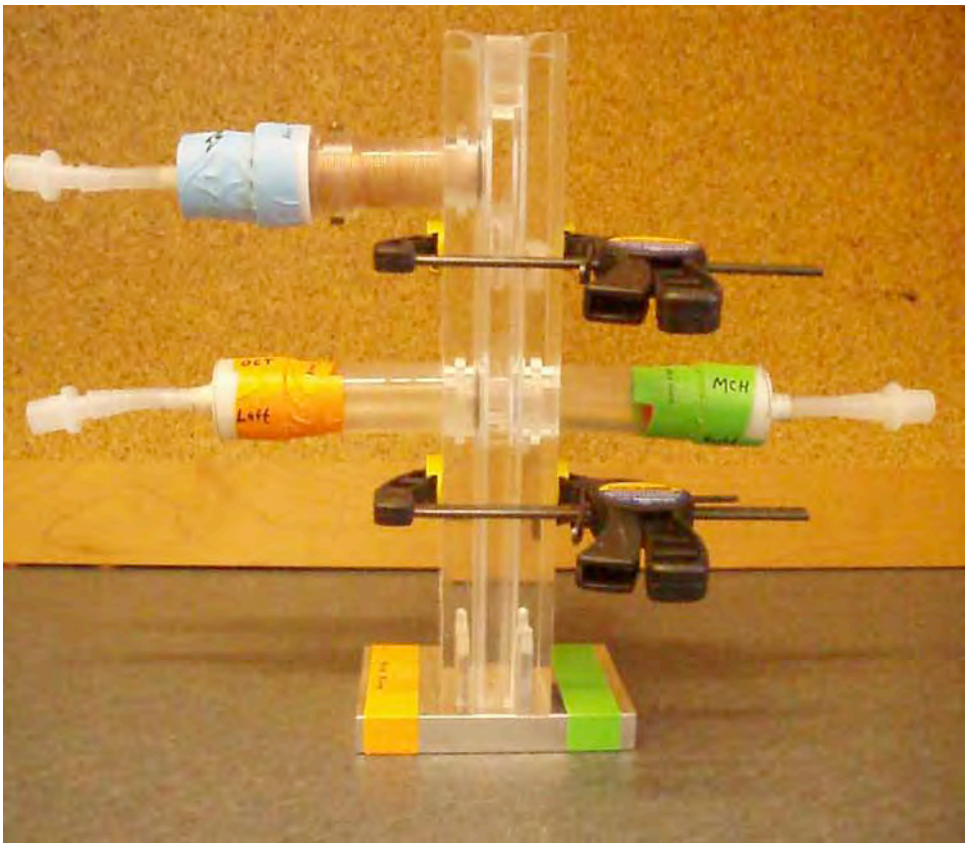

B.

$$\frac{\text{\# odor B (70) - \# odor A (30)}}{\text{total \# of flies (100)}}$$

Performance Index = 0.4

Figure I.3. Testing aversive olfactory learning/memory in a T-maze. (A) After training, flies are transported to a t-maze where they are allowed to choose between two odors they experienced during training. Naïve flies distribute equally between two arms of the maze whereas trained flies run away from the shock-associated odor. **(B)** A performance index is then calculated as the number of flies avoiding the shock-associated odor minus the number of flies going towards it, divided by the total number of flies. The assay is reciprocal and a different population of flies of the same genotype is trained to associate the other odor with shock. The final score is an average of two reciprocal half experiments. Thus, to show any performance in this assay, flies have to be able to associate the both odorants with shock.

Figure I.4

A.

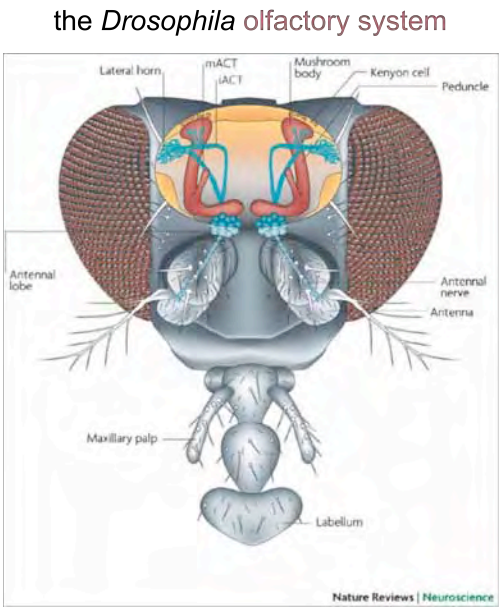
the *Drosophila* olfactory system
Lateral horn
mACT
iACT
Mushroom body
Kenyon cell
Peduncle
Antennal lobe
Antennal nerve
Antenna
Maxillary palp
Labellum
Nature Reviews | Neuroscience

B.

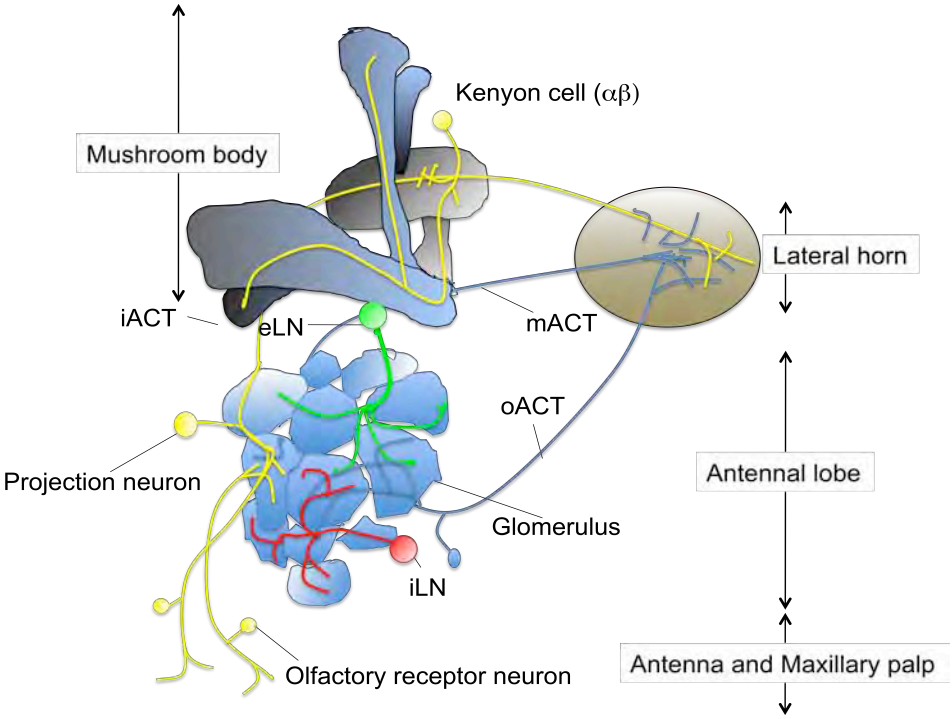
Kenyon cell (αβ)
Mushroom body
Lateral horn
iACT
eLN
mACT
oACT
Projection neuron
Antennal lobe
Glomerulus
iLN
Olfactory receptor neuron
Antenna and Maxillary palp

Figure I.4. *Drosophila melanogaster* olfactory circuit. (A) Cartoon *Drosophila melanogaster* head: Dorsal view of a cutaway fly head showing the main elements of the olfactory pathway. Odors are sensed by olfactory receptor neurons in the antennae and maxillary palps. These neurons project axons along the antennal nerve to the antennal lobe glomeruli, where they are sorted according to chemosensitivity. From there, the information is relayed by projection neurons in the inner and medial antennocerebral tract (iACT and mACT) to the mushroom body and to the lateral horn. Gustatory stimuli are sensed by gustatory receptor neurons in the labellum on the tip of the proboscis, the elongated fly mouthpiece. (Reproduced with permission from Keene and Waddell, 2007)

(B). Schematic representation of *Drosophila* olfactory circuit: Olfactory receptor neurons (ORNs) expressing the same olfactory receptor projects to the same glomerulus in the antennal lobe. Uniglomerular projection neurons following inner antennocerebral tracts carry the odor information form antennal lobe to mushroom body (MB) and lateral horn (LH). Some projection neurons bypass mushroom body and projects directly to lateral horns. Antennal lobe is also innervated by excitatory local interneurons and inhibitory local neurons. Abbreviations: mACT- medial antennocerebral tracts; oACT- outer antennocerebral tracts.; iLN- inhibitory local interneurons; eLN- excitatory local neurons.

Figure 1.5

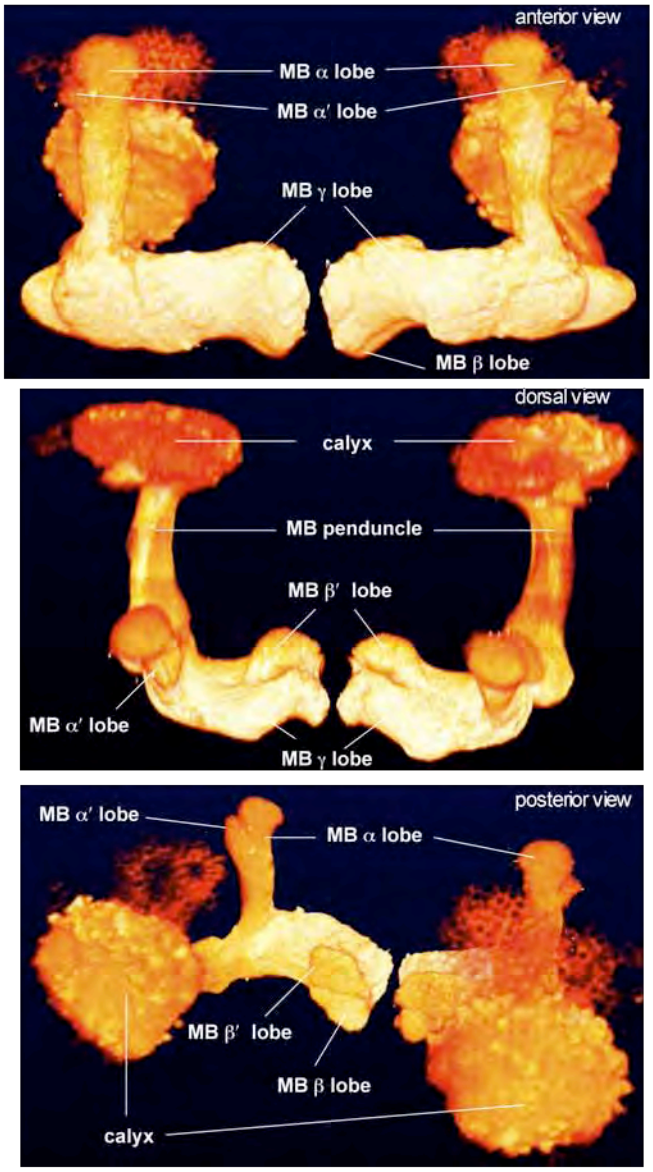

Figure 1.5. Three-dimensional model of the mushroom body. The panels illustrate major anatomical subdivisions of the *Drosophila* mushroom body. Kenyon cells extend their dendrites in the calyx. Beyond the calyx, Kenyon cell axons fasciculate to form the peduncle which projects towards the anterior protocerebrum. The Kenyon cell axons bifurcate upon reaching anterior

protocerebrum to form the mushroom body lobes. The lobes can be subdivided into the vertical α and α' lobes and the medial β, β' and γ lobes.

Figure I.6

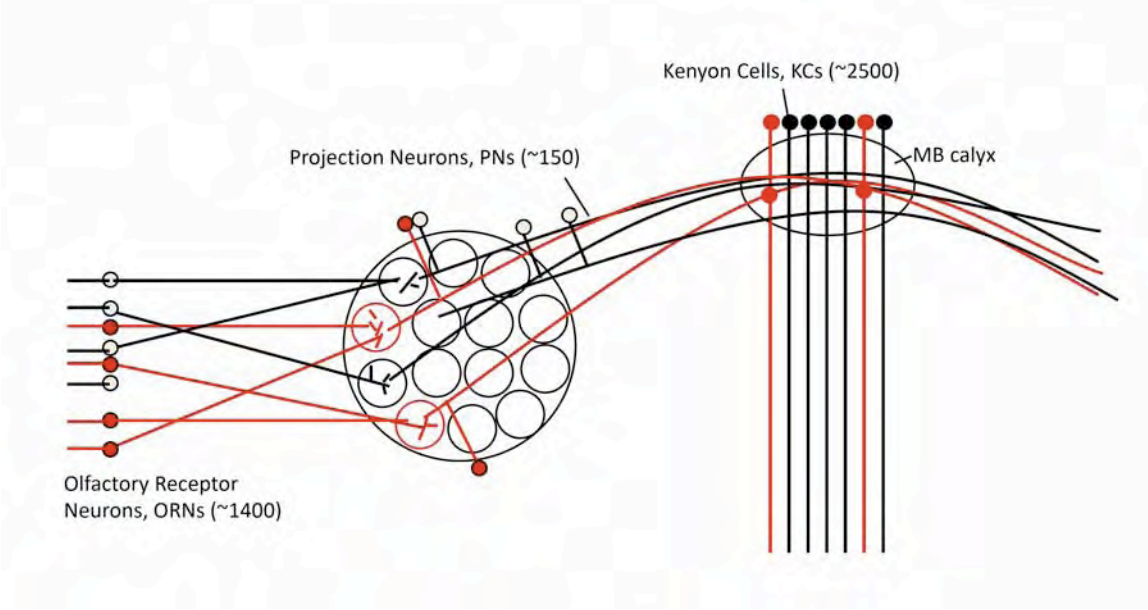

Figure I.6. Labeled-line theory of odor coding. Odors activate a combination of olfactory receptors. ORN activation patterns are relayed into PN activation patterns with 1:1 correlation. PN activation results in combinatorial activation of KCs.

Figure I.7

A.

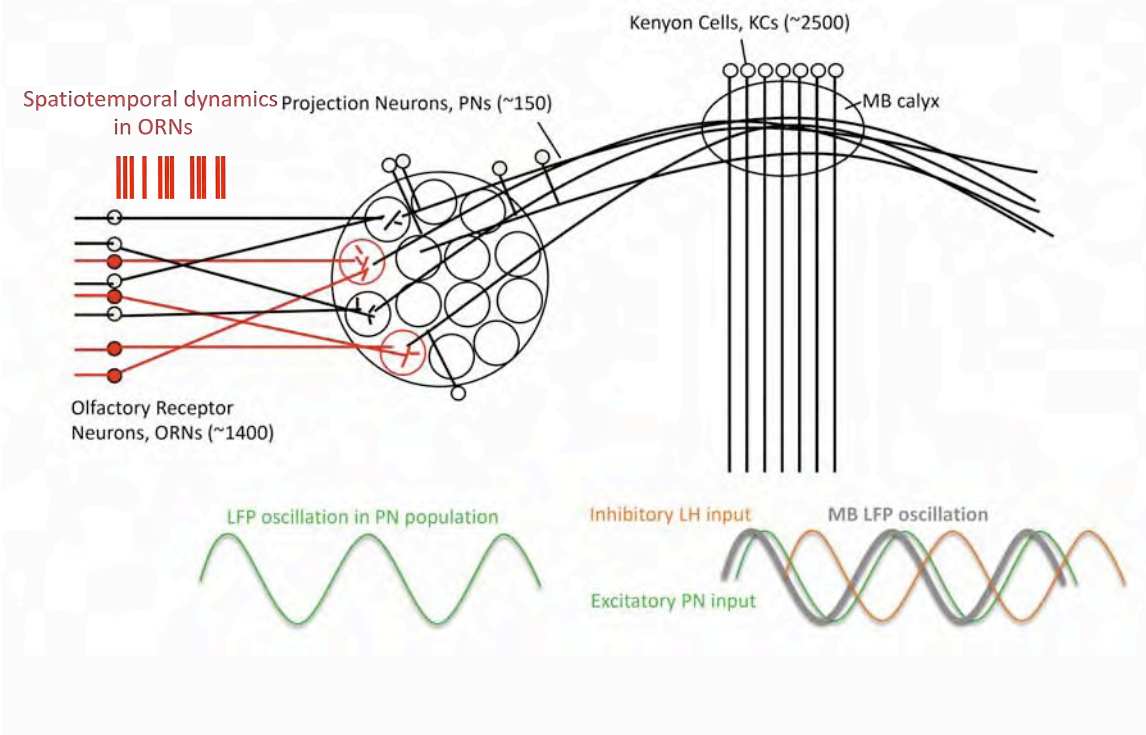
Kenyon Cells, KCs (~2500)
Spatiotemporal dynamics in ORNs
Projection Neurons, PNs (~150)
MB calyx
Olfactory Receptor Neurons, ORNs (~1400)
LFP oscillation in PN population
Inhibitory LH input
MB LFP oscillation
Excitatory PN input

B.

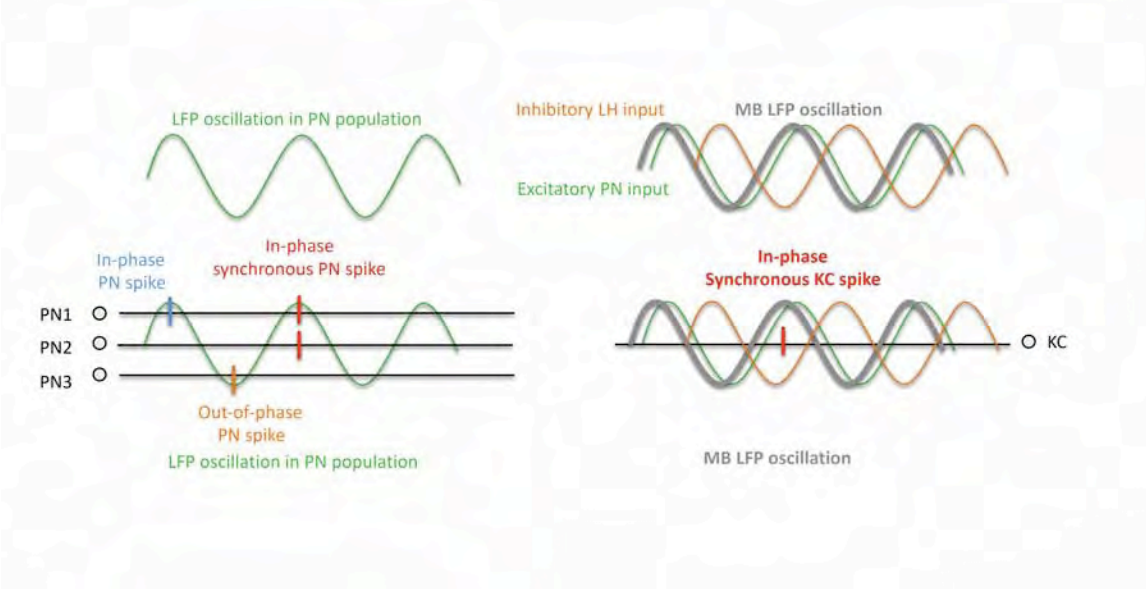
LFP oscillation in PN population
Inhibitory LH input
MB LFP oscillation
Excitatory PN input
In-phase PN spike
In-phase synchronous PN spike
PN1
PN2
PN3
In-phase Synchronous KC spike
KC
Out-of-phase PN spike
LFP oscillation in PN population
MB LFP oscillation

Figure I.7. Spatiotemporal coding of odors. **(A)** Odors evoke spatiotemporal activation patterns in ORNs. ORN activation patterns are decorrelated in the PN ensemble. ORN activity also results in oscillation in LFP of PN population. A similar oscillation in the LFP occurs in the KC population. However, LFP oscillation in the KCs is phase delayed because of phase-shifted inhibitory input from LH interneurons. **(B)** Individual PNs fire axon potentials at different phases of LFP oscillation. Spiking in KCs is triggered by PN spikes that are synchronous and in phase with the MB-LFP oscillations. Abbreviation: LFP- local field potential; LH- lateral horn.

Figure I.8

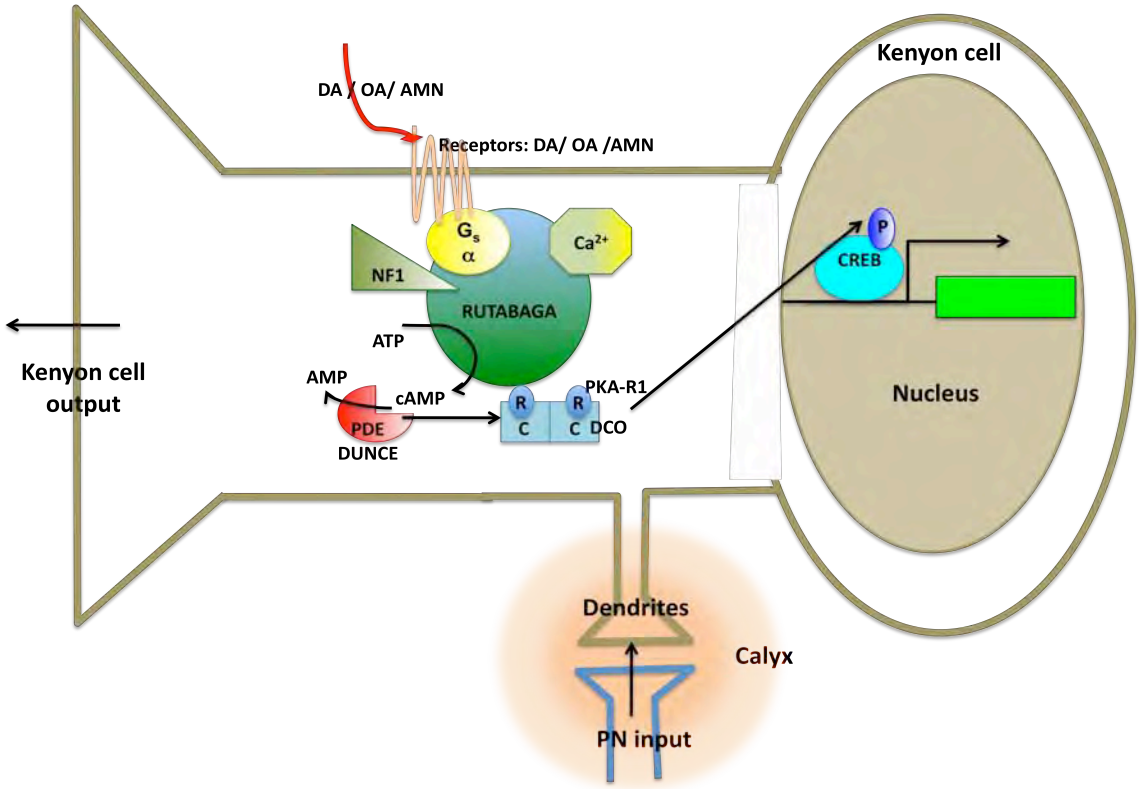

Figure I.8. A simplified molecular model for olfactory memory formation in *Drosophila* mushroom body. This cartoons depicts a single KC of the MB. Odor induced PN activity elevates intracellular Ca^{2+} level in KC whereas unconditioned stimulus information is carried to MB by monoamines like DA (for aversive US) / OA (for appetitive US), which activates specific GPCRs. When GPCR activation coincides with Ca2+ elevation, the adenylyl cyclase RUT is synergistically activated. The activation of RUT results in elevations in intracellular cAMP concentration. NF1 is thought to be involved in the maintenance of AC activity. DNC phosphodiesterase degrades cAMP. Cyclic AMP activates the protein kinase A (PKA-R1) tetramer by causing the release of

the inhibitory PKA-regulatory (PKA-R1) subunits from the catalytic subunits encoded by the *DC0* gene. The activation of PKA leads to either the phosphorylation (P) of a variety of substrates (including ion channels) for the establishment of short-term memory or the phosphorylation of CREB for the establishment of long-term memory. The DPM neurons (not shown) express AMN neuropeptides and provide input to the MB neurons for memory consolidation.

Abbreviations: DC0- *Drosophila* PKA catalytic subunit DC0; DA- dopamine; OA- octopamine; AMN-Amnesiac; NF1- Neurofibromin 1.

Figure I.9

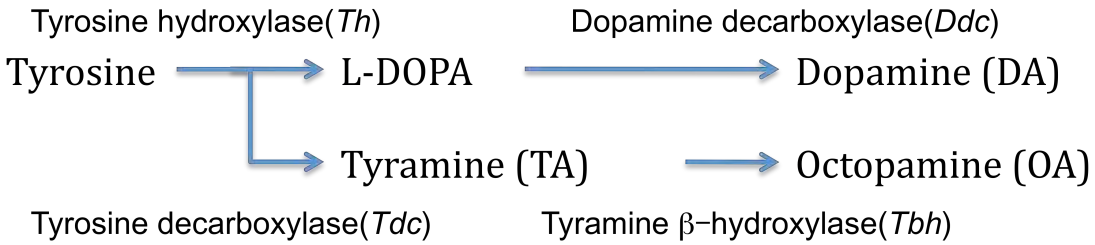

Figure I.9. Biosynthesis pathways for dopamine and octopamine in *Drosophila melanogaster.*

Figure I.10

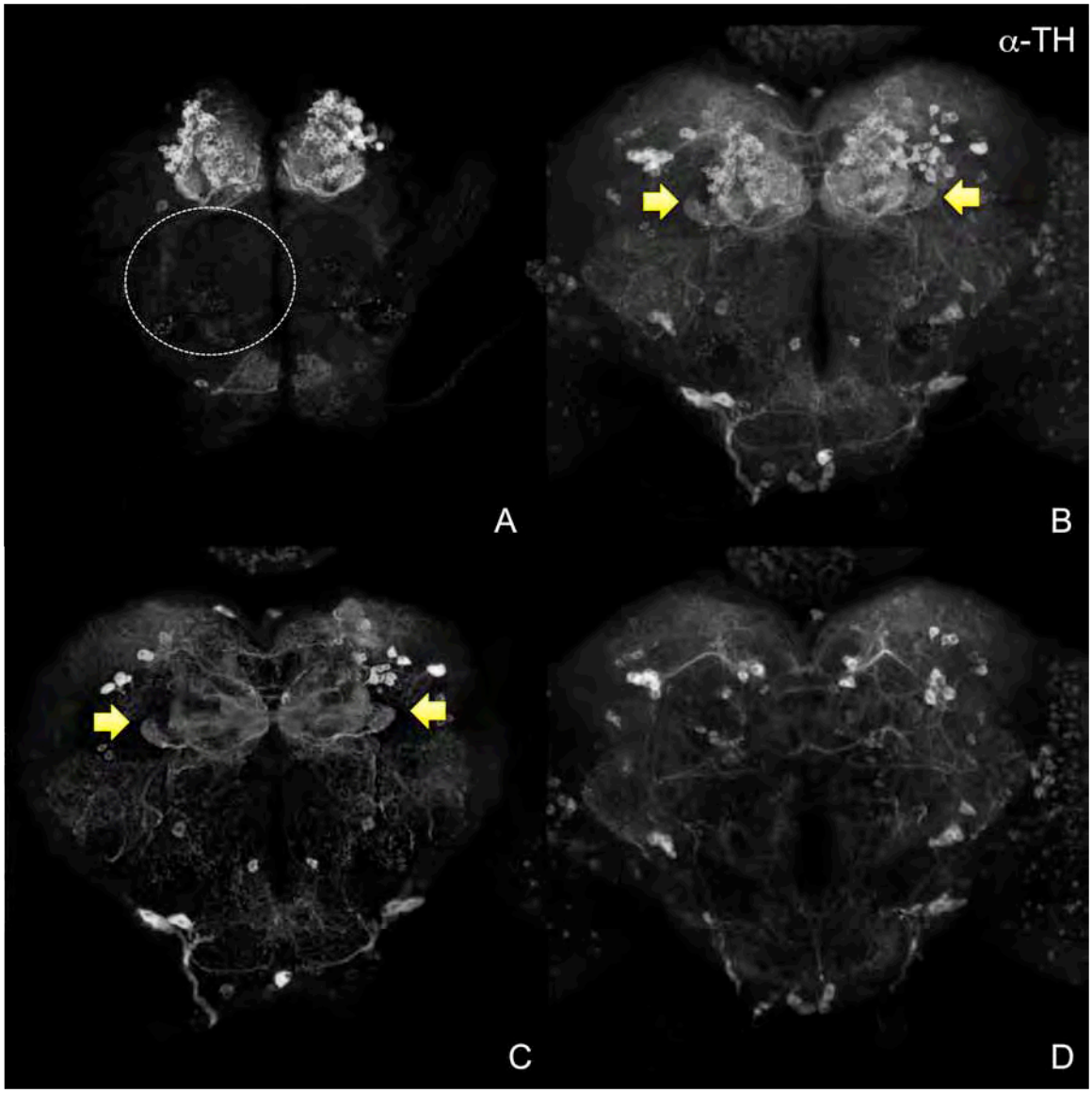

Figure I.10. Arborization pattern of dopaminergic neurons in the fly brain. Dopaminergic neurons are labeled by anti-tyrosine hydroxylase antibody. Partial projection of confocal stacks from a single brain are shown (Anterior-posterior A-D). Yellow arrows indicate mushroom body innervation. Antennal lobe is rarely innervated (open circle).

Figure I.11

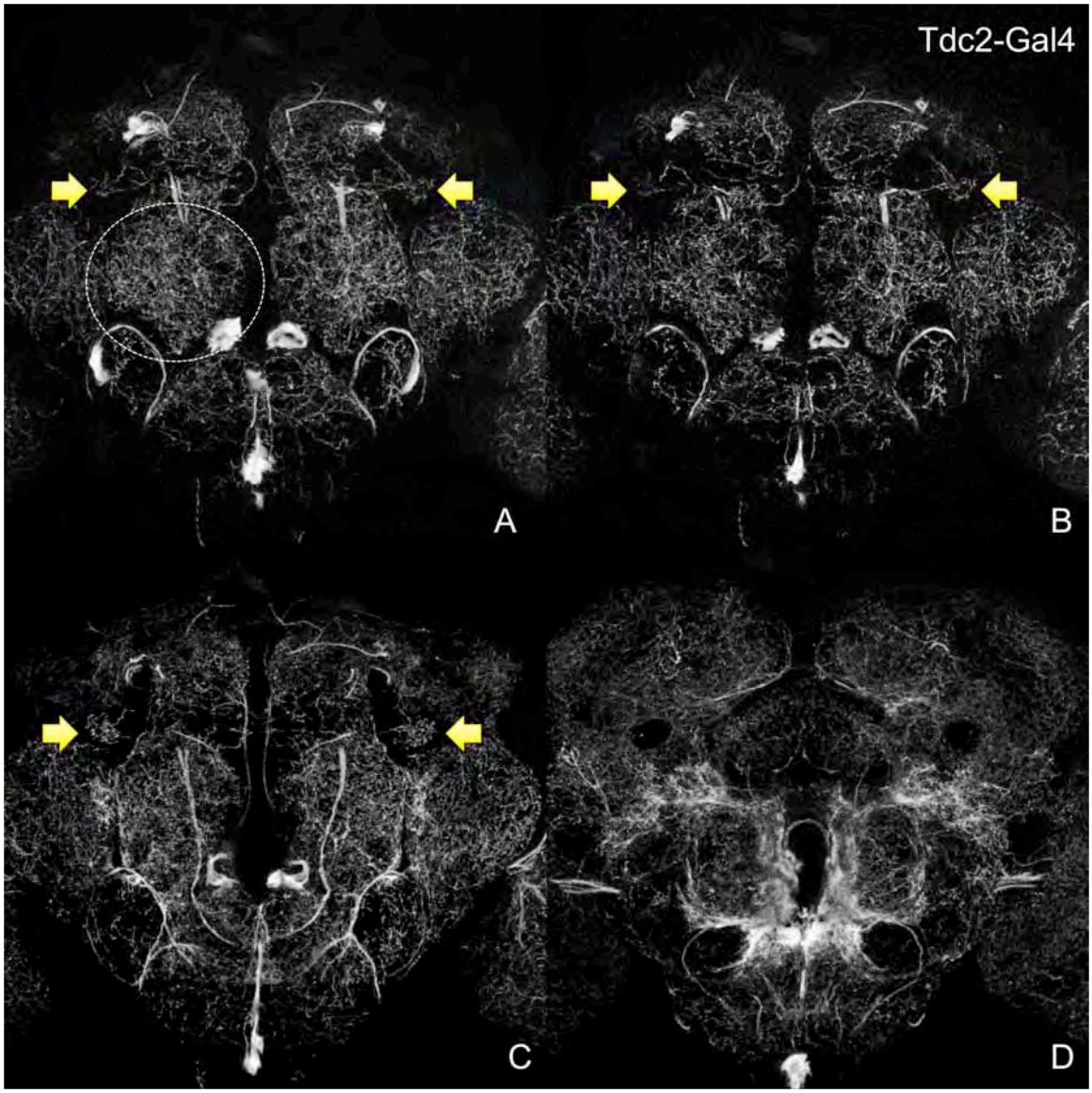

Figure I.11. Arborization pattern of octopaminergic and tyraminergic neurons in the fly brain. Octopaminergic and tyraminergic neurons are labeled by *Tdc2*-Gal4; uas-*mCD8::GFP*. Partial projections of a confocal stack from a single brain are shown (Anterior-posterior A-D). Yellow arrows indicate

mushroom body innervation. Note dense innervation in the antennal lobe (open circle).

Figure I.12

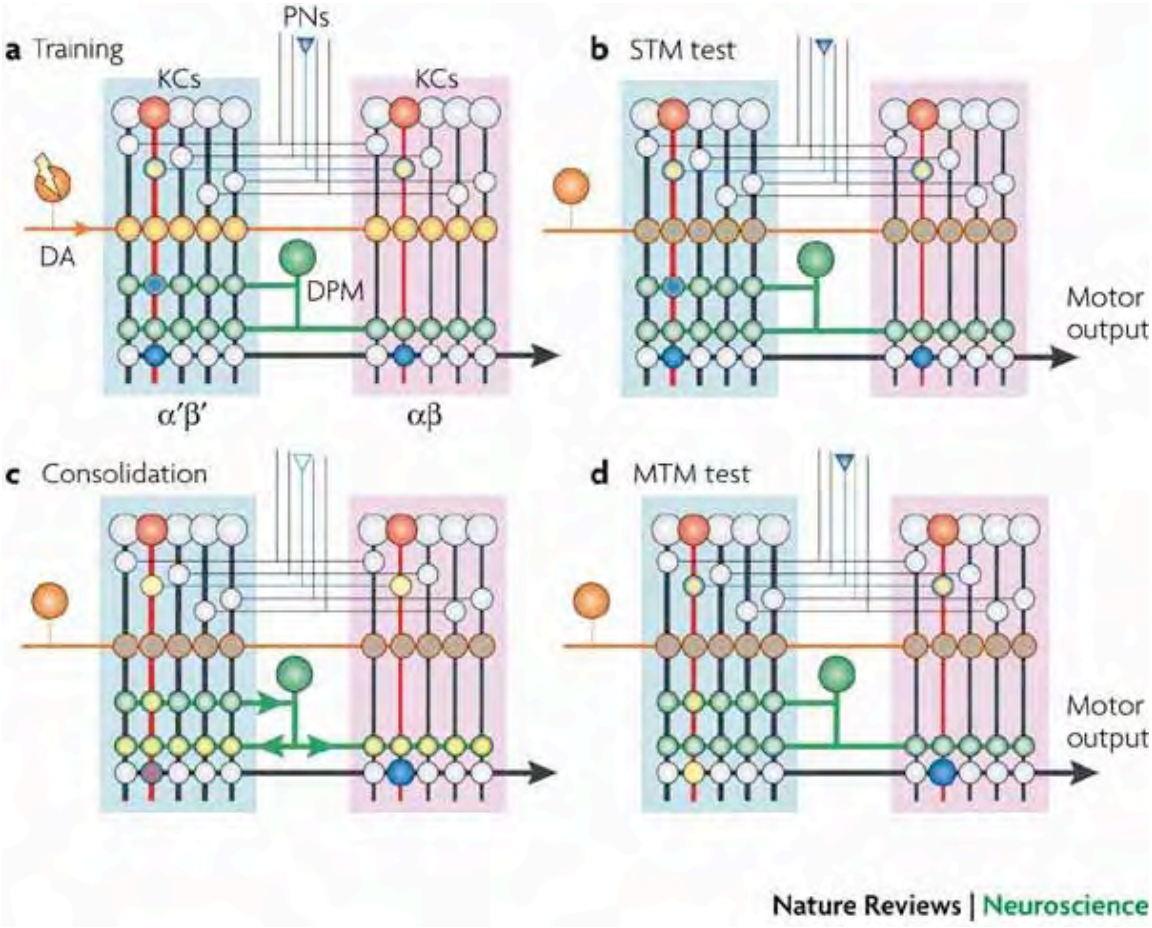

Figure I.12 Model for aversive olfactory conditioning and DPM neuron-dependent memory processing. (A). Training: Odor input through projection neurons (PNs) activates a sparse parallel array (red) of mushroom body Kenyon cells (KCs) that project in the α'β' (light blue) and αβ (pink) lobes. The reinforcing effect of punitive shock is delivered to the mushroom body by dopaminergic

modulatory neurons (DA, orange). Activated synapses are colored yellow. The encoded memory gains specificity through its reliance on coincident DA release onto Kenyon cells that have been activated by odor. Therefore, although DA is released onto all Kenyon cells, synaptic plasticity is only induced at the output synapses (blue circles) of the red neurons. **(B)** Short-term memory (STM) retrieval: Re-exposure to the conditioned odor activates the learning-modified Kenyon cells (red). Output through the modified Kenyon cell $\alpha'\beta'$ and $\alpha\beta$ output synapses (blue circles) leads to an aversive conditioned response. Plasticity was also induced at the $\alpha'\beta'$ Kenyon cell–dorsal paired medial (DPM) neuron synapse (blue/green), but transmission through this synapse is not required for short-term memory. **(C)** Memory consolidation: Spontaneous activity (open blue triangle) in the projection neurons after training occasionally drives the red $\alpha'\beta'$ and $\alpha\beta$ Kenyon cell neurons. Activity in the red $\alpha'\beta'$ neurons strongly drives DPM neurons (green) through the modified $\alpha'\beta'$ Kenyon cell–DPM synapse. DPM neurons feedback onto all $\alpha'\beta'$ and forward onto all $\alpha\beta$ Kenyon cells. Although DPM neurons release transmitter on all Kenyon cells, consolidation is neuron specific because it is reliant on the cells' history (that is, only the red neuron synapses that were modified during training can be consolidated) and coincident red Kenyon cell and DPM neuron activity after training. Each time the red Kenyon cells are spontaneously activated over the next hour, the recurrent $\alpha'\beta'$ Kenyon cell–DPM neuron loop consolidates the output synapses in the red $\alpha\beta$ Kenyon cells (larger blue circle), while plasticity in the red $\alpha'\beta'$ neuron output synapses (blue/red circle) wanes. **(D)** Middle-term memory (MTM) retrieval. Re-exposure to

the conditioned odor activates the red Kenyon cells. However, only transmission from the consolidated $\alpha\beta$ Kenyon cell output synapses (larger blue circle) is required to elicit the aversive conditioned response. (Reproduced with permission from Keene and Waddell, 2007).

Preface to Chapter II

This chapter has been published separately in:

DasGupta, S. & Waddell, S. (2008). Learned odor discrimination in *Drosophila* without combinatorial odor maps in the antennal lobe. Current Biology *18*: 1668-74.

DasGupta, S. performed the experiments

DasGupta, S. and Waddell, S. designed the experiments and wrote the manuscript.

Chapter II: Input to the system: Learned odor discrimination in *Drosophila* without combinatorial odor maps in the antennal lobe

II.A. Introduction:

In fruit flies, specific odorants interact with unique combinations of olfactory receptor neurons (ORNs) giving rise to a putative topographic odor code of activated glomeruli in the antennal lobe. To test the requirement of differential spatial encoding for odorant discrimination we reduced olfactory input complexity using *Or83b*^{2} null mutant flies (Larsson et al. 2004). OR83b is an essential subunit of odorant receptor (OR) containing odorant-gated cation channels (Larsson et al. 2004, Benton et al. 2006, Sato et al. 2008, Wicher et al. 2008). Most fruit fly ORNs co-express *Or83b* with a single unique (OR) gene and all those housed in basiconic and trichoid sensillae, with the exception of a highly specialized class that detect CO_2, require *Or83b* for function (Larsson et al. 2004, Benton et al. 2006, Jones et al. 2007, Kwon et al. 2007). *Or83b* is also co-expressed with *Or35a* in a broadly tuned class of coeloconic ORNs. The remaining coeloconic ORNs, that are narrowly tuned to select fatty acids, aldehydes and small amines, do not express *Or83b, Or* or *Gr* genes (Fishilevich et al. 2005, Couto et al. 2005, Yao et al. 2005). Therefore, *Or83b*^{2} mutant flies are anosmic to most odorants sensed by basiconic sensillae. Importantly, ORNs wire to the appropriate glomeruli in *Or83b* mutant flies and one can restore function to a single ORN class by expressing a uas-*Or83b* transgene using *Or*-specific GAL4 control (Fishilevich et al. 2005, Louis et al. 2008). Using this technique others demonstrated that larvae with a single ORN chemotax toward odorants that attract wild-type larvae (Fishilevich et al. 2005, Louis et al. 2008).

While clearly establishing a role for single ORNs, these studies did not investigate whether odorant-evoked activity through a single class of ORN can be decoded as a discrete odor percept. One way to do this is to assign value to an arbitrary odorant with associative conditioning and demonstrate that flies choose appropriately between odorants. If discrete spatial patterns of glomerular activation are essential for encoding odorant identity, flies with one ORN class will fail to discriminate odorants, because the glomerulus activated by all odorants is the same in these flies. Odorant discrimination with one class of ORNs would challenge a spatial encoding model.

We used an olfactory conditioning paradigm where flies associate one of two odorants with electric shock punishment and then choose between the two odorants (Tully and Quinn 1985). Trained flies preferentially avoid the T-maze arm with the conditioned odorant. A different population of the same genotype of flies is subsequently taught to associate the other odorant with punishment and a single learning score represents the average of the two reciprocal experiments. This design provides a rigorous test of odorant discrimination and controls against innate odorant bias.

II.B. Results:

Flies with single functional class of ORNs learn to discriminate between odorants

The electrophysiological response to a large panel of odorants has been reported for most *Drosophila* ORs (Hallem and Carlson 2006), allowing us to select and test ORNs and their cognate odorants. We first determined whether *Or83b*^{2} mutant flies can learn to discriminate between six pairs of odorants (6-methyl-5-hepten-2-one versus pentyl acetate, methyl salicylate versus methyl benzoate, isoamyl acetate versus methyl benzoate, methyl hexanoate versus di-ethyl succinate, methyl salicylate versus 4-methyl phenol and geranyl acetate versus ethyl acetate) selected because they activate defined ORs (Figure II.1A). As expected, wild-type flies showed robust learned discrimination with all six odorant pairs whereas *Or83b*^{2} mutant flies did not. Therefore, *Or83b* expressing ORNs are required to learn to discriminate between the chosen odorants and residual responses in *Or83b*^{2} mutant flies are not sufficient to support learned odorant discrimination.

We next tested flies in which the function of *Or46a*, *Or67a* or *Or98a*-expressing ORNs were restored individually. These ORNs are housed in different sensory sensilla (pb2, ab10 and ab7a) in the maxillary palp or antenna, project their axons to the spatially discrete VA7l, DM6 and VM5 glomeruli (Figure II.1B),

and respond to a subset of the odorant pairs used in Figure II.1A (Fishilevich et al. 2005, Couto et al. 2005, Hallem and Carlson 2006, Olsen et al. 2007). Furthermore, these receptors are not co-expressed with other functional ORs (Fishilevich et al. 2005, Couto et al. 2005, Goldman et al. 2005). We first used *Or46a*-GAL4 to express uas-*Or83b* in an otherwise $Or83b^2$ mutant fly and tested whether these flies could discriminate between two odorants reported to activate OR46a; 4-methyl phenol and methyl salicylate (Olsen et al. 2007). Restoring OR46a ORN function in this way faithfully restored odor-evoked responses to those approximating wild-type OR46a neurons (Olsen et al. 2007). We assayed wild-type, $Or83b^2$ mutant, *Or46a*-GAL4; $Or83b^2$ and uas-*Or83b*; $Or83b^2$ mutant flies in parallel for comparison (Figure II.1C). All flies without functional *Or83b*-expressing ORNs did not learn whereas flies with restored OR46a neurons learned to discriminate between 4-methyl phenol and methyl salicylate. As an indicator of specificity, we tested flies with restored OR67a neurons. OR67a is broadly tuned but apparently does not respond to 4-methyl phenol and methyl salicylate (Hallem and Carlson 2006, Olsen et al. 2007). Consistent with this, OR67a restored flies did not learn with these odorants (Figure II.1C). Therefore flies with a single class of functional *Or83b*-expressing ORNs can discriminate between two odorants if they activate the relevant OR.

The odor-tuning curve of OR67a partially overlaps with that of OR98a (Hallem and Carlson 2006). We therefore tested flies with restored OR67a or

OR98a neurons for learned discrimination between methyl benzoate and isoamyl acetate (Figure II.1D). As in the previous experiments, all flies without functional *Or83b*-expressing ORNs did not learn but robust learning was evident in flies with restored OR67a or OR98a neurons. Therefore *Or83b*^{2} mutant flies can use either OR67a or OR98a-restored ORNs to discriminate between methyl benzoate and isoamyl acetate.

OR67a also responds to pentyl acetate and 6-methyl-5-hepten-2-one (Hallem and Carlson 2006). We therefore tested whether flies with restored OR67a neurons could learn to discriminate between these two odorants (Figure II.1E). All flies without functional *Or83b*-expressing ORNs did not exhibit learning, whereas flies with restored OR67a ORNs learned. Therefore OR67a restored flies can learn to discriminate between at least two pairs of different odorants that activate OR67a. The preceding experiments demonstrate that flies can employ a single class of *Or83b*-expressing ORNs to learn to discriminate between two odorants that activate that ORN class, consistent with the notion that they can use neural activity in the same class of ORNs to differentially represent odorants.

Flies with single class of functional ORNs fail to recognize all components of an odorant mixture

Our findings using *Or83b*^{2} mutant flies suggest that *Or83b*-independent ORNs are not sufficient for learned discrimination with multiple odorant combinations (Figure II.1). Nevertheless, we further tested whether flies with restored OR67a neurons had other relevant ORNs by testing whether flies could simultaneously encode multiple odorant components, like wild-type flies. We combined the four odorants that flies with restored OR67a neurons can discriminate between; methyl benzoate, isoamyl acetate, pentyl acetate and 6-methyl-5-hepten-2-one, into two binary mixtures, trained the flies with these mixtures (Figure II.2A and B) and tested for discrimination between the component odorants. Whereas wild-type flies exhibited learned discrimination for all four component odorants, regardless of the mixture combination used during training, learned discrimination was only observed for the 6-methyl-5-hepten-2-one and pentyl acetate components in OR67a restored flies. These data suggest that OR67a restored flies encode one odor component at a time, consistent with the notion that these odorants activate the same ORNs.

To further test the model that odorants compete for ORs in OR67a restored flies, we trained flies with single odorants and tested discrimination with binary mixtures (Figure II.2C and D). We reasoned that a competing odorant in a

mixture during testing would mask learned behavior for the other odorant. Training wild-type flies with either 6-methyl-5-hepten-2-one versus pentyl acetate or isoamyl acetate versus methyl benzoate and testing with 6-methyl-5-hepten-2-one + isoamyl acetate versus methyl benzoate + pentyl acetate revealed learned discrimination in both cases (Figure II.2C). However, in flies with OR67a restored neurons, robust learned discrimination was only observed following training with 6-methyl-5-hepten-2-one versus pentyl acetate and not with isoamyl acetate versus methyl benzoate. We also tested learned discrimination with a different odorant combination; 6-methyl-5-hepten-2-one + methyl benzoate versus pentyl acetate + isoamyl acetate (Figure II.2D). Wild-type flies showed learned discrimination in both cases, whereas OR67a restored flies only showed learned discrimination when trained with 6-methyl-5-hepten-2-one versus pentyl acetate. Therefore these data are consistent with the notion that odorants compete at the ORN level in OR67a restored flies, providing further support that these flies have a single relevant ORN class (Figure II.5 and 6).

OR67a restored flies cross-adapt to odorants that activate OR67a neuron

We also tested the contribution of *Or83b*-independent ORNs using a cross-adaptation assay that does not require learning. We predicted OR67a restored flies would cross-adapt to odorants that activate OR67a ORNs if these odorants activated the same ORNs. We first used methyl benzoate and pentyl

acetate because odorant mixture experiments suggested these odorants compete for OR67a neurons (Figure II.3A and B). Wild-type and OR67a restored flies were adapted by pre-exposure to methyl benzoate for 30 minutes and tested for methyl benzoate or pentyl acetate avoidance behavior. Naive wild-type and OR67a flies avoided methyl benzoate but avoidance was abolished in both genotypes following adaptation (Figure II.3A), demonstrating the efficacy of the adaptation protocol. For cross-adaptation we tested separate groups of methyl benzoate adapted flies for pentyl acetate avoidance (Figure II.3A). Wild-type flies adapted with methyl benzoate avoided pentyl acetate indicating that pentyl acetate activates additional ORNs in wild-type flies that do not respond to methyl benzoate. However, OR67a restored flies adapted with methyl benzoate also adapted their behavioral response to pentyl acetate, suggesting that pentyl acetate activates the same ORNs in these flies that respond to methyl benzoate. We also performed reciprocal cross-adaptation experiments where flies were adapted to pentyl acetate and tested for pentyl acetate or methyl benzoate avoidance behavior (Figure II.3B). OR67a restored flies adapted to pentyl acetate also lost their response to methyl benzoate. In contrast, the same pentyl acetate pre-exposure partially altered the pentyl acetate and methyl benzoate response in wild-type flies. Therefore methyl benzoate and pentyl acetate activate overlapping ORNs in OR67a restored flies, again supporting the notion that odorants compete for a single relevant class of functional ORNs in OR67a restored flies.

We also used cross-adaptation to test whether odorants that can be discriminated by OR67a restored flies activate overlapping ORNs. Indeed, Or67a restored flies displayed reciprocal cross-adaptation to methyl benzoate and isoamyl acetate (Figure II.3A and C) and to pentyl acetate and 6-methyl-5-hepten-2-one (Figure II.3B and D). In addition, we demonstrated that OR67a restored flies discriminate between methyl benzoate and pentyl acetate (Figure II.7), two other odorants that they cross-adapt to. These data present further evidence that flies can discriminate between odorants using the same, and very likely a single class of, ORNs. Importantly, a purely spatial model for odorant encoding cannot account for discrimination between two odorants that activate the same class(es) of ORNs.

_Or83b_^{2} flies with functional OR67a neurons can discriminate odorants across changing concentration

Flies with a single class of functional *Or83b*-expressing ORNs could discriminate between odorants using odorant intensity (relative concentration) and / or identity (chemical structure) information. We therefore tested whether OR67a restored flies only coded odorant intensity by altering the concentration of one of the two odorants between training and testing discrimination. These manipulations

simultaneously changed absolute concentration of one of the odorants and the relationship between odorants. We used pentyl acetate and 6-methyl-5-hepten-2-one because the odor-evoked firing rate of *Or67a*-expressing ORNs to these odorants has been reported to vary between 10^{-2} and 10^{-4} dilutions (Hallem and Carlson 2006). We first trained flies with either 10^{-2}, 10^{-3} or 10^{-4} dilutions of 6-methyl-5-hepten-2-one versus a constant 10^{-3} dilution of pentyl acetate and tested all groups for discrimination between 10^{-3} 6-methyl-5-hepten-2-one versus 10^{-3} pentyl acetate (Figure II.4A). Learned discrimination scores varied little for wild-type and OR67a rescued flies with changing 6-methyl-5-hepten-2-one concentration demonstrating that both wild-type and OR67a rescued flies identify 6-methyl-5-hepten-2-one, despite a change in absolute and relative odorant intensity. We similarly manipulated pentyl acetate concentration between training and testing. In this case, learned discrimination in wild-type and OR67a restored flies was robust when training concentration was lower, or the same, as that at test (Figure II.4B). Both wild-type and OR67a restored flies performed most poorly when training concentration was higher than that at test. Since flies with restored OR67a neurons distinguish the appropriate odorant across changing concentration, they cannot be only coding absolute odorant intensity. Furthermore, since our experimental design also changed relative odorant intensity between training and testing, the flies do not utilize this parameter to discriminate odorants. Instead, these data suggest flies with restored OR67a neurons encode odorant identity.

II.C. Discussion

In conclusion, multiple classes of ORNs are not required for flies to discriminate odorants. Although flies without functional *Or83b*-expressing neurons cannot learn to discriminate between a number of chemically distinct odorants, providing a single class of *Or83b*-expressing ORNs restores learned discrimination between two odorants that activate that particular ORN class. These flies cross-adapt to odorants that activate the restored ORNs demonstrating that the relevant ORNs are the same, thus challenging a requirement for discrete spatial codes for odorants in the antennal lobe. As expected, flies with one class of *Or83b*-expressing ORNs have limitations and can apparently only encode one odorant that activates the appropriate receptor at a time. These data suggest a benefit of having multiple classes of ORNs is the ability to identify certain odorants present within a more complex milieu. Importantly, $Or83b^{2}$ mutant flies with one functional class of *Or83b*-expressing ORNs choose appropriately between two odorants even though the absolute and relative concentration is changed between training and testing, implying that they encode odorant identity, and do not only rely on encoding odorant intensity.

Finding that distinct combinatorial spatial patterns of ORN activation in the antennal lobe are not essential to represent odorant information implies an

important role for odorant-evoked temporal dynamics. Previous studies in insects and vertebrates have documented considerable temporal complexity in odor-evoked activity at successive layers of the olfactory system (Stopfer et al. 1997, Wehr et al. 1996, Friedrich and Laurent 2001, Muller et al. 2002, Perez-Orive et al. 2002, Lei et al. 2004, Friedrich et al. 2004, Wilson et al. 2004, Carleton et al. 2008) but few have investigated the behavioral relevance (Stopfer et al. 1997). Recent work has shown that excitatory and inhibitory lateral connectivity in the *Drosophila* antennal lobe can shape projection neuron responses (Louis et al. 2008, Wilson and Laurent 2005, Shang et al. 2007, Olsen and Wilson 2008, Kazama and Wilson 2008, Root et al. 2008), therefore we expect different temporal signals in the same ORNs to generate distinct temporal, and perhaps spatial, patterns of projection neuron activity. However, since flies with a single functional class of *Or83b*-expressing ORNs lack the lateral input driven by additional classes of ORN, it will be important to determine how lateral connectivity within the antennal lobe contributes to odorant discrimination in *Drosophila.*

II.D. Materials and methods

Fly strains

Fly stocks were raised on standard cornmeal food at 25°C and 40-50% relative humidity. The wild-type *Drosophila* strain is Canton-S. The uas-*n-syb::GFP* flies are described (Estes et al. 2000). *Or83b*^{2} mutant flies, *Or98a*-GAL4 (Fishilevich et al. 2005), and uas-*Or83b* transgenic flies were obtained from L. Vosshall (Rockefeller University). *Or67a*-GAL4 transgenic flies (Couto et al. 2005) were obtained from B. Dickson (IMP, Vienna) and Or46a-GAL4 (Fishilevich et al. 2005); *Or83b*^{2} flies were obtained from R. Wilson (Harvard University). All transgenic insertions are on the second chromosome. We generated *OrX*-GAL4/uas-*Or83b*; *Or83b*^{2} flies by crossing *OrX*-GAL4; *Or83b*^{2} flies to uas-*Or83b*; *Or83b*^{2} flies. Heterozygous uas-*Or83b*/+; *Or83b*^{2} and *OrX*-GAL4/+; *Or83b*^{2} flies were generated by crossing uas-*Or83b*; *Or83b*^{2} and *OrX*-GAL4; *Or83b*^{2} flies to *Or83b*^{2} flies. Mixed sex populations of flies, heterozygous for the listed transgenes, were tested for olfactory learning.

Behavioral analysis

The olfactory avoidance paradigm was essentially performed as described previously (Tully and Quinn 1985). The Performance Index (PI) was calculated as the number of flies avoiding the conditioned odor minus the number of flies

avoiding the unconditioned odor divided by the total number of flies in the experiment. A single PI value is the average score from flies of the identical genotype trained with each odor. For training, all odors were diluted 1:1000 in mineral oil (unless stated otherwise). For testing, all odors were diluted 1:1000 in mineral oil and adjusted so that naïve flies distributed equally between the odorant pair.

For olfactory adaptation experiments naïve flies or flies exposed to odorant A for 30min in the training chamber of the T-maze were tested for their preference between tubes with either odorant A versus air or for a different odorant versus air. Odorants were diluted approximately 1:1000 in mineral oil. Avoidance Index was calculated as the number of flies avoiding the odorant minus the number of flies avoiding the air divided by the total number of flies in the experiment.

To reduce variation within experiments, all genotypes were tested in each experimental session. Statistical analyses were performed using KaleidaGraph (Synergy Software). Overall analyses of variance (ANOVA) were followed by planned pairwise comparisons between the relevant groups with a Tukey HSD post-hoc test. Statistical significance from zero was determined using the Mann-Whitney U-test. All experiments are $n \geq 8$.

Methyl benzoate, isoamyl acetate, pentyl acetate, 6-methyl-5-hepten-2-one, 4-methyl phenol, methyl salicylate, methyl hexanoate, di-ethyl succinate, and ethyl acetate were obtained from Sigma and geranyl acetate from Fluka.

Immunohistochemistry

Adult brains expressing transgenic uas-*n-syb::GFP* (Estes et al. 2000) were removed from the head capsule and fixed in 4% paraformaldehyde in Phosphate Buffered Saline (PBS), [1.86mM NaH_2PO_4, 8.41mM Na_2HPO_4, 175mM NaCl] for 15 min, and rinsed in PBS-T (PBS containing 0.25% Triton X-100). Brains were incubated with 1:200 mAb anti-GFP (Invitrogen) and 1:100 mAb nc82 (Hybridoma Bank, University of Iowa) followed by the appropriate fluorescent secondary antibodies (Jackson Laboratories). Confocal analysis was performed on a Zeiss LSM 5 Pascal confocal microscope. Confocal stacks were processed using Amira, ImageJ and Adobe Photoshop.

Figure II.1

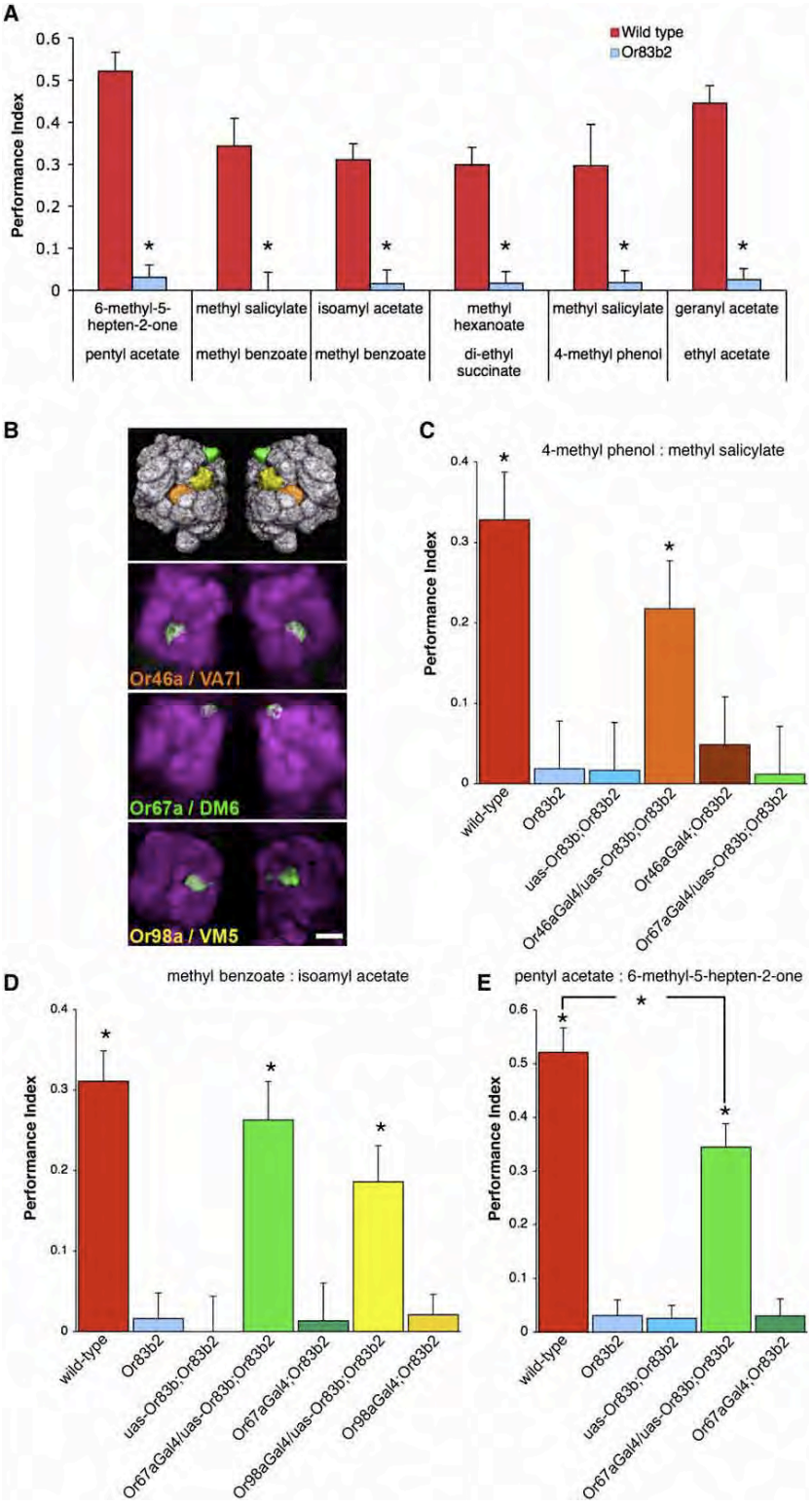
A
Wild type
Or83b2
Performance Index
6-methyl-5-hepten-2-one
pentyl acetate
methyl salicylate
methyl benzoate
isoamyl acetate
methyl benzoate
methyl hexanoate
di-ethyl succinate
methyl salicylate
4-methyl phenol
geranyl acetate
ethyl acetate
B
Or46a / VA7l
Or67a / DM6
Or98a / VM5
C
4-methyl phenol : methyl salicylate
Performance Index
wild-type
Or83b2
uas-Or83b;Or83b2
Or46aGal4/uas-Or83b;Or83b2
Or46aGal4;Or83b2
Or67aGal4/uas-Or83b;Or83b2
D
methyl benzoate : isoamyl acetate
Performance Index
wild-type
Or83b2
uas-Or83b;Or83b2
Or67aGal4/uas-Or83b;Or83b2
Or67aGal4;Or83b2
Or98aGal4/uas-Or83b;Or83b2
Or98aGal4;Or83b2
E
pentyl acetate : 6-methyl-5-hepten-2-one
Performance Index
wild-type
Or83b2
uas-Or83b;Or83b2
Or67aGal4/uas-Or83b;Or83b2
Or67aGal4;Or83b2

Figure II.1. *Or83b*^{2} flies with functional Or46a, Or67a or Or98a-expressing neurons learn to discriminate between odorants that activate these receptors. (**A**) *Or83b*^{2} mutant flies cannot learn to discriminate between odors. Wild-type flies can learn to discriminate between six pairs of odorants whereas *Or83b*^{2} mutant flies cannot. Asterisks indicate no significant difference to zero (all P>0.1, Mann Whitney U-test). **(B)** Upper panel, volume rendering of the fly antennal lobes highlighting the relative position of the VA7l (orange), DM6 (green) and VM5 (yellow) glomeruli innervated by Or46a, Or67a and Or98a expressing OSNs. Lower panels show corresponding confocal stack projections through the antennal lobes of flies expressing uas-*n-syb::GFP* driven by *Or46a*-GAL4, *Or67a*-GAL4 or *Or98a*-GAL4. N-syb::GFP is stained with anti-GFP (green) and neuropil is visualized with nc82 antibody (magenta) staining. Scale bar is 20μm and refers to all micrographs. (**C**) Flies with only functional OR46a neurons can learn to discriminate between 4-methyl phenol and methyl salicylate but flies with only OR67a neurons cannot. Asterisks indicate significant difference (all *P*<0.04, ANOVA) between the marked groups and all others. (**D**) Flies with only functional OR67a or OR98a neurons can learn to discriminate between methyl benzoate and isoamyl acetate. Asterisks indicate significant difference (all *P*<0.005, ANOVA) between the marked groups and all others. (**E**) Flies with only functional OR67a neurons can learn to discriminate between pentyl acetate and 6-methyl-5-hepten-2-one. Asterisks indicate significant difference (all *P*<0.005, ANOVA) between the marked groups and all others. Data are mean ± s.e.m.

Figure II.2

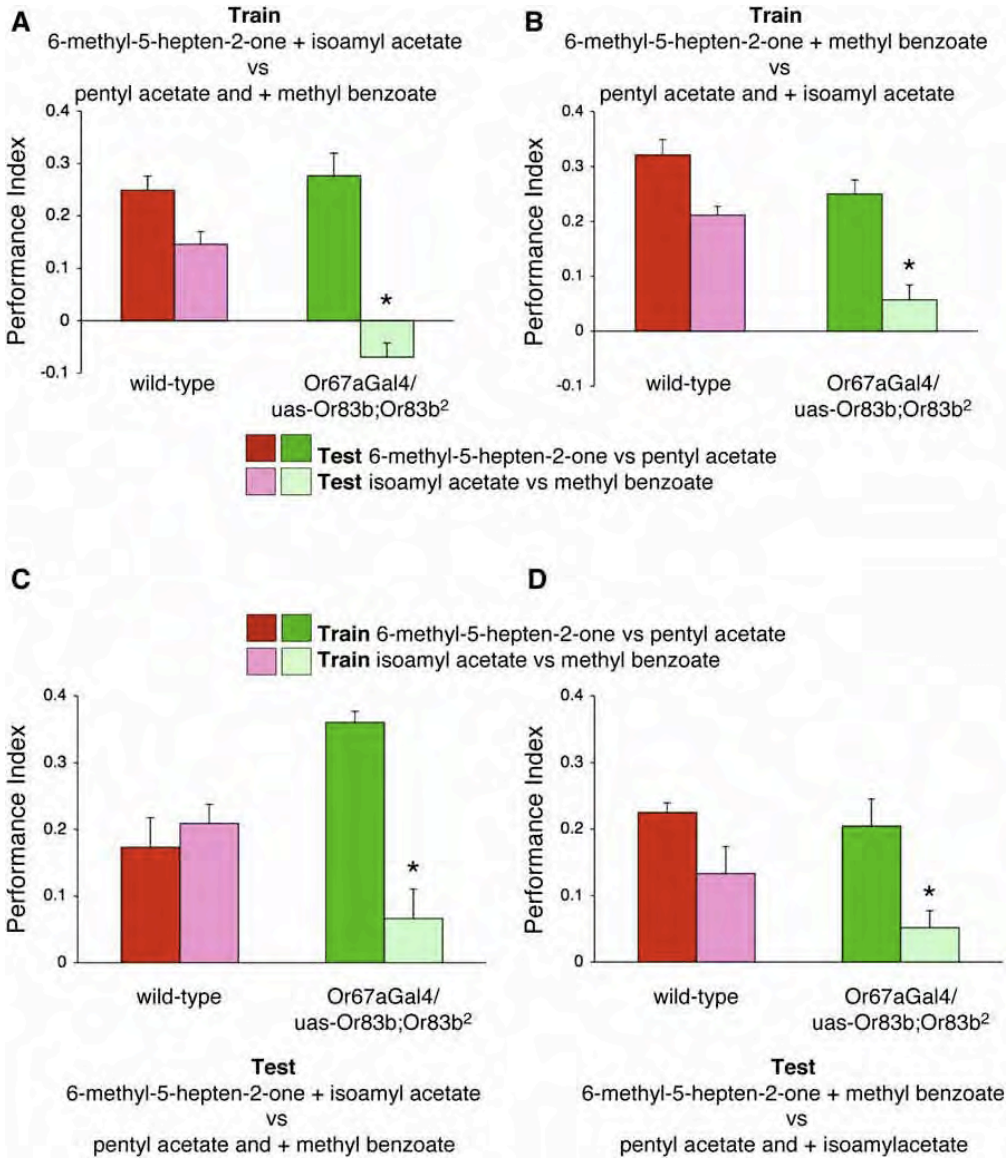
A
Train
6-methyl-5-hepten-2-one + isoamyl acetate
vs
pentyl acetate and + methyl benzoate
Performance Index
0.4
0.3
0.2
0.1
0
-0.1
*
wild-type
Or67aGal4/
uas-Or83b;Or83b2
B
Train
6-methyl-5-hepten-2-one + methyl benzoate
vs
pentyl acetate and + isoamyl acetate
Performance Index
0.4
0.3
0.2
0.1
0
-0.1
*
wild-type
Or67aGal4/
uas-Or83b;Or83b2
Test 6-methyl-5-hepten-2-one vs pentyl acetate
Test isoamyl acetate vs methyl benzoate
C
Train 6-methyl-5-hepten-2-one vs pentyl acetate
Train isoamyl acetate vs methyl benzoate
Performance Index
0.4
0.3
0.2
0.1
0
*
wild-type
Or67aGal4/
uas-Or83b;Or83b2
Test
6-methyl-5-hepten-2-one + isoamyl acetate
vs
pentyl acetate and + methyl benzoate
D
Performance Index
0.4
0.3
0.2
0.1
0
*
wild-type
Or67aGal4/
uas-Or83b;Or83b2
Test
6-methyl-5-hepten-2-one + methyl benzoate
vs
pentyl acetate and + isoamylacetate

Figure II.2. Limitations in learned behavior in *Or83b*^{2} flies with functional Or67a-expressing neurons. (A) Flies with only functional OR67a neurons learn one component of a binary blend. Flies were trained with 6-methyl-5-hepten-2-one + isoamyl acetate versus methyl benzoate + pentyl acetate mixtures. Wild-type flies show learning when tested with all components alone, whereas flies with only functional OR67a neurons exclusively show learned discrimination for the 6-methyl-5-hepten-2-one and pentyl acetate components**. (B)** Wild-type flies learn both components of a different binary blend, but OR67a-restored flies only learn one. Flies were trained with 6-methyl-5-hepten-2-one + methyl benzoate versus pentyl acetate + isoamyl acetate mixtures. Wild-type flies learn all components, whereas flies with restored OR67a neurons again only show learned discrimination for the 6-methyl-5-hepten-2-one and pentyl acetate components. **(C)** Flies with restored OR67a neurons do not show learned discrimination of isoamyl acetate and methyl benzoate when 6-methyl-5-hepten-2-one and pentyl acetate are also present during test. Wild-type flies trained with either set of single components show learned discrimination when tested with the additional complexity of binary mixtures, but flies with OR67a neurons only show robust performance if trained with 6-methyl-5-hepten-2-one versus pentyl acetate. **(D)** Flies with functional OR67a neurons do not show learned discrimination of isoamyl acetate and methyl benzoate when tested with a different composition of odorant mixtures. Wild-type flies trained with either set of single components, 6-methyl-5-hepten-2-one versus pentyl acetate or isoamyl

acetate versus methyl benzoate show learned discrimination when tested with binary mixtures, but flies with OR67a neurons only show robust performance if trained with 6-methyl-5-hepten-2-one versus pentyl acetate. Individual odor concentrations in the blends were the same as those used separately in Figures II.1D and 1E and when tested for component learning (Figures II.2A and 2B). Asterisks denote no significant difference to zero (all $p > 0.5$, Mann Whitney U test).

Figure II.3

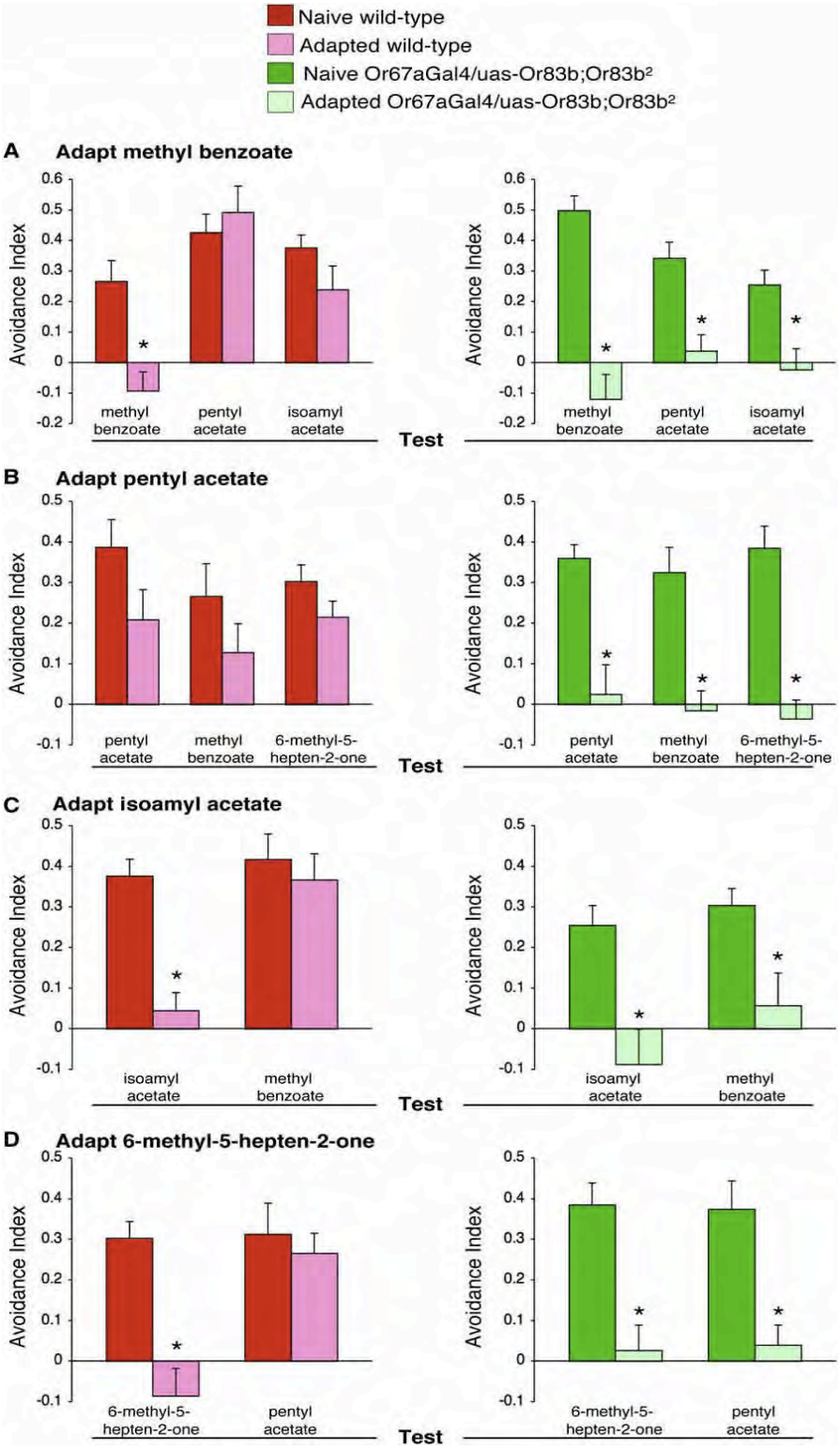
Naive wild-type
Adapted wild-type
Naive Or67aGal4/uas-Or83b;Or83b²
Adapted Or67aGal4/uas-Or83b;Or83b²
A
Adapt methyl benzoate
B
Adapt pentyl acetate
C
Adapt isoamyl acetate
D
Adapt 6-methyl-5-hepten-2-one
Avoidance Index
methyl benzoate
pentyl acetate
isoamyl acetate
6-methyl-5-hepten-2-one
Test

Figure II.3. OR67a restored flies cross-adapt to odorants that activate OR67a neurons. (A) Adaptation of innate odor avoidance behavior in wild-type and OR67a restored flies. Pre-exposing wild-type flies and those with restored OR67a neurons to methyl benzoate adapts methyl benzoate avoidance behavior. Flies with OR67a restored neurons, but not wild-type flies, cross-adapt to methyl benzoate, pentyl acetate and isoamyl acetate. Asterisk indicates significant difference ($P<0.002$, ANOVA) **(B)** Pre-exposure to pentyl acetate significantly adapts pentyl acetate avoidance behavior of flies with restored OR67a neurons ($P<0.002$, ANOVA) but does not significantly adapt wild-type flies ($P>0.1$, ANOVA). Pre-exposure to pentyl acetate cross-adapts methyl benzoate and 6-methyl-5-hepten-2-one avoidance in flies with OR67a restored neurons (both $P<0.001$, ANOVA) but not in wild-type flies ($P>0.2$, ANOVA). **(C)** Pre-exposure to isoamyl acetate cross-adapts the methyl benzoate avoidance behavior of flies with restored OR67a neurons ($P<0.002$, ANOVA) but does not significantly adapt wild-type flies ($P>0.1$, ANOVA). **(D)** Pre-exposure to 6-methyl-5-hepten-2-one cross-adapts pentyl acetate avoidance behavior of flies with restored OR67a neurons ($P<0.002$, ANOVA) but does not significantly adapt wild-type flies ($P>0.1$, ANOVA). Data are mean ± s.e.m.

Figure II.4

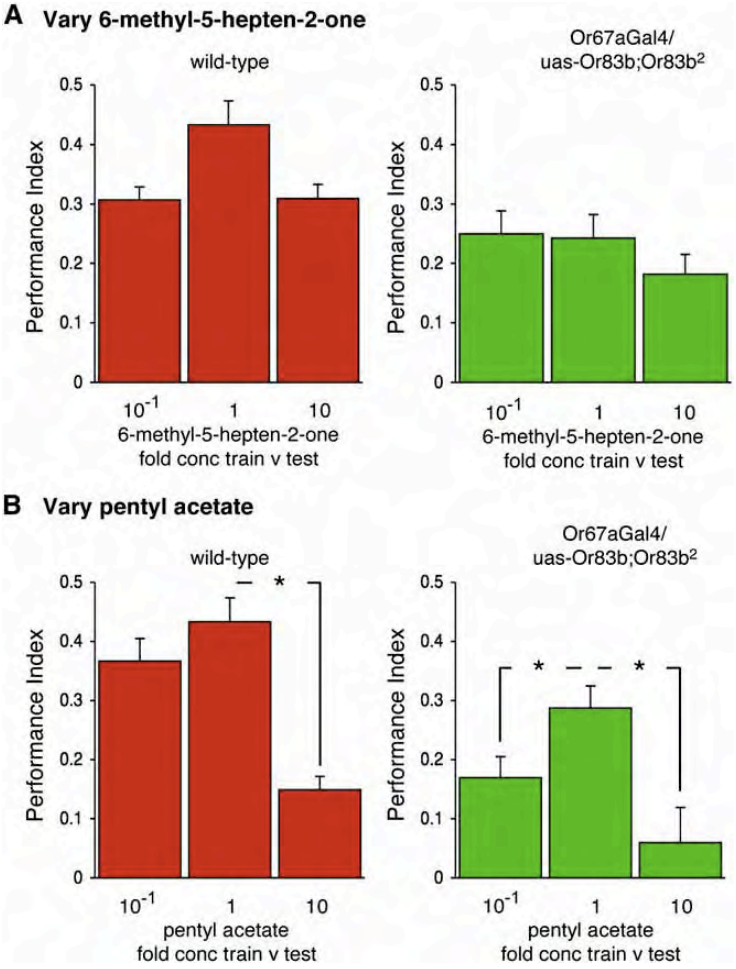
A Vary 6-methyl-5-hepten-2-one
wild-type
Or67aGal4/
uas-Or83b;Or83b2
Performance Index
0.5
0.4
0.3
0.2
0.1
0
10-1
1
10
6-methyl-5-hepten-2-one
fold conc train v test
B Vary pentyl acetate
wild-type
Or67aGal4/
uas-Or83b;Or83b2
*
pentyl acetate
fold conc train v test

Figure II.4. *Or83b*^{2} flies with functional OR67a neurons discriminate odorants across changing concentration. (A) Wild-type flies and OR67a restored flies were trained with 6-methyl-5-hepten-2-one concentrations that were 10X less, the same or 10X more than they were tested with, while pentyl acetate concentrations were kept constant. **(B)** Wild-type flies and those with restored OR67a neurons were trained with pentyl acetate concentrations that were 10X less, the same or 10X more than they were tested with, while 6-methyl-5-hepten-2-one concentrations were kept constant. Asterisks indicate significant difference (all $P<0.01$, ANOVA). Data are mean ± s.e.m.

Figure II.5

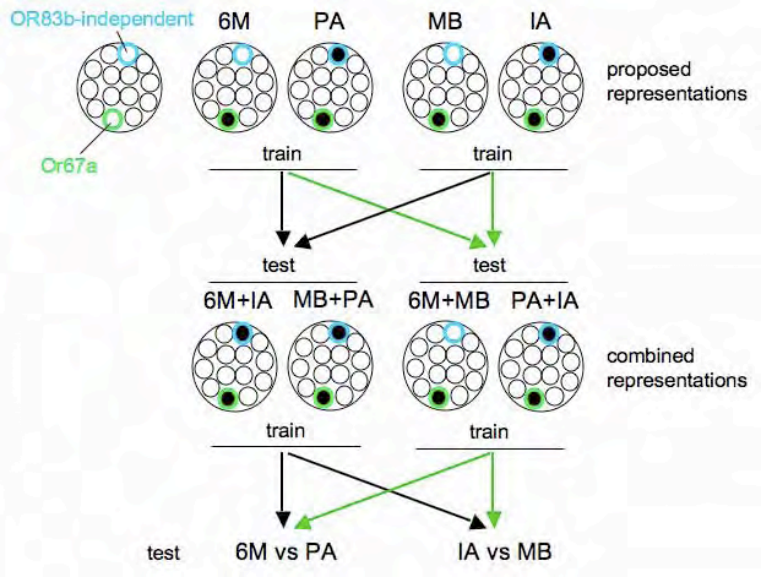

Figure II.5. Results from odor mixture experiments cannot be explained by the OR67a restored flies using spatial coding with OR67a neurons and another class of Or83b-independent neurons. In this model a black-filled circle represents an activated glomerulus. Green arrows represent predicted successful experiments and black arrows are predicted failure. OR67a restored flies can discriminate between 6-methyl-5-hepten-2-one (6M) and pentyl acetate (PA) (Figure II.2D) and between methyl benzoate (MB) and isoamyl acetate (IA) (Figure II.2C). Since all of these odorants activate OR67a neurons (green-edged glomerulus), a spatial coding model requires that only one of each discriminable odorant pair activates the other class of Or83b-independent neurons.

Irrespective of the odorant chosen to activate the Or83b-independent neurons, combining discriminable pairs into mixtures raises a scenario where two of the three mixtures generate identical spatial patterns of activation, and one is

unique. Such a spatial coding model predicts flies will be able to discriminate appropriately when trained with components and tested with 6M+MB versus PA+IA odor blends but that when trained with components and tested 6M+IA versus MB+PA there will be no evidence of learning. Our results do not fit this model because OR67a restored flies show learned discrimination for one of the odorant pairs when tested with either odorant mixture.

Similarly, our results from experiments training flies with mixtures and testing with components do not support a spatial model employing OR67a neurons and another class of Or83b-independent neurons. The spatial model predicts that training with the odorant mixtures will not produce component learning in one case and will produce learning for both components in the other instance. However, OR67a restored flies show learned discrimination for one odorant pair in each experiment.

Figure II.6.

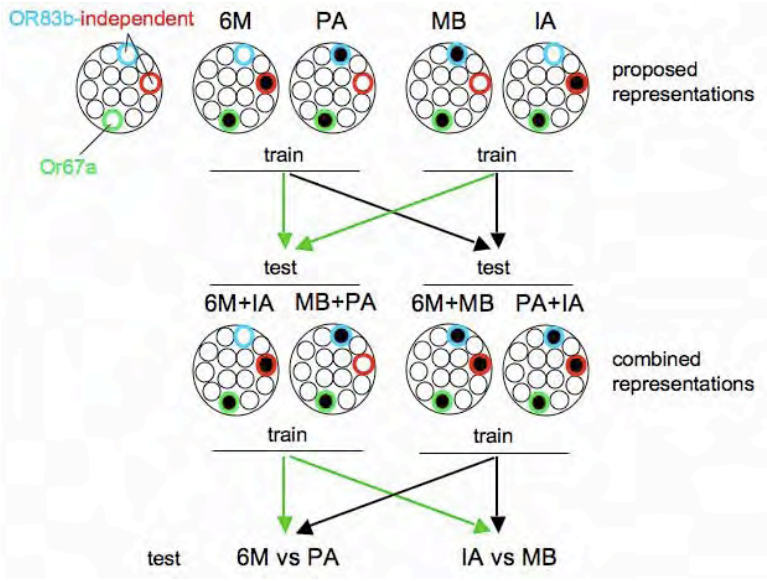

Figure II.6. Results from odor mixture experiments cannot be explained by the OR67a restored flies using spatial coding with OR67a neurons and 2 additional classes of Or83b-independent neurons. Our results show that OR67a restored flies learn one odor from a binary mixture and these results also cannot be explained by increasing the number of available Or83b-independent neurons to two that are activated in a non-overlapping manner. Even that scenario produces mixtures that cannot be discriminated using purely spatial encoding. One could continue to increase the number of putative Or83b-independent ORNs and eventually the flies would be predicted to encode both components of the mixture. However, OR67a restored flies encode one component of a binary mixture. Therefore the most parsimonious explanation is that they utilize a single class of Or83b-dependent ORNs in our experiments.

Figure II.7.

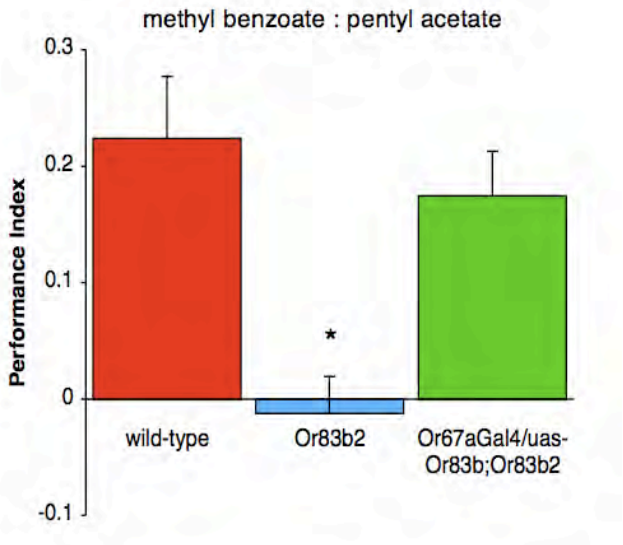

Figure II.7. Flies with only functional OR67a neurons can learn to discriminate between methyl benzoate and pentyl acetate. Asterisk indicates significant difference (*P*<0.005, ANOVA) between the marked group and the others. Data are mean ± s.e.m.

Preface to Chapter III

This chapter has been published separately in:

Krashes, M.J.*, **DasGupta, S*.,** Vreede, A., White, B., Armstrong, J.D., Waddell, S.. A neural circuit mechanism integrating motivational state with memory expression in *Drosophila*. **Cell** *in press.* * equal contribution

DasGupta, S. collected all confocal stacks, projected and processed the final images

Krashes, M.J. performed the behavior experiments

DasGupta, S. and Waddell, S. constructed fly strains

Vreede, A. designed and engineered the uas-*TRPM8* transgene

DasGupta, S., Krashes, M.J., Waddell, S. designed the experiments and wrote the manuscript

Chapter III: Output from the system: A neural circuit mechanism integrating motivational state with memory expression in *Drosophila*

III.A. Introduction

Motivation provides behavior with purpose and intensity and ensures that particular motor actions are expressed at the appropriate time. Although the concept of motivation has interested psychologists and ethologists for decades (Hull, 1951; Tolman, 1932; Thorpe, 1956; Bindra, 1959; Hinde, 1966; Lorenz, 1950; Dethier, 1976; Toates, 1986; Kennedy, 1987), a detailed neurobiological perspective of the mechanisms underlying state-dependent changes in behavior is lacking. Understanding how motivational systems are organized in the brain and how they impact neural circuits that direct behavior is a major question in neurobiology and addresses the functional connection between body and mind.

Hunger is perhaps the most heavily studied of the regulatory, or homeostatic, motivational drive states because food availability is easily manipulated in the laboratory. Hunger results from internally generated metabolic deficit signals and these signals in turn, increase the likelihood that the animal initiates food-seeking behavior (Dethier, 1976; Saper et al., 2002; Abizaid and Horvath, 2008). Models of motivation include learned representations of cues associated with food, such as smell and taste, that provide additional incentive and direction to locate a particular food source (Hull, 1951; Toates, 1986). When the food is located and consumed, the homeostatic process comes full-circle and the motivational drive to feed is neutralized. However, it is unclear how neural systems representing hunger and satiety are integrated with those of memory.

The idea that motivation could be approached experimentally in insects followed seminal studies of food-seeking behavior in the blowfly *Phormia regina* (Dethier, 1976). It was noted that although exposing gustatory receptor neurons on the proboscis to sugar always generated an electrophysiological response, the blowfly did not consistently respond by extending the proboscis. However, a food-deprived blowfly was more likely to respond with proboscis extension. A sophisticated genetic tool-kit for manipulating neural circuits (Keene and Waddell, 2007) coupled with robust behaviors makes the fruit fly *Drosophila melanogaster* ideal to understand the physiological mechanism that underlies such state-dependent behavior.

Drosophila can be efficiently trained to associate odorants with sucrose reward (Tempel et al., 1983; Krashes and Waddell, 2008). Importantly, fruit flies have to be hungry to effectively express appetitive memory performance (Krashes and Waddell, 2008). Therefore motivated decision-making and appetitive memory performance emerges in *Drosophila* when the incentive of the conditioned odor, the learned representation of that odor, and the internal motivational drive state of hunger are positively integrated. This apparent state-dependence implies that signals for hunger and satiety may interact with memory circuitry to regulate the behavioral expression of learned food-seeking behavior. The mushroom body (MB) in the fly brain is a critical site for appetitive memory (Schwaerzel et al., 2003; Keene et al., 2006; Krashes and Waddell, 2008).

Synaptic output from the MB α´β´ neurons is required to consolidate appetitive memory whereas output from the αβ subset is specifically required for memory retrieval (Krashes et al., 2007; Krashes and Waddell, 2008). This anatomy provides a foundation for understanding neural circuit integration between systems representing a motivational state and those for memory.

Neuropeptide Y (NPY) is a highly conserved 36 amino acid neuromodulator that stimulates food-seeking behavior in mammals (Tatemoto et al., 1982; Clark et al., 1984; Kalra, 1997). NPY mRNA levels are elevated in neurons in the arcuate nucleus of the hypothalamus of food-deprived mice (Sahu et al., 1988; Sanacora et al., 1990) and injection of NPY into the paraventricular nucleus increases feeding (Stanley and Leibowitz, 1985). Most impressively, ablating NPY expressing neurons from adult mice leads to starvation (Bewick et al., 2005; Gropp et al., 2005; Luquet et al., 2005). NPY exerts its effects through a family of NPY receptors and appears to have inhibitory function (Colmers et al., 1988; Colmers et al., 1991; Klapstein and Colmers, 1993; Qian et al., 1997; Rhim et al., 1997; Sun et al., 2003; Browning and Travagli, 2003; Lin et al., 2004). NPY therefore must repress the action of inhibitory pathways in order to promote feeding behavior. *Drosophila* Neuropeptide F is an ortholog of NPY, which has a C-terminal amidated phenylalanine instead of the amidated tyrosine in vertebrates (Brown et al., 1999). Evidence suggests that dNPF plays a similar role in appetitive behavior in flies. dNPF overexpression prolongs feeding in

larvae and delays the developmental transition from foraging to pupariation (Wu et al., 2003). Furthermore, overexpressing a dNPF receptor gene, *npfr1* (Garczynski et al., 2002), causes well-fed larvae to eat bitter-tasting food that wild-type larvae will only consume if they are hungry (Wu et al., 2005b).

In this study we exploited dNPF to identify a neural circuit that participates in motivational control of appetitive memory behavior in adult fruit flies. We show that stimulating dNPF neurons promotes appetitive memory performance in fed flies, mimicking the hungry state. *npfr1* is required in dopaminergic (DA) neurons that innervate the MB for satiety to suppress appetitive memory performance. Directly blocking the DA neurons during memory testing reveals performance in fed flies whereas stimulating them suppresses performance in hungry flies. These data suggest that six DA neurons are a key module of dNPF-regulated circuitry, through which the internal motivational states of hunger and satiety are represented in the MB.

III.B. Results

Stimulating dNPF neurons promotes memory retrieval in fed flies

Feeding flies after appetitive conditioning suppresses memory performance (Figure III.1A) and the suppression is reversed by re-starving flies (Krashes and Waddell, 2008). Food-deprivation is also required for efficient appetitive learning but a learning defect could simply result from satiated flies failing to ingest the reinforcing sucrose. In this study we specifically manipulated memory retrieval and in all experiments we ensured that flies were efficiently trained, by food-depriving them for 18hr before training. Immediately after training we transferred flies to vials with, or without, food for 3hr before testing appetitive memory. Flies starved before and after training display robust appetitive memory but memory performance steadily declines following 10-30min of feeding (Figure III.1A) indicating a continuum of performance relative to the satiety state of the flies.

Immunostaining for dNPF in adult fly brains reveals neurons in the subesophageal ganglion (SOG), the dorsal and lateral protocerebrum and the central complex (CC) (Wen et al., 2005; and Figure III.1B). One can control some of these neurons using a *dNPF* promoter-driven GAL4 to express GAL4-uas promoter driven transgenes (Wen et al., 2005). *dNPF*-GAL4 driven uas-*CD8::GFP* labels most of the dNPF-immunoreactive neurons whose cell bodies reside in the dorsal protocerebrum but not those whose somata are clustered in the SOG (Figure III.1B and 8).

We reasoned that dNPF release might represent the food-deprived state in the brain and so tested whether stimulating dNPF-expressing neurons could over-ride the suppression of memory performance by feeding. We expressed the heat-sensitive uas-*dTrpA1* transgene (Hamada et al., 2008) with *dNPF*-GAL4. *dTrpA1* encodes a Transient Receptor Potential (TRP) channel that is required in a small number of neurons in the brain for temperature preference in *Drosophila* (Hamada et al., 2008). Ectopically expressed dTRPA1 conducts Ca^{2+} and depolarizes neurons when flies are exposed to >25°C allowing one to stimulate specific neurons. We first food-deprived and trained wild-type, *dNPF*-GAL4, uas-*dTrpA1* and *dNPF*-GAL4; uas-*dTrpA1* flies, fed them *ad libitum* for 3-hours and tested appetitive memory at the permissive 23°C. No group showed robust appetitive memory under these conditions (Figure III.1C) and no statistical differences were apparent between groups (P>0.57). However, stimulating dNPF neurons for 30min before and during testing by shifting the flies to 31°C revealed memory performance in *dNPF*-GAL4;uas-*dTrpA1* flies that was statistically different from all other groups (P<0.006)(Figure III.1D). Therefore stimulating dNPF neurons mimics food-deprivation consistent with dNPF being a key factor in the internal state of hunger in the brain.

Localizing the relevant dNPF modulated circuit

We used a uas-RNA interference (RNAi) transgene against the dNPF receptor, uas-*npfr1*^{RNAi} (Wu et al., 2003; Wu et al., 2005b) to localize the relevant dNPF modulated neurons, reasoning that *npfr1* disruption would impair appetitive memory in hungry flies. We verified the efficacy of the uas-*npfr1*^{RNAi} transgene for our purpose by expressing it in all neurons using *n-synaptobrevin*-GAL4 and testing appetitive memory performance. As expected the memory performance of uas-*npfr*^{1RNAi};*n-syb*-GAL4 flies was impaired and was statistically different from all other control groups ($P<0.04$). However, uas-*npfr1*^{RNAi};*n-syb*-GAL4 flies were normal for aversive olfactory conditioning (Tully and Quinn, 1985)(Figure III.9). We next drove uas-*npfr1*^{RNAi} with GAL4 drivers that express in the dorsal protocerebrum and CC - c005, 210Y, 104Y and c061 and in all MB neurons or the MB αβ and γ neurons - OK107 and MB247. We food-deprived wild-type flies, flies with a piggyBac element in the *npfr1* locus (Bellen et al., 2004), flies expressing uas-*npfr1*^{RNAi} in specific neurons, and flies harboring GAL4 or uas-*npfr1*^{RNAi} alone, and tested appetitive memory 3 hr after training. The performance of *npfr1*[c01896] and c061;uas-*npfr1*^{RNAi} flies was statistically different (both $P<0.01$) from all other flies (Figure III.2). These data suggest c061 neurons mediate the effects of dNPF on appetitive memory expression.

Some c061 neurons innervate the MB

We visualized c061 neurons with uas-*CD8::GFP*. Confocal analysis revealed expression including intrinsic neurons of the MBs (Figure III.3A). Since MB expression of uas-*npfr1*^{RNAi} did not disrupt memory (Figure III.2), we crossed in a GAL80 transgene that blocks GAL4 activity in all MB neurons (MBGAL80; Krashes et al., 2007). MBGAL80 abolished MB expression but prominent expression remained in three neurons per hemisphere whose projections densely innervate the MB heel and peduncle. Another cluster of five neurons per hemisphere innervate a specific layer in the fan-shaped body of the CC (Figure III.3B, 5A, 15 and Movies S1 and S2). Higher resolution imaging revealed innervation of the MB peduncle occupied by αβ but not α´β´ neurons (Figure III.3E). Output from α´β´ neurons is required to consolidate appetitive memory whereas output from αβ neurons is required for appetitive memory retrieval (Krashes et al., 2007; Krashes and Waddell, 2008). Finding neurons that innervate the MB heel and αβ neurons is consistent with a model where satiety affects memory retrieval by modulating MB αβ and γ neurons.

The MB-innervating neurons are dopaminergic

Some DA neurons innervate the MB heel and base of the peduncle (Friggi-Grelin et al., 2003; Riemensperger et al., 2005; Tanaka et al., 2008, Figure III.11). We therefore immunostained c061;MBGAL80;uas-*CD8::GFP* brains with anti-

tyrosine hydroxylase (TH) antibody. TH specifically labels DA neurons in flies because they do not produce epinephrine or norepinephrine. This analysis revealed that the three c061 MB-innervating neurons double label with GFP and anti-TH (Figure III.3F) consistent with them releasing dopamine. Their position by the MB calyx defines them as belonging to the protocerebral posterior lateral 1 (PPL1) DA neuron cluster (Friggi-Grelin et al., 2003; Riemensperger et al., 2005). Finding the MB-innervating neurons label for TH allowed us to use a *TH*-promoter driven GAL80 (*TH*GAL80) to remove DA neuron expression (Sitaraman et al., 2008). We combined c061 and c061; MBGAL80 with *TH*GAL80 and uas-*CD8::GFP* and visualized brains co-labeled with anti-TH. *TH*GAL80 suppressed GFP expression in DA neuron somata (Figure III.3C, D and G) and eliminated expression in processes innervating the heel and peduncle region of the MB (Figure III.3C and 3D). Expression remained in c061; *TH*GAL80 brains in MB, fan-shaped body and SOG (Figure III.3C). In c061; MBGAL80/*TH*GAL80 brains, expression remained in the fan-shaped body and SOG (Figure III.3D). Therefore c061 DA neurons innervate the dorsal protocerebrum and MB heel and peduncle. Transgenic markers of neural polarity suggest DA processes in the dorsal protocerebrum are postsynaptic while those in the MB heel and peduncle are presynaptic (Zhang et al., 2007; and data not shown).

npfr1 expression in DA neurons is required for appetitive memory

We tested the importance of *npfr1* in DA neurons by expressing uas-*npfr1*^{RNAi} with *TH*-GAL4. We food-deprived flies before and after training and tested 3hr appetitive memory. Performance of *TH*-GAL4; uas-*npfr1*^{RNAi} flies was statistically different from that of wild-type, *TH*-GAL4 and uas-*npfr1*^{RNAi} control flies ($P<0.01$; Figure III.4A). We also used *TH*GAL80 to test whether DA neuron expression was required for the appetitive memory defect of c061;uas-*npfr1*^{RNAi} flies. Memory of c061;*TH*GAL80;uas-*npfr1*^{RNAi} flies was statistically indistinguishable from controls ($P>0.9$) and was statistically different from that of c061;uas-*npfr1*^{RNAi} and *TH*GAL4; uas-*npfr1*^{RNAi} flies (Figure III.4A). Therefore *npfr1* expression is required in DA neurons that innervate the MB for appetitive memory performance in hungry flies.

Blocking DA neurons promotes memory retrieval in fed flies

We used c061; MBGAL80 and *TH*GAL80 to test whether DA neurons were responsible for inhibiting memory performance in fed flies. We directly blocked their output during memory testing with the dominant temperature-sensitive uas-*shibire*^{ts1} (*shi*^{ts1}) transgene (Kitamoto, 2001). *shi*^{ts1} blocks membrane recycling and thus synaptic vesicle release at the restrictive temperature of 31°C and this blockade is reversible by returning flies to <25°C. Flies were food deprived, trained and immediately transferred to vials containing food before testing 3 hr

memory. We performed this experiment at 23°C throughout (Figure III.4B), or we blocked the neurons prior to, and during memory retrieval by shifting flies to 31°C for 1hr before testing (Figure III.4C). We tested wild-type and single transgene GAL4 and uas-*shi*^{ts1} flies in parallel. At 23°C performance was suppressed by feeding and there were no significant differences between groups (P>0.77; Figure III.4B). However, when c061; MBGAL80; uas-*shi*^{ts1} neurons were blocked prior to and during retrieval appetitive memory performance was statistically different from all other groups (all P<0.04) (Figure III.4C). Expressing uas-*shi*^{ts1} in c061; MBGAL80 neurons except the DA neurons did not enhance performance (Figure III.4C). Memory of c061; MBGAL80 /*TH*GAL80; uas-*shi*^{ts1} flies was statistically indistinguishable from the control groups (P>0.99). Importantly, blocking DA neurons did not further enhance hungry fly performance (all P>0.17; Figure III.4D). Therefore these data are consistent with the DA neurons limiting memory performance in fed flies. It is likely that dopamine provides the inhibition because the DA neurons do not label for the inhibitory transmitter gamma-aminobutyric acid, GABA (Figure III.10).

The DA neurons are MB-MP neurons

Similar neurons that innervate the MB have been described (Tanaka et al., 2008). NP2758 labels a single pair of MB-MP neurons, named according to the regions of the MB that they innervate: medial lobe and pedunculus (MP) (Figure

III.5B, 16 and Movies S3 and S4). From here we refer to MB-innervating DA neurons as MB-MP neurons. We also found that *krasavietz*-GAL4 (Dubnau et al., 2003; Shang et al., 2007) combined with MBGAL80 (Krashes et al., 2007) expresses in MB-MP neurons (Figure III.5C and Movies S5 and S6).

We counted the TH positive neurons in the PPL1 cluster in each GAL4 line (Figure III.5E and 11B). Three TH positive cells are labeled by GFP in each PPL1 cluster in c061; MBGAL80;uas-*CD8::GFP* flies. MBGAL80; *krasavietz*/uas-*CD8::GFP* also labels three TH neurons but two are MB-MP neurons and the other innervates the vertical MB α lobe (Figure III.5C and 11C). Lastly, we confirmed that NP2758;uas-*CD8::GFP* labels one MB-MP neuron per hemisphere. We combined the lines in pairs and counted cells co-labeled with GFP and anti-TH to determine whether c061, *krasavietz* and NP2758 label overlapping MB-MP neurons. Four cell bodies are labeled in PPL1 in c061; MBGAL80;*krasavietz* flies. One of these is the α lobe projecting *krasavietz* neuron (Figure III.5C, 5D and 11), so MBGAL80;*krasavietz* labels two of the three c061 MB-MP neurons. Three cell bodies are labeled in PPL1 in NP2758; MBGAL80; *krasavietz* flies showing that NP2758 labels one of the two MBGAL80; *krasavietz* MB-MP neurons. Therefore c061;MBGAL80 labels three MB-MP neurons, MBGAL80;*krasavietz* labels two of these and NP2758 labels one of the MB-MP neurons that is common to c061;MBGAL80 and MBGAL80;*krasavietz* (Figure III.5D). We did not observe more than three MB-MP

neurons on each side of the brain.

Blocking NP2758 or *krasavietz*;MBGAL80 neurons prior to, and during memory retrieval did not reveal performance in fed flies (Figure III.12). Therefore it is either necessary to block all six MB-MP neurons to release appetitive memory in fed flies or the two MB-MP neurons uniquely labeled by c061 could be responsible.

MB-MP stimulation inhibits appetitive memory expression in hungry flies

To further assess whether MB-MP neurons limit appetitive memory expression, we tested whether MB-MP neuron stimulation suppressed memory in hungry flies. We tested wild-type flies, flies expressing uas-*dTrpA1* in MB-MP neurons and GAL4 and uas-*dTrpA1* flies in parallel using two different temperature regimens; permissive 23°C throughout (Figure III.6A), or we stimulated neurons prior to, and during memory retrieval by shifting flies to 31°C (Figure III.6B). We starved flies, trained them and transferred them to empty vials before testing 3hr memory. All groups displayed robust appetitive memory at 23°C and there was no statistical difference between groups ($P>0.96$) (Figure III.6A). However, acute MB-MP neuron stimulation prior to, and during memory retrieval severely impaired memory (Figure III.6B). The performance of c061; MBGAL80/uas-*dTrpA1* flies, MBGAL80/uas-*dTrpA1*;*krasavietz* flies and NP2758;uas-*dTrpA1*

flies was statistically different from all other groups (P<0.04). These data suggest that stimulating two MB-MP neurons is sufficient to block appetitive memory performance.

The suppression of performance with MB-MP activation is not due to irreversible MB damage. Food-deprived c061;MBGAL80/uas-*dTrpA1* flies stimulated during acquisition (Figure III.13A) or for 1hr after training (Figure III.13B) showed normal 3 hr memory (P>0.58 and P>0.70 respectively). Furthermore, brief stimulation during testing is sufficient to suppress performance (P<0.005; Figure III.13C).

We also stimulated MB-MP neurons with the cold-sensitive uas-*TRPM8* transgene (Peabody et al., 2009). The mammalian TRPM8 channel is activated below 18°C (McKemy et al., 2002; Peier et al., 2002). We starved and trained flies and put them in empty food vials for 3 hr before testing appetitive memory. No statistical difference was apparent between the performance of flies at the permissive 23°C (P>0.50) (Figure III.6C). However, stimulating c061-MB-MP neurons by shifting flies to 16°C for 1hr before testing impaired memory (Figure III.6D). Performance of c061;MBGAL80;uas-*TRPM8* flies was statistically different from all other groups (P<0.03). Therefore stimulating MB-MP neurons with dTRPA1 or TRPM8 suppresses performance in hungry flies (Figure III.6B and D) and mimics feeding (Figure III.1A).

To exclude the possibility that manipulations with uas-*shi*^{ts1} and uas-*dTrpA1* interfere with olfaction or gustation, we tested the acuity of all flies used in this study. No significant differences were found between the relevant groups for either odor or sucrose acuity (Table III.1). Therefore blocking output from MB-MP neurons reveals appetitive memory performance in satiated flies whereas stimulating them suppresses appetitive memory expression in hungry flies. These data are consistent with MB-MP neurons being a neural mechanism through which satiety suppresses appetitive memory performance.

III.C. Discussion

Drosophila as a model for motivational systems

It is critical to an animal's survival that behaviors are expressed at the appropriate time. Motivational systems provide some of this behavioral control. Apart from the observation that motivational states are often regulated by hormones or neuromodulatory factors (Toates, 1986; Watts, 2003), we know little about how motivational states modulate specific neural circuitry. Hungry fruit flies form appetitive long-term memory following a 2 min pairing of odorant and sucrose and memory performance is only robust if the flies remain hungry (Krashes and Waddell, 2008). Therefore this paradigm includes key features of models for motivational systems (Toates, 1986): the conditioned odor provides the incentive cue predictive of food, there is a learned representation of the goal

object (odorant/sucrose), and the expression of learned behavior depends on the internal physiological state (hunger and not satiety). In this study we identified a neural circuit mechanism that integrates hunger/satiety and appetitive memory.

What normally regulates dNPF-expressing neurons?

We do not know the signals that ordinarily control dNPF-releasing neurons. In mammals NPY-expressing neurons are a critical part of a complex hypothalamic network that regulates food-intake and metabolism (Saper et al., 2002). In times of adequate nutrition, NPY-expressing neurons are inhibited by high levels of leptin and insulin that are transported into the brain following release from adipose tissue and the pancreas (Figlewicz and Benoit, 2009). In hungry mice, leptin and insulin levels fall leading to loss of inhibition of NPY neurons. Flies do not have leptin but they have several insulin-like peptides (Arquier et al., 2008), that may regulate dNPF neurons. Some NPY expressing neurons are directly inhibited by glucose (Levin et al., 2006). Fly neurons could sense glucose with the Bride of Sevenless receptor (Kohyama-Koganeya et al., 2008). In blowflies satiety involves mechanical tension of the gut and abdomen (Gelperin, 1967; Gelperin, 1971). Lastly, it will be interesting to test the role of other extracellular signals implicated in fruit fly feeding behavior including the hugin (Melcher and Pankratz, 2005) and take-out neuropeptides (Sarov-Blat et al., 2000; Meunier et al., 2007).

A model for the role of MB-MP neurons

NPY inhibits synaptic function in mammals (Colmers et al., 1988; Colmers et al., 1991; Klapstein and Colmers, 1993; Qian et al., 1997; Rhim et al., 1997; Sun et al., 2003; Browning and Travagli, 2003; Lin et al., 2004) and our data suggest that dNPF promotes appetitive memory performance by suppressing inhibitory MB-MP neurons. We propose a model where MB-MP neurons gate MB output (Figure 7). Appetitive memory performance is low in fed flies because the MB αβ and γ neurons are inhibited by tonic dopamine release from MB-MP neurons.

Hence, when the fly encounters the conditioned odorant during memory testing, the MB neurons encoding that olfactory memory respond, but the signal is not propagated beyond the MB due to the inhibitory influence of MB-MP neurons. However, when the flies are food-deprived dNPF levels rise and dNPF disinhibits MB-MP neurons, and other circuits, through the action of NPFR1. dNPF disinhibition of the MB-MP neurons opens the gate on the MB. Therefore, when hungry flies encounter the conditioned odorant during memory testing, the relevant MB neurons are activated and the signal propagates to downstream neurons, leading to expression of the conditioned behavior. Satiety and hunger are not absolute states. We sometimes observe above chance performance scores in fed flies and shorter periods of feeding after training suggest that inhibition of performance is graded. This could be accounted for by a competitive push-pull inhibitory mechanism between dNPF and MB-MP neurons.

By gating the MB through the MB-MP neurons, hunger and satiety are likely affecting the relative salience of learned odor cues in the fly brain. However, MB-MP neurons are unlikely to change the sensory representation of odor in the MB because flies trained with stimulated MB-MP neurons perform normally when tested for memory without stimulation (Figure III.13A). Therefore odors are likely perceived the same irrespective of MB-MP neuron activity. Furthermore, the MB-MP neurons did not affect naïve responses to the specific odorants used. It will be interesting to test whether MB-MP neurons change responses to other odorants and/or modulate arousal (Andretic et al., 2005; Kume et al., 2005; Seugnet et al., 2008), visual stimulus salience (Zhang et al., 2007) and attention-like phenomena (van Swinderen, 2007).

Structural and functional subdivision of DA neurons

There are eight different morphological classes of DA neurons that innervate the MB (Mao and Davis, 2009) and our data imply functional subdivision. Previous studies concluded that DA neurons convey aversive reinforcement (Schwaerzel et al., 2003; Schroll et al., 2006; Riemensperger et al., 2005 and see Figure III.14). We specifically manipulated the MB-MP DA neurons. MB-MP neurons are not required for acquisition of aversive olfactory memory ($P>0.94$)(Figure III.14) consistent with a distinct function in controlling the expression of appetitive memory. Since several studies have implicated the MB α lobe in memory

(Pascual and Preat, 2001; Yu et al., 2005; Yu et al., 2006), other DA neurons in PPL1 that innervate the α lobe (like those labeled in MBGAL80;*krasavietz*, Figure III.5C and 11) may provide reinforcement. The MB-MP neurons may also be functionally divisible and independently regulated to gate MB function. The idea that a specific DA circuit restricts stimulus-evoked behavior is reminiscent of literature tying dopamine to impulse control in mammals (Weintraub, 2008; Blum et al., 1996). Previous studies of DA neurons in *Drosophila* (Schwaerzel et al., 2003; Schroll et al., 2006; Seugnet et al., 2008; Andretic et al., 2005; Kume et al., 2005; Seugnet et al., 2008; Zhang et al., 2007) have simultaneously manipulated all, or large numbers of DA neurons. Our data suggest that the DA neurons should be considered as individuals, or small groups.

Motivation and learning in flies

Flies have to be hungry to efficiently acquire appetitive memory but whether this reflects a state-dependent neural mechanism or results from the failure to ingest enough sugar is unclear. Stimulating MB-MP neurons in hungry flies did not impair appetitive memory formation (Figure III.13A) and therefore MB-MP neurons are unlikely to constrain learning in fed flies. Other dNPF-regulated neurons may provide this control since NPY has been implicated in learning (Redrobe et al., 2004).

Hunger simultaneously regulates discrete neural circuit modules

The dNPF-expressing neurons innervate broad regions of the brain and may simultaneously modulate distinct neural circuits to promote food-seeking. MB-MP neurons represent a circuit through which the salience of learned food-relevant odorant cues is regulated by relative nutritional state. Given the apparent role of the MB as a locomotor regulator (Huber, 1967; Martin et al., 1998; Pitman et al., 2006; Joiner et al., 2006), MB-MP neurons may also generally promote exploratory behavior. There are likely to be independent circuits for other elements of food-seeking behavior including those that potentiate gustatory pathway sensitivity and promote ingestion. NPY stimulates feeding but inhibits sexual behavior in rats (Clark et al., 1985). Modulators exerting differential effects could provide a neural mechanism to establish a hierarchy of motivated states and coordinate behavioral control. dNPF may potentiate activity in food-seeking related circuits while suppressing circuits required for other potentially competing behaviors, eg. sexual pursuit.

Regulating behavior with inhibitory control

In this study we provide the first multi-level neural circuit perspective for a learned motivated behavior in fruit flies. Our work demonstrates a clear state-dependence for the expression of appetitive memory. Odorants that evoke conditioned appetitive behavior in hungry flies are ineffective at evoking appetitive behavior in satiated flies. Therefore the fly brain is not simply a

collection of input-output reflex units and includes neural circuits through which the internal physiological state of the animal establishes the appropriate context for behavioral expression.

Dethier (1976) proposed that ‘a satiated fly receives maximum inhibitory feedback so that sensory input is behaviorally ineffective. As deprivation increases inhibition wanes and sensory input becomes increasingly effective in initiating feeding’. Our data provide experimental evidence that this prediction is also likely to be accurate for expression of appetitive memory in the fruit fly where the mechanism involves neuromodulation in the central brain. The DA MB-MP neurons inhibit the expression of appetitive memory performance in satiated flies whereas dNPF disinhibits the MB-MP neurons in food-deprived flies. The likelihood that appetitive behavior is triggered by the conditioned odorant is therefore determined by the competition between inhibitory systems in the brain.

The concept that continuously active inhibitory forces in the insect brain control behavioral expression was also proposed many years ago (Roeder, 1955). Here we provide evidence that these neurons exist and that their hierarchical arrangement is a key determinant of behavioral control.

III.D. Experimental Procedures

Fly strains

Fly stocks were raised on standard cornmeal food at 23°C and 60% relative humidity. The wild-type *Drosophila* strain used was Canton-S. The *dNPF* (Wen et al., 2005), c061 (www.flytrap.org), 210Y, c005, 104Y (Liu et al., 2006), OK107 (Connolly et al., 1996) MB247 (Zars et al., 2000), TH-GAL4 (Friggi-Grelin et al., 2003), NP2758 (Tanaka et al., 2008) and *krasavietz* (Dubnau et al., 2003; Shang et al., 2007) GAL4 lines are described. *n-synaptobrevin*-GAL4 flies were a gift from Julie Simpson (HHMI Janelia Farm Research Campus). c061 and *krasavietz* were combined with the previously described MBGAL80 transgene (Krashes et al., 2007). The uas-*npfr1*^{RNAi} (Wu et al., 2003), uas-*dcr2* (Dietzl et al., 2007), *TH*GAL80 (Sitaraman et al., 2008), uas-*shi*^{ts1} (Kitamoto, 2001), uas-d*TrpA1* (Hamada et al., 2008) and MB-DsRED (Riemensperger et al., 2005) flies are described. *TH*GAL80 was combined with uas-*shi*^{ts1} on the 3rd chromosome. To express *dTRPA1* in dNPF neurons we crossed uas-*dTrpA1* females to *dNPF*-GAL4 male flies. To screen for neurons that required *npfr1* we crossed female uas-*npfr1*^{RNAi} flies to c061, c061; *TH*GAL80, 210Y, c005, 104Y, OK107, MB247, *TH*-GAL4, *n-syb* or *n-syb*; uas-*dcr2* males. c061 is located on the X-chromosome so female c061;MBGAL80 flies were crossed to uas-*shi*^{ts1} males. Similarly, we crossed c061;MBGAL80 females with *TH*GAL80; uas-*shi*^{ts1} males. To express uas-*shi*^{ts1} in MB-MP neurons female uas-*shi*^{ts1} flies were crossed to NP2758 or

MBGAL80; *krasavietz* males. Since NP2758 is on the X-chromosome, only female flies were assayed from the NP2758 cross. We expressed dTRPA1 in the MB-MP neurons by crossing female uas-*dTrpA1* flies to NP2758 or MBGAL80;*krasavietz* males or c061;MBGAL80 females with *uas-dTrpA1* males. All GAL4 and uas-transgene flies were crossed with wild-type females to create heterozygous controls. We visualized GAL4 expression by crossing to uas-*mCD8::GFP or* uas-*mCD8::GFP*; MB-DsRED flies (Lee and Luo, 1999; Riemensperger et al., 2005).

Behavioral analysis

All flies were food deprived for 16–20 hr before training in milk bottles containing a 10x6cm filter paper soaked with water. The olfactory appetitive paradigm was performed as described (Krashes and Waddell, 2008). Following training, flies were stored for 3hr in vials with food or containing only a water-damp filter paper. All experiments performed after feeding included a control group of food-deprived flies. The performance index (PI) was calculated as the number of flies choosing the conditioned odor minus the number of flies choosing the unconditioned odor divided by the total number of flies in the experiment. A single PI value is the average score from flies of the identical genotype tested with each odor (3-Octanol or 4-Methylcyclohexanol). Olfactory and gustatory acuity was performed according to Keene et al. (2006).

Statistical analyses were performed using KaleidaGraph (Synergy Software). Overall analyses of variance (ANOVA) were followed by planned pairwise comparisons between the relevant groups with a Tukey HSD post-hoc test. Unless stated otherwise, all experiments are n≥8.

Immunohistochemistry

Adult female flies were collected 3-5 days after eclosion, brains or entire central nervous systems were dissected in ice-cold PBS [1.86mM NaH_2PO_4, 8.41mM Na_2HPO_4, 175mM NaCl] and fixed in 2% paraformaldehyde solution in PBS for 10min at room temperature (RT). Samples were then washed 5X for 15min with PBS containing 0.25% Triton-X100 (PBT), blocked for 1hr with PBT containing 5% NGS (all at RT) and incubated with primary antibody in blocking solution for 2 days at 4°C. Samples were washed 5X for 15 min in PBT, incubated with secondary antibody in PBT for 12 hr at 4°C and washed 10X for 15min with PBT, 2X in PBS for 15min and mounted in Vectashield (Vector Labs) for confocal microscopy. Imaging was performed on a Zeiss LSM 5 Pascal confocal microscope and images were processed in ImageJ, Adobe Photoshop and Amira software. In some cases, debris on the brain surface was manually deleted from the relevant confocal sections to permit construction of a clear projection view of the z-stack. Antibodies were diluted: mouse IgG_{2a} anti-GFP (Invitrogen 1:200);

rabbit anti- Tyrosine hydroxylase (Chemicon 1:100); rabbit anti-dNPF (gift from P. Shen 1:2000); rabbit anti-GABA (Sigma 1:100); mouse monoclonal 4B1 anti-Drosophila ChAT (Hybridoma Bank, University of Iowa 1:100), FITC conjugated anti-Mouse IgG_{2a}(Jackson Laboratory 1:200); Cy3 conjugated anti-Rabbit (Jackson Laboratory 1:200); Cy5 conjugated anti-Mouse $IgG_{1\gamma}$ (Jackson Laboratory 1:200).

Figure III.1

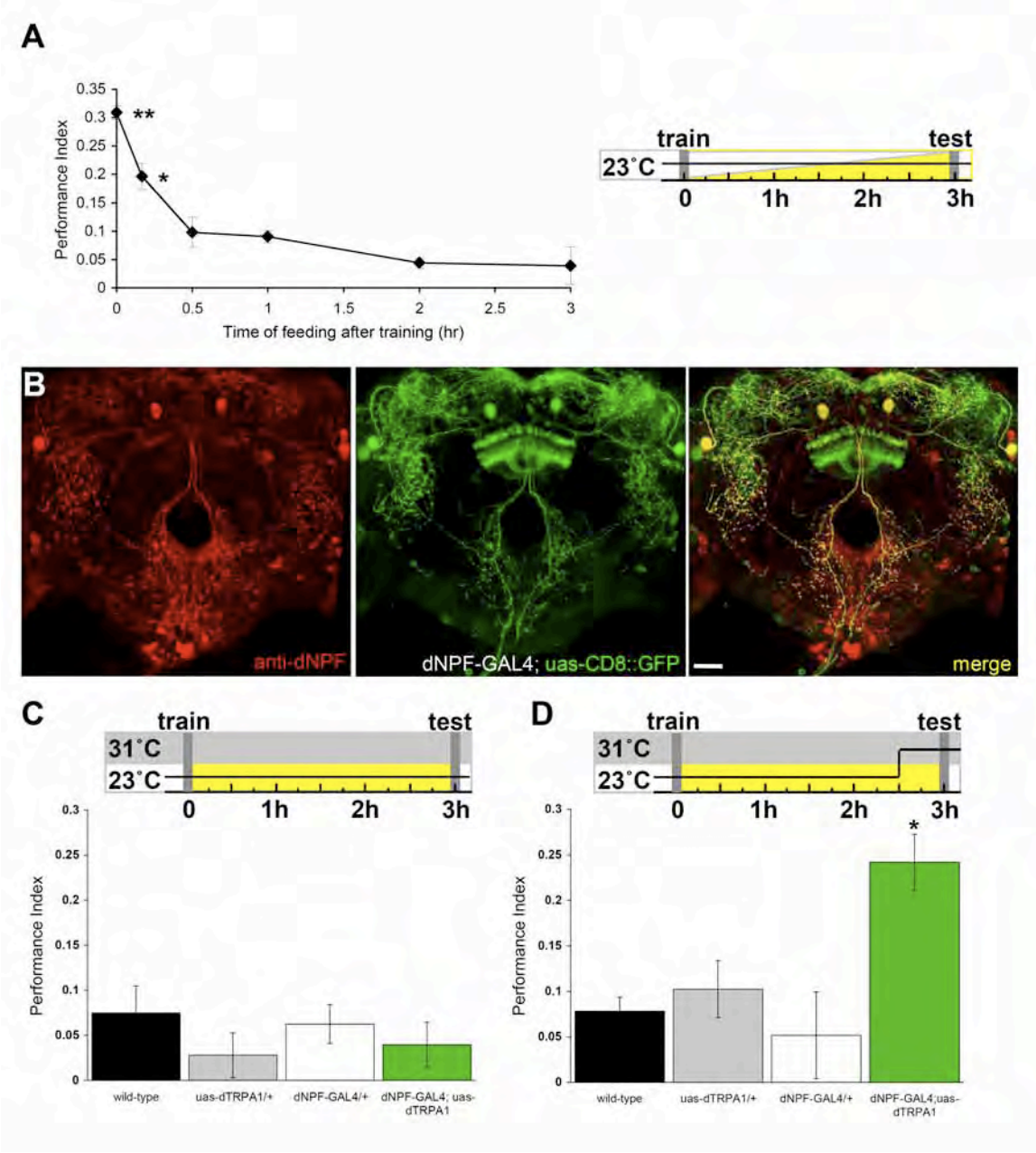

Figure III.1. Stimulating dNPF-expressing neurons promotes appetitive memory expression in satiated flies. (A). Feeding for 3hr after training

suppresses appetitive memory performance. Double asterisk, significant difference ($P<0.007$) from all other groups. Single asterisk, significant difference ($P<0.03$) from all other groups. The temperature shift protocols are shown pictographically. A white bar represents storage of flies in empty vials, while a yellow bar indicates flies stored in food vials. This figure format is used throughout this study. **(B)** dNPF is expressed in large neurons that densely innervate the dorsal and lateral protocerebrum, the subesophageal ganglion and the central complex. Immunostaining with an anti-dNPF antibody (red), partially overlaps (yellow, merge) with expression of *dNPF*-GAL4 driven CD8::GFP (green). The dNPF positive cell bodies in the subesophageal ganglion are not labeled by *dNPF*-GAL4. Furthermore, the anti-dNPF antibody only labels the upper layer of the fan-shaped body of the central complex, consistent with the processes in the ellipsoid body and lower layer of the fan-shaped body being post-synaptic regions of *dNPF*-expressing neurons. Scale bar represents 20μm. **(C)** Feeding flies after training at the permissive temperature of 23˚C suppresses 3 hr memory performance. All flies were food-deprived, trained, fed and tested at 23˚C. **(D)** Stimulating dNPF neurons for 30 minutes before testing produces memory performance in fed flies. All flies were food-deprived, trained, and fed for 150min at 23˚C. At that time all flies were transferred to 31˚C for 30min and tested for appetitive memory performance. Asterisk denotes significant difference ($P<0.05$, ANOVA) from other unmarked groups. Data are mean ± standard error of the mean (SEM).

Figure III.2.

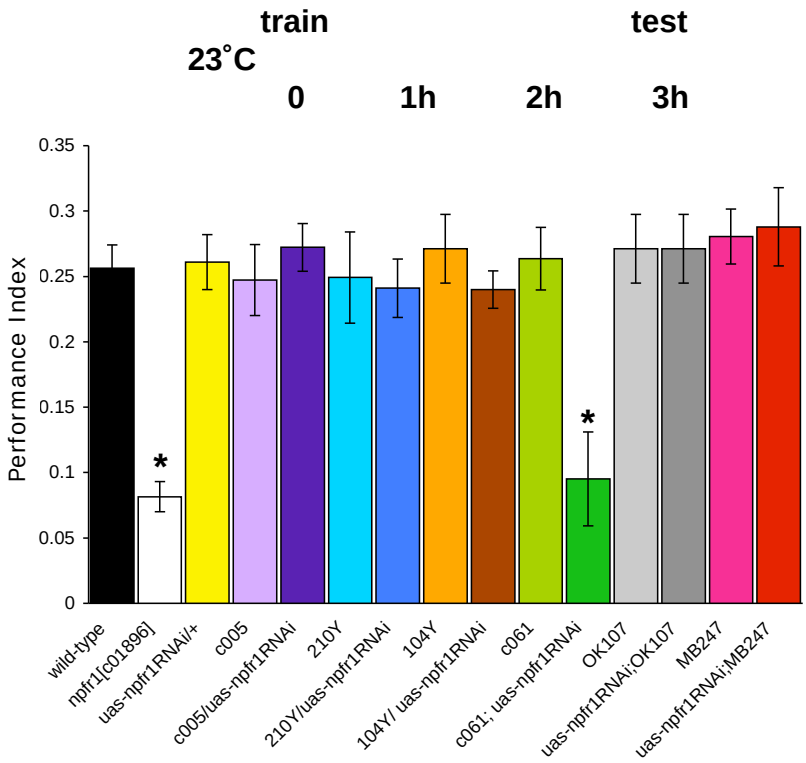

Figure III.2. Region-specific disruption of *npfr1* expression impairs appetitive olfactory memory in food-deprived flies. (A) Expressing a uas-*npfr1*^{RNAi} transgene with c061 impairs 3 hr appetitive memory in food-deprived flies whereas expressing the uas-*npfr1*^{RNAi} with 210Y, c005, 104Y, OK107 or MB247 GAL4 control has no effect. Asterisk denotes significant difference ($P<0.05$, ANOVA) from other unmarked groups. Data are mean ± SEM.

Figure III.3

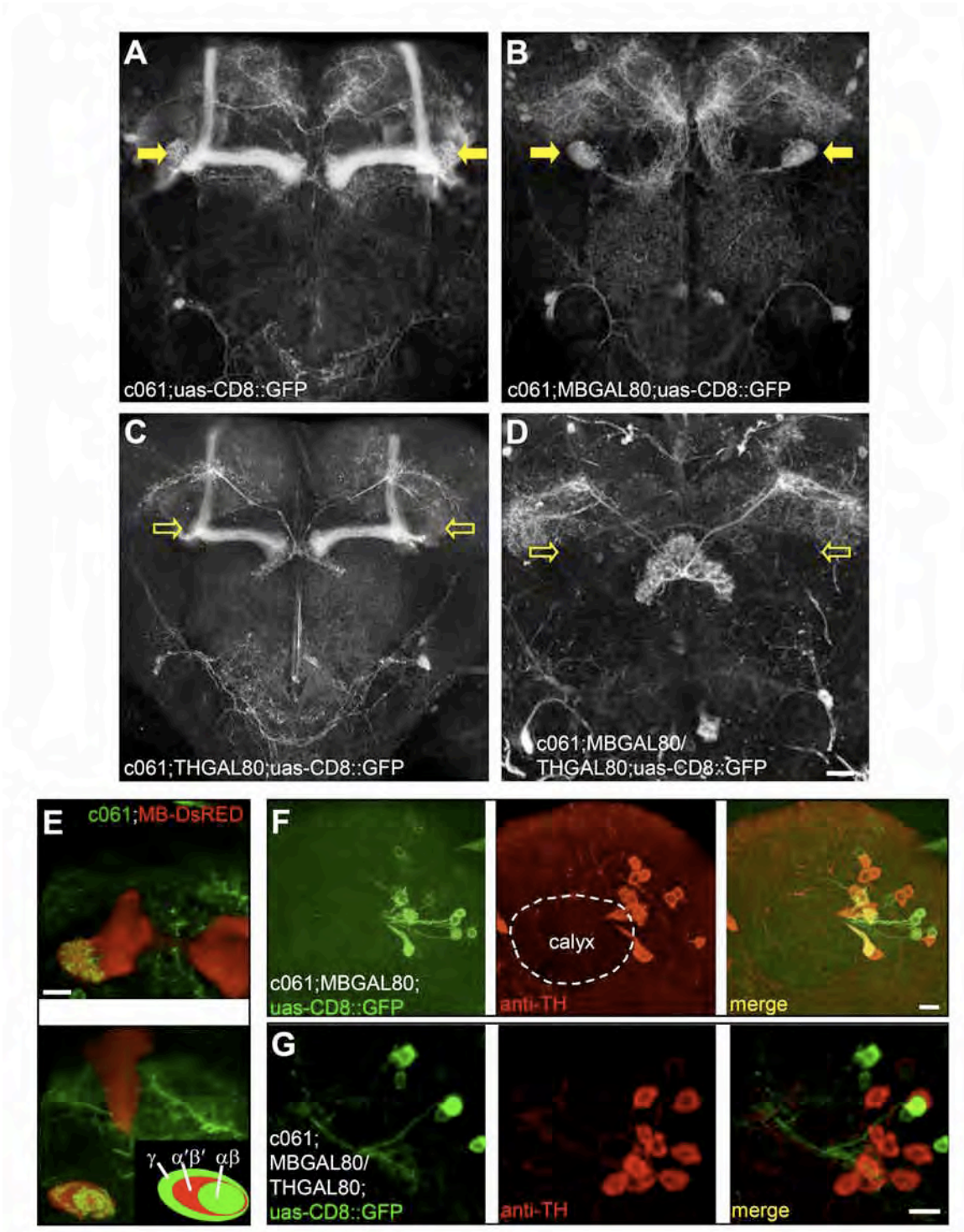
A
c061;uas-CD8::GFP
B
c061;MBGAL80;uas-CD8::GFP
C
c061;THGAL80;uas-CD8::GFP
D
c061;MBGAL80/
THGAL80;uas-CD8::GFP
E
c061;MB-DsRED
γ
α′β′
αβ
F
c061;MBGAL80;
uas-CD8::GFP
calyx
anti-TH
merge
G
c061;
MBGAL80/
THGAL80;
uas-CD8::GFP
anti-TH
merge

Figure III.3. c061 labels six dopaminergic neurons that innervate the mushroom bodies. (A) Projection view of a c061; uas-*CD8::GFP* brain. Yellow arrows mark innervation of the heel region of the MB (filled yellow arrows) resembling that in *TH*-GAL4 labeled brains (Figure S4A) as well as a few neurons innervating the fan-shaped body of the central complex and a few neurons in the subesophageal ganglion. **(B)** Combining MBGAL80 with c061; uas-*CD8::GFP* eliminates MB neuron expression and reveals the detailed morphology of the neurons that innervate the heel region of the mushroom bodies (filled yellow arrows). Also see Movies S1 and S2. **C.** Combining *TH*GAL80 with c061; uas-*CD8::GFP* eliminates expression in the neurons innervating the dorsal protocerebrum region between the mushroom body lobes and the MB heel (hollow arrows) but leaves expression elsewhere intact. **(D)** Projection view of a c061;MBGAL80/THGAL80;uas-*CD8::GFP* brain. A *TH*50 promoter driven GAL80 removes expression from the neurons that innervate the dorsal protocerebrum and MB heel (hollow arrows) labeled by c061; MBGAL80 and leaves prominent expression in the fan-shaped body and elsewhere intact. Scale bar represents 20μm. **(E)** Higher magnification single confocal section views of the MB heel and peduncle region from a c061; uas-*CD8::GFP* brain. Moving anterior to posterior from top to bottom. Top panel shows extensive innervation of the MB heel. Bottom panel detailing innervation in the base of the peduncle. Inset, schematic cross section through the peduncle explaining zones

occupied by the αβ, α´β´ and γ MB neurons. The MB is co-labeled in both panels with a MB-expressed DsRED transgene. **(F)** A confocal section through a c061;MBGAL80; uas-*CD8::GFP* brain at the level of the MB calyx (outlined). GFP (green) labels 3 large cell bodies at the side of the calyx and 5 more lateral cell bodies. Counter staining with an anti-tyrosine hydroxylase antibody (red) labels 12 cell bodies in that region of the brain (known as the PPL1 cluster), and 3 of them overlap (merge, yellow) with c061;MBGAL80 driven GFP. Scale bar represents 10μm. **(G)** A confocal section through a c061;MBGAL80/THGAL80; uas-*CD8::GFP* brain at the level of the PPL1 cluster of DA neurons. GFP (green) labels 5 cell bodies and none of these overlap with anti-TH staining. Scale bar represents 10μm.

Figure III.4

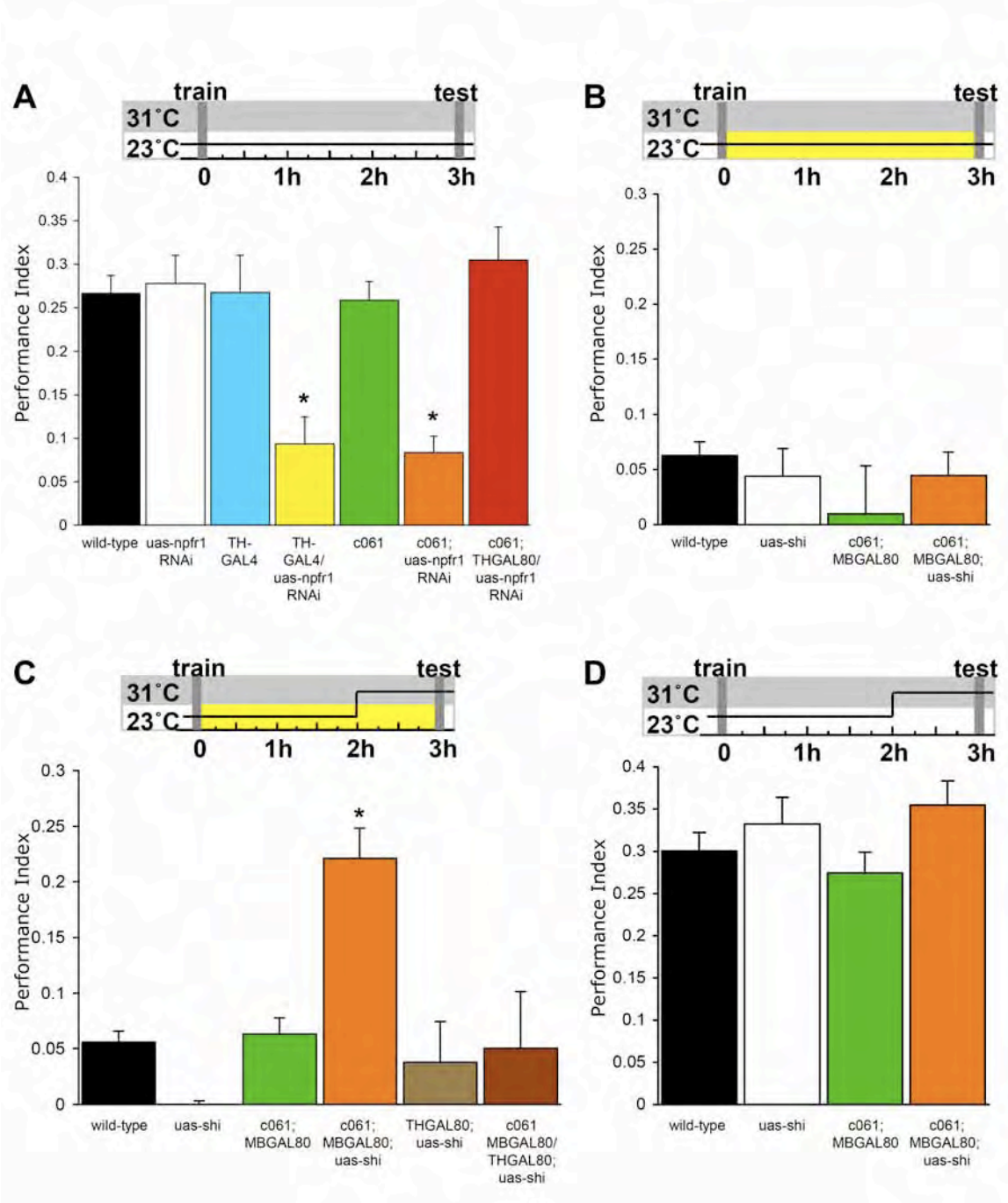
A
train
test
31˚C
23˚C
0
1h
2h
3h
Performance Index
wild-type
uas-npfr1 RNAi
TH-GAL4
TH-GAL4/ uas-npfr1 RNAi
c061
c061; uas-npfr1 RNAi
c061; THGAL80/ uas-npfr1 RNAi
B
wild-type
uas-shi
c061; MBGAL80
c061; MBGAL80; uas-shi
C
wild-type
uas-shi
c061; MBGAL80
c061; MBGAL80; uas-shi
THGAL80; uas-shi
c061 MBGAL80/ THGAL80; uas-shi
D
wild-type
uas-shi
c061; MBGAL80
c061; MBGAL80; uas-shi

Figure III.4. c061 labeled dopaminergic neurons are critical for regulating appetitive memory performance. The temperature shift protocols are shown pictographically above each graph. **(A)** Expressing the uas-*npfr1*^{RNAi} transgene in all dopaminergic neurons with *TH*-GAL4 or in a subset of dopaminergic neurons with c061 impairs 3 hr appetitive memory in food-deprived flies. Expressing uasnpfr1RNAi in all c061 neurons except the dopaminergic neurons (c061;*TH*GAL80;uas-*npfr1*^{RNAi} flies) does not affect appetitive memory. **(B)** Feeding flies after training suppresses 3 hr memory performance of all groups used in this experiment. All genotypes were food-deprived, trained, fed and tested at the permissive temperature of 23˚C. **C.** Blocking synaptic output from the c061; MBGAL80 labeled neurons for one hour before testing using uas-*shi*^{ts1} reveals memory performance in satiated flies. Removing uas-*shi*^{ts1} expression from the dopaminergic neurons reverses the memory promoting effect (c061;MBGAL80/*TH*GAL80;uas-*shi*^{ts1} flies). All genotypes were food-deprived, trained and stored in food vials for 120min at 23˚C. Vials were then shifted to 31˚C for 60min before flies were tested for appetitive memory at 31˚C. **(D)** Blocking synaptic output from the c061; MBGAL80 labeled neurons for one hour before testing does not enhance memory performance in food-deprived flies. All genotypes were food-deprived, trained and stored in empty vials for 120min at 23˚C. Vials were then shifted to 31˚C for 60min before flies were tested for appetitive memory at 31˚C. Asterisks denote significant difference ($P<0.05$,ANOVA) from other unmarked groups. Data are mean ± SEM.

Figure III.5

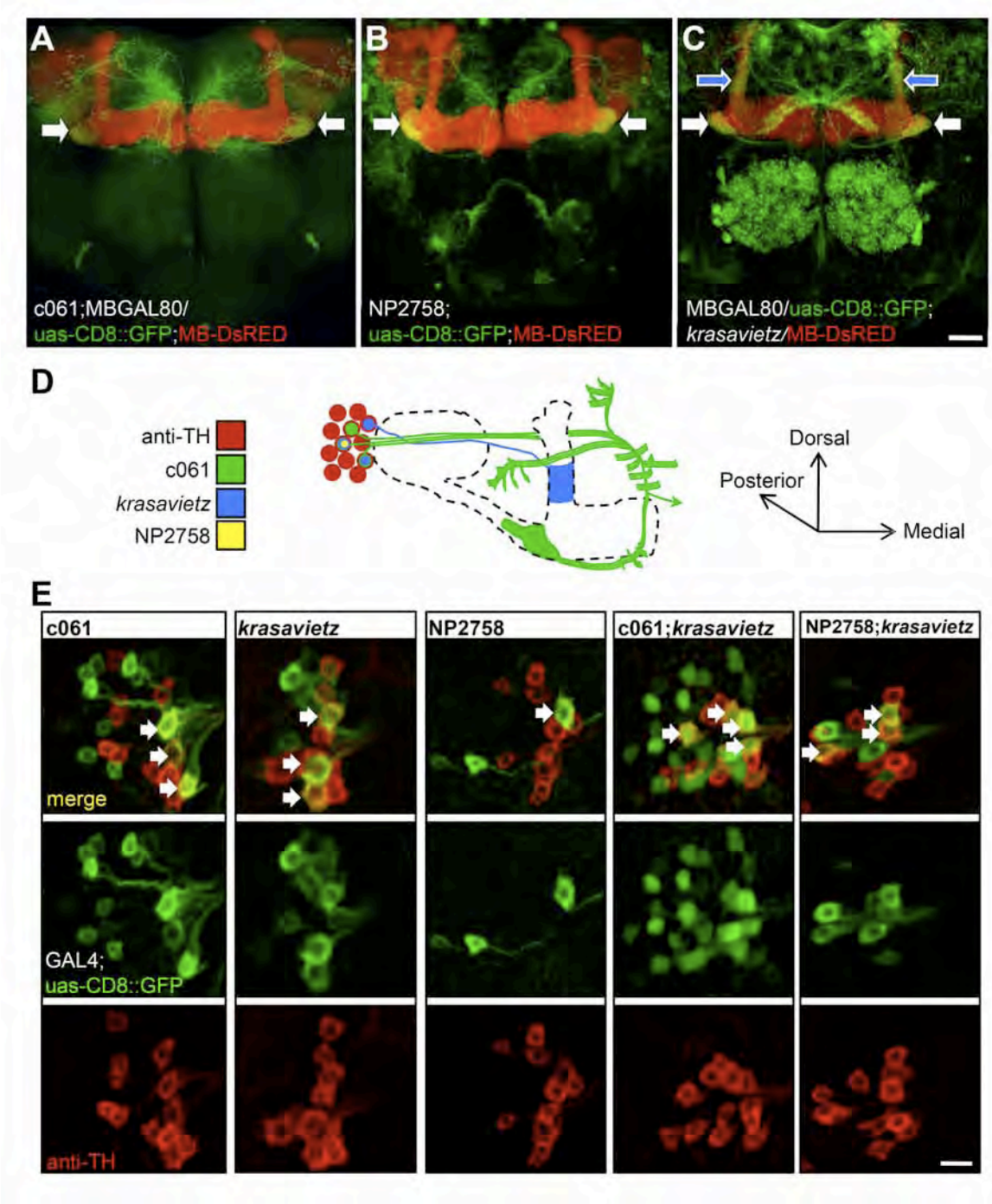
A
B
C
c061;MBGAL80/
uas-CD8::GFP;MB-DsRED
NP2758;
uas-CD8::GFP;MB-DsRED
MBGAL80/uas-CD8::GFP;
krasavietz/MB-DsRED
D
anti-TH
c061
krasavietz
NP2758
Dorsal
Posterior
Medial
E
c061
krasavietz
NP2758
c061;krasavietz
NP2758;krasavietz
merge
GAL4;
uas-CD8::GFP
anti-TH

Figure III.5. The dopaminergic c061 neurons are MB-MP neurons. (A) Projection view of a c061; MBGAL80; uas-*CD8::GFP* brain showing labeling in MB-MP neurons (white arrows) and in the subesophageal ganglion (also see Movies S1 and S2). **(B)** Projection view of a NP2758; uas-*CD8::GFP* brain showing labeling in MB-MP neurons (white arrows) and in the subesophageal ganglion (also see Movies S3 and S4). **(C)** Projection view of a MBGAL80; *krasavietz*/uas-*CD8::GFP* brain showing expression in MB-MP neurons (white arrows). Expression is also visible in dopaminergic neurons innervating the α stalk of the MB lobes (blue arrows, also see Figure III.S4C), neurons in the fan-shaped body of the central complex and local neurons in the antennal lobe (also see Movies S5 and S6). The MB is co-labeled with a MB-expressed DsRED transgene. **(D)** Cartoon illustrating the gross structure of MB-MP neurons and the expression pattern of each GAL4 line used in this study. The MB is shown as an outline. Dopaminergic neuron cell bodies (red, anti-TH) of a single PPL1 cluster are shown with the labeling of each GAL4 line overlayed. The organization of the cell bodies is not stereotyped and it is difficult to distinguish the projection patterns of each MB-MP neuron. No order or detail is inferred here. At least one MB-MP neuron sends a contralateral projection to the other MB (green arrow head). **(E)** *krasavietz* and NP2758 label a subset of c061 labeled MB-MP neurons. Each column shows the separate and merged channels from confocal images of a PPL1 cluster in brains counter-labeled with GAL4 driven GFP (green) and anti-TH antibody (red). Double-labeled neurons are marked with an

arrow in the merged images. c061 and *krasavietz*;MBGAL80 driven GFP label 3 somata that counter-stain with anti-TH whereas NP2758 driven GFP labels only one anti-TH labeled cell body. c061;MBGAL80; *krasavietz* driven GFP labels 4 somata that counter-stain with anti-TH indicating that c061 and *krasavietz* expression overlaps in 2 neurons. NP2758;MBGAL80;*krasavietz* driven GFP labels 3 somata that counter-stain with anti-TH indicating that NP2758 labels one of the 2 MB-MP neurons in *krasavietz*; MBGAL80 (For quantification of neuron numbers see Figure S4B). Scale bar represents 20μm (A, B, C) or 10μm (E).

Figure III.6

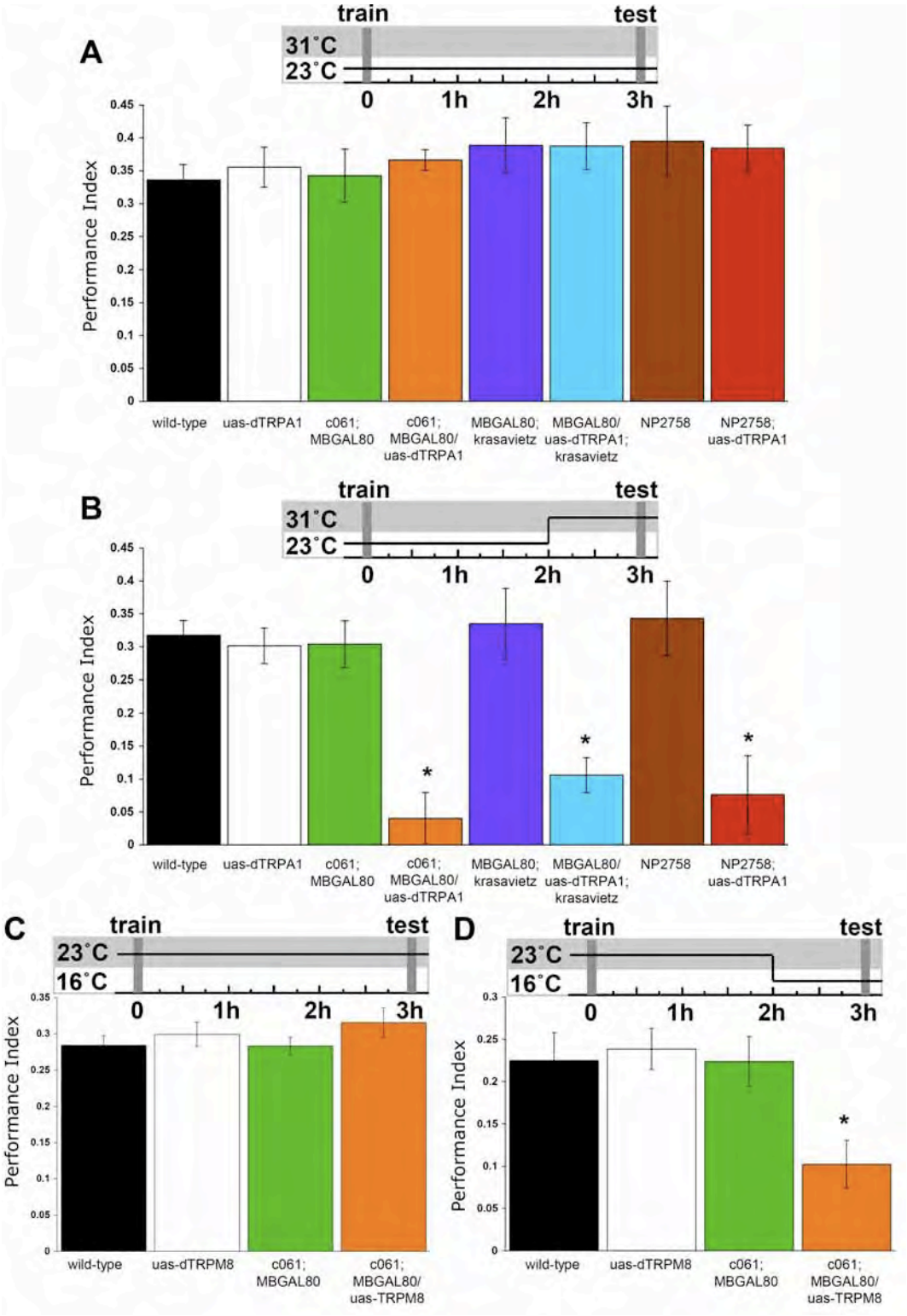
A
train
test
31˚C
23˚C
0
1h
2h
3h
Performance Index
0.45
0.4
0.35
0.3
0.25
0.2
0.15
0.1
0.05
0
wild-type
uas-dTRPA1
c061; MBGAL80
c061; MBGAL80/ uas-dTRPA1
MBGAL80; krasavietz
MBGAL80/ uas-dTRPA1; krasavietz
NP2758
NP2758; uas-dTRPA1
B
train
test
31˚C
23˚C
0
1h
2h
3h
Performance Index
*
*
*
wild-type
uas-dTRPA1
c061; MBGAL80
c061; MBGAL80/ uas-dTRPA1
MBGAL80; krasavietz
MBGAL80/ uas-dTRPA1; krasavietz
NP2758
NP2758; uas-dTRPA1
C
train
test
23˚C
16˚C
0
1h
2h
3h
Performance Index
0.35
0.3
0.25
0.2
0.15
0.1
0.05
0
wild-type
uas-dTRPM8
c061; MBGAL80
c061; MBGAL80/ uas-TRPM8
D
train
test
23˚C
16˚C
0
1h
2h
3h
Performance Index
0.3
0.25
0.2
0.15
0.1
0.05
0
*
wild-type
uas-dTRPM8
c061; MBGAL80
c061; MBGAL80/ uas-TRPM8

Figure III.6. Stimulating MB-MP neurons before testing suppresses appetitive memory expression in hungry flies. The temperature shift protocols are shown pictographically above each graph. **(A)** The permissive temperature of 23˚C does not affect 3 hr appetitive odor memory of any of the lines used in this study. All genotypes were starved, trained, stored for 3 hr in empty vials and tested for appetitive memory at 23˚C. **(B)** Stimulating 6, 4 or 2 MB-MP neurons with uas-*dTrpA1* before and during testing attenuates memory performance in starved flies. All genotypes were food-deprived, trained and stored in empty vials for 120min at 23˚C and were then shifted to 31˚C for 60min before and during testing. **(C)** The permissive temperature of 23˚C does not affect 3 hr appetitive odor memory of any of the lines used in this study. All genotypes were starved, trained, stored in empty vials for 3 hr and tested for appetitive memory at 23˚C. **(D)** Stimulating 6 MB-MP neurons with uas-*TRPM8* before and during testing attenuates memory performance in starved flies. All genotypes were food deprived, trained and stored in empty food vials for 120min at 23˚C and were then shifted to 16˚C for 60min before and during testing. Asterisk denotes significant difference ($P<0.05$, ANOVA) from other unmarked groups. Data are mean ± SEM.

Figure III.7

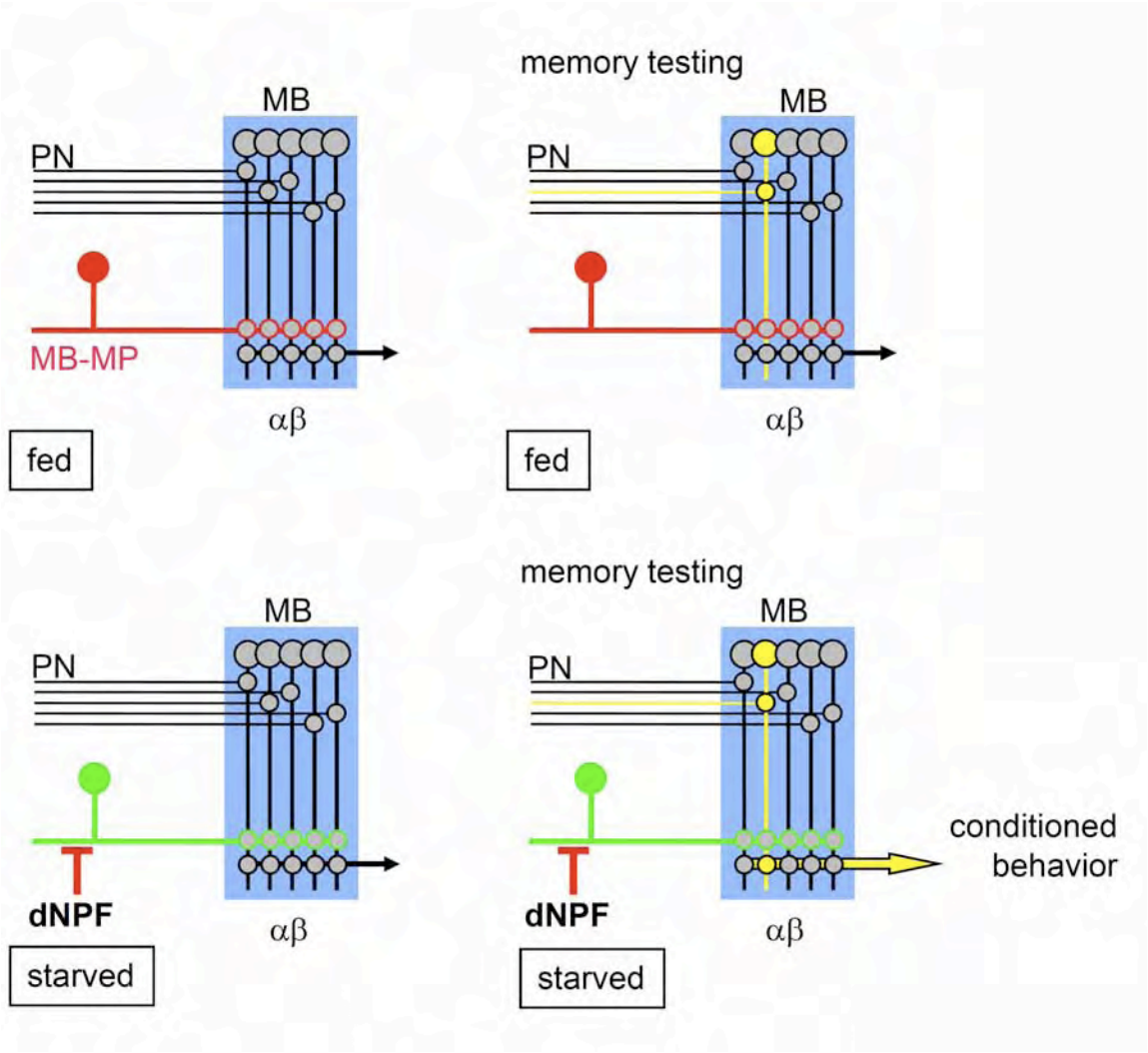

Figure III.7. Model for the role of MB-MP neurons. Left panels illustrate the state of the inhibitory control exerted upon the MB in the fed state (top) and starved state (bottom). When fed flies are exposed to the conditioned odor during memory testing (right panels) the appropriate projection neurons and MB neurons are activated (yellow). However, the signal only propagates beyond the

MB neurons in hungry flies when the MB-MP neuron ‘gate’ is open. Red lines denote inhibition and green lines relief from inhibition. See discussion for more detail.

Table III.1

	OCT		MCH		sucrose acuity
	23˚C	31˚C	23˚C	31˚C	23˚C
uas-npfr1RNAi	0.51+/-0.06		0.60+/-0.07		0.61+/-0.05
c061	0.52+/-0.03		0.59+/-0.10		0.57+/-0.08
c061; uas-npfr1RNAi	0.57+/-0.05		0.55+/-0.09		0.59+/-0.08
syb-GAL4	0.56+/-0.06		0.57+/-0.05		0.61+/-0.05
uas-dcr2; syb-GAL4	0.54+/-0.06		0.53+/-0.07		-
uas-dcr2	0.51+/-0.04		0.53+/-0.06		-
uas-dcr2;uas-npfr1RNAi	0.56+/-0.08		0.55+/-0.05		0.58+/-0.04
uas-dcr2;uas-npfr1RNAi;syb-GAL4	0.52+/-0.06		0.63+/-0.08		0.65+/-0.06
uas-npfr1RNAi/TH-GAL4	0.61+/-0.09		0.70+/-0.07		0.60+/-0.07
wild-type		0.52+/-0.03		0.59+/-0.11	0.59+/-0.04
uas-shi		0.51+/-0.03		0.63+/-0.10	0.62+/-0.05
c061; MBGAL80		0.54+/-0.05		0.60+/-0.11	0.62+/-0.05
c061; MBGAL80; uas-shi		0.57+/-0.11		0.64+/-0.10	0.62+/-0.06
NP2758		0.62+/-0.09		0.53+/-0.06	0.61+/-0.05
NP2758; uas-shi		0.55+/-0.05		0.58+/-0.04	0.65+/-0.02
MBGAL80; krasavietz		0.65+/-0.07		0.57+/-0.03	0.59+/-0.07
MBGAL80; krasavietz/ uas-shi		0.56+/-0.03		0.56+/-0.03	0.64+/-0.10
THGAL80; uas-shi		0.56+/-0.06		0.59+/-0.06	0.64+/-0.07
c061; MBGAL80/THGAL80; uas-shi		0.54+/-0.02		0.56+/-0.04	0.67+/-0.06
uas-dTRPA1		0.51+/-0.06		0.65+/-0.10	0.58+/-0.09
dNPF-GAL4		0.50+/-0.04		0.60+/-0.07	0.69+/-0.05
c061; MBGAL80/uas-dTRPA1		0.56+/-0.07		0.60+/-0.12	0.59+/-0.07
dNPF-GAL4/uas-dTRPA1		0.51+/-0.05		0.57+/-0.09	0.70+/-0.03
NP2758; uas-dTRPA1		0.61+/-0.07		0.57+/-0.07	0.68+/-0.06
MBGAL80/uas-dTRPA1; krasavietz		0.64+/-0.08		0.54+/-0.03	0.61+/-0.04

Table III.1. Olfactory and Sucrose Acuity for strains used in this study. All genotypes were either tested for odor acuity at 23˚C or at the restrictive temperature for uas-*shi*ts1 or uas-*dTrpA1* of 31°C. All genotypes were tested for sucrose acuity at the permissive temperature of 23°C. No statistical differences were apparent between the relevant groups. (OCT 23˚C P>0.98; MCH 23˚C P>0.80; OCT 31˚C P>0.88; MCH 31˚C P>0.99; sucrose P>0.89). All n≥6.

Figure III.8

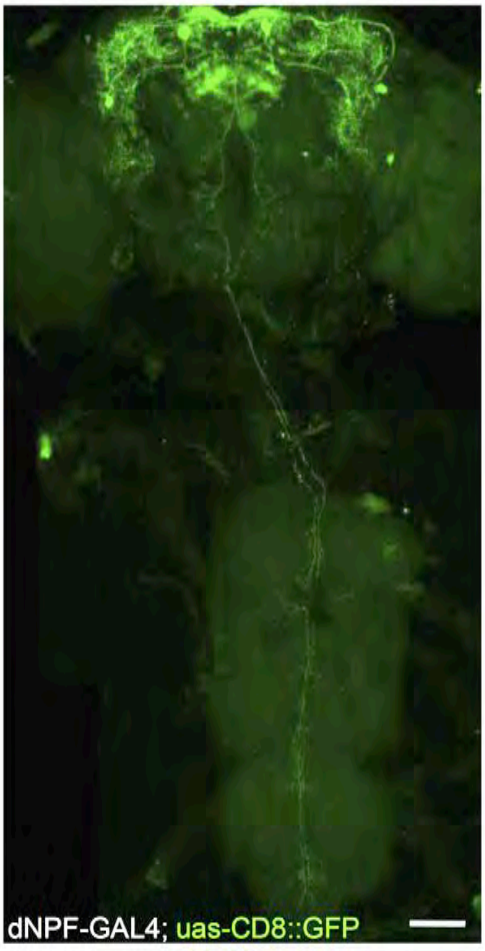

Figure III.8. *dNPF*-GAL4 does not label somata in the ventral ganglion.

dNPF-GAL4 driven CD8::GFP (green) shows strong expression in the brain and fibres descending into the ventral ganglion. However, no somata are labeled in the ventral ganglion. Scale bar represents 50μm.

Figure III.9

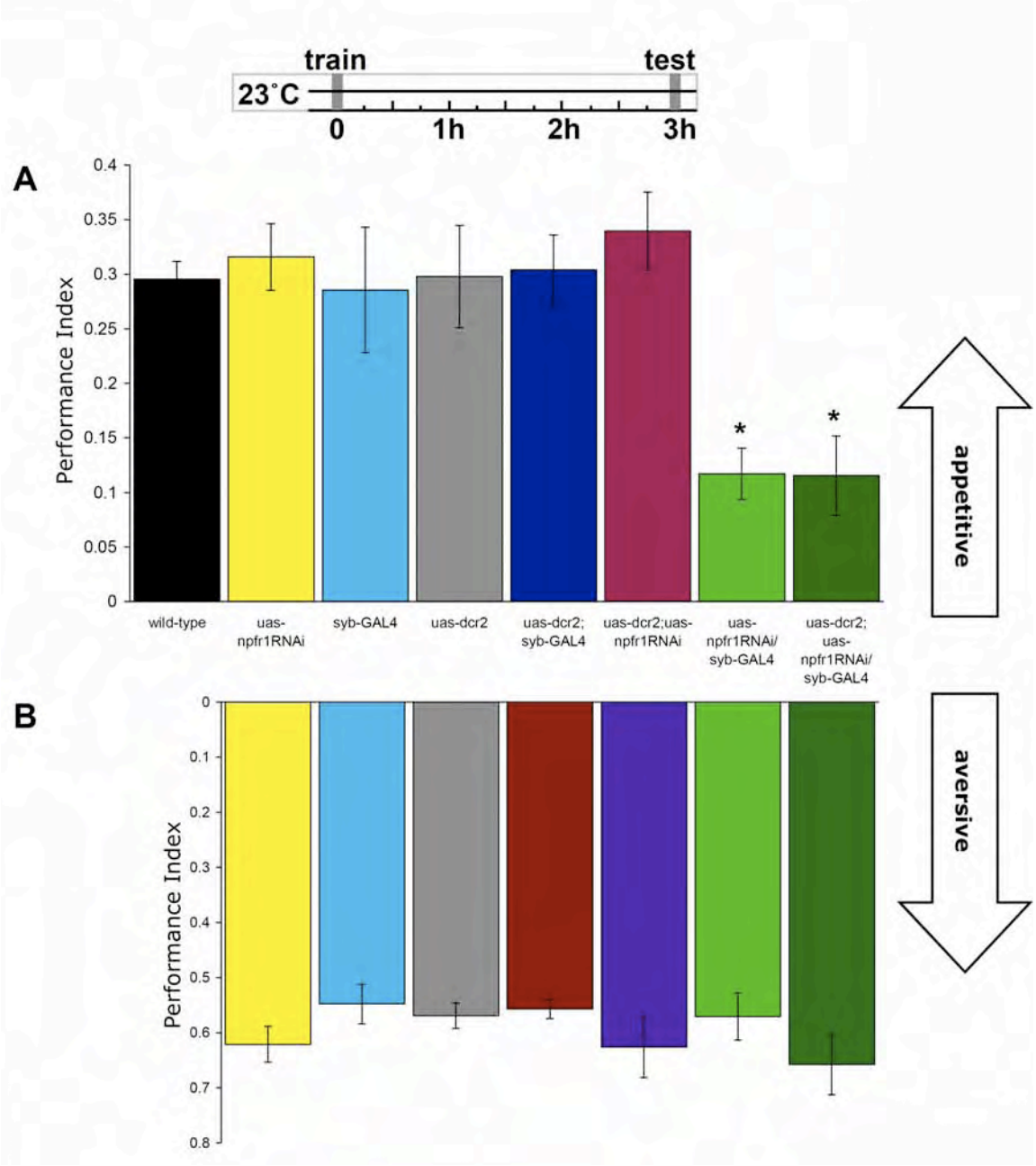

Figure III.9. Silencing *npfr1* in all neurons specifically disrupts 3 hr appetitive olfactory memory. (A) Driving the uas-*npfr1*^{RNAi} globally throughout

the brain using syb-GAL4 in the presence or absence of uas-*dicer2* attenuates memory performance in hungry animals. uas-*npfr1*^{RNAi}/syb-GAL4 and uas-*dcr2*; *npfr1*^{RNAi}/syb-GAL4 flies are statistically different than wild-type, uas-*npfr1*^{RNAi}, syb-GAL4, uas-*dcr2*, uas-*dcr2*; syb-GAL4/+ and uas-*dcr2*; uas-*npfr1*^{RNAi} controls. **(B)** Driving the uas-*npfr1*RNAi globally throughout the brain using syb-GAL4 in the presence or absence of uas-*dicer2* does not affect 3 minute aversive memory performance. Data are mean ± SEM. Asterisks denote significant difference ($P<0.05$, ANOVA) from other unmarked groups. Data are mean ± SEM.

Figure III.10

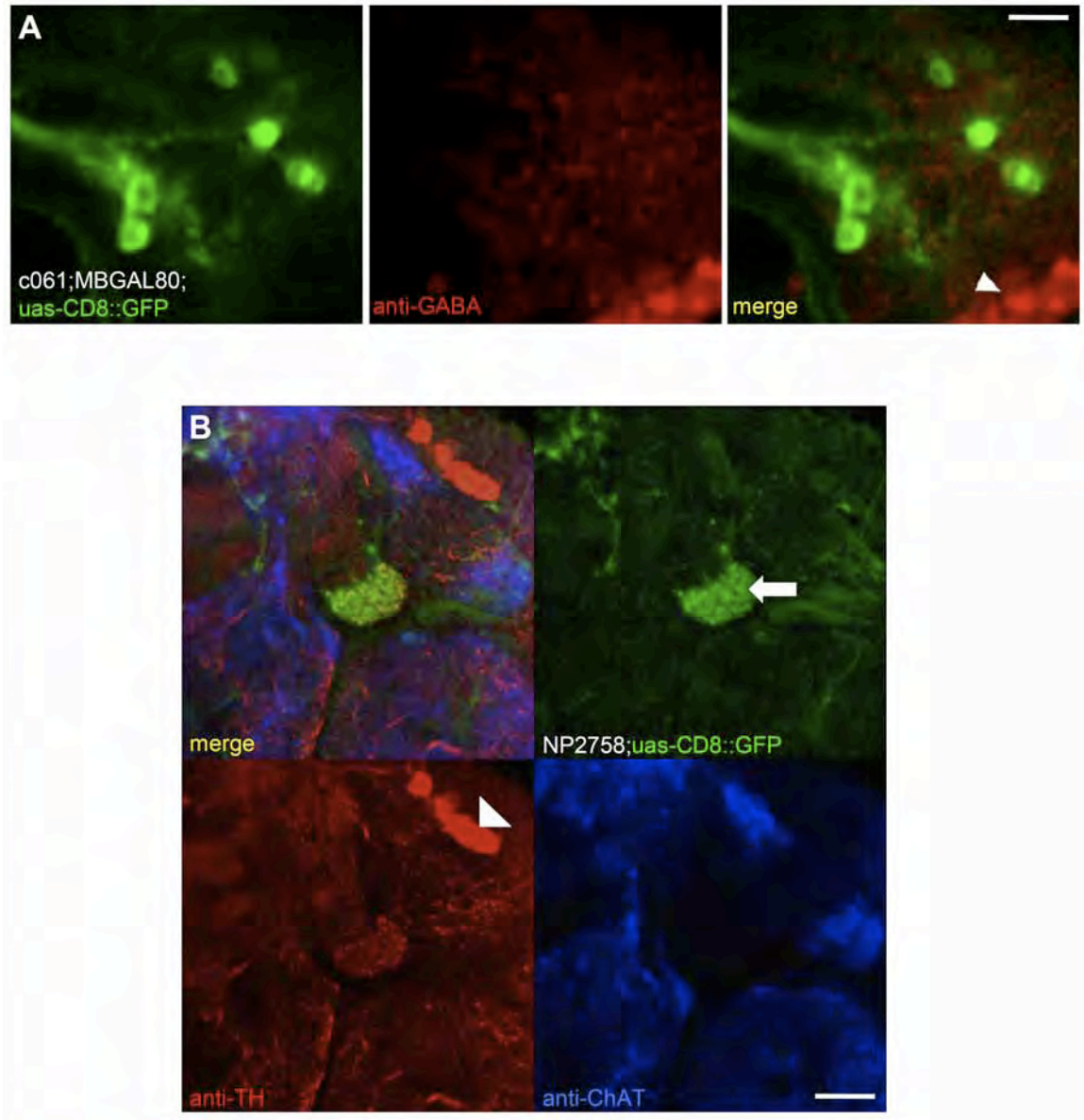

Figure III.10. MB-MP neurons do not contain GABA or acetylcholine. (A) The separate and merged channels from confocal images of a PPL1 cluster in a c061;MBGAL80;uas-*CD8::GFP* brain counter-labeled with GFP (green) and an

anti-GABA antibody (red). (**B)** The separate and merged channels of a confocal image at the level of the MB heel in an NP2758;uas-*CD8::GFP* brain counter-labeled with GFP (green) and anti-TH antibody (red) and anti-ChAT (choline acetyl transferase) antibody. GFP strongly labels the heel region of the MB (white arrow). This region is also innervated by dopaminergic processes in the anti-TH labeled image. Anti-TH also strongly labels dopaminergic neuron cell bodies at that level of the brain (white arrow head). Anti-ChAT strongly labels many processes in the brain but is notably absent from the heel region of the MB. Scale bar represents 10μm.

Figure III.11

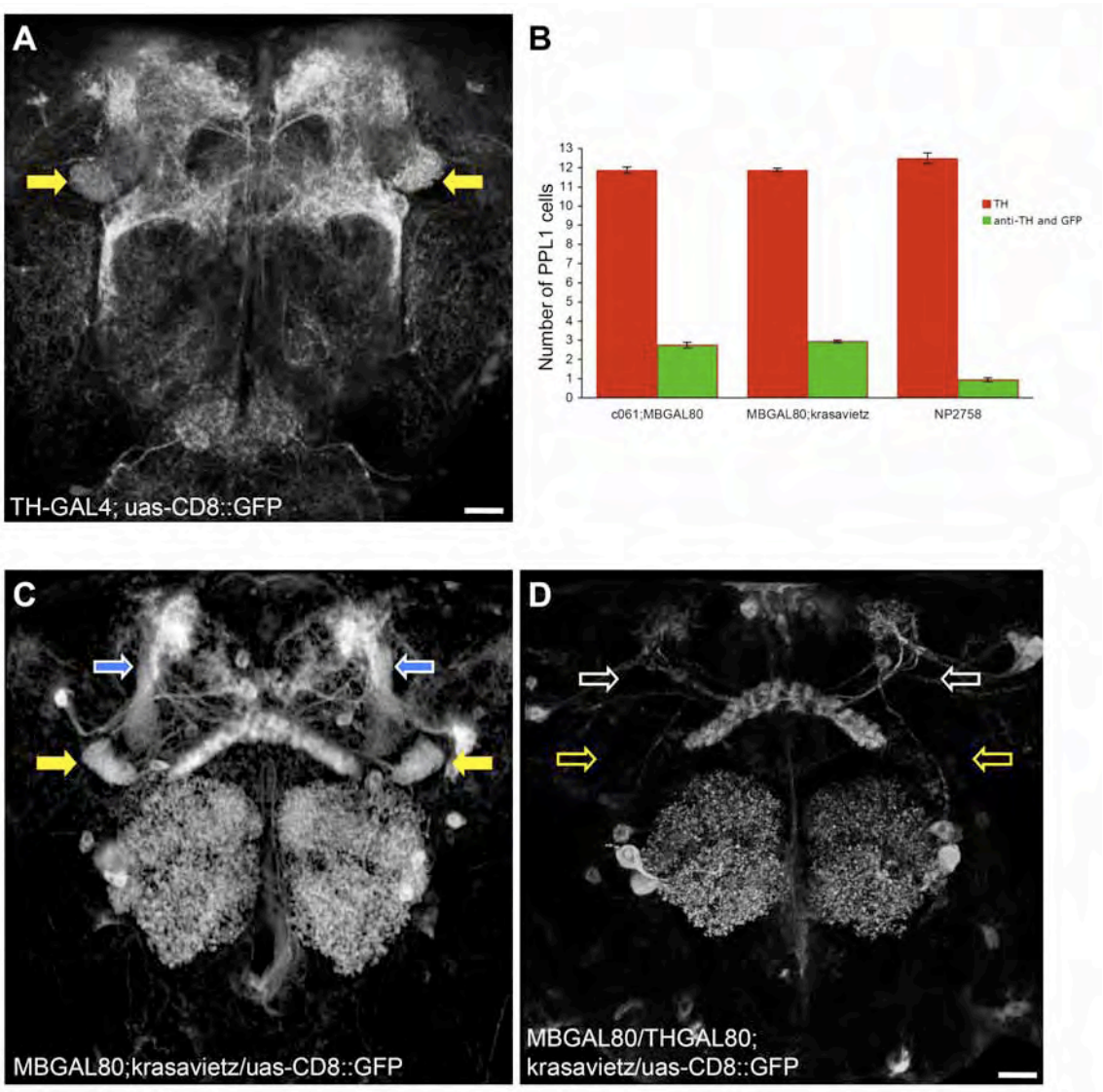

Figure III.11. Analysis of expression in subsets of dopaminergic neurons. **(A)** A projection view of frontal sections from a brain containing labeled dopaminergic neurons with *TH*-GAL4 driven uas-*CD8::GFP* reveals dense innervation of specific domains in the dorsal protocerebrum including the heel of

the MB (yellow arrows). **(B)** Quantification of the number of anti-TH labeled neurons and GFP-positive neurons in the PPL1 cluster of the three GAL4 lines, c061;MBGAL80, MBGAL80;*krasavietz* and NP2758, used in this study. Data are mean ± SEM. n=16 PPL1 clusters from 8 brains per genotype. **(C)** The MBGAL80;*krasavietz* line labels two MB-MP neurons and one additional dopaminergic neuron in each PPL1 cluster that projects to the stalk of the α lobe. Projection view of a MBGAL80;*krasavietz*/uas-*CD8::GFP* brain reveals the MB-MP neuron processes in the heel of the MB (yellow arrows) as well as projections from other neurons on the stalk of the MB α lobe (blue arrows). (**D)** Projection view of a MBGAL80/*TH*GAL80;*krasavietz*/uas-*CD8::GFP* brain reveals that the *TH*GAL80 transgene removes expression from the MB-MP neurons and the neurons projecting to the stalk of the a lobe (hollow arrows). Scale bar represents 20µm.

Figure III.12

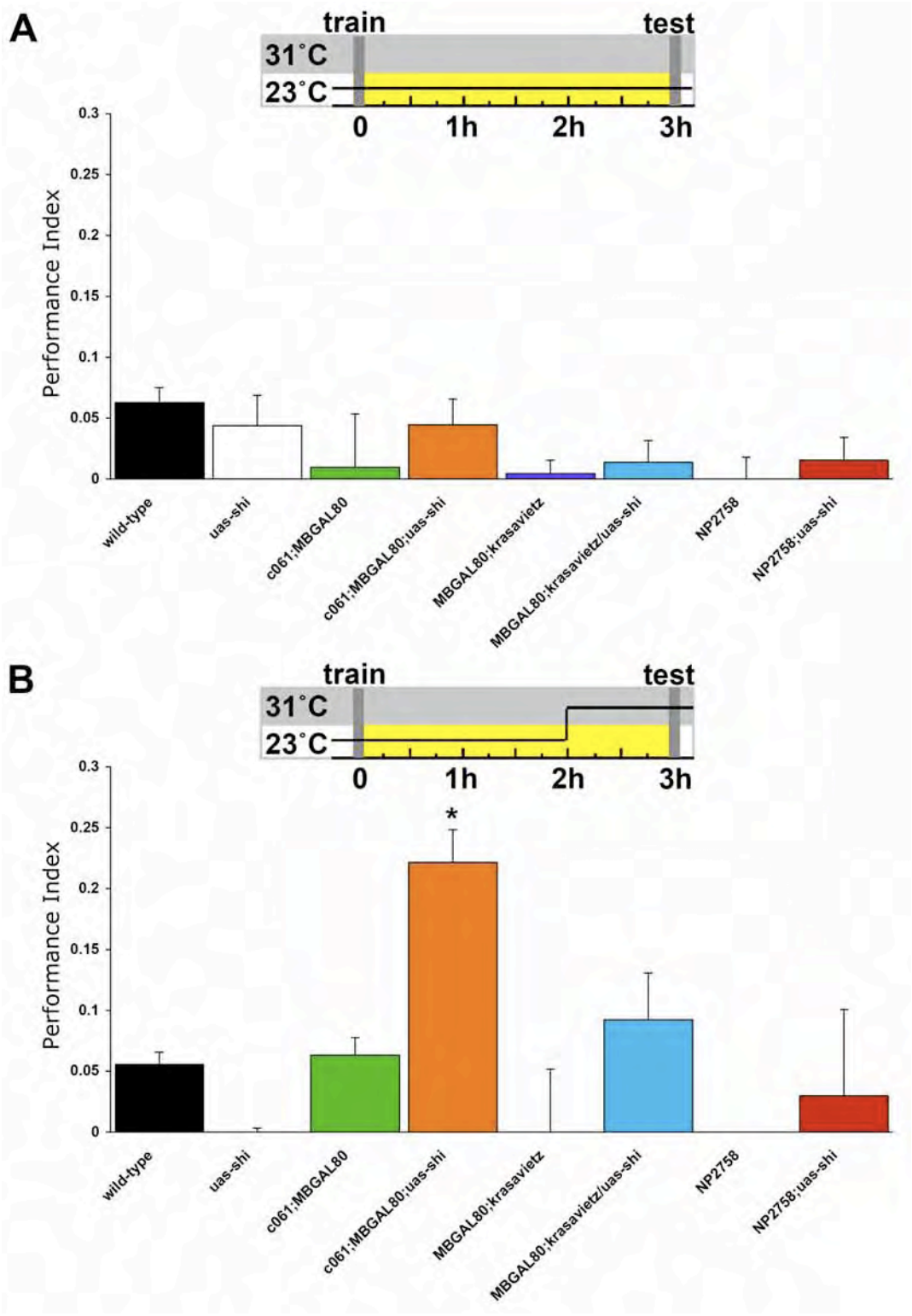

Figure III.12. Blocking only 2 or 4 of the 6 MB-MP neurons does not release appetitive memory performance in fed flies. (A) Feeding flies after training suppresses 3 hr memory performance of all groups used in this experiment. All genotypes were food-deprived, trained, fed and tested at the permissive temperature of 23˚C. **(B)** Blocking synaptic output from 6 MB-MP neurons with c061; MBGAL80 for one hour before testing using uas-*shi*^{ts1} reveals memory performance in satiated flies but blocking 4 with MBGAL80;*krasavietz* or 2 with NP2758 does not. All genotypes were food-deprived, trained and stored in food vials for 120min at 23˚C. Vials were then shifted to 31˚C for 60min before flies were tested for appetitive memory at 31˚C. Data are mean ± SEM.

Figure III.13

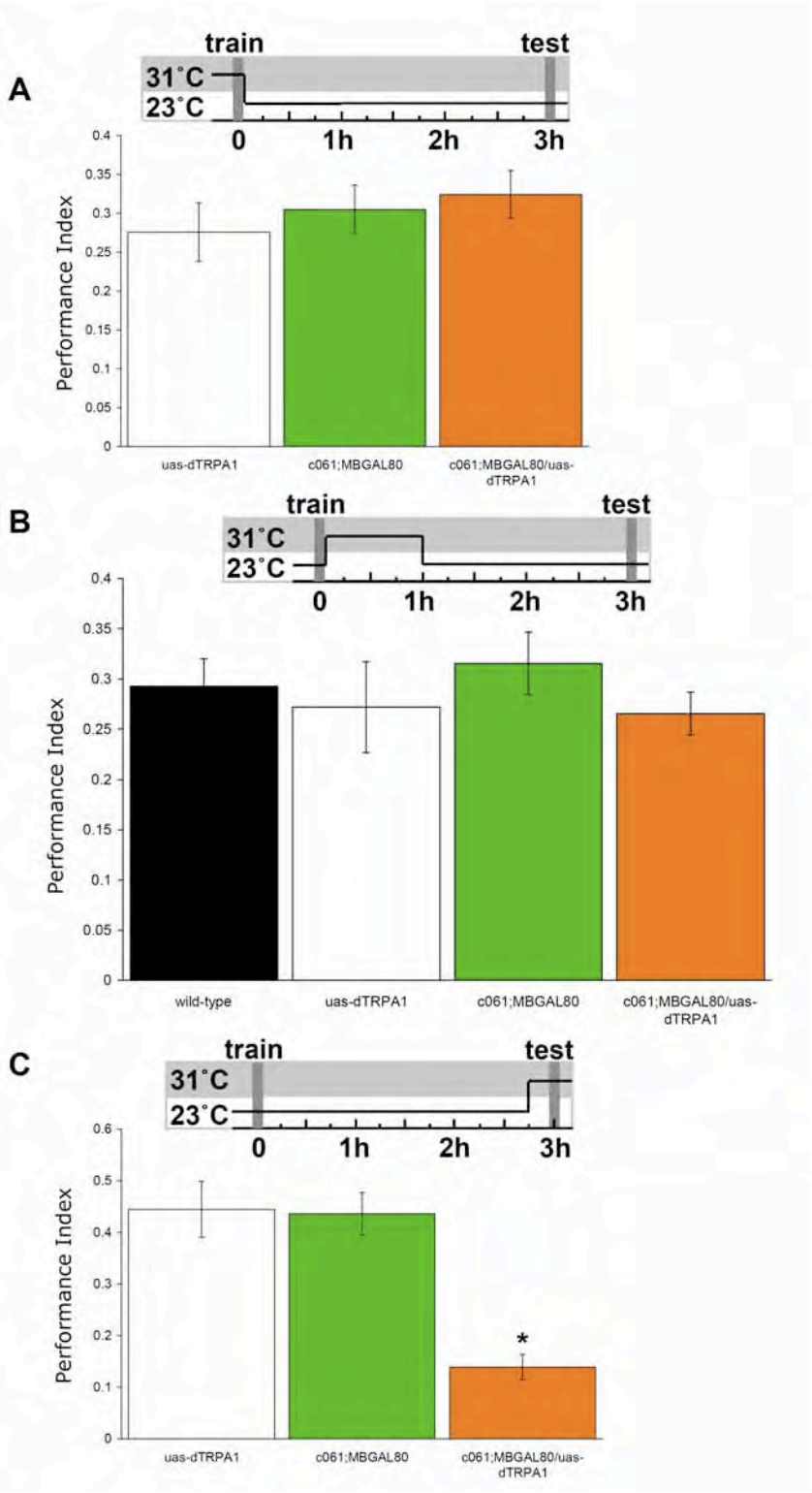

Figure III.13. Stimulating MB-MP neurons during testing suppresses appetitive memory performance but stimulating during acquisition or temporarily after training does not. (A) All genotypes were food-deprived, trained and stored in food vials for 120min at 23˚C. Vials were then shifted to 31˚C for 15min before flies were tested for appetitive memory at 31˚C. **(B)** All genotypes were food-deprived and trained at 23˚C. They were then immediately transferred to food vials at 31˚C for 60min and returned to 23˚C for 120min before being tested for memory at 23˚C. **(C)** All genotypes were food-deprived at 23˚C and 30min before training they were transferred to 31˚C and trained. After training they were stored in food vials for 180min at 23˚C before flies were tested for appetitive memory at 23˚C. Asterisk denotes significant difference ($P<0.05$, ANOVA) from other unmarked groups. Data are mean ± SEM.

Figure III.14

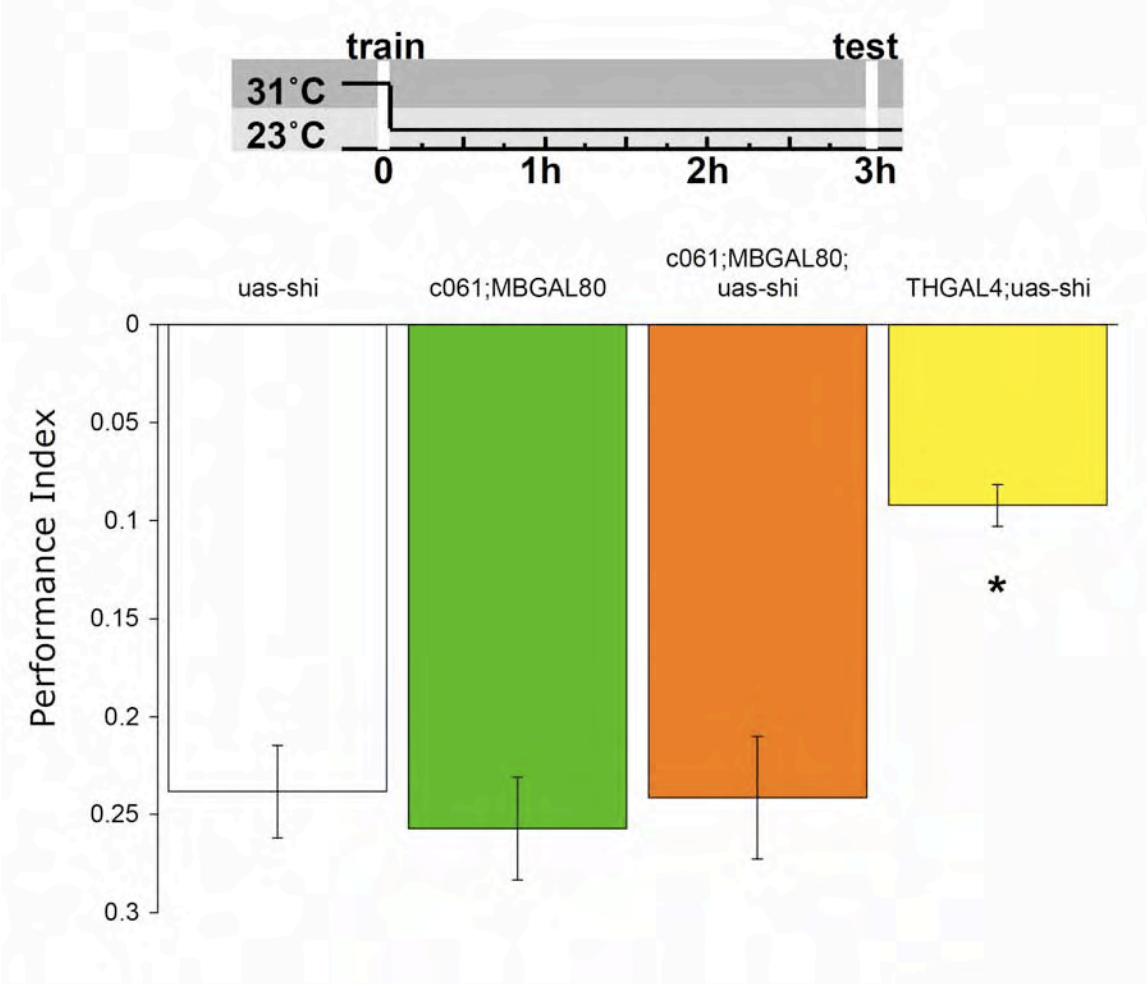

Figure III.14. Blocking MB-MP neurons does not impair acquisition of aversive odor memory. All flies were incubated at 31˚C for 30min before and during training with the aversive odor and shock protocol. Immediately after training all flies were returned to 23˚C and tested for 3 hr aversive odor memory. Asterisk denotes significant difference ($P<0.05$, ANOVA) from other unmarked groups. Data are mean ± SEM.

Figure III.15

A.

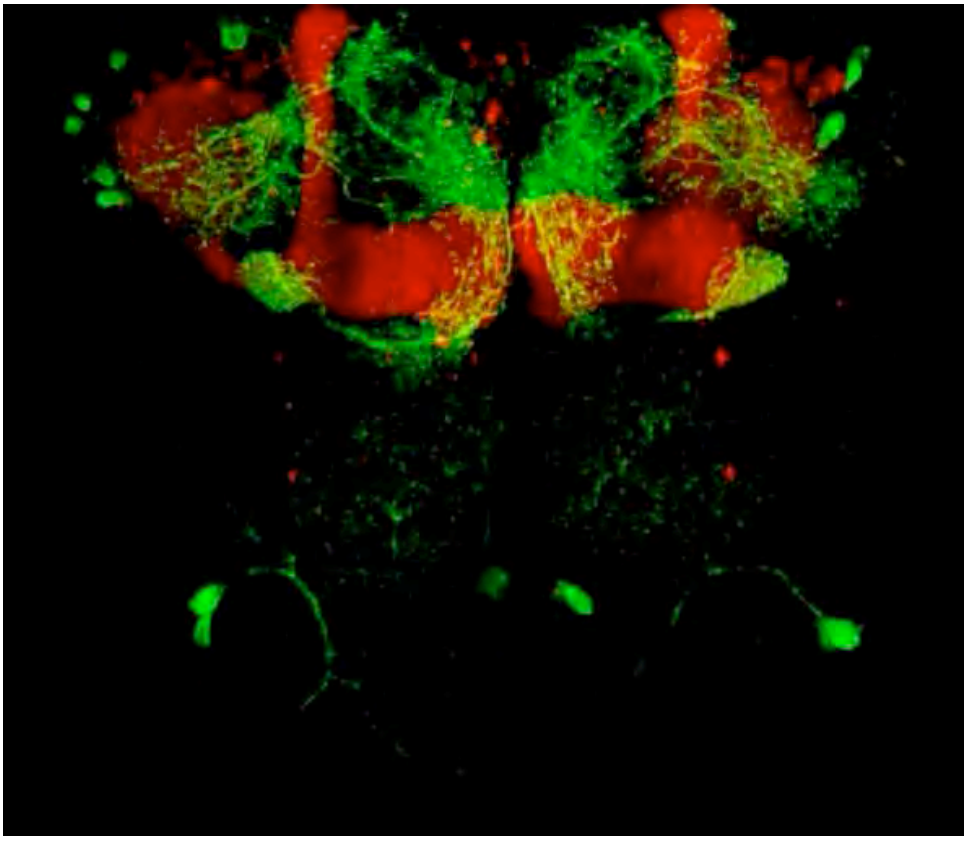

B.

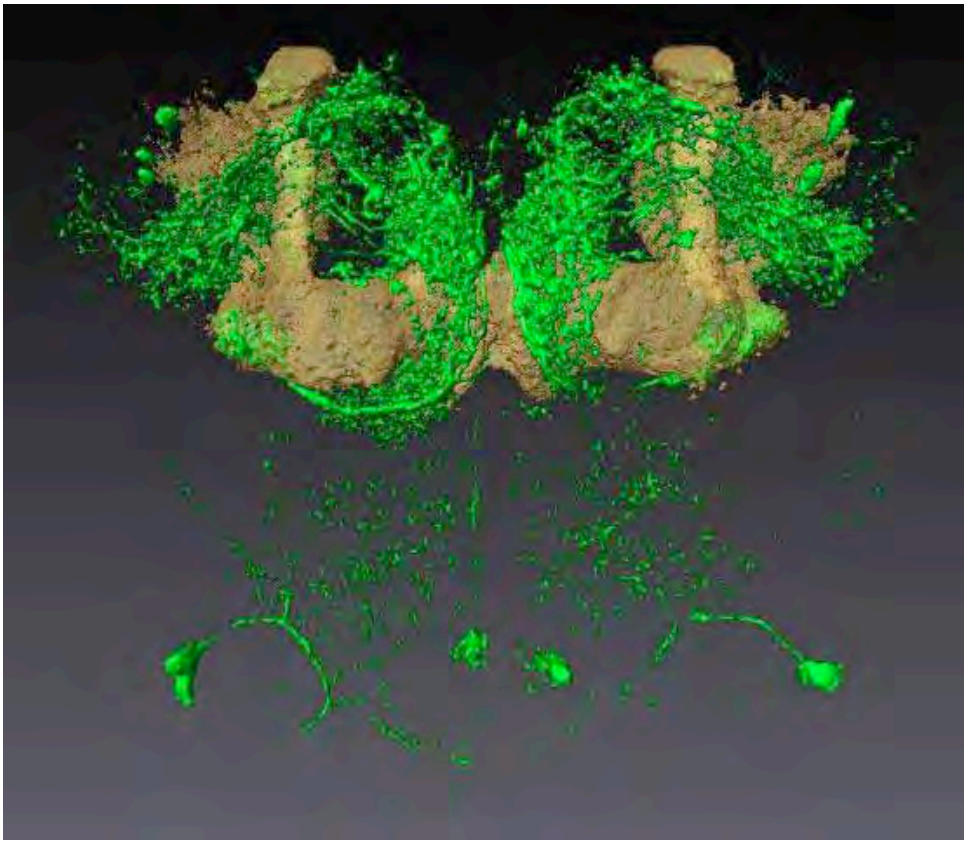

Figure III.15. Projection pattern of c061;MBGAL80. (A) 3-dimensional projection view of a confocal stack of a c061;MBGAL80/uas-*CD8::GFP*;MB-DsRed brain. To produce this movie the green channel was thresholded to reveal the projections of MB-MP neurons in more detail. Thresholding made the neurons that project to the fan-shaped body of the central complex invisible. **(B)** A 3D volume rendered view of a c061;MBGAL80/uas-*CD8::GFP*;MBDsRed brain using Amira software.

Figure III.16

A.

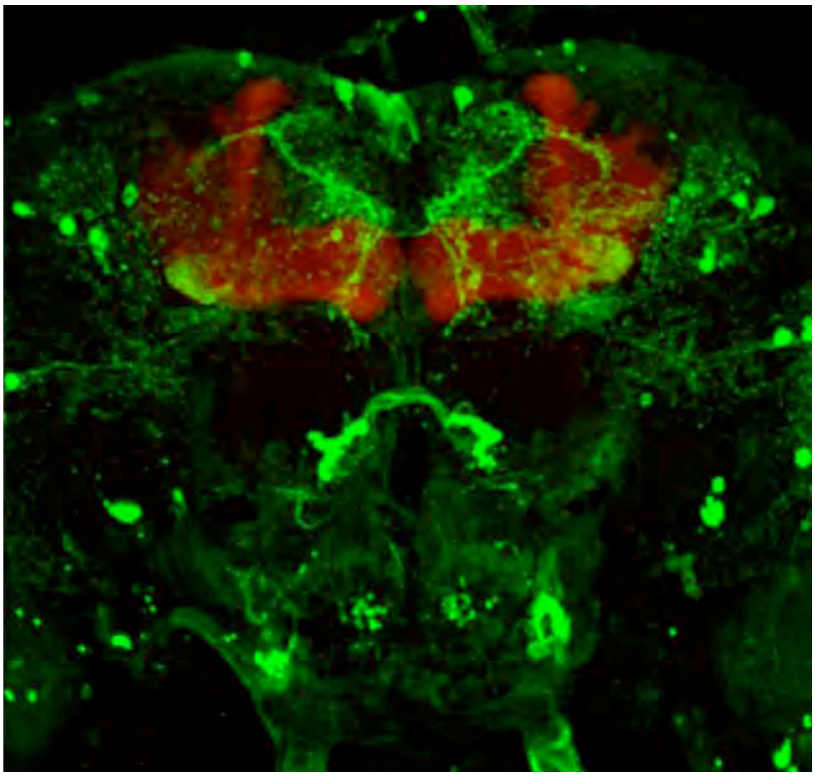

B.

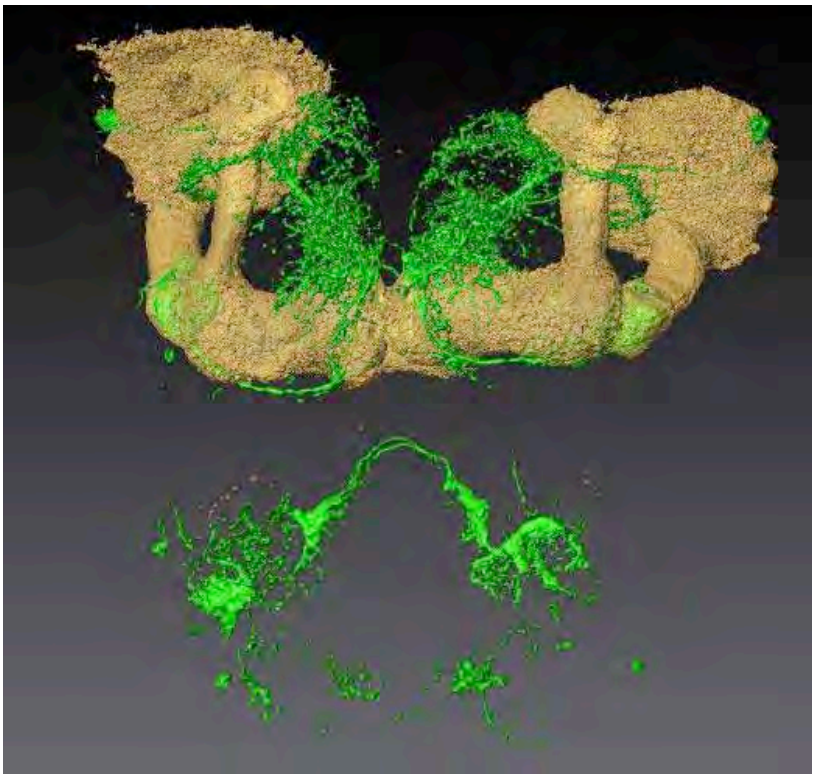

Figure III.16. Projection pattern of NP2758. (A) A 3-dimensional projection view of a confocal stack of an NP2758;uas-*CD8::GFP*;MB-DsRed brain. **(B)** 3D volume rendered view of a c061;MBGAL80/uas-*CD8::GFP*;MBDsRed brain using Amira software.

Figure III.17

A.

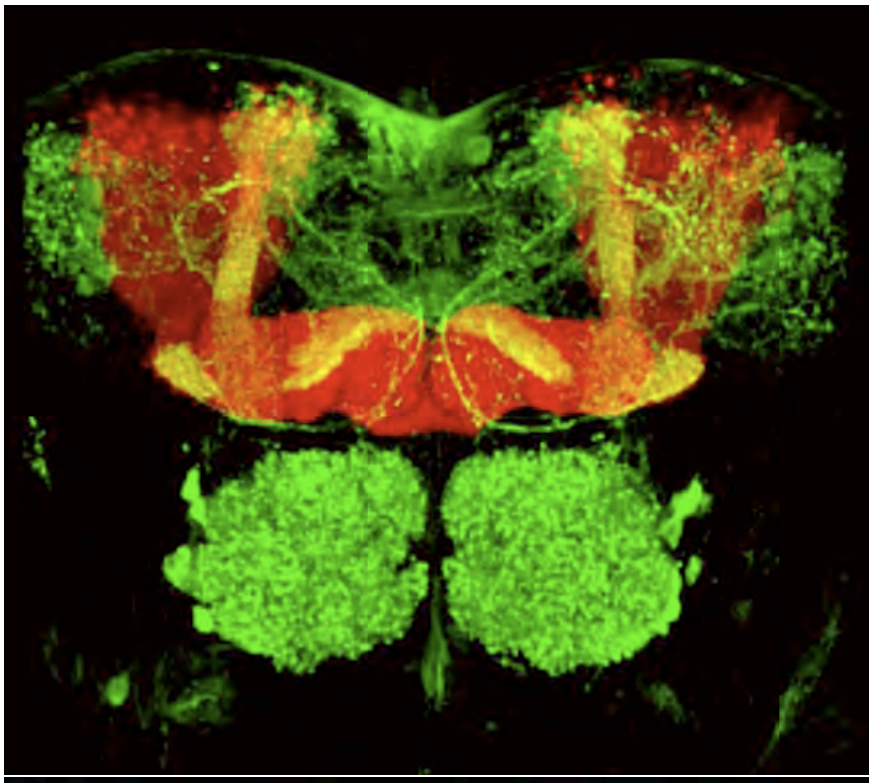

B.

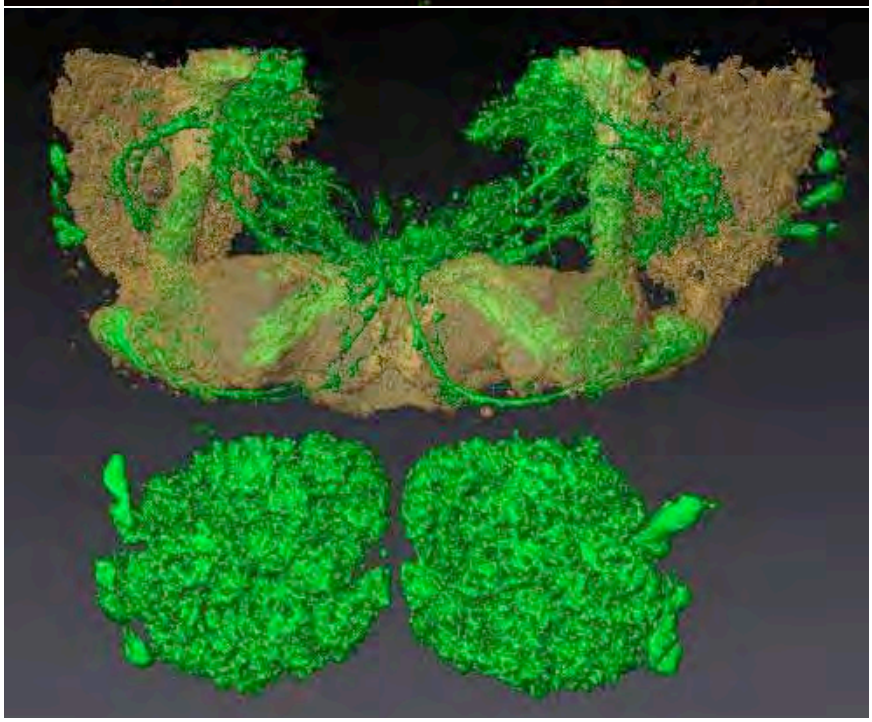

Figure 17. Projection pattern of MBGAL80; *krasavietz*. (A) 3-dimensional projection view of confocal stack of an MBGAL80/ uas-*CD8::GFP; krasavietz/*MB-DsRed brain. **(B)** A 3D volume rendered view of an MBGAL80/uas-*CD8::GFP; krasavietz/*MB-DsRed brain using Amira software

Chapter IV. Final Summary, conclusions and future directions

IV.A. Odor Coding:

Temporal coding in ORNs: The topographical organization of the antennal lobe segregates incoming odor information into combinatorial maps of activated ORNs. One prominent theory suggests that insects and mammals discriminate odors using distinct combinatorial spatial codes (Figure I.6, Ng et al., 2002; Wang et al.,2003). Using the genetic tools available in *Drosophila*, we tested the combinatorial coding hypothesis by engineering flies that have only one class of functional ORNs and therefore cannot support combinatorial maps. These files can be taught to discriminate between two odorants that activate the single functional class of ORN. They can also identify an odorant across a range of concentrations, demonstrating that a combinatorial code is not required to support learned odor discrimination. In addition, these data suggest that odorant identities can be distinguished using differences in the odor-evoked temporal firing patterns in the same ORNs. Electrophysiological studies will be required to address how PN populations respond to different temporal patterns of ORN activity.

Intensity coding: Spatiotemporal patterns of ORN activity vary with changing odor intensity. It is still unclear how the olfactory circuit compensates for changes in odor concentration to maintain appropriate coding of odor identity. Since more classes of ORN are activated with increasing odorant concentration, a combinatorial code would not support odor-generalization across a concentration range. Electrophysiological studies in locust have reported existence of concentration-invariant spatiotemporal features in the PN ensemble (Stopfer et al., 2003) activity but such features have not been reported in *Drosophila* to date. Two recent studies have reported that a purely combinatorial code mediates innate odor attraction in *Drosophila* larvae and adults. Kreher at al. (2008) demonstrated that two receptors Or42a and Or42b mediate the larval response to ethyl acetate and the net behavioral response is a linear summation of the individual olfactory neuron responses. A similar study on odor attraction of adult flies came to a similar conclusion (Semmelhack and Wang, 2009). However these studies did not test odor discrimination. A purely combinatorial code also cannot explain how larvae with a single class of functional ORNs can track odorants across an intensity gradient (Louis et al., 2008). Behavioral studies have found that larvae with a single class of functional ORNs are more sensitive to changes in odorant concentration and this enhanced sensitivity is mediated by iLNs (Asahina et al., 2009). Our preliminary studies of intensity discrimination in adult flies with a class of functional ORNs indicated that these flies are more

sensitive to changes in odor concentration (Figure IV.1). It will be interesting to test the role of iLNs for this enhanced sensitivity.

How to correlate different approaches?

A major roadblock in understanding odor coding has been the lack of correlation between data from different labs. The problem stems from the different approaches used to study odor coding. It is unclear how data collected using the different approaches; functional imaging with synaptic release based sensors or Ca^{2+} sensors and electrophysiological analyses using patch-clamp electrodes, sharp-electrodes and field-recording as well as population-based behavioral paradigms, relate to one another.

Odor is a very complex stimulus and ORN responses to odors vary immensely depending on the odor-delivery system. In the field, it is customary to express odor concentration as the odor-dilutions used in the master stock. However, the actual amount of odor that reaches the fly antennae depends on the flow-rate of the carrier airstream. Since odor responses vary greatly with odor concentration, non-standard odor delivery systems make it difficult to compare data from different labs. Moreover the airstream itself may trigger PN responses, which

makes it critical to establish a standardized protocol for baseline correction and odor delivery.

Another problem in comparing behavioral data with physiology data has been the absence of a good single-fly learning assay. Ideally one would like to compare physiology and behavioral data using the same preparation. However, a typical 3-hour memory score in a T-maze based assay is PI=0.3 which means 65% of the population of flies displays the appropriate response. The reason for this low response probability is unclear. It is possible that the non-perfect response probability is built into the system and reflects the probability of eliciting a learned response in the network. This makes the task of developing a single fly learning assay extremely difficult. A population-based assay smoothes-out the variability of the system but with a single fly assay it might take an extremely large sample size to reach statistically significant data. For example a typical sample size in a T-maze assay is n=6, which means the data, comes from 1200 flies per genotype. To reach a similar sample size with a single fly assay one might need to perform over 1000 individual experiments per genotype. Thus a fresh approach to fly behaviors might be essential to overcome this obstacle. Another problem in comparing behavior data with physiology data is the difference in the exposure time to the odor stimulus. The longest odor-exposure time used in physiology experiments is 1-2 seconds whereas T-maze behavior uses 1-2 minutes of odor-exposure. It is unclear how increased duration of odor-exposure

affects the neuronal response to odors. Flies actively tracking an odor-stream move in and out of the odor-plume, presumably to prevent adaptations of ORNs (Duistermars et al., 2008). Moreover, in free-flight, cross-modal integration between visual, mechanical and olfactory stimuli is essential for a fly to actively track an odor (Duistermars et al., 2008). While the t-maze assay does a fantastic job in reducing the complexity of the response, a richer behavioral assay might be required to fully appreciate the information-coding capacity of the system.

IV.B. The role of the mushroom bodies in memory processes:

IV.B.1. Improved anatomical specificity of MB-GAL4 drivers:

Like other *Drosophila* labs, we rely heavily on the GAL4/UAS system (Brand and Perrimon 1993) to drive expression of transgenes in subpopulations of neurons. Using this approach, our lab has demonstrated that blocking DPM and MB $\alpha'\beta'$ neuron output during acquisition or within the first hour after training (during the period of memory consolidation) severely impairs aversive and appetitive olfactory memory but blocking MB $\alpha\beta$ neurons during these time periods has no effect (Keene et al., 2004; Krashes et al., 2007). Instead MB $\alpha\beta$ neuron output is essential for memory retrieval when output from DPM and MB $\alpha'\beta'$ neurons is dispensable (Krashes et al., 2007; Krashes and Waddell, 2008). A caveat to the

use of GAL4 system is that the expression pattern of most GAL4 enhancer trap lines is rarely exclusive to the cells of interest. Our lab has utilized genetic techniques to improve the resolution of the analyses in MB neurons. We introduced the use of a MB expressed GAL80 transgene to block GAL4 activity in MB neurons and assess the role of other neurons labeled by MB-expressing GAL4 lines (Krashes et al., 2007) and recently we developed a technique to restrict gene expression exclusively to different subsets of mushroom body neurons.

We have used a pan-MB expressed LexA transgene (247-LexA) to express a LexA-operator driven FLP recombinase (lexAop-*FLP*) in all MB neurons. The FLP recombinase activity can then be used to remove either a STOP cassette from a uas>STOP>X transgene (where '>' denotes a FLP Recombinase Target, FRT site, X denotes gene of interest) or a GAL80 cassette from a tub>GAL80> transgene (tub denotes the tubulin promoter). When combined with a mushroom body GAL4 line the uas-X transgene is only expressed where MB-GAL4 and 247-LexA expressions overlap, i.e. in specific subsets of MB neurons (Figure IV.2-6). Flipping-out the >STOP> cassette preceding a transgene requires putting fewer transgenes in a single fly but it requires construction of a new trangene including the >STOP> cassette. Using the tub>GAL80> method allows one to use any pre-existing uas-transgene but

one must deal with possible perdurance of GAL80 even after FLP-out of the transgene.

Both these approaches dramatically improve the specificity of existing MB-GAL4 drivers. Moreover, this allows us to sub-divide the MB based on neurotransmitter use. For example GAD1-GAL4 labels GABAergic neurons in the fly brain including some MB neurons but broad expression of GAD1-GAL4 makes it unsuitable for behavioral studies. Using the FLP-out approach we can manipulate GABAergic kenyon cells for behavioral studies (Figure IV.6).

We are currently using this technique to investigate the roles of the different mushroom body neuron subsets in memory processes. In addition, we are using this approach to perform a gene-expression analysis between the different subsets of MB neurons. These new techniques will help us to develop a greater understanding of MB function.

IV.B.2. Role of cAMP signaling in synaptic plasticity:

The cAMP signaling pathway is believed to be critical for numerous cellular processes including synaptic plasticity (Review Keene and Waddell 2007, Figure I.8 and 12). The current model for memory formation suggests the nature of memory formed following classical conditioning depends on the duration of cAMP

elevation after training. A transient increase in cAMP level results in formation of short-term memory whereas a prolonged increase in cAMP level produces persistent PKA activity, activation of the transcription factor cAMP response-element binding protein (CREB) and results in formation of long-term memory (Review Keene and Waddell 2007, Figure I.8 and 12). However the available tools for modulating the cAMP cascade involve mutant-rescues and pharmacological manipulation, neither of which provides acute spatiotemporal control over cAMP signaling. Thus, a central tenet of memory formation is difficult to tested directly using currently available tools.

A light-inducible cAMP system: To address this problem, we adapted the photo-activated adenylyl cyclase (PAC) from *Euglena gracilis* as a light-inducible cAMP system for *Drosophila*. PAC mediates photoavoidance in *Euglena* and is a tetrameric enzyme consisting of two subunits of PACα and two PACβ. Both subunits independently exhibit adenylyl cyclase activity that is enhanced by blue light. However, catalytic activity of the tetramer is higher than that of the individual subunits (Iseki et al., 2002).

We made multiple fly-lines carrying PACα and PACβ subunit transgenes under the control of the UAS_{GAL4} promoter. This allowed us to express the PAC subunits in specific cells using GAL4 enhancer-trap fly lines. We combined PACα and PACβ lines with a cAMP-response element promoter-driven luciferase

transgene (CRE-luciferase) and monitored light-induced changes in cAMP levels by using a luciferase assay system (Figure IV.7).

We used two independent UAS-PACα and one UAS-PACβ line for our preliminary analysis and discovered that PACα alone is sufficient to elevate cAMP level following exposure to blue-light. Moreover, PACβ appears to have an inhibitory effect on cAMP induction in *Drosophila* (Figure IV.7). An independent study by Schroder-Lang et al. (2007) came to a similar conclusion. To test the utility of the PACα system we collaborated with Vivian Budnik's laboratory to explore the role of cAMP signaling in modulating developmental synaptic plasticity. Our preliminary data indicates that PACα mediated elevation of cAMP can induce synaptic growth at the larval neuromuscular junction (Koon et al. unpublished data).

A single-trial of aversive conditioning produces short-term memory that lasts for a few hours (Tully and Quinn, 1985) whereas a single trial of appetitive conditioning produces long-term memory that persists for days (Krashes and Waddell, 2008). It is possible that appetitive conditioning produces a prolonged change in cAMP level in the MB and thereby allows formation of a more stable memory. If this is true, artificial elevation of cAMP in the MB with the PACα system might allow us to promote LTM following single-trial aversive conditioning.

IV.C. Motivational control of behavior:

Appetitive memory in *Drosophila* provides an excellent system to study motivational control of behavior because the motivational state of hunger promotes appetitive memory performance whereas satiety suppresses it. We found that activation of neuropeptide F (dNPF) neurons in fed flies releases appetitive memory performance from satiety-mediated suppression. Through a GAL4 screen, we identified six dopaminergic neurons that are a substrate for dNPF regulation. In satiated flies, these neurons inhibit mushroom body output, thereby suppressing appetitive memory performance. Hunger promotes dNPF release, which blocks the inhibitory dopaminergic neurons. The motivational drive of hunger thus affects behavior through a hierarchical inhibitory control mechanism: satiety inhibits memory performance through a subset of dopaminergic neurons, and hunger promotes appetitive memory retrieval via dNPF-mediated disinhibition of these neurons. This study establishes *Drosophila* as a model organism to study motivational systems and resolves motivation to a neural mechanism involving dNPF and dopamine that imparts state-dependent control on appetitive memory. The hierarchical arrangement of opposing inhibitory systems may be a common motif in the conditional control of behavior. Future studies will determine whether other motivational states such as thirst utilize control systems resembling the dNPF/DA system we have identified for hunger.

Figure IV.1

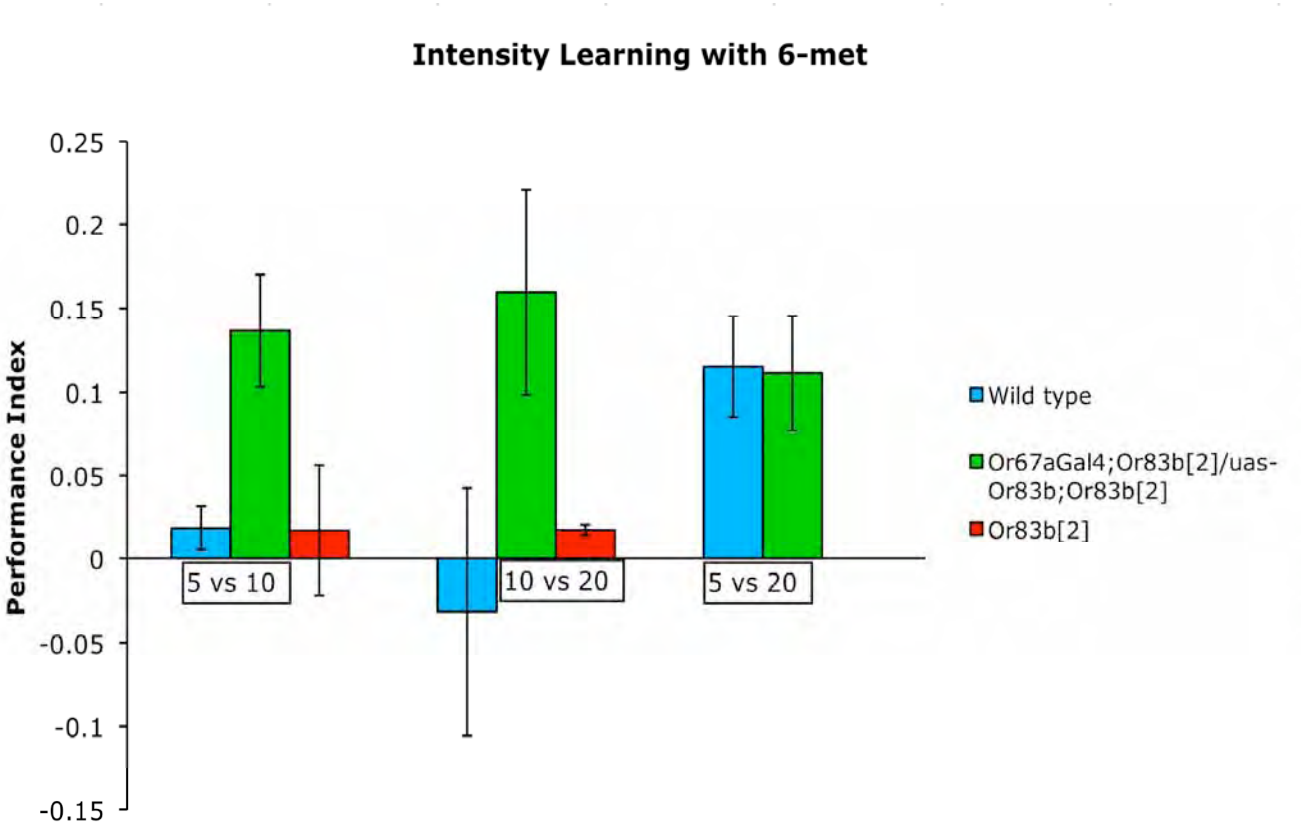

Figure IV.1. *Or83b*^{2} flies with OR67a functional ORNs are more sensitive to concentration difference. OR67a rescue flies are tested for their ability to discriminate between two different concentrations of 6-methyl-5-hepten-2-one (6-met). Unlike OR67a rescue flies, wild type flies cannot discriminate between small differences in concentrations. Numbers on X-axis indicate dilutions of odorants X 10^{-3}

Figure IV.2

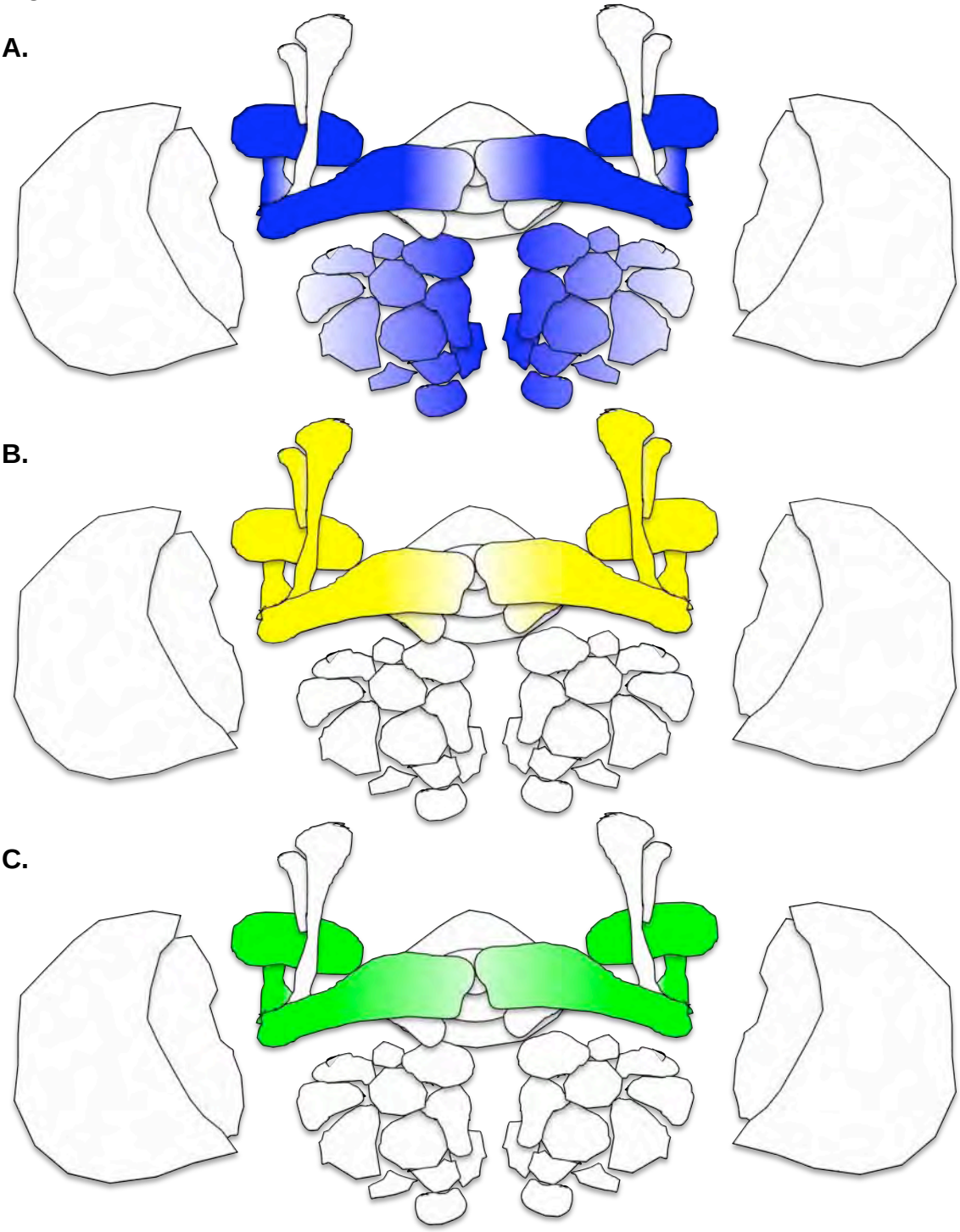

Figure IV.2. Strategy for restricting Gal4 expression within mushroom body subsets. (A) MB1-Gal4 is expressed in γ lobes and in antennal lobes (blue). (B) MB2-LexA is expressed in all lobes of mushroom body. (C) Target gene is expressed where MB1-Gal4 and MB2-LexA expression overlaps, i.e. in mushroom body γ lobes.

Figure IV.3

A.

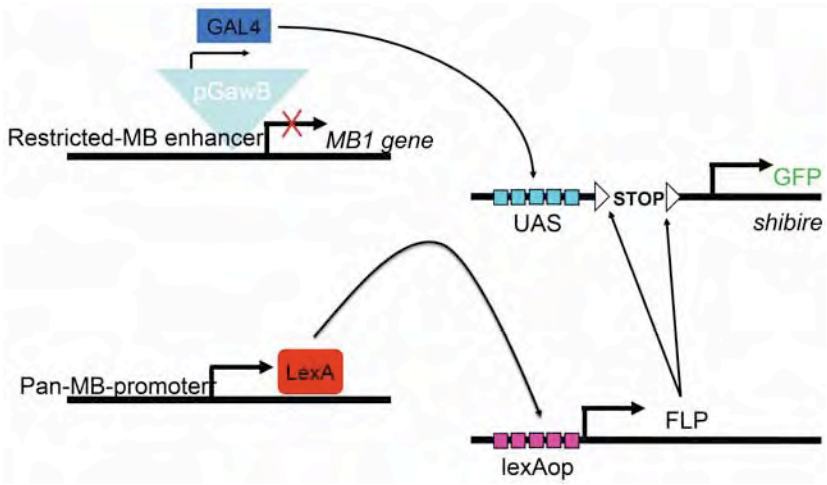

B.

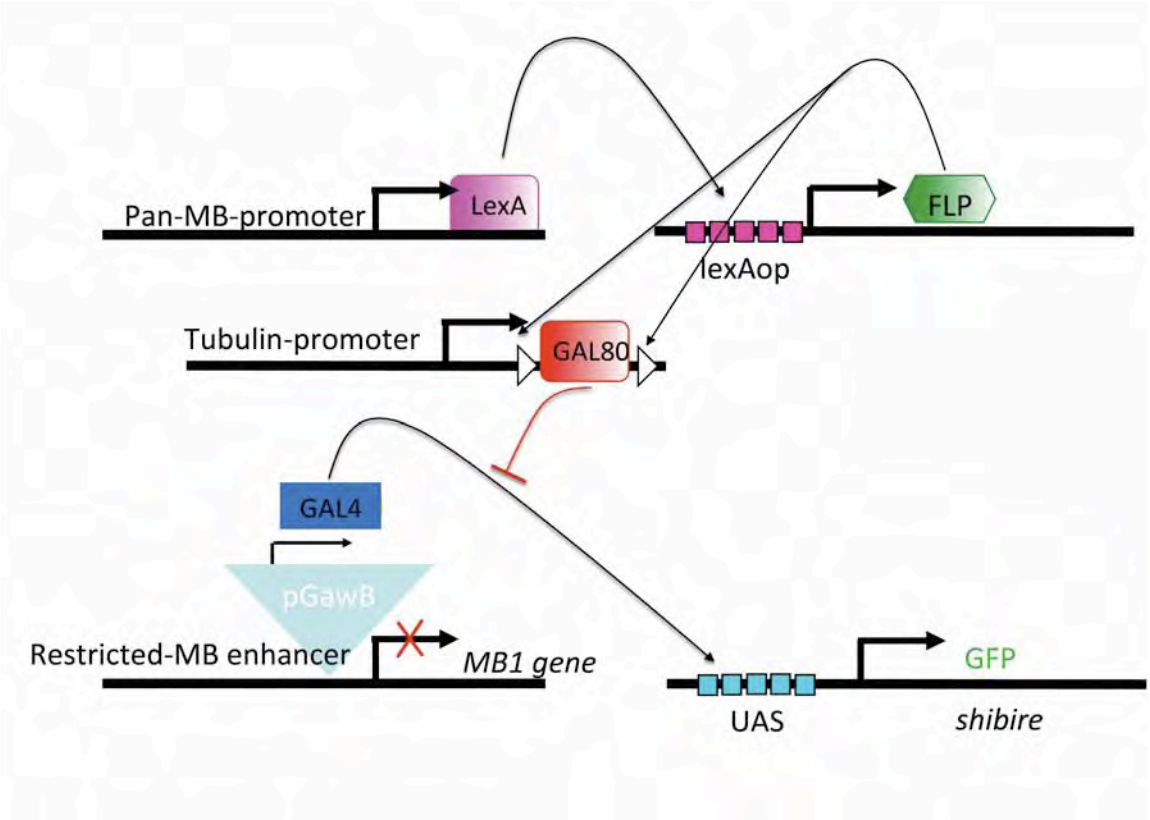

Figure IV.3. Alternative genetic strategies for restricting Gal4 expression within mushroom body subsets. (A) A pan-neuronal mushroom body-LexA driver is used to express FLP-recombinase, which removes the STOP cassette from a uas>STOP>GFP transgene. A MB GAL4 driver can then be used to drive the uas-GFP in MB subsets. **(B)** A restricted MB GAL4 can drive expression of GFP, but the expression is inhibited by the presence of GAL80 transgene driven with ubiquitous Tubulin promoter. In the same fly, a pan-neural mushroom body-LexA driver is used to express FLP-recombinase. FLP removes the GAL80 from the Tub>GAL80> cassette in MB, allowing expression of the GFP only in overlapping neurons.

Figure IV.4

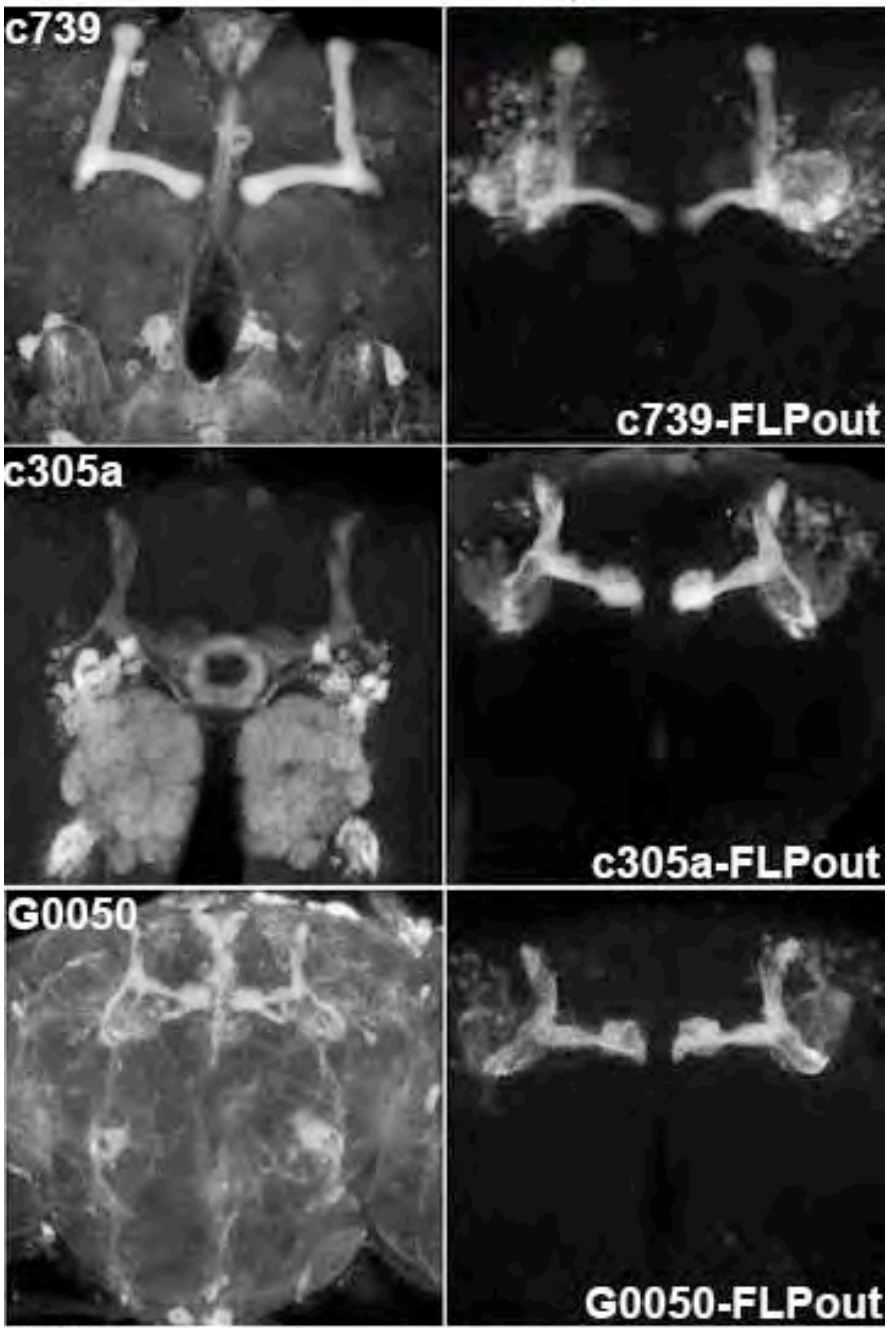

Figure IV.4. Improved specificity with uas>STOP> FLP-out approach: Whole brain projections showing standard GAL4 patterns (left panels) and enhanced specificity with ‘FLP-out’.

Figure IV.5

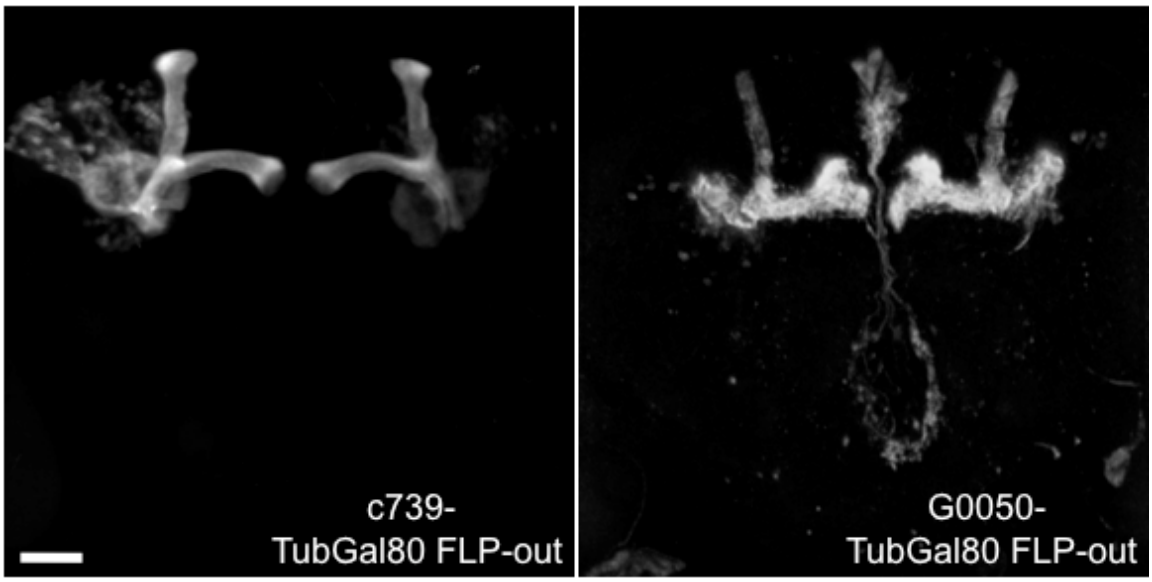

Figure IV.5. Improved specificity with Tubulin>GAL80> FLP-out approach. Whole brain projections showing enhanced specificity with Tub>GAL80> ‘FLP-out’. Scale bar represents 20μm.

Figure IV.6

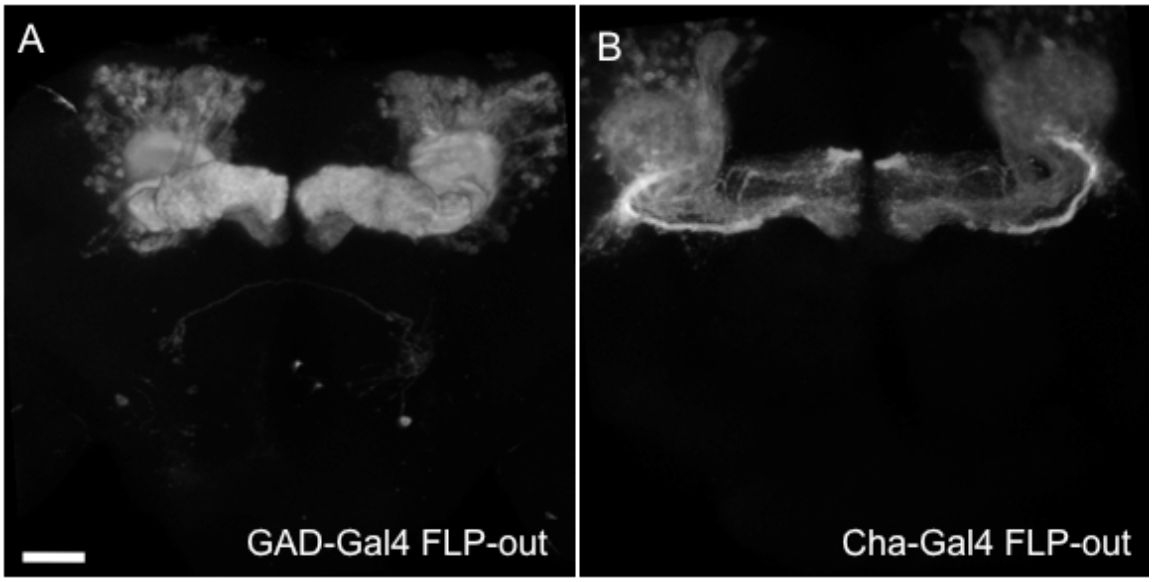

Figure IV.6 Subdividing mushroom body according to transmitter use.

(A) GABAergic neurons of mushroom body are labeled with GAD-Gal4 'FLP-out'.

(B) Cholinergic Kenyon cells are labeled with Cha-Gal4 'FLP-out'. Scale bar represents 20μm.

Figure IV.7

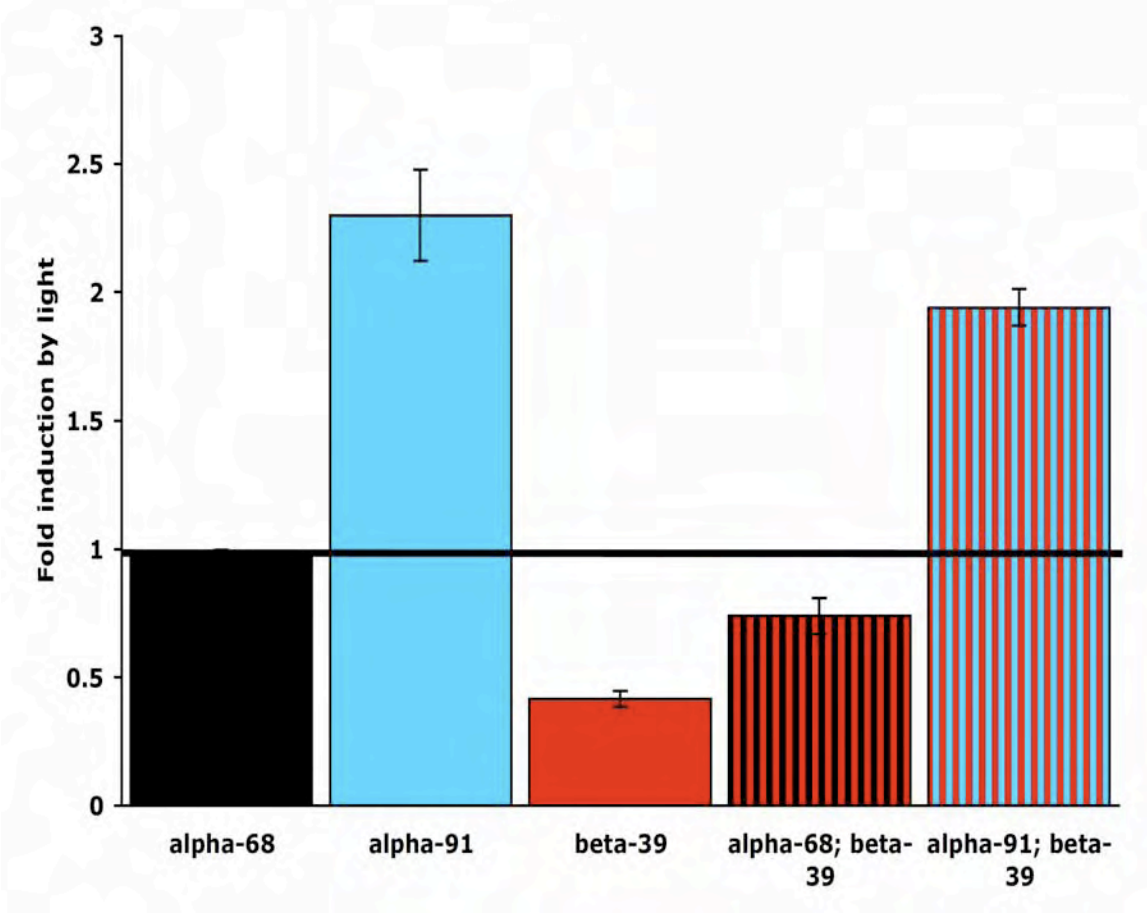

Figure IV.7. Blue light exposure activates PACα alone. Relative changes in luciferase activity induced by exposing transgenic flies to blue light (400-500 nm). All flies harbor the CRE-luciferase reporter and one (alpha-68, alpha-91 or beta-39) or both of the PAC subunit transgenes.

Preface to Appendix

This chapter has been published separately in:

Rickmyre, J. L., **DasGupta, S.,** Ooi, D. L., Keel, J., Lee, E., Kirschner, M. W., Waddell, S., and Lee, L. A. (2007). The Drosophila homolog of MCPH1, a human microcephaly gene, is required for genomic stability in the early embryo. J. Cell. Sci 120, 3565-3577.

DasGupta, S. performed the experiments described in Figure 8.

The *Drosophila* homolog of *MCPH1*, a human microcephaly gene, is required for genomic stability in the early embryo

Jamie L. Rickmyre[1], Shamik DasGupta[2], Danny Liang-Yee Ooi[3], Jessica Keel[1], Ethan Lee[1], Marc W. Kirschner[3], Scott Waddell[2] and Laura A. Lee[1,*]

[1]Department of Cell and Developmental Biology, Vanderbilt University Medical Center, U-4200 MRBIII, 465 21st Avenue South, Nashville, TN 37232-8240, USA
[2]Department of Neurobiology, University of Massachusetts Medical School, 364 Plantation Street, Worcester, MA 01605, USA
[3]Department of Systems Biology, Harvard Medical School, 200 Longwood Avenue, Boston, MA 02115, USA
*Author for correspondence (e-mail: laura.a.lee@vanderbilt.edu)

Accepted 20 August 2007
Journal of Cell Science 120, 3565-3577 Published by The Company of Biologists 2007
doi:10.1242/jcs.016626

Summary

Mutation of human microcephalin (*MCPH1*) causes autosomal recessive primary microcephaly, a developmental disorder characterized by reduced brain size. We identified *mcph1*, the *Drosophila* homolog of *MCPH1*, in a genetic screen for regulators of S-M cycles in the early embryo. Embryos of null *mcph1* female flies undergo mitotic arrest with barrel-shaped spindles lacking centrosomes. Mutation of Chk2 suppresses these defects, indicating that they occur secondary to a previously described Chk2-mediated response to mitotic entry with unreplicated or damaged DNA. *mcph1* embryos exhibit genomic instability as evidenced by frequent chromatin bridging in anaphase. In contrast to studies of human *MCPH1*, the ATR/Chk1-mediated DNA checkpoint is intact in *Drosophila mcph1* mutants. Components of this checkpoint, however, appear to cooperate with MCPH1 to regulate embryonic cell cycles in a manner independent of Cdk1 phosphorylation. We propose a model in which MCPH1 coordinates the S-M transition in fly embryos: in the absence of *mcph1*, premature chromosome condensation results in mitotic entry with unreplicated DNA, genomic instability, and Chk2-mediated mitotic arrest. Finally, brains of *mcph1* adult male flies have defects in mushroom body structure, suggesting an evolutionarily conserved role for MCPH1 in brain development.

Supplementary material available online at
http://jcs.biologists.org/cgi/content/full/120/20/3565/DC1

Key words: *Drosophila*, Embryogenesis, Microcephaly, Cell cycle, Mitosis, DNA checkpoint, BRCT domain

Introduction

Drosophila melanogaster is an ideal model organism for study of the cell cycle during development (reviewed by Foe et al., 1993; Lee and Orr-Weaver, 2003). *Drosophila* achieves rapid embryogenesis by using a streamlined cell cycle that is not dependent on transcription or growth. The first 13 embryonic cell cycles are nearly synchronous nuclear divisions without cytokinesis occurring in the shared cytoplasm of the syncytial blastoderm. These cycles differ from canonical G1-S-G2-M cycles in that they have no intervening gaps; instead DNA replication and mitosis rapidly oscillate. Maternal RNA and protein stockpiles drive these abbreviated 'S-M' cycles (~10 minutes each). In mammalian embryos, rapid peri-gastrulation divisions that occur later in development share many features and have been proposed to be related by evolutionary descent to early embryonic divisions of flies and frogs (O'Farrell et al., 2004). Thus, advances gained from studies of these streamlined cycles in 'simple' model organisms likely have relevance for understanding mammalian cell cycles.

In a genetic screen for regulators of embryonic S-M cycles, we identified the *Drosophila* homolog of a human disease gene, *MCPH1* (microcephalin). Mutation of human *MCPH1* causes autosomal recessive primary microcephaly, a developmental disorder characterized by severe reduction of cerebral cortex size (Jackson et al., 2002). *Mcph1* is highly expressed in the developing forebrain of fetal mice, consistent with its proposed role in regulating the number neuronal precursor cell divisions and, ultimately, brain size (Jackson et al., 2002). Human MCPH1 protein is predicted to contain three BRCA1 C-terminal (BRCT) domains (reviewed by Glover et al., 2004; Huyton et al., 2000), which mediate phosphorylation-dependent protein-protein interactions in cell-cycle checkpoint and DNA repair functions.

Several studies have implicated human MCPH1 in the cellular response to DNA damage. The DNA checkpoint is engaged at critical cell-cycle transitions in response to DNA damage or incomplete replication and serves as a mechanism to preserve genomic integrity (reviewed by Nyberg et al., 2002). Triggering of this checkpoint causes cell-cycle delay, presumably to allow time for correction of DNA defects. When a cell senses DNA damage or incomplete replication, a kinase cascade is activated. Activated ATM and ATR kinases phosphorylate their targets, including the checkpoint kinase Chk1, which is activated to phosphorylate its targets. The first clue that MCPH1 plays a role in the DNA damage response came from siRNA-mediated knockdown studies in cultured mammalian cells demonstrating a requirement for MCPH1 in the intra-S phase and G2-M checkpoints in response to ionizing

radiation (Lin et al., 2005; Xu et al., 2004). Two recent reports have further implicated MCPH1 in the DNA checkpoint, although puzzling discrepancies remain to be resolved (reviewed by Bartek, 2006). One report indicates that MCPH1 functions far downstream in the pathway, at a level between Chk1 and one of its targets, Cdc25 (Alderton et al., 2006). Another report (Rai et al., 2006) suggests that MCPH1 is a proximal component of the DNA damage response required for radiation-induced foci formation (i.e. recruitment of checkpoint and repair proteins to damaged chromatin).

Additional functions have been reported for MCPH1. *MCPH1*$^{-}$ lymphocytes of microcephalic patients exhibit premature chromosome condensation (PCC) characterized by an abnormally high percentage of cells in a prophase-like state, suggesting that MCPH1 regulates chromosome condensation and/or cell-cycle timing (Trimborn et al., 2004). A possible explanation for the PCC phenotype is that *MCPH1*-deficient cells have high Cdk1-cyclin B activity, which drives mitotic entry; decreased inhibitory phosphorylation of Cdk1 was found to be responsible for elevated Cdk1 activity in *MCPH1*-deficient cells (Alderton et al., 2006). It is not clear whether MCPH1's role in regulating mitotic entry in unperturbed cells is related to its checkpoint function; intriguingly, Chk1 has similarly been reported to regulate timing of mitosis during normal division (Kramer et al., 2004). *MCPH1* (also called *Brit1*) was independently identified in a screen for negative regulators of telomerase, suggesting that it may function as a tumor suppressor (Lin and Elledge, 2003). Further evidence for such a role comes from a study showing that gene copy number and expression of *MCPH1* is reduced in human breast cancer cell lines and epithelial tumors (Rai et al., 2006).

We report here the identification and phenotypic characterization of *Drosophila* mutants null for *mcph1*. We show that syncytial embryos from *mcph1* females exhibit genomic instability and undergo mitotic arrest due to activation of a DNA checkpoint kinase, Chk2. We find that, in contrast to reports of MCPH1 function in human cells, the ATR/Chk1-mediated DNA checkpoint is intact in *Drosophila mcph1* mutants. We propose that *Drosophila* MCPH1, like its human counterpart, is required for proper coordination of cell-cycle events; in early embryos lacking *mcph1*, chromosome condensation prior to completion of DNA replication causes genomic instability and Chk2-mediated mitotic arrest.

Results

Screen for *Drosophila* cell-cycle mutants identifies *absent without leave* (*awol*)

In an effort to identify genes required for S-M cycles of the early embryo, we previously screened (Lee et al., 2003) a maternal-effect lethal subset of a collection of ethylmethanesulfonate (EMS)-mutagenized lines from Charles Zuker's lab (Koundakjian et al., 2004). We screened ~2400 lines by examining DAPI-stained embryos of homozygous females. Because early embryonic development is entirely regulated by maternally deposited mRNA and protein, only the maternal genotype is relevant in this screen. We identified 33 lines (12 chromosome II and 21 chromosome III mutants) representing 26 complementation groups in which the majority of embryos from mutant females arrest at the syncytial blastoderm stage. We previously identified two alleles of *giant nuclei*, which prevents excessive DNA replication in S-M cycles (Freeman et al., 1986; Renault et al., 2003), from this collection (Lee et al., 2003). We have now identified alleles of four well-known regulators of the cell cycle from the same screen (supplementary material Table S1). All four genes encode protein kinases with conserved roles in cell-cycle regulation. *wee1*, *grapes*, *telomere fusion* and *aurora* encode *Drosophila* orthologs of Wee1 (a Cdk1 inhibitory kinase), DNA checkpoint kinases Chk1 and ATM (ataxia telangiectasia mutated), and the mitotic kinase Aurora A, respectively (Fogarty et al., 1997; Glover et al., 1995; Oikemus et al., 2004;

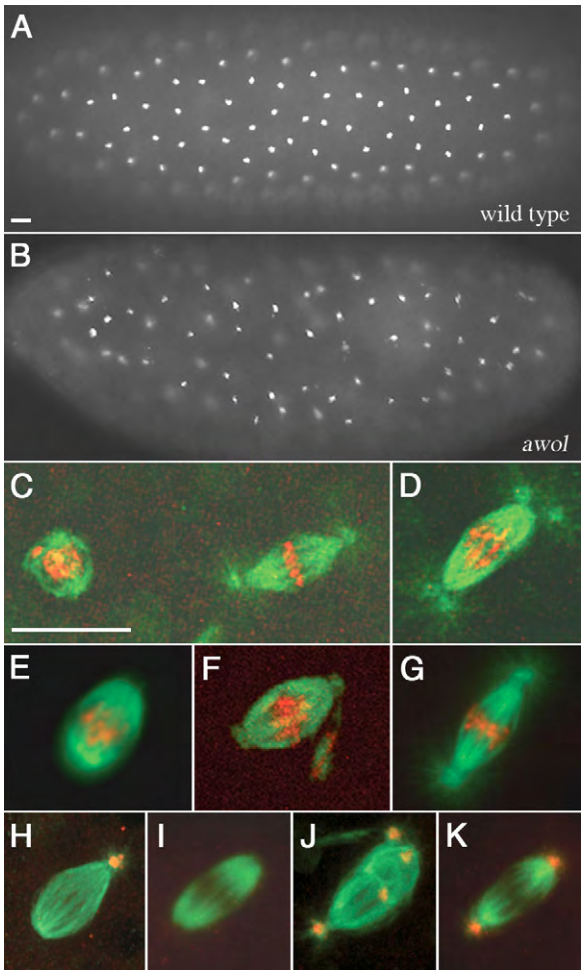

Fig. 1. The *awol* phenotype. Representative syncytial embryos (A,B) and mitotic spindles (C-K) in embryos from wild-type or *awol*^{Z1861}/*awol*^{Z0978} females. (A,B) DNA staining of embryos from *awol* females shows arrest with condensed chromosomes and unevenly spaced nuclei (B) compared to wild type (A). (C-G) Microtubules are in green and DNA in red. (C) Asynchronous neighboring nuclei in embryo from *awol* female (left, interphase; right, mitosis). (D) Metaphase spindle with duplicated centrosomes in embryo from *awol* female shows asynchronous nuclear and centrosome cycles (duplication normally occurs in telophase). (E) Shortened, barrel-shaped spindle in embryo from *awol* female. (F) DNA displaced from metaphase plate is tethered by microtubules to spindle pole in embryo from *awol* female. (G) Wild-type spindle. (H-K) Microtubules are in green and centrosomes in red. (H-I) *awol* spindles with missing or ectopic centrosomes. (K) Wild-type spindle. Bars, 20 μm.

Table 1. Mitotic spindle defects in *mcph1* embryos and suppression by *mnk*

Genotype	MI*	Centrosome number (% spindles)†		Other spindle defects (% spindles)†		
		Decreased‡	Increased§	Barrel	Interacting¶	Multipolar
Wild type	54.1	0.2	0.0	0.1	0.0	0.0
*mcph1***	88.8	43.6	46.0	97.5	0.0	0.2
mnk	54.2	0.2	0.1	0.0	0.2	0.0
mnk mcph1^{Z1861}	57.5	0.2	1.2	0.0	15.0	6.0

*Mitotic index=% embryos in mitosis/total number of embryos (>100 embryos scored per genotype). The presence of both condensed chromosomes and a mitotic spindle was used as the criterion for scoring mitotic embryos.
†To quantify spindle defects, >500 spindles from 25 embryos were scored per genotype.
‡Spindles with centrosomal detachment at one or both poles.
§Spindles with >1 centrosome per pole (one or both poles) or ectopic centrosomes within spindle. Telophase spindles were not scored because centrosome duplication normally occurs at this phase in the early embryo.
¶Two spindles connected by microtubules.
***mcph1*^{Z1861}/*mcph1*^{Z0978}.

Price et al., 2000). Identification of these alleles of bona fide cell-cycle regulators validates our screen.

We chose for further study the largest complementation group on chromosome II (comprising *ZII-0978*, *ZII-1861* and *ZII-4050*) identified in our screen. Females homozygous or transheterozygous for any of these mutations are completely sterile, producing embryos that arrest in a metaphase-like state (~90% of embryos) in cycles 1-8 (the majority in cycles 6-8). Unevenly spaced, asynchronously dividing nuclei and centrosome duplication prior to chromosome segregation are often seen (Fig. 1B-D; Table 1); all of these are consistent with failure of nuclear divisions. Tubulin foci are frequently missing from one or both poles of mitotic spindles, which are typically shorter and more barrel-shaped than those of wild type (Fig. 1E; Table 1). Chromosomes are poorly aligned and occasionally displaced from the metaphase plate (Fig. 1F). Staining for Centrosomin, a core centrosomal component (Li and Kaufman, 1996), revealed that lack of tubulin foci at one or both poles in mutant-derived embryos is due to an absence of centrosomes (Fig. 1H,I; Table 1); we occasionally see ectopic centrosomes embedded in spindles (Fig. 1J; Table 1). On the basis of the phenotype of acentrosomal mitotic spindles, we have given the name '*absent without leave*' ('*awol*') to mutants of this complementation group.

awol encodes the *Drosophila* homolog of *MCPH1*

We localized *awol* to a region including five genes by a combination of mapping strategies (see Materials and Methods for details). A candidate in this region was the *Drosophila* homolog of the human disease gene, *MCPH1* (Jackson et al., 2002). Sequencing of PCR-amplified *mcph1* coding region from homozygous mutant genomic DNA revealed that *awol*^{Z0978} and *awol*^{Z4050} are distinct missense mutations in *mcph1* causing non-conservative amino acid changes and *awol*^{Z1861} is a nonsense mutation resulting in severe truncation of the protein (Fig. 2A). Thus, all three EMS-induced *awol* alleles represent mutations affecting MCPH1 protein. Furthermore, females carrying any of these *awol* alleles in

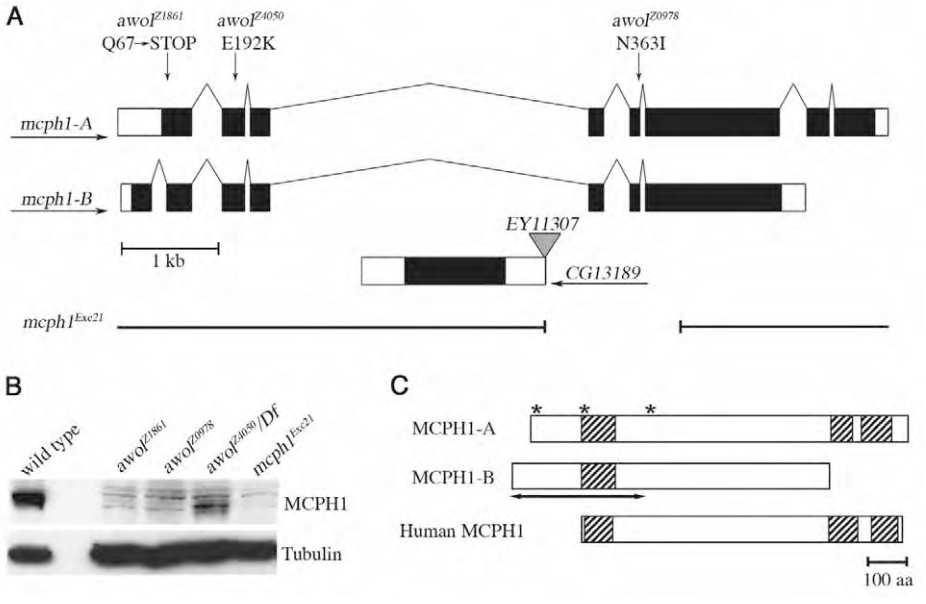

Fig. 2. *mcph1* is the *awol* gene. (A) The *Drosophila mcph1* gene structure. Exons are represented by filled boxes, 5′- and 3′-UTRs by open boxes, and splicing events by thin lines. The gene *CG13189* lies within the largest intron of *mcph1*. Alternative splicing produces transcript *mcph1-RA* or *-RB*. Arrows below gene or transcript names indicate direction of transcription. Positions of the point mutations in each of the three EMS-induced alleles of *awol* and resulting amino acid changes (numbers refer to MCPH1-B) are indicated above the *mcph1* gene. Imprecise excision of *P*-element *EY11307* (inverted triangle) generated allele *mcph1*^{Exc21} (deleted region indicated by gap). (B) Western analysis reveals trace amounts of or no MCPH1 protein in extracts of *awol* embryos relative to wild type (loading control: anti-α-tubulin). The excision allele (*Exc21*) of *mcph1* serves as negative control. *Df=Df(2R)BSC39*, which removes the *mcph1* genomic locus. (C) Comparison of the BRCT domain content (hatched boxes) of the two *Drosophila* MCPH1 isoforms (MCPH1-A and -B) and human MCPH1 protein (bottom). Positions of the amino acid changes in each of the three EMS-induced alleles of *awol* are indicated by asterisks. A double-sided arrow indicates the region of MCPH1-B used for antibody production.

trans to a deletion of the *mcph1* genomic locus produce embryos with phenotypes indistinguishable from that of homozygous mutant females (data not shown), suggesting that all three Zuker *awol* alleles behave genetically as nulls.

To confirm that mutation of *mcph1* is responsible for the awol phenotype, we generated a null allele ($mcph1^{Exc21}$) by imprecise P-element excision (Fig. 2A). $mcph1^{Exc21}$ homozygous females produce embryos with the awol phenotype; similar results were obtained for females carrying this excision in *trans* to any of the EMS-induced *awol* alleles or a deletion of the *mcph1* genomic locus (data not shown), further confirming that mutation of *mcph1* causes the awol phenotype. Importantly, expression of transgenic *mcph1* using the UAS-Gal4 system (Brand and Perrimon, 1993; Rorth, 1998) restored fertility to $awol^{Z0978}/awol^{Z4050}$ females, resulting in a hatch rate of ~40% of their embryos (supplementary material Table S2). Thus, *mcph1* is the *awol* gene. We used the MCPH1 isoform that is most abundant in the early embryo for transgenic rescue; it is possible that full rescue of the maternal-effect lethality of *awol* mutants might additionally require expression of the less abundant isoform (see below for description of MCPH1 isoforms; Fig. 2A and supplementary material Fig. S1B).

To further characterize our *mcph1* alleles, we generated polyclonal antibodies against an MBP-MCPH1 fusion. Anti-MCPH1 antibodies recognize a major band of ~90 kDa, consistent with the predicted size of MCPH1-B, when used to probe immunoblots of wild-type embryo extracts (Fig. 2B). In contrast, for all *mcph1* alleles identified here, we detect greatly reduced or no MCPH1 protein in mutant-derived embryos. Thus, all of these alleles are null (or nearly null) for MCPH1 protein.

MCPH1 isoforms differ in expression pattern and BRCT domain content

Our genetic data revealed that *mcph1* null alleles are homozygous viable and that *mcph1* is required maternally for early embryonic development. To measure MCPH1 levels throughout *Drosophila* development, we probed immunoblots of extracts from various developmental stages with anti-MCPH1 antibodies (supplementary material Fig. S1A). As expected, MCPH1 is abundant in ovaries and early embryos, whereas older embryos under zygotic control have relatively low amounts. MCPH1 is present in larval brains and imaginal discs but undetectable in adult brain extracts. Although high levels of MCPH1 are present in adult testes, it is not required for male fertility (data not shown).

Two major isoforms of MCPH1 were detected by immunoblotting: ~90 kDa (predominant in ovaries and embryos) and ~110 kDa (predominant in testes). Both isoforms were detected in larval tissues. The most recent *mcph1* gene model annotated by FlyBase predicts two splice variants (A and B) differing at their 5′-ends that encode proteins with distinct amino termini (Grumbling and Strelets, 2006). We compared sizes of recombinant MCPH1-A and -B proteins (produced by in vitro transcription-translation reactions) to that of endogenous MCPH1 isoforms by immunoblotting. We found that the gel mobilities of MCPH1-A and -B closely match that of MCPH1 in testes and ovaries, respectively; thus, MCPH1-A is the ~110 kDa isoform that is abundant in testes, and MCPH1-B is the ~90 kDa isoform that is abundant in ovaries and early embryos (supplementary material Fig. S1B).

We observed a discrepancy between relative sizes of MCPH1-A and -B on our immunoblots (A larger than B; supplementary material Fig. S1B) and as predicted by FlyBase [779 versus 826 amino acids, respectively (Grumbling and Strelets, 2006)]. We were unable to find 3′-end sequence data for *mcph1-A* on public databases, so we fully sequenced a representative clone (LP15451) and found it to encode a protein of 981 amino acids, which closely matches our estimated size of 110 kDa for endogenous MCPH1-A. Furthermore, our sequencing revealed that *mcph1-A* contains coding sequence from both *mcph1* and *CG30038*, a gene predicted to overlap the 3′-end of *mcph1* (Fig. 2A). Thus, *mcph1-A* and *-B* are alternatively spliced at both ends, producing proteins that differ in their N- and C-terminal regions (Fig. 2C), and predicted gene *CG30038* comprises alternatively spliced exons of *mcph1-A*.

MCPH1-A and -B proteins both contain BRCT domains (three or one, respectively). The arrangement of BRCT domains within MCPH1-A (one N-terminal and two paired C-terminal) resembles that of human MCPH1 (Fig. 2C). *Drosophila* and human MCPH1 have highest sequence identity in their BRCT domains (37.6%, 52.5% and 26.8% between the N-terminal, first C-terminal, and second C-terminal domains, respectively). The presence of extended amino termini in both *Drosophila* isoforms relative to human MCPH1 raises the possibility that the reported human sequence (Jackson et al., 2002) may not be full-length.

MCPH1 is a nuclear protein

Because *Drosophila* MCPH1 contains BRCT domains, we hypothesized that it has a nuclear function. In syncytial embryos, MCPH1 signal localizes to interphase nuclei and disappears in mitosis (supplementary material Fig. S2). As control for antibody specificity, no MCPH1 signal was detected in interphase nuclei of embryos derived from *mcph1* null females. Because MCPH1 protein is readily detectable throughout the cell cycle (by immunoblotting of extracts from staged embryos; data not shown), the disappearance of MCPH1 signal in mitosis, as observed by immunostaining, is probably due to its dispersal into the cytoplasm upon nuclear envelope breakdown. Human MCPH1 has been reported to localize to the nucleus (Lin et al., 2005) as well as to centrosomes (Jeffers et al., 2007; Zhong et al., 2006); we observe no centrosomal localization for MCPH1 in syncytial embryos of *Drosophila*.

Mitotic arrest in *mcph1* syncytial embryos is a consequence of Chk2 activation

The defective mitotic spindles of embryos derived from *mcph1* females (hereafter referred to as '*mcph1* embryos') exhibit key features reminiscent of Chk2-mediated centrosomal inactivation. In particular, these spindles are short, barrel-shaped, anastral, and associated with poorly aligned chromosomes (Fig. 1). Late syncytial embryos of *Drosophila* use a two-stage response to DNA damage or replication defects (Sibon et al., 2000). The DNA checkpoint mediated by Meiotic 41 (MEI-41) and Grapes (GRP), the *Drosophila* orthologs of ATR (ATM-Rad3-related) and Chk1 kinases, respectively, delays mitotic entry via inhibitory phosphorylation of Cdk1 to

allow repair of DNA damage or completion of replication (Sibon et al., 1999; Sibon et al., 1997). When this checkpoint fails, a secondary damage-control system operating in mitosis is activated; resulting changes in spindle structure block chromosome segregation, presumably to stop propagation of defective DNA (Sibon et al., 2000; Takada et al., 2003). This damage-control system, known as centrosomal inactivation, is mediated by the checkpoint kinase Chk2 (Takada et al., 2003).

Loss of γ-tubulin from centrosomes of mitotic spindles is another characteristic feature of Chk2-mediated centrosomal inactivation. We detected decreased γ-tubulin staining of centrosomes during mitosis in *mcph1* embryos compared to wild type (supplementary material Fig. S3). We typically observe complete detachment of centrosomes from spindles in *mcph1* embryos. High levels of DNA damage induced by intense laser illumination can similarly cause complete centrosomal detachment from spindle poles of wild-type embryos (Takada et al., 2003), suggesting that the spindle changes we observe in *mcph1* embryos represent an extreme form of centrosomal inactivation.

To determine whether mitotic defects in *mcph1* embryos are due to Chk2-mediated centrosomal inactivation, we created lines doubly mutant for *mcph1* and *maternal nuclear kinase* (*mnk*), also known as *loki*, which encodes *Drosophila* Chk2 (Abdu et al., 2002; Brodsky et al., 2004; Masrouha et al., 2003; Xu et al., 2001). A similar approach has been used to demonstrate Chk2-mediated centrosomal inactivation in *grp*, *mei-41* and *wee1* embryos (Stumpff et al., 2004; Takada et al., 2003). Null *mnk* mutants are viable and fertile, but they are highly sensitive to ionizing radiation (Xu et al., 2001). Remarkably, we found that *mnk* suppresses many of the mitotic defects of *mcph1* embryos (Fig. 3A-D; Table 1). Mitotic spindles are restored to near-normality: in contrast to the short, barrel-shaped, anastral spindles of *mcph1* embryos, *mnk mcph1* embryos have elongated spindles with attached centrosomes. Thus, Chk2 activation contributes significantly to the *mcph1* phenotype in syncytial embryos.

In addition to suppressing the mitotic spindle defects of *mcph1* embryos, *mnk* strikingly suppresses their developmental arrest (Fig. 3G-K). Whereas *mcph1* embryos uniformly (100%) arrest in early to mid-syncytial cycles (cycles 1-8), most (>95%) *mnk mcph1* embryos complete syncytial divisions, cellularize, and cease developing near gastrulation. Thus, Chk2 activation causes *mcph1* embryos to arrest at the syncytial stage. Cellularized *mnk mcph1* embryos show irregularities in cell size and shape and intensity of DNA staining; gastrulation is grossly aberrant. We conclude that mutation of *mnk* removes the 'brakes' from *mcph1* embryos, allowing further nuclear divisions and development in the face of DNA defects, which eventually become so severe that embryos die peri-gastrulation.

mcph1 syncytial embryos exhibit a high frequency of chromatin bridging

We sought to understand the primary defects leading to Chk2 activation in *mcph1* embryos. Known triggers of Chk2-mediated centrosomal inactivation are mitotic entry with incompletely replicated or damaged DNA (Sibon et al., 2000; Takada et al., 2003). Although *mnk* suppresses many of the cell-cycle defects of *mcph1* embryos, we occasionally observe abnormal DNA aggregates shared by more than one spindle and multipolar spindles in *mnk mcph1* embryos that progress beyond the usual *mcph1* arrest point (Fig. 3E; Table 1). These defects are not observed in *mnk* embryos, suggesting that they are due to a lack of *mcph1*. In whole mounts of both *mnk mcph1* and *mcph1* embryos, we frequently observe chromatin bridging, which represents a physical linkage of chromosomes that prevents their segregation to opposite poles at anaphase (Fig. 3F; data not shown); this bridging could result from mitotic entry with unreplicated, damaged, and/or improperly condensed chromosomes. We were prohibited from quantifying this phenotype, however, as yolk proteins obscure nuclei that lie deep within the interior of early syncytial embryos. We circumvented this problem by adapting a larval

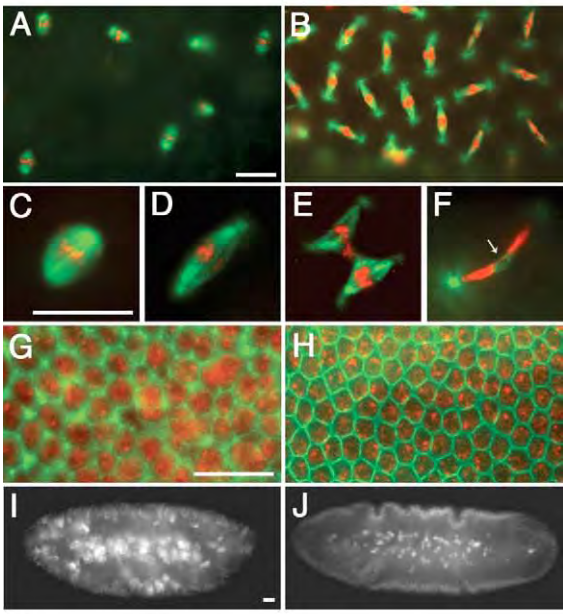

K

Genotype	Gastrulation[a] (% Embryos)	Embryos (n)
wild type	98.6	220
mcph1	0	200
mnk	83.3	180
mnk mcph1	95.9	170

[a]Embryos that initiate gastrulation

Fig. 3. Suppression of *mcph1* by *Chk2* (*mnk*). (A-J) Representative mitotic spindles in syncytial embryos and whole-mount embryos from $mcph1^{Z1861}$, *mnk* $mcph1^{Z1861}$ and wild-type females. Bars, 20 μm. (A-F) Microtubules are in green and DNA in red; low (A,B) and high (C-F) magnification views. *mcph1* embryos have *awol*-type (barrel-shaped, acentrosomal) spindles (A,C). *awol* phenotype is suppressed in *mnk mcph1* embryos (B,D): note restoration of elongated spindles and attached centrosomes. Other defects are seen in *mnk mcph1* embryos, such as DNA shared by two spindles (E) and DNA bridging (F, arrow). (G,H) Cellularized embryos (2-3 hours) stained for actin (green) and DNA (red). *mnk mcph1* embryos reach gastrulation with irregular cell size and DNA content (G) compared to wild type (H). (I,J) DNA-stained embryos (3-4 hours). *mnk mcph1* embryos (I) arrest peri-gastrulation with aberrant morphology compared to wild type (J). (K) Quantification of suppression of developmental arrest of $mcph1^{Z1861}$ embryos by *mnk*.

A

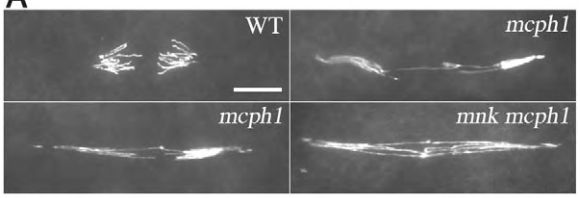

B

Genotype	Chromatin bridging (% A/T[a] figures)	Embryos (n[b])	Late A/T figures (n[b])
wild type	2.9	12	549
mcph1	68.3	14	60
mnk	10.6	6	113
mnk mcph1^{Z1861}	80.8	10	468

[a]A/T represents late anaphase to telophase.
[b]n represents the number of embryos or A/T figures scored.

Fig. 4. Chromatin bridging in *mcph1* embryos. Syncytial embryos were squashed and the DNA stained. (A) Representative late anaphase-to-telophase figures (images shown at same magnification). DNA bridging and increased pole-to-pole distances are seen in squashes of *mcph1*^{Z1861}/*mcph1*^{Z0978} and *mnk mcph1*^{Z1861} embryos. Bars, 10 μm. (B) Quantification of DNA bridging in *mcph1*^{Z1861}/*mcph1*^{Z0978} and *mnk mcph1*^{Z1861} embryo squashes. Wild-type and *mnk* embryos served as controls.

brain squash protocol for this developmental stage that allowed us to more clearly observe chromosomes of early embryos.

Using this approach, we found a high frequency of chromatin bridging in *mcph1* embryos (68% of late anaphase-to-telophase figures) in cycles 4-6, prior to their Chk2-mediated arrest (Fig. 4). Multiple bridges are often present between segregating chromosomes. Spindle pole-to-pole distances are increased dramatically compared to wild-type figures, presumably due to an extended anaphase B in a failed attempt to separate chromosomes that remain physically linked. All *mcph1* alleles reported here exhibit a similar degree of bridging, whereas this phenotype was rarely observed (<3%) in squashes of wild-type embryos (Fig. 4 and data not shown). Chromatin bridging probably represents a primary defect of *mcph1* embryos because it occurs at a similar frequency (81%) in *mnk mcph1* embryos that lack the Chk2-mediated checkpoint. We hypothesize that *mcph1* embryos incur chromosomal lesions that cause Chk2-mediated centrosomal inactivation and mitotic arrest as secondary consequences.

We occasionally observe apparent DNA breakage (evidenced by gaps in DAPI staining) along the length of bridging chromatin that is extensively stretched between poles in *mcph1* and *mnk mcph1* embryos (data not shown). We propose that DNA breakage is not a primary defect in *mcph1* embryos but rather occurs secondary to bridging. Our attempts to confirm the presence of DNA breaks in syncytial embryos (*mcph1* or irradiated wild type) by phospho-histone H2Av or TUNEL staining have been unsuccessful.

mcph1 is not required for the DNA checkpoint in *Drosophila*

Chk2-mediated centrosomal inactivation can be triggered in *Drosophila* syncytial embryos by DNA damaging agents, the DNA-replication inhibitor aphidicolin, or mutation of DNA checkpoint components (MEI-41 or GRP) or WEE1, a kinase that prohibits mitotic entry via inhibitory phosphorylation of Cdk1 (Sibon et al., 2000; Stumpff et al., 2004; Takada et al., 2003). Human *MCPH1*-deficient cells show defective G2-M and intra-S phase checkpoint responses following DNA damage (Alderton et al., 2006; Lin et al., 2005; Xu et al., 2004). In light of these studies linking human *MCPH1* to the ATR/Chk1 pathway and our results that *Drosophila mcph1* embryos undergo Chk2-mediated arrest, we sought to determine if MCPH1 is required for the DNA checkpoint in *Drosophila*.

Because MEI-41 and GRP are required during larval stages for the DNA checkpoint (Brodsky et al., 2000; Jaklevic and Su, 2004), we tested whether MCPH1 is required. In response to ionizing radiation (IR), eye-antennal imaginal disc cells of wild-type larvae undergo G2 arrest. We found that *mcph1* larvae also exhibit IR-induced G2 arrest under conditions in which *mei-41* larvae fail to arrest (Fig. 5A). We next tested the intra-S phase response to IR in larval brain cells. *mcph1* brains exhibited IR-induced intra-S phase arrest similar to that of wild type, whereas no arrest was seen in *mei-41* brains (Fig. 5B). We also tested sensitivity of *mcph1* larvae to hydroxyurea (HU), which blocks DNA replication. Under conditions in which no *mei-41* larvae survived, *mcph1* larvae were HU resistant, surviving at near-Mendelian ratios (Fig. 5C). We conclude that MCPH1 is not required for the DNA checkpoint in larval tissues. We also found that *mcph1* larvae, in contrast to *mei-41*, survive normally following low-dose IR exposure (Fig. 5D), indicating that MCPH1 is not required for DNA repair (Jaklevic and Su, 2004).

The MEI-41/GRP-mediated DNA-replication checkpoint is also developmentally activated at the midblastula transition (MBT) (Sibon et al., 1999; Sibon et al., 1997). Rapid S-M cycles of the early embryo are under maternal genetic control, and the switch to zygotic control occurs at the MBT after cycle 13. During late syncytial cycles (11-13), titration of a maternal DNA-replication factor is thought to induce a *mei-41*/*grp*-dependent checkpoint that causes Cdk1 inhibitory phosphorylation. Mitotic entry is thereby slowed, presumably to allow time to complete replication. Embryos from *mei-41* or *grp* females fail to lengthen interphase in late syncytial cycles and undergo extra S-M cycles (Sibon et al., 1999; Sibon et al., 1997).

We asked if MCPH1 is required for the MEI-41/GRP-dependent DNA-replication checkpoint at the MBT. *mcph1* embryos undergo arrest due to Chk2 activation prior to their reaching cortical divisions (cycles 10-13). Thus, to test whether *mcph1* is required for cell-cycle delay at the MBT, we performed live analysis of cortical divisions in *mnk mcph1* embryos that lack a functional Chk2-mediated checkpoint. We reasoned that any primary defects in cell-cycle timing due to mutation of *mcph1* would still be apparent in *mnk mcph1* embryos. This assumption is strengthened by a recent study showing that *mnk grp* embryos that progress through the MBT due to lack of Chk2-mediated arrest retain the cell-cycle timing defects of *grp* embryos (Takada et al., 2007). We monitored timing of nuclear envelope breakdown and reformation by differential interference contrast microscopy (DIC) and found no significant differences in interphase or mitosis lengths in *mnk mcph1* and wild-type embryos (Fig. 6A).

To further confirm that the DNA-replication checkpoint is

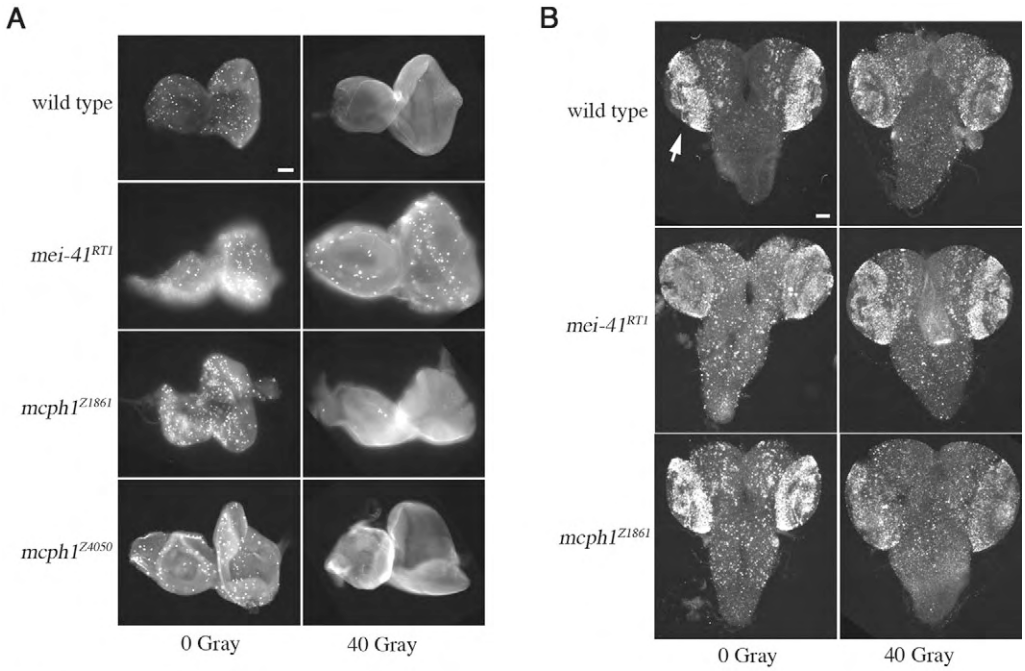

C

Sensitivity to hydroxyurea

Genotype	Percent homozygotes -HU	+HU
mei-41^{RT1}	59.2 (130)	0 (100)
mcph1^{Z1861}/ *mcph1*^{Z0978}	18.4 (163)	22.6 (288)
mcph1^{Exc21}	26.7 (101)	40.6 (101)

D

Eclosion after irradiation

Genotype	Percent eclosion 0 Gray	10 Gray
wild type	86.6 (134)	90.2 (153)
mei-41^{RT1}	79.8 (109)	3.3 (121)
mcph1^{Z1861}	85.1 (114)	82.4 (125)

Fig. 5. *mcph1* larvae have intact DNA checkpoints and normal sensitivity to DNA-damaging agents. (A,B) Cell-cycle checkpoints in *mcph1* larvae. Bars, 50 μm. (A) G2-M checkpoint. Eye-antennal imaginal disks were dissected from untreated (left) or irradiated (right) larvae, fixed, and stained with antibodies against phosphorylated Histone H3 (anti-PH3), a marker of mitotic cells. Lack of anti-PH3 staining post-IR indicates G2 arrest. Representative disks are shown (with at least twelve discs scored per genotype). (B) Intra-S phase checkpoint. Brains were dissected from untreated (left) or irradiated (right) larvae and labeled with BrdU. Decreased BrdU staining in brain lobes (arrows) post-IR indicates intra-S phase arrest. Representative brains are shown (with at least six brains scored per genotype). (C,D) Survival of *mcph1* larvae following exposure to DNA-damaging agents. (C) Sensitivity to hydroxyurea (HU). Larvae were grown on food minus or plus HU and allowed to develop. For each genotype, the ratio of homozygous mutant to total progeny is expressed as a percentage with total number of adult flies scored shown in parentheses. (D) Sensitivity to IR. Third instar larvae were untreated or exposed to low-dose irradiation and allowed to develop. For each genotype, the ratio of eclosed adults to total pupae is expressed as a percentage with total pupae shown in parentheses.

intact in *mnk mcph1* embryos, we assessed the extent of inhibitory phosphorylation of Cdk1 and found it to be comparable to that of wild type (Fig. 6B). We also found wild-type levels of Cyclin B and Cyclin A in *mnk mcph1* embryos (Fig. 6C; data not shown). Low levels of Chk1 protein have been reported in *MCPH1* siRNA human cells (Lin et al., 2005; Xu et al., 2004), but we detected normal levels of Grapes (Chk1) in *mcph1* and *mnk mcph1* embryos (Fig. 6D). Thus, our data do not support a role for *Drosophila* MCPH1 in control of cell-cycle timing in syncytial embryos via regulation of Cdk1 phosphorylation, Cyclin B, or Grapes levels.

mcph1 cooperates with *mei-41* and *grp* to regulate syncytial divisions

Previous studies of *grp* and *mei-41* embryos largely focused on mitotic defects in cortical nuclear divisions, which are amenable to live analysis (Sibon et al., 2000; Takada et al., 2003). Given the earlier arrest point of *mcph1* embryos, we initially concluded that *mcph1* and *mei-41*/*grp* must have discrete roles. We subsequently found, however, that a sizeable fraction of embryos (17-33%) from homozygous or hemizygous *grp* females arrest in pre-cortical cycles (1-9) with acentrosomal, barrel-shaped spindles nearly identical to that of *mcph1* (Fig. 7A). We obtained similar results for all three *grp* alleles tested (Fig. 7B), including the null *grp*^{209} (Larocque et al., 2007). Our data and a previous report of defective Cyclin A proteolysis in pre-cortical *grp* embryos (Su et al., 1999) have established a role for *grp* in regulating the cell cycles of early syncytial embryos. We also found that *mcph1* dominantly enhances a weak *mei-41* phenotype to a degree similar to that of *grp* (Fig. 7C). Intriguingly, by immunoblotting, we consistently observe an upward mobility shift in MCPH1 in *grp* or *mei-41* embryonic extracts (Fig. 7D). Taken together, these data suggest that MCPH1 cooperates with MEI-41 and GRP to regulate the cell cycles of the early embryo via a mechanism independent of Cdk1 phosphorylation.

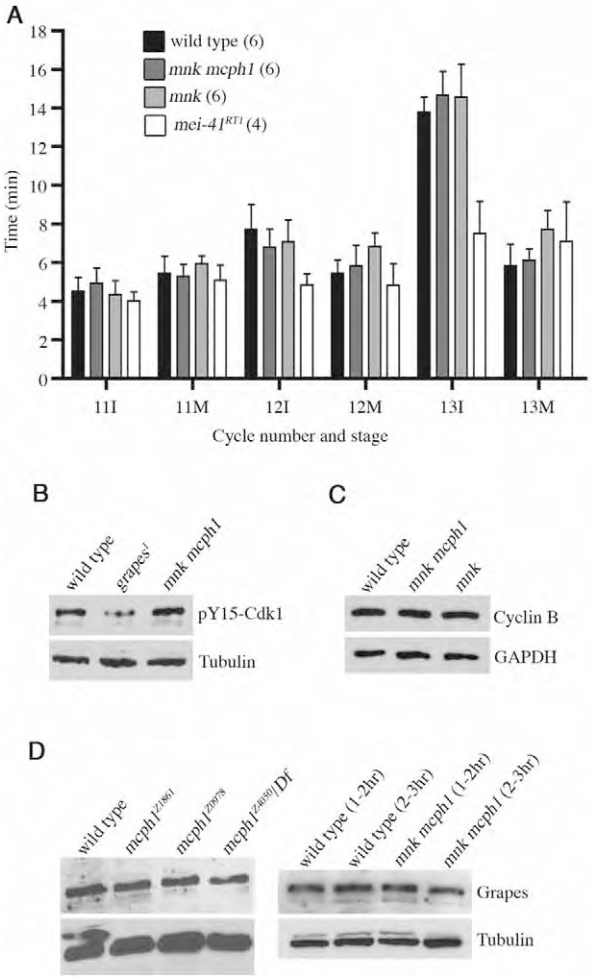

Fig. 6. Intact DNA-replication checkpoint and normal Cyclin B levels in *mcph1* embryos. (A) Quantification of cell-cycle timing during cortical divisions of early embryogenesis. No significant differences in interphase (I) or mitosis (M) lengths were observed for *mnk mcph1*^{Z1861} embryos compared to wild-type or *mnk* controls, whereas shorter interphases were apparent in *mei-41* embryos (cycles 12 and 13). Average times with standard deviations (error bars) are shown. Numbers of embryos scored for each genotype are shown in parentheses. (B) Western analysis using phospho-specific antibodies against Cdk1 reveals wild-type levels of pY15-Cdk1 in extracts of *mnk mcph1*^{Z1861} embryos (1-2 hours). Control *grp* embryos have reduced pY15-Cdk1 levels. (C) Western analysis reveals normal Cyclin B levels in *mnk mcph1*^{Z1861} embryos (1-2 hours). (D) Western analysis reveals normal GRP levels in *mcph1* and *mnk mcph1*^{Z1861} embryos (1-2 hours unless otherwise indicated). Loading controls: anti-α-tubulin or anti-GAPDH.

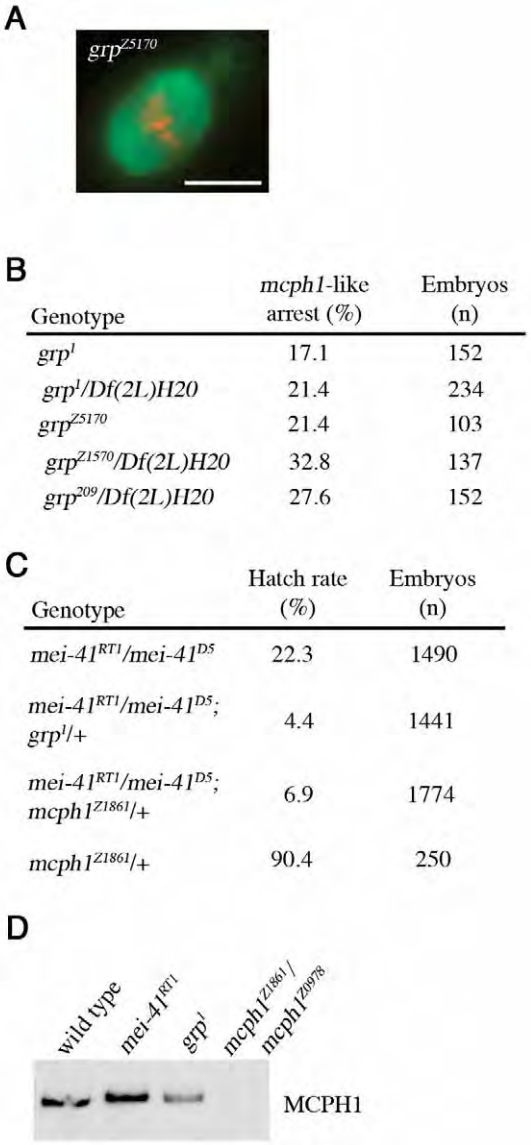

Fig. 7. *mcph1* cooperates with *mei-41* and *grp* in the early embryo. (A) Mitotic spindle from a pre-cortically arrested *grapes*^{Z5170} embryo resembles *awol*-type spindles of *mcph1* embryos. Microtubules are in green and DNA in red. Scale bar: 10 μm. (B) Quantification of *mcph1*-like arrest in *grp* embryos (2-4 hours). (C) *mcph1* dominantly enhances *mei-41* embryonic lethality. Introduction of one copy of *mcph1*^{Z1861} into a semi-sterile *mei-41* background (*mei-41*^{RT1}/*mei-41*^{D5}) reduces embryonic hatch rate more than threefold. (D) Immunoblotting shows slower gel mobility of MCPH1 in *mei-41*^{RT1} or *grp*^{1} embryos (1-2 hours) relative to wild type.

mcph1 males exhibit defects in adult brain structure

On the basis of the reduced brain size of patients with mutation of *mcph1*, we tested whether mutation of *Drosophila mcph1* affects brain development. We did not observe an obvious change in overall brain size, but we did observe morphological defects in central brain structures. The mushroom bodies (MBs) of the *Drosophila* adult brain are bilaterally symmetrical structures required for olfactory memory and other complex adaptive behaviors (de Belle and Heisenberg, 1994). MB structure is stereotyped, and gross morphological brain defects often uncover structural defects in MBs. The 2500 intrinsic neurons in each MB can be subdivided into at least three morphologically well-defined subsets (αβ, α′β′ or γ) based on bundling of their axonal projections in the region of the MBs called the lobes (Crittenden et al., 1998). Each MB neuron contributing to the αβ subdivision bifurcates and sends one axon branch vertically to the α lobe and one horizontally to the β lobe. Anti-Fasciclin II (FasII) antibodies strongly

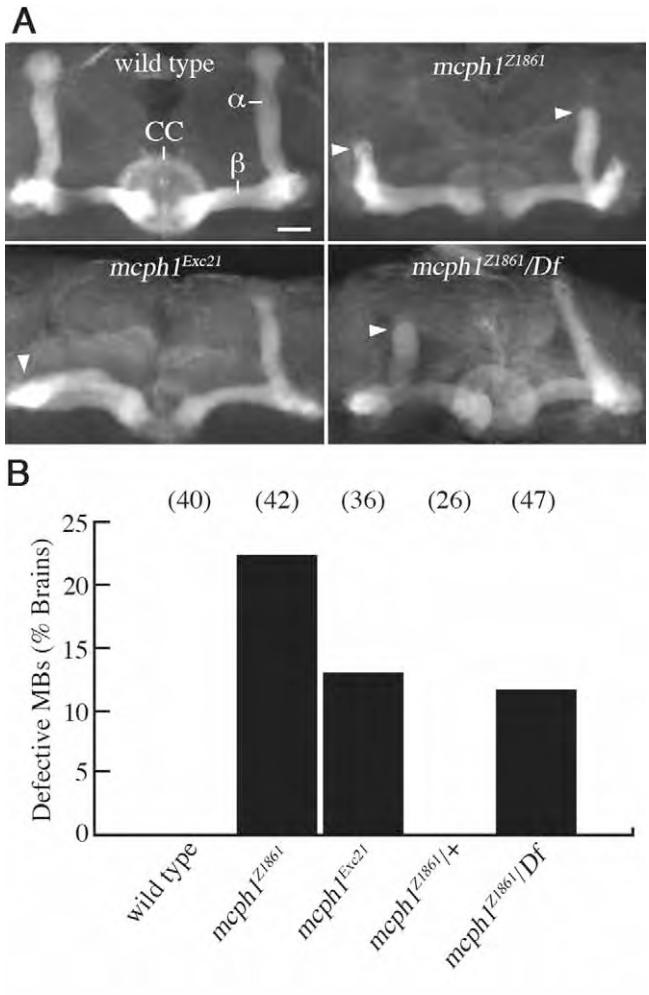

Fig. 8. Defects in male *mcph1* brains. Adult male brains were stained with anti-FasII antibodies to visualize mushroom body (MB) αβ lobes and the ellipsoid body of the central complex (CC). (A) MB αβ lobes of wild-type brains are symmetric, whereas MBs of *mcph1* brains are occasionally defective with missing or diminished αβ lobes (arrowheads). *Df=Df(2R)BSC39*, which removes the *mcph1* genomic locus. (B) Quantification of brain defects in *mcph1* males. Sample number for each genotype is indicated in parentheses (top).

label MB neurons that lie in the αβ lobes (Grenningloh et al., 1991), thereby allowing straightforward visualization of developmental defects.

Our initial analysis revealed obvious morphological MB defects in brains of $mcph1^{Z1861}$ and $mcph1^{Exc21}$ male flies (Fig. 8A). The nature of the MB defects was variable, ranging from missing or malformed lobes to complete absence of lobes, and defects were often asymmetric. For unknown reasons, we never observed MB defects in brains of female *mcph1* flies (data not shown). Quantification revealed defects in 22% of $mcph1^{Z1861}$ and 13% of $mcph1^{Exc21}$ male brains (Fig. 8B). We similarly found defects in 11.5% of brains from males carrying $mcph1^{Z1861}$ in trans to a deletion of the *mcph1* genomic locus; no defects were found in control heterozygous ($mcph1^{Z1861}$/+) male brains. These data establish a role for *mcph1* in *Drosophila* brain development.

Discussion

We identified *Drosophila mcph1*, the homolog of the human primary microcephaly gene *MCPH1*, in a genetic screen for cell-cycle regulators and have shown that it is required for genomic stability in the early embryo. Three additional primary microcephaly (*MCPH*) genes have been identified in humans: *ASPM*, *CDK5RAP2*, and *CENPJ* (reviewed by Cox et al., 2006). Much of our understanding of the biological functions of the proteins encoded by human *MCPH* genes has come from studies of their *Drosophila* counterparts. Mutation of *abnormal spindle* (*asp*), the *Drosophila* ortholog of *ASPM*, results in cytokinesis defects and spindles with poorly focused poles (do Carmo Avides and Glover, 1999; Wakefield et al., 2001). The *Drosophila* ortholog of *CDK5RAP2*, *centrosomin* (*cnn*), is required for proper localization of other centrosomal components (Li and Kaufman, 1996; Megraw et al., 1999). *Sas-4*, the *Drosophila* ortholog of *CENPJ*, is essential for centriole production, and the mitotic spindle is often misaligned in asymmetrically dividing neuroblasts of *Sas-4* larvae (Basto et al., 2006). Whereas all of these primary microcephaly genes are critical regulators of spindle and centrosome functions, mitotic defects in *Drosophila mcph1* mutants are largely secondary to Chk2 activation in response to DNA defects; thus, *mcph1* probably represents a distinct class of primary microcephaly genes.

MCPH1 is a BRCT domain-containing protein, suggesting that it plays a role in the DNA damage response. Conflicting models of MCPH1 function, however, have emerged from studies of human cells as it has been proposed to function at various levels in this pathway: upstream, at the level of damage-induced foci formation (Rai et al., 2006) and further downstream, to augment phosphorylation of targets by the effector Chk1 (Alderton et al., 2006). The phenotype of embryos from null *mcph1* females is more severe than that of embryos from null *grp* females, suggesting that enhancement of phosphorylation of GRP (Chk1) substrates is not the sole function of MCPH1. Furthermore, we found both the DNA checkpoint in larval stages and its developmentally regulated use at the MBT to be intact in *mcph1* mutants, suggesting a requisite role for MCPH1 in the DNA checkpoint evolved in higher organisms.

Studies of human cells suggest a role for MCPH1 in regulation of chromosome condensation. Microcephalic patients homozygous for a severely truncating mutation in MCPH1 show increased frequency of G2-like cells displaying premature chromosome condensation (PCC) with an intact nuclear envelope (Alderton et al., 2006; Trimborn et al., 2004). Depletion of Condensin II subunits by RNAi in *MCPH1*-deficient cells leads to reduction in the frequency of PCC, suggesting that MCPH1 is a negative regulator of chromosome condensation (Trimborn et al., 2006). Alderton et al. (Alderton et al., 2006) observed a decreased level of inhibitory phosphates on Cdk1 that correlated with PCC in *MCPH1*-deficient cells. The authors proposed that MCPH1 maintains Cdk1 phosphorylation in an ATR-independent manner because PCC is not seen in cells of patients with Seckel syndrome, which is caused by mutation of *ATR*; residual ATR present in these cells, however, may be sufficient to prevent PCC (O'Driscoll et al., 2003). Furthermore, in several experimental systems, ATR and Chk1 have been implicated in an S-M checkpoint that prevents premature mitotic entry with

unreplicated DNA (reviewed by Petermann and Caldecott, 2006).

We have shown that embryos from *grp* (*Chk1*) females occasionally undergo *mcph1*-like arrest in early syncytial cycles, prior to the time at which inhibitory phosphorylation of Cdk1 is thought to control mitotic entry. Thus, decreased signaling through the DNA checkpoint resulting in less Cdk1 phosphorylation is unlikely to explain this *mcph1*-like arrest. In contrast to studies of *MCPH1*-deficient human cells, we detect no decrease in pY15-Cdk1 levels in *mcph1* embryos allowed to progress beyond their normal arrest point by mutation of *mnk* (*Chk2*). Based on these data and the PCC phenotype associated with loss of *MCPH1* in humans, we propose a model in which MEI-41/GRP cooperate with MCPH1 in syncytial embryos in a Cdk1-independent manner to delay chromosome condensation until DNA replication is complete (Fig. 9). In the absence of *mcph1*, we hypothesize that embryos condense chromosomes before finishing S phase, resulting in DNA defects (bridging chromatin), Chk2 activation, and mitotic arrest. We were precluded from directly monitoring chromosome condensation in *mnk mcph1* embryos expressing Histone-GFP as previously described (e.g. Brodsky et al., 2000) because we were unable to establish fly stocks carrying this transgene in the *mnk* background. Live imaging of *mcph1* embryos was not technically feasible because they arrest prior to cortical stages, and yolk proteins obscure more interior nuclei in early embryos. *grp* embryos have been reported to initiate chromosome condensation with normal kinetics (Yu et al., 2000), although a subtle PCC phenotype might be difficult to detect.

Support for our model that MCPH1 allows completion of S phase by delaying chromosome condensation comes from the observation that inhibition of DNA replication in syncytial embryos (via injection of aphidicolin or HU) results in phenotypes similar to those observed in *mcph1* embryos, including chromatin bridging, which is presumably a direct consequence of progressing through mitosis with unreplicated chromosomes (Raff and Glover, 1988), and Chk2 activation (Takada et al., 2003). Alternatively, *mcph1* might be required during S phase for timely completion of DNA synthesis; in this case, *mcph1* embryos would initiate chromosome condensation with normal kinetics prior to completing replication. Coordination of S-phase completion and mitotic entry may be particularly critical in the rapid cell cycles of the early embryo that lack gap phases and may explain why loss of *Drosophila mcph1* is most apparent at this developmental stage. Interestingly, even in the absence of exogenous genotoxic stress, *MCPH1*-deficient human cells also exhibit a high frequency of chromosomal aberrations (Rai et al., 2006), which may be a consequence of PCC.

An evolutionary role for *mcph1* in expansion of brain size along primate lineages has emerged in recent years (reviewed by Woods et al., 2005). In brains of *Drosophila mcph1* males, we find low-penetrance defects in MB structure. Both MCPH1 isoforms are expressed in larval brains, and all *mcph1* mutations described here affect both isoforms, so it is unclear whether MB formation requires one or both isoforms. The lack of MB defects in *mcph1* females is puzzling because both isoforms are found in male and female larval brains (data not shown); other sex-specific factors are probably involved. Larval brains of *mcph1* males show no obvious aneuploidy (data not shown) or spindle orientation defects (Andrew Jackson, personal communication), so the cellular basis for these defects remains to be determined. It will be interesting to test in future studies whether *mei-41* and *grp*, which cooperate with *mcph1* to regulate early embryogenesis, are similarly required in *Drosophila* males for brain development.

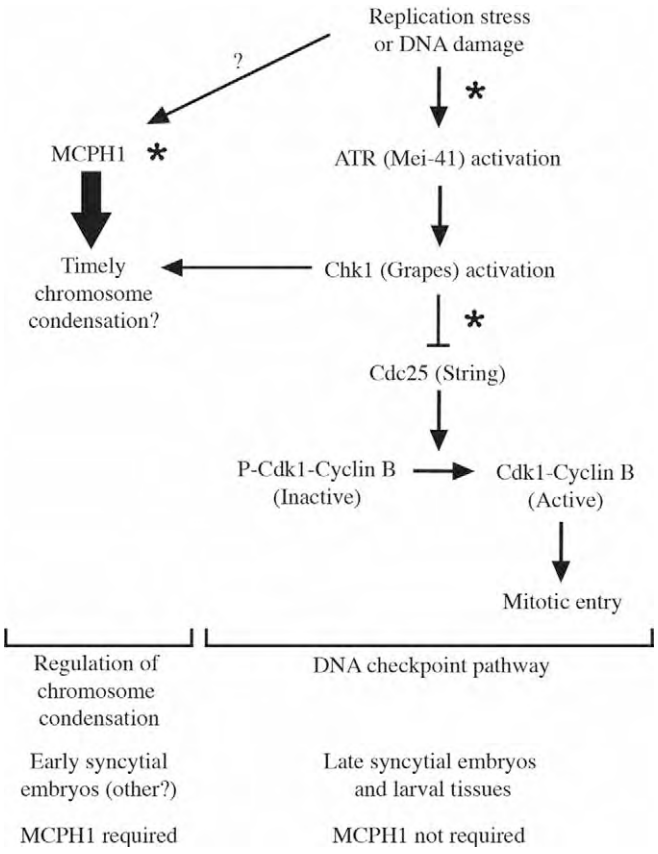

Fig. 9. Proposed model of *Drosophila* MCPH1 function. Asterisks represent key points at which human MCPH1 reportedly functions. Our data suggest that MCPH1 cooperates with MEI-41/GRP in a Cdk1-independent manner to promote genomic integrity in embryos, possibly by controlling timing of chromosome condensation.

In conclusion, we have demonstrated an essential role for *Drosophila* MCPH1 in maintaining genomic integrity in the early embryo. Our data suggest that, in contrast to the mammalian protein, *Drosophila* MCPH1 is not required for the DNA checkpoint, although its role in regulating other processes (e.g. chromosome condensation) may be conserved. We predict that the early embryo of *Drosophila* will continue to be an important model genetic system for unraveling the biological functions of MCPH1, a critical determinant of brain size in humans.

Materials and Methods

Drosophila stocks

Flies were maintained at 25°C using standard techniques (Greenspan, 2004). Wild-type stocks used were *y w* or *Oregon-R*. Zuker alleles of *mcph1* are *cn bw* and balanced over *CyO*. Zuker stock designations have been shortened and superscripted to indicate that they are alleles of *mcph1* (e.g. *ZII-1861* becomes $mcph1^{Z1861}$). Deficiency strains, P-element lines for mapping, mutants for complementation

testing (*grp*^{1}, *aurora*^{1}, *wee1*^{ES1}), *nanos-Gal4:VP16* stock, and *mei-41* mutants were from Bloomington Stock Center. *mcph1* P-element insertions were from Bloomington Stock Center (*EY11307*), Kyoto Stock Center (*NP6229-5-1*), or a gift from Steven Hou (*l(2)SH0220*). *tefu*^{356}, *mnk*^{6006} and *grp*^{209} stocks were gifts from Mike Brodsky, Bill Theurkauf and Tin Tin Su, respectively.

Identification of new alleles of cell-cycle regulators

A combination of female meiotic recombination, deficiency mapping and direct complementation testing of candidates was used to identify mutants from our screen. Complementation testing with known cell-cycle regulators was performed by assessing fertility of females carrying a Zuker chromosome in trans to a known mutation. We used the following alleles: *wee1*^{ES1} (Price et al., 2000), *grp*^{1} (Fogarty et al., 1997), *tefu*$^{\Delta 356}$ (Oikemus et al., 2004) and *aur*^{1} (Glover et al., 1995).

Quantification of embryonic hatch rates

For hatch rate assays, embryos (0-4 hours) were collected on grape plates, counted and aged ~40 hours at 25°C. The number of hatched embryos was determined by subtracting the number of unhatched (intact) embryos from the total number collected. Hatch rate is the ratio of hatched to total embryos expressed as a percentage.

Genetic and molecular mapping of *awol*

The *awol* gene was localized by a combination of mapping strategies. We first screened a collection of deficiencies on the second chromosome for non-complementation of the female sterility of *awol*^{Z1861}. We found that females carrying *awol*^{Z1861} in trans to *Df(2R)BSC39* produced embryos with the awol phenotype; similar results were obtained for *awol*^{Z0978} and *awol*^{Z4050}. Thus, *awol* lies between the breakpoints of *Df(2R)BSC39* in the polytene interval 48C5-E1, a region that contains ~35 genes. We mapped *awol* by P-element-induced male recombination (Chen et al., 1998) relative to the following insertion lines: *Mtor*^{k03905}, *ERp60*^{BG01854}, *KG04952*, *otk*^{EP2017} and *CG8378*^{EP2501}. We thereby narrowed *awol* to a region of five genes (including *mcph1*) that lie distal to *ERp60*^{BG01854} and proximal to *KG04952*. The *awol* stock used (*cn ZII-1861 bw/CyO*) has visible flanking markers *cn* and *bw*. The source of transposase was *Delta2-3 Sb*. Multiple independent recombinant chromosomes were recovered for each P-element line tested. Genomic DNA was extracted from whole flies homozygous for *awol* mutations essentially as previously described (Ballinger and Benzer, 1989). *mcph1* coding regions were PCR-amplified from genomic DNA and sequenced.

Generation of *mcph1* excision line

P-element insertions have been identified in the 5′-UTR of *mcph1* (*NP6229-5-1*) and within its largest intron (*l(2)k06612*, *l(2)SH0220* and *EY11307*) (Grumbling and Strelets, 2006). *l(2)k06612* is no longer available from stock centers. We mapped the lethality of line *l(2)SH0220* (Oh et al., 2003) outside of the *mcph1* genomic region (data not shown). We found that *EY11307* homozygous and *EY11307/mcph1*^{Z1861} transheterozygous females are viable, fertile and produce embryos with nearly wild-type levels of MCPH1 protein, indicating that this P-insertion has little effect on *mcph1* transcription; similar results were obtained for *NP6229-5-1* (data not shown). *EY11307* is inserted in the 5′-UTR of *CG13189*, which encodes a putative metal ion transporter, and the largest intron of *mcph1* (Fig. 2A). All EMS-induced *mcph1* mutations described here lie outside of *CG13189* (including two beyond its 3′ end), thereby making it unlikely that decreased *CG13189* activity causes the awol phenotype. We performed imprecise P-element excision of *EY11307* to generate *mcph1*^{Exc21}, which lacks two internal exons and part of the 3′-most exon of *mcph1*; this excision left the 5′-UTR, coding region and 3′-UTR of *CG13189* intact, but probably removed some of its promoter (Fig. 2A).

Embryo fixation, staining and microscopy

Embryos (1-2 hours unless otherwise indicated) were collected for staining using standard techniques (Rothwell and Sullivan, 2000). For mouse anti-α-tubulin (DM1α, 1:500, Sigma) or rabbit anti-Centrosomin (1:10,000, a gift from W. Theurkauf) staining, embryos were dechorionated in 50% bleach, fixed, and devitellinized by shaking in a mixture of methanol and heptane (1:1). For staining with guinea pig anti-MCPH1 (1:200) or mouse anti-actin (1:400, MP Biomedicals) or co-staining with anti-α-tubulin (YL1/2, Serotec, 1:250) and anti-γ-tubulin (GTU-88, 1:250, Sigma), embryos were fixed fore 20 minutes in a mixture of 3.7% formaldehyde in PBS and heptane (1:1). The aqueous layer containing formaldehyde was removed and embryos devitellinized as described above. Embryos were incubated in primary antibodies at 4°C overnight except for anti-MCPH1 (4°C for three days). Secondary antibodies were conjugated to Cy2 (Jackson ImmunoResearch). Embryos were stained with propidium iodide (Sigma) and cleared as previously described (Fenger et al., 2000). A Nikon Eclipse 80i microscope equipped with a CoolSNAP ES camera (Photometrics) and Plan-Apo (20×, 100×) or Plan-Fluor 40× objectives was used; for confocal images, we used a Zeiss LSM510 microscope equipped with a Plan-Neofluar 100× objective.

Embryo squashes and quantification of DNA bridging

Methanol-fixed embryos (40-80 minutes) were placed in 2-μl drops of 45% acetic acid on coverslips for 1-2 minutes. Slides were lowered onto coverslips, inverted and embryos squashed by hand between blotting paper. Samples were snap-frozen in liquid nitrogen, coverslips removed, and slides immersed in ethanol at –20°C for 10 minutes and air-dried. Vectashield mounting medium with DAPI (Vector Labs) and new coverslips were added to slides. Fluorescence microscopy (100× objective) was used to visualize DNA. Late anaphase and telophase figures (cycle-5 to -7 embryos) were examined. The presence of one or more linkages between DNA masses segregating to opposite poles was scored as a bridging defect.

Live embryo imaging

For analysis of cell-cycle timing, embryos (0-1.5 hours) were dechorionated in 50% bleach, glued (octane extract of tape) to glass-bottomed culture dishes (MatTek Corp.), and covered with halocarbon oil 27 (Sigma). DIC images of dividing embryos at 21.5-22.5°C were captured (20-second intervals) using a Nikon Eclipse TE2000-E inverted microscope with a CoolSNAP HQ CCD camera (Photometrics), Plan-Apo 20× objective, and IPLab image acquisition software (BD Biosciences). Interphase length was determined by counting frame numbers from nuclear envelope formation to breakdown. Mitosis length was determined by counting frame numbers from nuclear envelope breakdown to reformation. Cycle number was determined by nuclear size and density.

mcph1 cDNA clones and transgenes

cDNA clones encoding MCPH1-B (LD43341) or MCPH1-A (LP15451) were from the Drosophila Gene Collection or Drosophila Genomics Resource Center, respectively. MCPH1-B coding region was PCR-amplified from LD43341, subcloned into UASp (Rorth, 1998), and transformed into *y w* flies (Spradling, 1986). To generate IVT constructs, MCPH1-B coding region was subcloned into pCS2. The BRCT domains of MCPH1 were identified using ScanProsite. Descriptions of FlyBase's annotation of *mcph1* were based on version FB2006_01 (Grumbling and Strelets, 2006). GenBank accession number for LP15451 encoding MCPH1-A is EF587234.

Polyclonal antibodies against MCPH1

Maltose-binding protein (MBP) fused to MCPH1-B protein (residues 1-352) was used to produce antibodies. N-terminal MCPH1-B sequence was PCR-amplified from LD43341 and subcloned into pMAL (New England Biolabs). MBP-N-MCPH1-B was made in bacterial cells, purified using amylose beads, and injected into guinea pigs for antibody production (Covance). Anti-MCPH1 antibodies were affinity purified using standard techniques.

Protein extracts and immunoblots

Protein extracts were made by homogenizing either embryos (1-2 hours old unless otherwise indicated) or dissected tissues in urea sample buffer as described previously (Tang et al., 1998). Proteins were transferred to nitrocellulose for immunoblotting using standard techniques. MCPH1-A and -B (unlabeled proteins) were made by coupled transcription-translation of LP15451 and LD43341, respectively, according to the manufacturer's protocol (Promega). Antibodies were used as follows: guinea pig anti-MCPH1 (1:200-500), mouse anti-Cyclin B (F2F4, 1:200, Developmental Studies Hybridoma Bank), rabbit anti-pY15-Cdk1 (1:1000, Upstate), rabbit anti-Grapes (1:500, a gift from T. T. Su) (Purdy et al., 2005), mouse anti-α-tubulin (DM1α, 1:5000, Sigma), mouse anti-GAPDH (1:1000, Abcam). HRP-conjugated secondary antibodies and chemiluminescence were used to detect primary antibodies.

DNA damage response assays

We used a Mark I cesium-137 irradiator as a source of irradiation (IR). To test the G2-M checkpoint post-IR, we used the method of Brodsky et al. (Brodsky et al., 2000) except that fluorescently coupled secondary antibodies were used. To test the intra-S phase checkpoint post-IR, we used the method of Jaklevic and Su (Jaklevic and Su, 2004) except that larvae were exposed to 40 Gray (4000 Rad). To test sensitivity to irradiation, third instar larvae were untreated or exposed to 10 Gray (1000 Rad), transferred to food, and allowed to pupate and eclose as adults. Mutant chromosomes were balanced over *CyO, arm-GFP* (Sullivan et al., 2000) and homozygotes identified by lack of GFP signal. Numbers of pupae formed and empty pupal cases (due to eclosion) were scored up to 10 days post-IR. Percentage eclosion (measure of survival) is the number of empty pupal cases expressed as a percentage of total pupae. All irradiated larvae formed pupae in these experiments. To test hydroxyurea (HU) sensitivity, heterozygous adults (ten males and ten virgin females) were added to vials. After embryo collection (48 hours), adults were removed and 500 ml of 20 μM HU in water was added to food 24 hours later. Adult progeny were scored after 2 weeks. HU sensitivity is indicated by preferential loss of a specific genotypic class.

Adult brain immunostaining

Adult brains were fixed, immunostained and examined by confocal microscopy as previously described (Krashes et al., 2007) using mouse anti-Fasciclin II antibodies (1D4, 1:4, Developmental Studies Hybridoma Bank).

The maternal-effect mutant collection was kindly provided by Charles Zuker. We thank Edmund Koundakjian, David Cowan and Robert Hardy for establishing the collection and the labs of Barbara Wakimoto, Dan Lindsley and Mike McKeown for identifying the female-sterile subset. We gratefully acknowledge Terry Orr-Weaver, in whose lab the screen was performed (with support from NIH grant GM39341 and NSF grant MCB0132237 to T.O.-W.) and her lab members for participation in the screen. We thank Irina Kaverina and Saeko Takada for expert advice on live analysis of embryos by DIC microscopy. Erin Loggins, Audrey Frist and Joshua Tarkoff provided technical assistance. Curtis Thorne helped map *awol*. Bill Theurkauf, Tin Tin Su and Mike Brodsky provided antibodies and fly stocks. We thank Bill Theurkauf and Tin Tin Su for helpful discussions and Andrew Jackson for sharing unpublished data. Daniela Drummond-Barbosa, Andrea Page-McCaw, Terry Orr-Weaver and members of the Lee lab provided critical comments on the manuscript. This work was supported by a Basil O'Connor Starter Scholar Research Award (Grant 5-FY05-29) and Grant 1-FY07-456 from the March of Dimes Foundation and NIH grant GM074044 to L.A.L.

References

Abdu, U., Brodsky, M. and Schupbach, T. (2002). Activation of a meiotic checkpoint during Drosophila oogenesis regulates the translation of Gurken through Chk2/Mnk. *Curr. Biol.* **12**, 1645-1651.

Alderton, G. K., Galbiati, L., Griffith, E., Surinya, K. H., Neitzel, H., Jackson, A. P., Jeggo, P. A. and O'Driscoll, M. (2006). Regulation of mitotic entry by microcephalin and its overlap with ATR signalling. *Nat. Cell Biol.* **8**, 725-733.

Ballinger, D. G. and Benzer, S. (1989). Targeted gene mutations in Drosophila. *Proc. Natl. Acad. Sci. USA* **86**, 9402-9406.

Bartek, J. (2006). Microcephalin guards against small brains, genetic instability, and cancer. *Cancer Cell* **10**, 91-93.

Basto, R., Lau, J., Vinogradova, T., Gardiol, A., Woods, C. G., Khodjakov, A. and Raff, J. W. (2006). Flies without centrioles. *Cell* **125**, 1375-1386.

Brand, A. H. and Perrimon, N. (1993). Targeted gene expression as a means of altering cell fates and generating dominant phenotypes. *Development* **118**, 401-415.

Brodsky, M. H., Sekelsky, J. J., Tsang, G., Hawley, R. S. and Rubin, G. M. (2000). mus304 encodes a novel DNA damage checkpoint protein required during Drosophila development. *Genes Dev.* **14**, 666-678.

Brodsky, M. H., Weinert, B. T., Tsang, G., Rong, Y. S., McGinnis, N. M., Golic, K. G., Rio, D. C. and Rubin, G. M. (2004). Drosophila melanogaster MNK/Chk2 and p53 regulate multiple DNA repair and apoptotic pathways following DNA damage. *Mol. Cell. Biol.* **24**, 1219-1231.

Chen, B., Chu, T., Harms, E., Gergen, J. P. and Strickland, S. (1998). Mapping of Drosophila mutations using site-specific male recombination. *Genetics* **149**, 157-163.

Cox, J., Jackson, A. P., Bond, J. and Woods, C. G. (2006). What primary microcephaly can tell us about brain growth. *Trends Mol. Med.* **12**, 358-366.

Crittenden, J. R., Skoulakis, E. M., Han, K. A., Kalderon, D. and Davis, R. L. (1998). Tripartite mushroom body architecture revealed by antigenic markers. *Learn. Mem.* **5**, 38-51.

de Belle, J. S. and Heisenberg, M. (1994). Associative odor learning in Drosophila abolished by chemical ablation of mushroom bodies. *Science* **263**, 692-695.

do Carmo Avides, M. and Glover, D. M. (1999). Abnormal spindle protein, Asp, and the integrity of mitotic centrosomal microtubule organizing centers. *Science* **283**, 1733-1735.

Fenger, D. D., Carminati, J. L., Burney-Sigman, D. L., Kashevsky, H., Dines, J. L., Elfring, L. K. and Orr-Weaver, T. L. (2000). PAN GU: a protein kinase that inhibits S phase and promotes mitosis in early Drosophila development. *Development* **127**, 4763-4774.

Foe, V. E., Odell, G. M. and Edgar, B. A. (1993). Mitosis and morphogenesis in the *Drosophila* embryo: point and counterpoint. In *The Development of Drosophila melanogaster* (ed. M. Bate and A. Martinez Arias), pp. 149-300. Cold Spring Harbor, NY: Cold Spring Harbor Laboratory Press.

Fogarty, P., Campbell, S. D., Abu-Shumays, R., Phalle, B. S., Yu, K. R., Uy, G. L., Goldberg, M. L. and Sullivan, W. (1997). The Drosophila grapes gene is related to checkpoint gene chk1/rad27 and is required for late syncytial division fidelity. *Curr. Biol.* **7**, 418-426.

Freeman, M., Nusslein-Volhard, C. and Glover, D. M. (1986). The dissociation of nuclear and centrosomal division in gnu, a mutation causing giant nuclei in Drosophila. *Cell* **46**, 457-468.

Glover, D. M., Leibowitz, M. H., McLean, D. A. and Parry, H. (1995). Mutations in aurora prevent centrosome separation leading to the formation of monopolar spindles. *Cell* **81**, 95-105.

Glover, J. N., Williams, R. S. and Lee, M. S. (2004). Interactions between BRCT repeats and phosphoproteins: tangled up in two. *Trends Biochem. Sci.* **29**, 579-585.

Greenspan, R. J. (2004). *Fly Pushing: The Theory and Practice of Drosophila Genetics*. Cold Spring Harbor, NY: Cold Spring Harbor Laboratory Press.

Grenningloh, G., Rehm, E. J. and Goodman, C. S. (1991). Genetic analysis of growth cone guidance in Drosophila: fasciclin II functions as a neuronal recognition molecule. *Cell* **67**, 45-57.

Grumbling, G. and Strelets, V. (2006). FlyBase: anatomical data, images and queries. *Nucleic Acids Res.* **34**, D484-D488.

Huyton, T., Bates, P. A., Zhang, X., Sternberg, M. J. and Freemont, P. S. (2000). The BRCA1 C-terminal domain: structure and function. *Mutat. Res.* **460**, 319-332.

Jackson, A. P., Eastwood, H., Bell, S. M., Adu, J., Toomes, C., Carr, I. M., Roberts, E., Hampshire, D. J., Crow, Y. J., Mighell, A. J. et al. (2002). Identification of microcephalin, a protein implicated in determining the size of the human brain. *Am. J. Hum. Genet.* **71**, 136-142.

Jaklevic, B. R. and Su, T. T. (2004). Relative contribution of DNA repair, cell cycle checkpoints, and cell death to survival after DNA damage in Drosophila larvae. *Curr. Biol.* **14**, 23-32.

Jeffers, L. J., Coull, B. J., Stack, S. J. and Morrison, C. G. (2007). Distinct BRCT domains in Mcph1/Brit1 mediate ionizing radiation-induced focus formation and centrosomal localization. *Oncogene* doi:10.1038/sj.onc.1210595.

Koundakjian, E. J., Cowan, D. M., Hardy, R. W. and Becker, A. H. (2004). The Zuker collection: a resource for the analysis of autosomal gene function in Drosophila melanogaster. *Genetics* **167**, 203-206.

Kramer, A., Mailand, N., Lukas, C., Syljuasen, R. G., Wilkinson, C. J., Nigg, E. A., Bartek, J. and Lukas, J. (2004). Centrosome-associated Chk1 prevents premature activation of cyclin-B-Cdk1 kinase. *Nat. Cell Biol.* **6**, 884-891.

Krashes, M. J., Keene, A. C., Leung, B., Armstrong, J. D. and Waddell, S. (2007). Sequential use of mushroom body neuron subsets during drosophila odor memory processing. *Neuron* **53**, 103-115.

Larocque, J. R., Jaklevic, B. R., Su, T. T. and Sekelsky, J. (2007). Drosophila ATR in double-strand break repair. *Genetics* **175**, 1023-1033.

Lee, L. A. and Orr-Weaver, T. L. (2003). Regulation of cell cycles in Drosophila development: intrinsic and extrinsic cues. *Annu. Rev. Genet.* **37**, 545-578.

Lee, L. A., Van Hoewyk, D. and Orr-Weaver, T. L. (2003). The Drosophila cell cycle kinase PAN GU forms an active complex with PLUTONIUM and GNU to regulate embryonic divisions. *Genes Dev.* **17**, 2979-2991.

Li, K. and Kaufman, T. C. (1996). The homeotic target gene centrosomin encodes an essential centrosomal component. *Cell* **85**, 585-596.

Lin, S. Y. and Elledge, S. J. (2003). Multiple tumor suppressor pathways negatively regulate telomerase. *Cell* **113**, 881-889.

Lin, S. Y., Rai, R., Li, K., Xu, Z. X. and Elledge, S. J. (2005). BRIT1/MCPH1 is a DNA damage responsive protein that regulates the Brca1-Chk1 pathway, implicating checkpoint dysfunction in microcephaly. *Proc. Natl. Acad. Sci. USA* **102**, 15105-15109.

Masrouha, N., Yang, L., Hijal, S., Larochelle, S. and Suter, B. (2003). The Drosophila chk2 gene loki is essential for embryonic DNA double-strand-break checkpoints induced in S phase or G2. *Genetics* **163**, 973-982.

Megraw, T. L., Li, K., Kao, L. R. and Kaufman, T. C. (1999). The centrosomin protein is required for centrosome assembly and function during cleavage in Drosophila. *Development* **126**, 2829-2839.

Nyberg, K. A., Michelson, R. J., Putnam, C. W. and Weinert, T. A. (2002). Toward maintaining the genome: DNA damage and replication checkpoints. *Annu. Rev. Genet.* **36**, 617-656.

O'Driscoll, M., Ruiz-Perez, V. L., Woods, C. G., Jeggo, P. A. and Goodship, J. A. (2003). A splicing mutation affecting expression of ataxia-telangiectasia and Rad3-related protein (ATR) results in Seckel syndrome. *Nat. Genet.* **33**, 497-501.

O'Farrell, P. H., Stumpff, J. and Su, T. T. (2004). Embryonic cleavage cycles: how is a mouse like a fly? *Curr. Biol.* **14**, R35-R45.

Oh, S. W., Kingsley, T., Shin, H. H., Zheng, Z., Chen, H. W., Chen, X., Wang, H., Ruan, P., Moody, M. and Hou, S. X. (2003). A P-element insertion screen identified mutations in 455 novel essential genes in Drosophila. *Genetics* **163**, 195-201.

Oikemus, S. R., McGinnis, N., Queiroz-Machado, J., Tukachinsky, H., Takada, S., Sunkel, C. E. and Brodsky, M. H. (2004). Drosophila atm/telomere fusion is required for telomeric localization of HP1 and telomere position effect. *Genes Dev.* **18**, 1850-1861.

Petermann, E. and Caldecott, K. W. (2006). Evidence that the ATR/Chk1 pathway maintains normal replication fork progression during unperturbed S phase. *Cell Cycle* **5**, 2203-2209.

Price, D., Rabinovitch, S., O'Farrell, P. H. and Campbell, S. D. (2000). Drosophila wee1 has an essential role in the nuclear divisions of early embryogenesis. *Genetics* **155**, 159-166.

Purdy, A., Uyetake, L., Cordeiro, M. G. and Su, T. T. (2005). Regulation of mitosis in response to damaged or incompletely replicated DNA require different levels of Grapes (Drosophila Chk1). *J. Cell Sci.* **118**, 3305-3315.

Raff, J. W. and Glover, D. M. (1988). Nuclear and cytoplasmic mitotic cycles continue in Drosophila embryos in which DNA synthesis is inhibited with aphidicolin. *J. Cell Biol.* **107**, 2009-2019.

Rai, R., Dai, H., Multani, A. S., Li, K., Chin, K., Gray, J., Lahad, J. P., Liang, J., Mills, G. B., Meric-Bernstam, F. et al. (2006). BRIT1 regulates early DNA damage response, chromosomal integrity, and cancer. *Cancer Cell* **10**, 145-157.

Renault, A. D., Zhang, X. H., Alphey, L. S., Frenz, L. M., Glover, D. M., Saunders, R. D. and Axton, J. M. (2003). giant nuclei is essential in the cell cycle transition from meiosis to mitosis. *Development* **130**, 2997-3005.

Rorth, P. (1998). Gal4 in the Drosophila female germline. *Mech. Dev.* **78**, 113-118.

Rothwell, W. F. and Sullivan, W. (2000). Fluorescent analysis of Drosophila embryos. In *Drosophila Protocols* (ed. W. Sullivan, M. Ashburner and R. S. Hawley), pp. 141-157. Cold Spring Harbor, NY: Cold Spring Harbor Laboratory Press.

Sibon, O. C., Stevenson, V. A. and Theurkauf, W. E. (1997). DNA-replication checkpoint control at the Drosophila midblastula transition. *Nature* **388**, 93-97.

Sibon, O. C., Laurencon, A., Hawley, R. and Theurkauf, W. E. (1999). The Drosophila ATM homologue Mei-41 has an essential checkpoint function at the midblastula transition. *Curr. Biol.* **9**, 302-312.

Sibon, O. C., Kelkar, A., Lemstra, W. and Theurkauf, W. E. (2000). DNA-replication/DNA-damage-dependent centrosome inactivation in Drosophila embryos. *Nat. Cell Biol.* **2**, 90-95.

Spradling, A. C. (1986). P-element-mediated transformation. In *Drosophila: A Practical Approach* (ed. D. B. Roberts), pp. 175-197. Oxford: IRL Press.

Stumpff, J., Duncan, T., Homola, E., Campbell, S. D. and Su, T. T. (2004). Drosophila Wee1 kinase regulates Cdk1 and mitotic entry during embryogenesis. *Curr. Biol.* **14**, 2143-2148.

Su, T. T., Campbell, S. D. and O'Farrell, P. H. (1999). Drosophila grapes/CHK1 mutants are defective in cyclin proteolysis and coordination of mitotic events. *Curr. Biol.* **9**, 919-922.

Sullivan, K. M., Scott, K., Zuker, C. S. and Rubin, G. M. (2000). The ryanodine receptor is essential for larval development in Drosophila melanogaster. *Proc. Natl. Acad. Sci. USA* **97**, 5942-5947.

Takada, S., Kelkar, A. and Theurkauf, W. E. (2003). Drosophila checkpoint kinase 2 couples centrosome function and spindle assembly to genomic integrity. *Cell* **113**, 87-99.

Takada, S., Kwak, S., Koppetsch, B. S. and Theurkauf, W. E. (2007). grp (chk1) replication-checkpoint mutations and DNA damage trigger a Chk2-dependent block at the Drosophila midblastula transition. *Development* **134**, 1737-1744.

Tang, T. T., Bickel, S. E., Young, L. M. and Orr-Weaver, T. L. (1998). Maintenance of sister-chromatid cohesion at the centromere by the Drosophila MEI-S332 protein. *Genes Dev.* **12**, 3843-3856.

Trimborn, M., Bell, S. M., Felix, C., Rashid, Y., Jafri, H., Griffiths, P. D., Neumann, L. M., Krebs, A., Reis, A., Sperling, K. et al. (2004). Mutations in microcephalin cause aberrant regulation of chromosome condensation. *Am. J. Hum. Genet.* **75**, 261-266.

Trimborn, M., Schindler, D., Neitzel, H. and Hirano, T. (2006). Misregulated chromosome condensation in MCPH1 primary microcephaly is mediated by condensin II. *Cell Cycle* **5**, 322-326.

Wakefield, J. G., Bonaccorsi, S. and Gatti, M. (2001). The drosophila protein asp is involved in microtubule organization during spindle formation and cytokinesis. *J. Cell Biol.* **153**, 637-648.

Woods, C. G., Bond, J. and Enard, W. (2005). Autosomal recessive primary microcephaly (MCPH): a review of clinical, molecular, and evolutionary findings. *Am. J. Hum. Genet.* **76**, 717-728.

Xu, J., Xin, S. and Du, W. (2001). Drosophila Chk2 is required for DNA damage-mediated cell cycle arrest and apoptosis. *FEBS Lett.* **508**, 394-398.

Xu, X., Lee, J. and Stern, D. F. (2004). Microcephalin is a DNA damage response protein involved in regulation of CHK1 and BRCA1. *J. Biol. Chem.* **279**, 34091-34094.

Yu, K. R., Saint, R. B. and Sullivan, W. (2000). The Grapes checkpoint coordinates nuclear envelope breakdown and chromosome condensation. *Nat. Cell Biol.* **2**, 609-615.

Zhong, X., Pfeifer, G. P. and Xu, X. (2006). Microcephalin encodes a centrosomal protein. *Cell Cycle* **5**, 457-458.

Table S1

Table S1. New alleles of known cell-cycle regulators in *Drosophila*

Chromosome	Gene	New alleles	Vertebrate homolog
II	*wee1*	*ZII-2186*	Wee1
	grapes	*ZII-5170*[a]	Chk1
III	*giant nuclei*	*ZIII-0591*[b]	None
		ZIII-3770[b]	
	aurora	*ZIII-2400*	Aurora A
		ZIII-2973	
		ZIII-5137	
	telomere fusion	*ZIII-5190*	ATM

[a]Independently identified as *grapes* allele by LaRocque et al. (2006).
[b]Previously described by Lee et al. (2003).

Table S2

Table S2. Effects of maternal overexpression of transgenic *mcph1* on development of *awol* or wild-type embryos

Genotype	Hatch rate (%)	Embryos (n)
Wild type	95.6	139
awol[a]	0	215
awol[a]; *UASp-mcph1*[b]/*nanos-Gal4:VP16*	38.4	164
awol[a]; *UASp-mcph1*[b]/+	0.5	193
awol[a]; *nanos-Gal4:VP16*/+	0	230
UASp-mcph1/*nanos-Gal4:VP16*	86.9	260

[a]$awol^{Z4050}/awol^{Z0978}$ transheterozygotes.
[b]cDNA encoding MCPH1-B was used to make transgenic construct.

Fig. S1

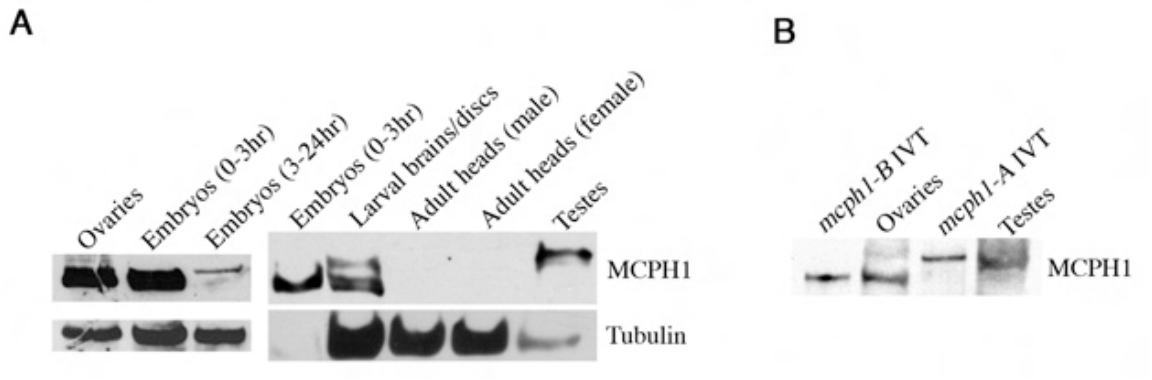

Fig. S1. Developmental expression of alternate MCPH1 isoforms. (A,B) MCPH1 immunoblots. (A) Developmental western of wild-type extracts shows MCPH1 protein is present in a variety of tissues and at several life-cycle stages. Extracts of embryos and testes were relatively underloaded (loading control: anti-α-tubulin). (B) Type A and B MCPH1 isoforms produced in vitro co-migrate on SDS-PAGE with endogenous MCPH1 isoforms abundant in testes and ovaries, respectively.

Fig. S2

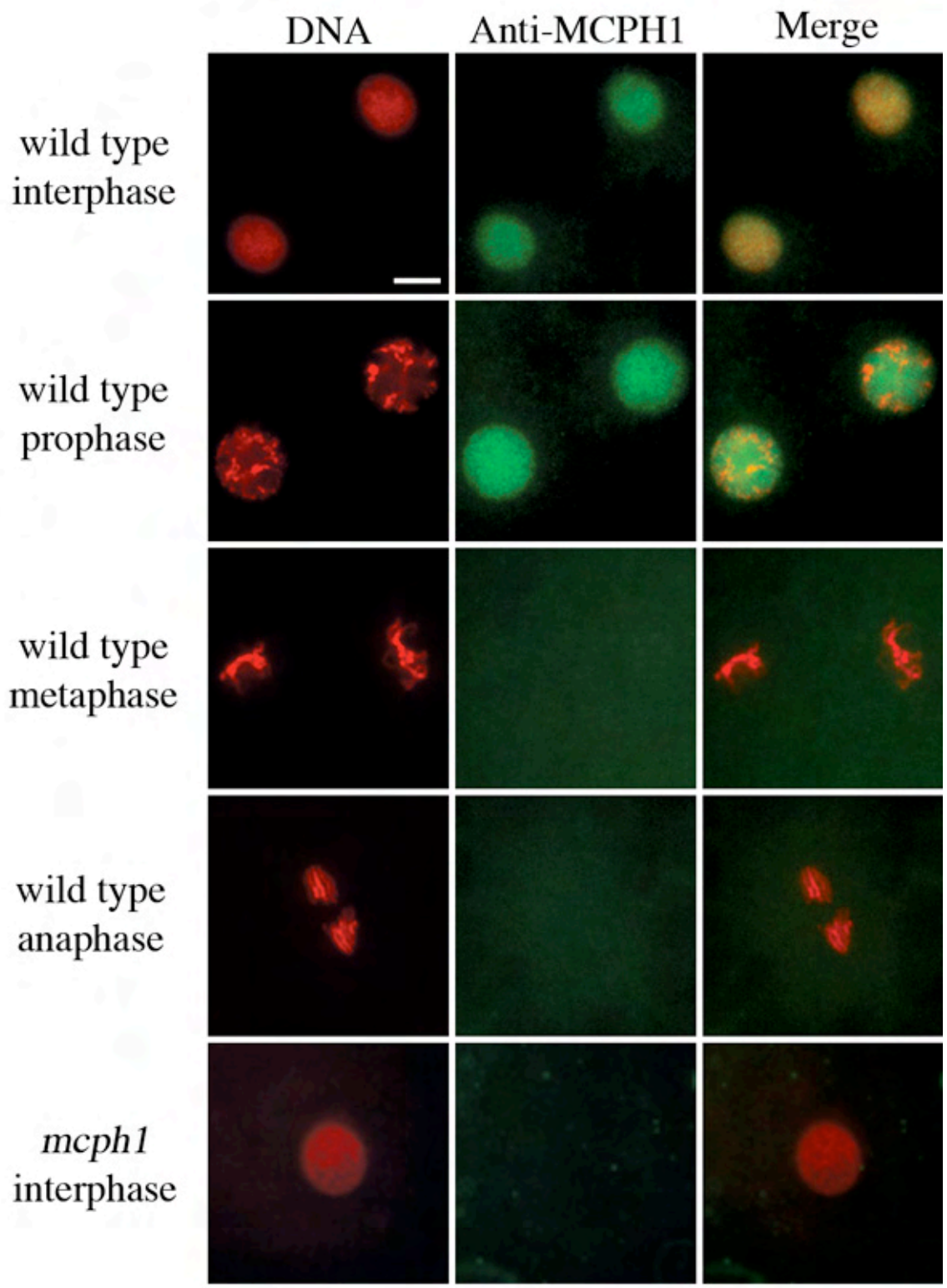
DNA
Anti-MCPH1
Merge
wild type interphase
wild type prophase
wild type metaphase
wild type anaphase
mcph1 interphase

Fig. S2. MCPH1 is a nuclear protein. Wild-type syncytial embryos were fixed and stained with an antibody against MCPH1 (green) and DNA dye (red). Representative embryos in various cell-cycle stages are shown. MCPH1 localizes to the nucleus during interphase and prophase and is no longer detectable during later stages of mitosis (following nuclear envelope breakdown). No MCPH1 signal is detected in interphase nuclei of *mcph1*^{Z1861} mutants (negative control). Bar, 10 µm.

Fig. S3

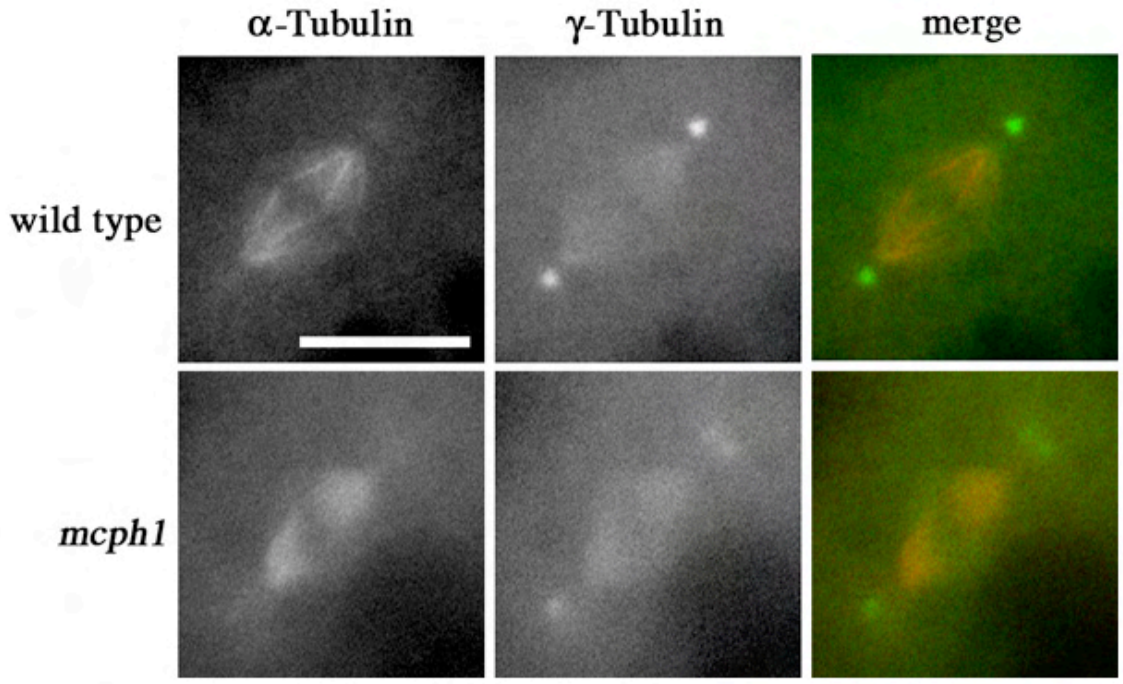

Fig. S3. Decreased γ-tubulin staining of centrosomes in *mcph1* embryos. Syncytial embryos from wild-type or *mcph1*^{Exc21} females were fixed and co-stained with antibodies against α-tubulin (red) and γ-tubulin (green). Representative mitotic spindles are shown. Bar, 10 µm.

Bibliography

Abizaid, A., and Horvath, T. L. (2008). Brain circuits regulating energy homeostasis. Regul. Pept 149, 3-10.

Amrein, H., and Thorne, N. (2005). Gustatory perception and behavior in Drosophila melanogaster. Curr. Biol 15, R673-684.

Andretic, R., van Swinderen, B., and Greenspan, R. J. (2005). Dopaminergic modulation of arousal in Drosophila. Curr. Biol 15, 1165-1175.

Antonov, I., Antonova, I., Kandel, E. R., and Hawkins, R. D. (2003). Activity-dependent presynaptic facilitation and Hebbian LTP are both required and interact during classical conditioning in Aplysia. Neuron 37, 135-147.

Asahina, K., Louis, M., Piccinotti, S., and Vosshall, L. B. (2009). A circuit supporting concentration-invariant odor perception in Drosophila. J. Biol 8, 9.

Ashraf, S. I., McLoon, A. L., Sclarsic, S. M., and Kunes, S. (2006). Synaptic protein synthesis associated with memory is regulated by the RISC pathway in Drosophila. Cell 124, 191-205.

Assisi, C., Stopfer, M., Laurent, G., and Bazhenov, M. (2007). Adaptive regulation of sparseness by feedforward inhibition. Nat. Neurosci 10, 1176-1184.

Bathellier, B., Buhl, D. L., Accolla, R., and Carleton, A. (2008). Dynamic ensemble odor coding in the mammalian olfactory bulb: sensory information at different timescales. Neuron 57, 586-598.

de Belle, J. S., and Heisenberg, M. (1994). Associative odor learning in Drosophila abolished by chemical ablation of mushroom bodies. Science 263, 692-695.

Benton, R., Sachse, S., Michnick, S. W., and Vosshall, L. B. (2006). Atypical membrane topology and heteromeric function of Drosophila odorant receptors In Vivo. PLoS Biol 4, e20.

Benton, R., Vannice, K. S., Gomez-Diaz, C., and Vosshall, L. B. (2009). Variant ionotropic glutamate receptors as chemosensory receptors in Drosophila. Cell 136, 149-162.

Bewick, G. A., Gardiner, J. V., Dhillo, W. S., Kent, A. S., White, N. E., Webster, Z., Ghatei, M. A., and Bloom, S. R. (2005). Post-embryonic ablation of AgRP

neurons in mice leads to a lean, hypophagic phenotype. FASEB J 19, 1680-1682.

Bindra, D. (1959). Motivation : a systematic reinterpretation (New York :: Ronald Press Co).

Blum, K., Sheridan, P. J., Wood, R. C., Braverman, E. R., Chen, T. J., Cull, J. G., and Comings, D. E. (1996). The D2 dopamine receptor gene as a determinant of reward deficiency syndrome. J R Soc Med 89, 396-400.

Brand, A. H., and Perrimon, N. (1993). Targeted gene expression as a means of altering cell fates and generating dominant phenotypes. Development 118, 401-415.

Brown, M. R., Crim, J. W., Arata, R. C., Cai, H. N., Chun, C., and Shen, P. (1999). Identification of a Drosophila brain-gut peptide related to the neuropeptide Y family. Peptides 20, 1035-1042.

Browning, K. N., and Travagli, R. A. (2003). Neuropeptide Y and peptide YY inhibit excitatory synaptic transmission in the rat dorsal motor nucleus of the vagus. J. Physiol. (Lond.) 549, 775-785.

Buck, L. B. (1996). Information coding in the vertebrate olfactory system. Annu. Rev. Neurosci 19, 517-544.

Byers, D., Davis, R. L., and Kiger, J. A. (1981). Defect in cyclic AMP phosphodiesterase due to the dunce mutation of learning in Drosophila melanogaster. Nature 289, 79-81.

Cassenaer, S., and Laurent, G. (2007). Hebbian STDP in mushroom bodies facilitates the synchronous flow of olfactory information in locusts. Nature 448, 709-713.

Castellucci, V., and Kandel, E. R. (1976). Presynaptic facilitation as a mechanism for behavioral sensitization in Aplysia. Science 194, 1176-1178.

Chen, C. N., Denome, S., and Davis, R. L. (1986). Molecular analysis of cDNA clones and the corresponding genomic coding sequences of the Drosophila dunce+ gene, the structural gene for cAMP phosphodiesterase. Proc. Natl. Acad. Sci. U.S.A 83, 9313-9317.

Chen, C. N., Malone, T., Beckendorf, S. K., and Davis, R. L. (1987). At least two genes reside within a large intron of the dunce gene of Drosophila. Nature 329, 721-724.

Cherry, J. A., and Davis, R. L. (1995). A mouse homolog of dunce, a gene important for learning and memory in Drosophila, is preferentially expressed in olfactory receptor neurons. J. Neurobiol 28, 102-113.

Clark, J. T., Kalra, P. S., Crowley, W. R., and Kalra, S. P. (1984). Neuropeptide Y and human pancreatic polypeptide stimulate feeding behavior in rats. Endocrinology 115, 427-429.

Clark, J. T., Kalra, P. S., and Kalra, S. P. (1985). Neuropeptide Y stimulates feeding but inhibits sexual behavior in rats. Endocrinology 117, 2435-2442.

Clyne, P. J., Warr, C. G., and Carlson, J. R. (2000). Candidate taste receptors in Drosophila. Science 287, 1830-1834.

Colmers, W. F., Klapstein, G. J., Fournier, A., St-Pierre, S., and Treherne, K. A. (1991). Presynaptic inhibition by neuropeptide Y in rat hippocampal slice in vitro is mediated by a Y2 receptor. Br. J. Pharmacol 102, 41-44.

Colmers, W. F., Lukowiak, K., and Pittman, Q. J. (1988). Neuropeptide Y action in the rat hippocampal slice: site and mechanism of presynaptic inhibition. J. Neurosci 8, 3827-3837.

Connolly, J. B., Roberts, I. J., Armstrong, J. D., Kaiser, K., Forte, M., Tully, T., and O'Kane, C. J. (1996). Associative learning disrupted by impaired Gs signaling in Drosophila mushroom bodies. Science 274, 2104-2107.

Couto, A., Alenius, M., and Dickson, B. J. (2005). Molecular, anatomical, and functional organization of the Drosophila olfactory system. Current Biology 15, 1535-1547.

Crittenden, J. R., Skoulakis, E. M., Han, K. A., Kalderon, D., and Davis, R. L. (1998). Tripartite mushroom body architecture revealed by antigenic markers. Learn. Mem 5, 38-51.

Dahanukar, A., Foster, K., van der Goes van Naters, W. M., and Carlson, J. R. (2001). A Gr receptor is required for response to the sugar trehalose in taste neurons of Drosophila. Nat. Neurosci 4, 1182-1186.

Dahanukar, A., Lei, Y., Kwon, J. Y., and Carlson, J. R. (2007). Two Gr genes underlie sugar reception in Drosophila. Neuron 56, 503-516.

DasGupta, S., and Waddell, S. (2008). Learned odor discrimination in Drosophila without combinatorial odor maps in the antennal lobe. Current Biology 18, 1668-1674.

Dauwalder, B., and Davis, R. L. (1995). Conditional rescue of the dunce learning/memory and female fertility defects with Drosophila or rat transgenes. J. Neurosci 15, 3490-3499.

Davis, R. L. (2005). Olfactory memory formation in Drosophila: from molecular to systems neuroscience. Annu. Rev. Neurosci 28, 275-302.

de Bruyne, M., Clyne, P. J., and Carlson, J. R. (1999). Odor coding in a model olfactory organ: the Drosophila maxillary palp. J. Neurosci 19, 4520-4532.

de Bruyne, M., Foster, K., and Carlson, J. R. (2001). Odor coding in the Drosophila antenna. Neuron 30, 537-552.

Dethier, V. G. (1976). The Hungry Fly: Physiological study of behaviour associated with feeding (Harvard University Press).

Devaud, J., Keane, J., and Ferrús, A. (2003). Blocking sensory inputs to identified antennal glomeruli selectively modifies odorant perception in Drosophila. J. Neurobiol 56, 1-12.

Dobritsa, A. A., van der Goes van Naters, W., Warr, C. G., Steinbrecht, R. A., and Carlson, J. R. (2003). Integrating the molecular and cellular basis of odor coding in the Drosophila antenna. Neuron 37, 827-841.

Doty, R. L. (1997). On the protheticity of olfactory pleasantness and intensity. Percept Mot Skills 85, 1439-1449.

Drain, P., Folkers, E., and Quinn, W. G. (1991). cAMP-dependent protein kinase and the disruption of learning in transgenic flies. Neuron 6, 71-82.

Dubnau, J., Grady, L., Kitamoto, T., and Tully, T. (2001). Disruption of neurotransmission in Drosophila mushroom body blocks retrieval but not acquisition of memory. Nature 411, 476-480.

Duistermars, B. J., and Frye, M. A. (2008). Crossmodal visual input for odor tracking during fly flight. Current Biology 18, 270-275.

Quinn, W. G., and Dudai, Y. (1976). Memory phases in Drosophila. Nature 262, 576-577.

Figlewicz, D. P., and Benoit, S. C. (2009). Insulin, leptin, and food reward: update 2008. Am. J. Physiol. Regul. Integr. Comp. Physiol 296, R9-R19.

Fishilevich, E., Domingos, A. I., Asahina, K., Naef, F., Vosshall, L. B., and Louis, M. (2005). Chemotaxis behavior mediated by single larval olfactory neurons in Drosophila. Curr. Biol 15, 2086-2096.

Fishilevich, E., and Vosshall, L. B. (2005). Genetic and functional subdivision of the Drosophila antennal lobe. Curr. Biol 15, 1548-1553.

Friedrich, R. W., and Laurent, G. (2001). Dynamic optimization of odor representations by slow temporal patterning of mitral cell activity. Science 291, 889-894.

Friedrich, R. W., Habermann, C. J., and Laurent, G. (2004). Multiplexing using synchrony in the zebrafish olfactory bulb. Nat Neurosci 7, 862-871.

Friggi-Grelin, F., Coulom, H., Meller, M., Gomez, D., Hirsh, J., and Birman, S. (2003). Targeted gene expression in Drosophila dopaminergic cells using regulatory sequences from tyrosine hydroxylase. J. Neurobiol 54, 618-627.

Gao, Q., Yuan, B., and Chess, A. (2000). Convergent projections of Drosophila olfactory neurons to specific glomeruli in the antennal lobe. Nat Neurosci 3, 780-785.

Garczynski, S. F., Brown, M. R., Shen, P., Murray, T. F., and Crim, J. W. (2002). Characterization of a functional neuropeptide F receptor from Drosophila melanogaster. Peptides 23, 773-780.

Gelperin, A. (1967). Stretch receptors in the foregut of the blowfly. Science 157, 208-210.

Goldman, A. L., Van der Goes van Naters, W., Lessing, D., Warr, C. G., and Carlson, J. R. (2005). Coexpression of two functional odor receptors in one neuron. Neuron 45, 661-666.

Hallem, E. A., and Carlson, J. R. (2006). Coding of odors by a receptor repertoire. Cell 125, 143-160.

Hallem, E. A., Dahanukar, A., and Carlson, J. R. (2006). Insect odor and taste receptors. Annu. Rev. Entomol 51, 113-135.

Hallem, E. A., Ho, M. G., and Carlson, J. R. (2004). The molecular basis of odor coding in the Drosophila antenna. Cell 117, 965-979.

Hammer, M., and Menzel, R. (1993). An identified neuron mediated the unconditioned stimulus in associative olfactory learning in honeybees. Nature 366, 59-63.

Han, K. A., Millar, N. S., and Davis, R. L. (1998). A novel octopamine receptor with preferential expression in Drosophila mushroom bodies. J. Neurosci 18, 3650-3658.

Han, K. A., Millar, N. S., Grotewiel, M. S., and Davis, R. L. (1996). DAMB, a novel dopamine receptor expressed specifically in Drosophila mushroom bodies. Neuron 16, 1127-1135.

Han, P. L., Levin, L. R., Reed, R. R., and Davis, R. L. (1992). Preferential expression of the Drosophila rutabaga gene in mushroom bodies, neural centers for learning in insects. Neuron 9, 619-627.

Hebb, D. (1949). The Organization of Behavior: A Neuropsychological Theory (New York: Wiley (Interscience)).

Heisenberg, M. (2003). Mushroom body memoir: from maps to models. Nat. Rev. Neurosci 4, 266-275.

Heisenberg, M., Borst, A., Wagner, S., and Byers, D. (1985). Drosophila mushroom body mutants are deficient in olfactory learning. J. Neurogenet 2, 1-30.

Hinde, R. (1966). Animal behaviour: A synthesis of ethology and comparative psychology (New York: McGraw-Hill).

Huber, F. (1967). Central control of movements and behavior of invertebrates. In Invertebrate nervous systems, C.A.G. Wiersma, ed. (Chicago and London: University of Chicago Press), pp. 333–351.

Hull, C. (1951). Essentials of Behavior (New Haven,CT: Yale University Press).

Hull, C. D., and Cribb, B. W. (2001). Olfaction in the Queensland fruit fly, Bactrocera tryoni. II: Response spectra and temporal encoding characteristics of the carbon dioxide receptors. J. Chem. Ecol 27, 889-906.

Iseki, M., Matsunaga, S., Murakami, A., Ohno, K., Shiga, K., Yoshida, K., Sugai, M., Takahashi, T., Hori, T., and Watanabe, M. (2002). A blue-light-activated adenylyl cyclase mediates photoavoidance in Euglena gracilis. Nature 415, 1047-1051.

Ito, I., Ong, R. C., Raman, B., and Stopfer, M. (2008). Sparse odor representation and olfactory learning. Nat. Neurosci 11, 1177-1184.

Jayaraman, V., and Laurent, G. (2007). Evaluating a genetically encoded optical sensor of neural activity using electrophysiology in intact adult fruit flies. Front Neural Circuits 1, 3.

Jefferis, G. S. X. E., Potter, C. J., Chan, A. M., Marin, E. C., Rohlfing, T., Maurer, C. R., and Luo, L. (2007). Comprehensive maps of Drosophila higher olfactory

centers: spatially segregated fruit and pheromone representation. Cell 128, 1187-1203.

Joiner, W. J., Crocker, A., White, B. H., and Sehgal, A. (2006). Sleep in Drosophila is regulated by adult mushroom bodies. Nature 441, 757-760.

Jones, W. D., Cayirlioglu, P., Kadow, I. G., and Vosshall, L. B. (2007). Two chemosensory receptors together mediate carbon dioxide detection in Drosophila. Nature 445, 86-90.

Jortner, R. A., Farivar, S. S., and Laurent, G. (2007). A simple connectivity scheme for sparse coding in an olfactory system. J. Neurosci 27, 1659-1669.

Kalra, S. P. (1997). Appetite and body weight regulation: is it all in the brain? Neuron 19, 227-230.

Kazama, H., and Wilson, R. I. (2008). Homeostatic matching and nonlinear amplification at identified central synapses. Neuron 58, 401-413.

Kazama, H., and Wilson, R. I. (2009). Origins of correlated activity in an olfactory circuit. Nat. Neurosci 12, 1136-1144.

Keene, A. C., Krashes, M. J., Leung, B., Bernard, J. A., and Waddell, S. (2006). Drosophila dorsal paired medial neurons provide a general mechanism for memory consolidation. Curr. Biol 16, 1524-1530.

Keene, A. C., Stratmann, M., Keller, A., Perrat, P. N., Vosshall, L. B., and Waddell, S. (2004). Diverse odor-conditioned memories require uniquely timed dorsal paired medial neuron output. Neuron 44, 521-533.

Keene, A. C., and Waddell, S. (2007). Drosophila olfactory memory: single genes to complex neural circuits. Nat. Rev. Neurosci 8, 341-354.

Kennedy, J. (1987). Animal Motivation: The Beginning of the End? In Perspectives in Chemoreception and Behavior, R. F. Chapman and E. A. Bernays, eds. (Springer).

Kim, Y., Lee, H., and Han, K. (2007). D1 dopamine receptor dDA1 is required in the mushroom body neurons for aversive and appetitive learning in Drosophila. J. Neurosci 27, 7640-7647.

Kim, Y., Lee, H., Seong, C., and Han, K. (2003). Expression of a D1 dopamine receptor dDA1/DmDOP1 in the central nervous system of Drosophila melanogaster. Gene Expr. Patterns 3, 237-245.

Kitamoto, T. (2001). Conditional modification of behavior in Drosophila by targeted expression of a temperature-sensitive shibire allele in defined neurons. J. Neurobiol 47, 81-92.

Klapstein, G. J., and Colmers, W. F. (1993). On the sites of presynaptic inhibition by neuropeptide Y in rat hippocampus in vitro. Hippocampus 3, 103-111.

Kohyama-Koganeya, A., Kim, Y., Miura, M., and Hirabayashi, Y. (2008). A Drosophila orphan G protein-coupled receptor BOSS functions as a glucose-responding receptor: loss of boss causes abnormal energy metabolism. Proc. Natl. Acad. Sci. U.S.A 105, 15328-15333.

Koulakov, A., Gelperin, A., and Rinberg, D. (2007). Olfactory coding with all-or-nothing glomeruli. J. Neurophysiol 98, 3134-3142.

Krashes, M.J., DasGupta, S., Vreede, A., White, B., Armstrong, J.D., Waddell, S. (2009). A neural circuit mechanism integrating motivational state with memory expression in Drosophila. Cell *in press*.

Krashes, M. J., Keene, A. C., Leung, B., Armstrong, J. D., and Waddell, S. (2007). Sequential use of mushroom body neuron subsets during Drosophila odor memory processing. Neuron 53, 103-115.

Krashes, M. J., and Waddell, S. (2008). Rapid consolidation to a radish and protein synthesis-dependent long-term memory after single-session appetitive olfactory conditioning in Drosophila. J. Neurosci 28, 3103-3113.

Kreher, S. A., Mathew, D., Kim, J., and Carlson, J. R. (2008). Translation of sensory input into behavioral output via an olfactory system. Neuron 59, 110-124.

Kwon, J. Y., Dahanukar, A., Weiss, L. A., and Carlson, J. R. (2007). The molecular basis of CO2 reception in Drosophila. Proceedings of the National Academy of Sciences 104, 3574-3578.

Kume, K., Kume, S., Park, S. K., Hirsh, J., and Jackson, F. R. (2005). Dopamine is a regulator of arousal in the fruit fly. J. Neurosci 25, 7377-7384.

Lai, S., Awasaki, T., Ito, K., and Lee, T. (2008). Clonal analysis of Drosophila antennal lobe neurons: diverse neuronal architectures in the lateral neuroblast lineage. Development 135, 2883-2893.

Larsson, M. C., Domingos, A. I., Jones, W. D., Chiappe, M. E., Amrein, H., and Vosshall, L. B. (2004). Or83b encodes a broadly expressed odorant receptor essential for Drosophila olfaction. Neuron 43, 703-714.

Lee, H., Seong, C., Kim, Y., Davis, R. L., and Han, K. (2003). Octopamine receptor OAMB is required for ovulation in Drosophila melanogaster. Dev. Biol 264, 179-190.

Lee, T., Lee, A., and Luo, L. (1999). Development of the Drosophila mushroom bodies: sequential generation of three distinct types of neurons from a neuroblast. Development 126, 4065-4076.

Lee, T., and Luo, L. (1999). Mosaic analysis with a repressible cell marker for studies of gene function in neuronal morphogenesis. Neuron 22, 451-461.

Lei, H., Christensen, T. A., and Hildebrand, J. G. (2004). Spatial and temporal organization of ensemble representations for different odor classes in the moth antennal lobe. J. Neurosci. 24, 11108-11119.

Levin, B. E., Kang, L., Sanders, N. M., and Dunn-Meynell, A. A. (2006). Role of neuronal glucosensing in the regulation of energy homeostasis. Diabetes 55, S122-S130.

Levin, L. R., Han, P. L., Hwang, P. M., Feinstein, P. G., Davis, R. L., and Reed, R. R. (1992). The Drosophila learning and memory gene rutabaga encodes a Ca2+/Calmodulin-responsive adenylyl cyclase. Cell 68, 479-489.

Lin, H., Lai, J. S., Chin, A., Chen, Y., and Chiang, A. (2007). A map of olfactory representation in the Drosophila mushroom body. Cell 128, 1205-1217.

Lin, S., Boey, D., and Herzog, H. (2004). NPY and Y receptors: lessons from transgenic and knockout models. Neuropeptides 38, 189-200.

Liu, X., and Davis, R. L. (2009). The GABAergic anterior paired lateral neuron suppresses and is suppressed by olfactory learning. Nat. Neurosci 12, 53-59.

Liu, X., Krause, W. C., and Davis, R. L. (2007). GABAA receptor RDL inhibits Drosophila olfactory associative learning. Neuron 56, 1090-1102.

Livingstone, M. S., Sziber, P. P., and Quinn, W. G. (1984). Loss of calcium/calmodulin responsiveness in adenylate cyclase of rutabaga, a Drosophila learning mutant. Cell 37, 205-215.

Lorenz, K.Z. (1950). The comparative method in studying innate behaviour patterns. In Symposia of the society for experimental biology, No. 4, Physiological mechanisms in animal behaviour. (New York: Academic Press), pp. 221-268.

Louis, M., Huber, T., Benton, R., Sakmar, T. P., and Vosshall, L. B. (2008). Bilateral olfactory sensory input enhances chemotaxis behavior. Nat Neurosci 11, 187-199.

Luquet, S., Perez, F. A., Hnasko, T. S., and Palmiter, R. D. (2005). NPY/AgRP neurons are essential for feeding in adult mice but can be ablated in neonates. Science 310, 683-685.

Malnic, B., Hirono, J., Sato, T., and Buck, L. B. (1999). Combinatorial receptor codes for odors. Cell 96, 713-723.

Mao, Z., and Davis, R. L. (2009). Eight different types of dopaminergic neurons innervate the Drosophila mushroom body neuropil: anatomical and physiological heterogeneity. Front Neural Circuits 3, 5.

Mao, Z., Roman, G., Zong, L., and Davis, R. L. (2004). Pharmacogenetic rescue in time and space of the rutabaga memory impairment by using Gene-Switch. Proc. Natl. Acad. Sci. U.S.A 101, 198-203.

Marella, S., Fischler, W., Kong, P., Asgarian, S., Rueckert, E., and Scott, K. (2006). Imaging taste responses in the fly brain reveals a functional map of taste category and behavior. Neuron 49, 285-295.

Martin, J. R., Ernst, R., and Heisenberg, M. (1998). Mushroom bodies suppress locomotor activity in Drosophila melanogaster. Learn. Mem 5, 179-191.

Mazor, O., and Laurent, G. (2005). Transient dynamics versus fixed points in odor representations by locust antennal lobe projection neurons. Neuron 48, 661-673.

Mayford, M., Bach, M. E., Huang, Y., Wang, L., Hawkins, R. D., and Kandel, E. R. (1996). Control of memory formation through regulated expression of a CaMKII transgene. Science 274, 1678-1683.

McGuire, S. E., Le, P. T., and Davis, R. L. (2001). The role of Drosophila mushroom body signaling in olfactory memory. Science 293, 1330-1333.

McGuire, S. E., Le, P. T., Osborn, A. J., Matsumoto, K., and Davis, R. L. (2003). Spatiotemporal rescue of memory dysfunction in Drosophila. Science 302, 1765-1768.

McKemy, D. D., Neuhausser, W. M., and Julius, D. (2002). Identification of a cold receptor reveals a general role for TRP channels in thermosensation. Nature 416, 52-58.

Melcher, C., and Pankratz, M. J. (2005). Candidate gustatory interneurons modulating feeding behavior in the Drosophila brain. PLoS Biol 3, e305.

Meunier, N., Belgacem, Y. H., and Martin, J. (2007). Regulation of feeding behaviour and locomotor activity by takeout in Drosophila. J. Exp. Biol 210, 1424-1434.

Miesenböck, G., De Angelis, D. A., and Rothman, J. E. (1998). Visualizing secretion and synaptic transmission with pH-sensitive green fluorescent proteins. Nature 394, 192-195.

Mombaerts, P., Wang, F., Dulac, C., Chao, S. K., Nemes, A., Mendelsohn, M., Edmondson, J., and Axel, R. (1996). Visualizing an olfactory sensory map. Cell 87, 675-686.

Murthy, M., Fiete, I., and Laurent, G. (2008). Testing odor response stereotypy in the Drosophila mushroom body. Neuron 59, 1009-1023.

Müller, D., Abel, R., Brandt, R., Zöckler, M., and Menzel, R. (2002). Differential parallel processing of olfactory information in the honeybee, Apis mellifera. J. Comp. Physiol. A Neuroethol. Sens. Neural. Behav. Physiol 188, 359-370.

Ng, M., Roorda, R. D., Lima, S. Q., Zemelman, B. V., Morcillo, P., and Miesenböck, G. (2002). Transmission of olfactory information between three populations of neurons in the antennal lobe of the fly. Neuron 36, 463-474.

Oda, Y., Kawasaki, K., Morita, M., Korn, H., and Matsui, H. (1998). Inhibitory long-term potentiation underlies auditory conditioning of goldfish escape behaviour. Nature 394, 182-185.

Okada, R., Awasaki, T., and Ito, K. (2009). Gamma-aminobuyric acid (GABA)-mediated neural connections in the Drosophila antennal lobe. J. Comp. Neurol 514, 74-91.

Olsen, S. R., Bhandawat, V., and Wilson, R. I. (2007). Excitatory interactions between olfactory processing channels in the Drosophila antennal lobe. Neuron 54, 89-103.

Olsen, S. R., and Wilson, R. I. (2008). Lateral presynaptic inhibition mediates gain control in an olfactory circuit. Nature 452, 956-960.

Pascual, A., and Préat, T. (2001). Localization of long-term memory within the Drosophila mushroom body. Science 294, 1115-1117.

Peabody, N. C., Pohl, J. B., Diao, F., Vreede, A. P., Sandstrom, D. J., Wang, H., Zelensky, P. K., and White, B. H. (2009). Characterization of the decision

network for wing expansion in Drosophila using targeted expression of the TRPM8 channel. J. Neurosci 29, 3343-3353.

Peier, A. M., Moqrich, A., Hergarden, A. C., Reeve, A. J., Andersson, D. A., Story, G. M., Earley, T. J., Dragoni, I., McIntyre, P., Bevan, S., et al. (2002). A TRP channel that senses cold stimuli and menthol. Cell 108, 705-715.

Perazzona, B., Isabel, G., Preat, T., and Davis, R. L. (2004). The role of cAMP response element-binding protein in Drosophila long-term memory. J. Neurosci 24, 8823-8828.

Perez-Orive, J., Mazor, O., Turner, G. C., Cassenaer, S., Wilson, R. I., and Laurent, G. (2002). Oscillations and sparsening of odor representations in the mushroom body. Science 297, 359-365.

Pitman, J. L., DasGupta, S., Krashes, M. J., Leung, B., Perrat, P. N., and Waddell, S. (2009). There are many ways to train a fly. Fly (Austin) 3, 3-9.

Pitman, J. L., McGill, J. J., Keegan, K. P., and Allada, R. (2006). A dynamic role for the mushroom bodies in promoting sleep in Drosophila. Nature 441, 753-756.

Quinn, W. G., and Dudai, Y. (1976). Memory phases in Drosophila. Nature 262, 576-577.

Quinn, W. G., Harris, W. A., and Benzer, S. (1974). Conditioned behavior in Drosophila melanogaster. Proc. Natl. Acad. Sci. U.S.A 71, 708-712.

Quinn, W. G., Sziber, P. P., and Booker, R. (1979). The Drosophila memory mutant amnesiac. Nature 277, 212-214.

Redrobe, J. P., Dumont, Y., Herzog, H., and Quirion, R. (2004). Characterization of neuropeptide Y, Y(2) receptor knockout mice in two animal models of learning and memory processing. J. Mol. Neurosci 22, 159-166.

Ressler, K. J., Sullivan, S. L., and Buck, L. B. (1994). Information coding in the olfactory system: evidence for a stereotyped and highly organized epitope map in the olfactory bulb. Cell 79, 1245-1255.

Rhim, H., Kinney, G. A., Emmerson, P. J., and Miller, R. J. (1997). Regulation of neurotransmission in the arcuate nucleus of the rat by different neuropeptide Y receptors. J. Neurosci 17, 2980-2989.

Riemensperger, T., Völler, T., Stock, P., Buchner, E., and Fiala, A. (2005). Punishment prediction by dopaminergic neurons in Drosophila. Curr. Biol 15, 1953-1960.

Roeder, K. D. (1955). Spontaneous activity and behavior. The Scientific Monthly 80, 362-370.

Rogan, M. T., Staubli, U. V., and LeDoux, J. E. (1997). Fear conditioning induces associative long-term potentiation in the amygdala. Nature 390, 604-607.

Roman, G., Endo, K., Zong, L., and Davis, R. L. (2001). P[Switch], a system for spatial and temporal control of gene expression in Drosophila melanogaster. Proc. Natl. Acad. Sci. U.S.A 98, 12602-12607.

Root, C. M., Masuyama, K., Green, D. S., Enell, L. E., Nässel, D. R., Lee, C., and Wang, J. W. (2008). A presynaptic gain control mechanism fine-tunes olfactory behavior. Neuron 59, 311-321.

Sahu, A., Kalra, P. S., and Kalra, S. P. (1988). Food deprivation and ingestion induce reciprocal changes in neuropeptide Y concentrations in the paraventricular nucleus. Peptides 9, 83-86.

Sanacora, G., Kershaw, M., Finkelstein, J. A., and White, J. D. (1990). Increased hypothalamic content of preproneuropeptide Y messenger ribonucleic acid in genetically obese Zucker rats and its regulation by food deprivation. Endocrinology 127, 730-737.

Saper, C. B., Chou, T. C., and Elmquist, J. K. (2002). The need to feed: homeostatic and hedonic control of eating. Neuron 36, 199-211.

Sarov-Blat, L., So, W. V., Liu, L., and Rosbash, M. (2000). The Drosophila takeout gene is a novel molecular link between circadian rhythms and feeding behavior. Cell 101, 647-656.

Sato, K., Pellegrino, M., Nakagawa, T., Nakagawa, T., Vosshall, L. B., and Touhara, K. (2008). Insect olfactory receptors are heteromeric ligand-gated ion channels. Nature 452, 1002-1006.

Schroder-Lang, S., Schwarzel, M., Seifert, R., Strunker, T., Kateriya, S., Looser, J., Watanabe, M., Kaupp, U. B., Hegemann, P., and Nagel, G. (2007). Fast manipulation of cellular cAMP level by light in vivo. Nat Meth 4, 39-42.

Schroll, C., Riemensperger, T., Bucher, D., Ehmer, J., Völler, T., Erbguth, K., Gerber, B., Hendel, T., Nagel, G., Buchner, E., et al. (2006b). Light-induced activation of distinct modulatory neurons triggers appetitive or aversive learning in Drosophila larvae. Curr. Biol 16, 1741-1747.

Schwaerzel, M., Monastirioti, M., Scholz, H., Friggi-Grelin, F., Birman, S., and Heisenberg, M. (2003). Dopamine and octopamine differentiate between

aversive and appetitive olfactory memories in Drosophila. J. Neurosci 23, 10495-10502.

Scott, K., Brady, R., Cravchik, A., Morozov, P., Rzhetsky, A., Zuker, C., and Axel, R. (2001). A chemosensory gene family encoding candidate gustatory and olfactory receptors in Drosophila. Cell 104, 661-673.

Semmelhack, J. L., and Wang, J. W. (2009). Select Drosophila glomeruli mediate innate olfactory attraction and aversion. Nature 459, 218-223.

Seugnet, L., Suzuki, Y., Vine, L., Gottschalk, L., and Shaw, P. J. (2008). D1 receptor activation in the mushroom bodies rescues sleep-loss-induced learning impairments in Drosophila. Curr. Biol 18, 1110-1117.

Shang, Y., Claridge-Chang, A., Sjulson, L., Pypaert, M., and Miesenböck, G. (2007). Excitatory Local Circuits and Their Implications for Olfactory Processing in the Fly Antennal Lobe. Cell 128, 601-612.

Sinakevitch, I., and Strausfeld, N. J. (2006). Comparison of octopamine-like immunoreactivity in the brains of the fruit fly and blow fly. J. Comp. Neurol 494, 460-475.

Sitaraman, D., Zars, M., Laferriere, H., Chen, Y., Sable-Smith, A., Kitamoto, T., Rottinghaus, G. E., and Zars, T. (2008). Serotonin is necessary for place memory in Drosophila. Proc. Natl. Acad. Sci. U.S.A 105, 5579-5584.

Skoulakis, E. M., Kalderon, D., and Davis, R. L. (1993). Preferential expression in mushroom bodies of the catalytic subunit of protein kinase A and its role in learning and memory. Neuron 11, 197-208.

Slone, J., Daniels, J., and Amrein, H. (2007). Sugar receptors in Drosophila. Curr. Biol 17, 1809-1816.

Stanley, B. G., and Leibowitz, S. F. (1985). Neuropeptide Y injected in the paraventricular hypothalamus: a powerful stimulant of feeding behavior. Proc. Natl. Acad. Sci. U.S.A 82, 3940-3943.

Stopfer, M., Bhagavan, S., Smith, B. H., and Laurent, G. (1997). Impaired odour discrimination on desynchronization of odour-encoding neural assemblies. Nature 390, 70-74.

Stopfer, M., Jayaraman, V., and Laurent, G. (2003). Intensity versus identity coding in an olfactory system. Neuron 39, 991-1004.

Strauss, R., and Heisenberg, M. (1993). A higher control center of locomotor behavior in the Drosophila brain. J. Neurosci 13, 1852-1861.

Sun, Q., Baraban, S. C., Prince, D. A., and Huguenard, J. R. (2003). Target-specific neuropeptide Y-ergic synaptic inhibition and its network consequences within the mammalian thalamus. J. Neurosci 23, 9639-9649.

Tanaka, N. K., Awasaki, T., Shimada, T., and Ito, K. (2004). Integration of chemosensory pathways in the Drosophila second-order olfactory centers. Curr. Biol 14, 449-457.

Tanaka, N. K., Ito, K., and Stopfer, M. (2009). Odor-evoked neural oscillations in Drosophila are mediated by widely branching interneurons. J. Neurosci 29, 8595-8603.

Tanaka, N. K., Tanimoto, H., and Ito, K. (2008). Neuronal assemblies of the Drosophila mushroom body. J. Comp. Neurol 508, 711-755.

Tatemoto, K., Carlquist, M., and Mutt, V. (1982). Neuropeptide Y--a novel brain peptide with structural similarities to peptide YY and pancreatic polypeptide. Nature 296, 659-660.

Tempel, B. L., Bonini, N., Dawson, D. R., and Quinn, W. G. (1983). Reward learning in normal and mutant Drosophila. Proc. Natl. Acad. Sci. U.S.A 80, 1482-1486.

Thorpe, W. (1956). Learning and Instinct in Animals (Cambridge: Harvard University Press).

Thum, A. S., Jenett, A., Ito, K., Heisenberg, M., and Tanimoto, H. (2007). Multiple memory traces for olfactory reward learning in Drosophila. J. Neurosci 27, 11132-11138.

Toates, F. (1986). Motivational Systems (Cambridge: Cambridge University Press).

Tolman, E. (1932). Purposive behavior in animals and men (New York: The Century Co.).

Tsien, J. Z., Huerta, P. T., and Tonegawa, S. (1996). The essential role of hippocampal CA1 NMDA receptor-dependent synaptic plasticity in spatial memory. Cell 87, 1327-1338.

Tsvetkov, E., Carlezon Jr., W. A., Benes, F. M., Kandel, E. R., and Bolshakov, V. Y. (2002). Fear conditioning occludes LTP-induced presynaptic enhancement of synaptic transmission in the cortical pathway to the lateral amygdala. Neuron 34, 289-300.

Tully, T., and Quinn, W. G. (1985). Classical conditioning and retention in normal and mutant Drosophila melanogaster. J. Comp. Physiol. A 157, 263-277.

Turner, G. C., Bazhenov, M., and Laurent, G. (2008). Olfactory representations by Drosophila mushroom body neurons. J. Neurophysiol 99, 734-746.

van Swinderen, B. (2007). Attention-like processes in Drosophila require short-term memory genes. Science 315, 1590-1593.

Vassar, R., Chao, S. K., Sitcheran, R., Nuñez, J. M., Vosshall, L. B., and Axel, R. (1994). Topographic organization of sensory projections to the olfactory bulb. Cell 79, 981-991.

Vosshall, L. B., Wong, A. M., and Axel, R. (2000). An olfactory sensory map in the fly brain. Cell 102, 147-159.

Waddell, S., Armstrong, J. D., Kitamoto, T., Kaiser, K., and Quinn, W. G. (2000). The amnesiac gene product is expressed in two neurons in the Drosophila brain that are critical for memory. Cell 103, 805-813.

Wang, J. W., Wong, A. M., Flores, J., Vosshall, L. B., and Axel, R. (2003). Two-photon calcium imaging reveals an odor-evoked map of activity in the fly brain. Cell 112, 271-282.

Wang, Y., Chiang, A., Xia, S., Kitamoto, T., Tully, T., and Zhong, Y. (2003). Blockade of neurotransmission in Drosophila mushroom bodies impairs odor attraction, but not repulsion. Curr. Biol 13, 1900-1904.

Wang, Y., Guo, H., Pologruto, T. A., Hannan, F., Hakker, I., Svoboda, K., and Zhong, Y. (2004). Stereotyped odor-evoked activity in the mushroom body of Drosophila revealed by green fluorescent protein-based Ca2+ imaging. J. Neurosci 24, 6507-6514.

Wang, Z., Singhvi, A., Kong, P., and Scott, K. (2004). Taste representations in the Drosophila brain. Cell 117, 981-991.

Wehr, M., and Laurent, G. (1996). Odour encoding by temporal sequences of firing in oscillating neural assemblies. Nature 384, 162-166.

Weintraub, D. (2008). Dopamine and impulse control disorders in Parkinson's disease. Ann. Neurol 64 Suppl 2, S93-100.

Wen, T., Parrish, C. A., Xu, D., Wu, Q., and Shen, P. (2005). Drosophila neuropeptide F and its receptor, NPFR1, define a signaling pathway that acutely modulates alcohol sensitivity. Proc. Natl. Acad. Sci. U.S.A 102, 2141-2146.

Wicher, D., Schafer, R., Bauernfeind, R., Stensmyr, M. C., Heller, R., Heinemann, S. H., and Hansson, B. S. (2008). Drosophila odorant receptors are both ligand-gated and cyclic-nucleotide-activated cation channels. Nature 452, 1007-1011.

Wilson, R. I., and Laurent, G. (2005). Role of GABAergic inhibition in shaping odor-evoked spatiotemporal patterns in the Drosophila antennal lobe. J. Neurosci 25, 9069-9079.

Wilson, R. I., and Mainen, Z. F. (2006). Early events in olfactory processing. Annu. Rev. Neurosci 29, 163-201.

Wilson, R. I., Turner, G. C., and Laurent, G. (2004). Transformation of olfactory representations in the Drosophila antennal lobe. Science 303, 366-370.

Watts, A.G. (2003). Motivation. In The handbook of brain theory and neural networks. M.A. Arbib, ed. (Cambridge, MA: Bradford Books, MIT Press), pp. 680-683.

Wu, C., Xia, S., Fu, T., Wang, H., Chen, Y., Leong, D., Chiang, A., and Tully, T. (2007). Specific requirement of NMDA receptors for long-term memory consolidation in Drosophila ellipsoid body. Nat. Neurosci 10, 1578-1586.

Wu, Q., Wen, T., Lee, G., Park, J. H., Cai, H. N., and Shen, P. (2003). Developmental control of foraging and social behavior by the Drosophila neuropeptide Y-like system. Neuron 39, 147-161.

Wu, Q., Zhang, Y., Xu, J., and Shen, P. (2005). Regulation of hunger-driven behaviors by neural ribosomal S6 kinase in Drosophila. Proc. Natl. Acad. Sci. U.S.A 102, 13289-13294.

Wu, Q., Zhao, Z., and Shen, P. (2005). Regulation of aversion to noxious food by Drosophila neuropeptide Y- and insulin-like systems. Nat. Neurosci 8, 1350-1355.

Xia, S., Miyashita, T., Fu, T., Lin, W., Wu, C., Pyzocha, L., Lin, I., Saitoe, M., Tully, T., and Chiang, A. (2005). NMDA receptors mediate olfactory learning and memory in Drosophila. Curr. Biol 15, 603-615.

Yao, C. A., Ignell, R., and Carlson, J. R. (2005). Chemosensory coding by neurons in the coeloconic sensilla of the Drosophila antenna. J. Neurosci 25, 8359-8367.

Yin, J. C., Del Vecchio, M., Zhou, H., and Tully, T. (1995). CREB as a memory modulator: induced expression of a dCREB2 activator isoform enhances long-term memory in Drosophila. Cell 81, 107-115.

Yin, J. C., Wallach, J. S., Del Vecchio, M., Wilder, E. L., Zhou, H., Quinn, W. G., and Tully, T. (1994). Induction of a dominant negative CREB transgene specifically blocks long-term memory in Drosophila. Cell 79, 49-58.

Yu, D., Akalal, D. G., and Davis, R. L. (2006). Drosophila alpha/beta mushroom body neurons form a branch-specific, long-term cellular memory trace after spaced olfactory conditioning. Neuron 52, 845-855.

Yu, D., Ponomarev, A., and Davis, R. L. (2004). Altered representation of the spatial code for odors after olfactory classical conditioning; memory trace formation by synaptic recruitment. Neuron 42, 437-449.

Yuan, N., and Lee, D. (2007). Suppression of excitatory cholinergic synaptic transmission by Drosophila dopamine D1-like receptors. Eur. J. Neurosci 26, 2417-2427.

Zars, T., Fischer, M., Schulz, R., and Heisenberg, M. (2000). Localization of a short-term memory in Drosophila. Science 288, 672-675.

Zhang, K., Guo, J. Z., Peng, Y., Xi, W., and Guo, A. (2007). Dopamine-mushroom body circuit regulates saliency-based decision-making in Drosophila. Science 316, 1901-1904.

Zhu, S., Chiang, A., and Lee, T. (2003). Development of the Drosophila mushroom bodies: elaboration, remodeling and spatial organization of dendrites in the calyx. Development 130, 2603-2610.